Fangping Yan

THE DEPOSITION AND LIGHT ABSORPTION PROPERTY OF CARBONACEOUS MATTER IN THE HIMALAYAS AND TIBETAN PLATEAU

ACTA UNIVERSITATIS LAPPEENRANTAENSIS 910

Fangping Yan

THE DEPOSITION AND LIGHT ABSORPTION PROPERTY OF CARBONACEOUS MATTER IN THE HIMALAYAS AND TIBETAN PLATEAU

Dissertation for the degree of Doctor of Science (Technology) to be presented with due permission for public examination and criticism at Lappeenranta-Lahti University of Technology LUT, Lappeenranta, Finland on the 29th of June, 2020, at 10:00 am.

Acta Universitatis
Lappeenrantaensis 910

Supervisors Professor Satu-Pia Reinikainen
LUT School of Engineering Science
Lappeenranta-Lahti University of Technology LUT
Finland

Associate professor Chaoliu Li
Key Laboratory of Tibetan Environment Changes and Land Surface Processes, Institute of Tibetan Plateau Research
Chinese Academy of Sciences
China

Reviewers Professor Yuan Cheng
School of Environment
Harbin Institute of Technology
Harbin, China

Research Scientist Guofeng Shen
College of Urban and Environmental Sciences
Peking University
Beijing, China

Opponent Professor Yuan Cheng
School of Environment
Harbin Institute of Technology
Harbin, China

ISBN 978-952-335-525-5
ISBN 978-952-335-526-2 (PDF)
ISSN-L 1456-4491
ISSN 1456-4491

Lappeenranta-Lahti University of Technology LUT
LUT University Press 2020

Abstract

Fangping Yan
The deposition and light absorption property of carbonaceous matter in the Himalayas and Tibetan Plateau
Lappeenranta 2020
89 pages
Acta Universitatis Lappeenrantaensis 910
Diss. Lappeenranta-Lahti University of Technology LUT
ISBN 978-952-335-525-5, ISBN 978-952-335-526-2 (PDF), ISSN-L 1456-4491, ISSN 1456-4491

The Himalayas and Tibetan Plateau (HTP), known as the “Third Pole” and “world roof”, contains the largest amount of glaciers outside the Arctic and Antarctic. Carbonaceous matter, mainly including black carbon (BC) and organic carbon (OC), plays important role in climate forcing of the atmosphere and glacier retreat after its deposition on the glacier surface in the HTP. With the rapid climate change and glacier retreat, the study on carbonaceous matter in the HTP has become a hotspot in recent few decades. Although a series of studies on carbonaceous matter in the atmosphere and glacier regions of the HTP have been conducted, large uncertainties still existed. Therefore, this work was carried out to first discuss the uncertainties in previous studies and adjust the reported data of carbonaceous matter in the HTP. Then in-situ observations were conducted at three remote stations and an urban site in the HTP to comprehensively investigate reliable concentrations and deposition rates of carbonaceous mater in precipitation, and the atmospheric dry deposition rates of particulate carbon. Meanwhile, the scavenging mechanisms of carbonaceous matter in the atmosphere were discussed. Furthermore, the OC, especially the water-insoluble fraction, exerts strong light absorption particularly in the UV wavelength rage. However, the methods in previous studies to investigate the light absorption of this water-insoluble organic carbon (WIOC) have large uncertainties. To accurately estimate its light absorption, the uncertainties in previous methods to extract WIOC with methanol were discussed, and a new method was developed in this work.

The results in this work indicated that the previously reported concentrations of the atmospheric BC and OC were overestimated due to the influence of inorganic carbon (e.g. carbonate) in mineral dust because of the wide distribution of arid and desert regions across the HTP. Thus, the previously reported BC concentrations at two remote stations of the HTP, Nam Co and Everest were adjusted to 61 and 151 ng m^{-3}, respectively. Meanwhile, the previous BC atmospheric deposition rates estimated using the lake cores were also overestimated due to the large contribution of catchment input.

An average BC deposition rate of 17.9±5.3 mg m^{-2} yr^{-1} in glacier regions of the HTP was then reached using the relatively consistent data from snow pits and ice cores.

The in-situ investigation indicated that the concentrations and deposition rates of three components of carbonaceous matter (BC, dissolved OC (DOC) and WIOC) in precipitation were in accordance with those in other mountain and remote regions, reflecting the relatively clean atmosphere in the HTP. Among the three components, DOC is the major fraction while BC is the smallest fraction in precipitation, which was attributed to their different characteristics and scavenging processes. Wet deposition rates of the carbonaceous components exhibited obvious temporal and spatial variations due to the distinct monsoon/non-monsoon periods and complex topography of the HTP. Moreover, the in-situ investigation also indicated that dry deposition rates of particulate carbon factions (BC and WIOC) were unexpectedly higher than those previously anticipated in the HTP. For instance, the BC dry deposition rates at Nam Co Station and Lhasa city were approximately 1.6 and 8.5 times higher than the corresponding wet deposition rates, which indicated that dry deposition was the dominated removal process for the particulate carbon in most parts of the HTP. However, the dry deposition rates had been underestimated by the modeling and empirical algorithms, while the corresponding wet deposition rates were overestimated.

The mass absorption cross-section (MAC) of precipitation DOC which represented the light absorption of DOC from the cloud altitude to the near surface was consistently lower than those of the corresponding near-surface aerosols (i.e., MAC of water-soluble OC (WSOC)) at three remote stations. Additionally, by comparing the previous methods with the one we proposed to extract atmospheric OC with methanol, we found that the previous extraction methods ignored the particulate carbon detachment and largely overestimated the methanol-soluble OC (MeS-OC) mass, leading to the underestimation of its MAC value. However, the new method can avoid this problem, and it was found that OC could be extracted by methanol in a short time; the sonication and long-term soaking in previous studies did not significantly increase the amount of methanol extractable OC. Therefore, this new method could quantitatively provide reliable light absorption of atmospheric OC. The MAC values of WIOC at 365 nm by this new method were approximately 2.3 and 1.6 times higher than the values of WSOC for the biomass and ambient aerosols, respectively, in this study, indicating that WIOC was more representative than WSOC acting as proxy of brown carbon. Thus, further related work should be carried out to obtain a comprehensive understanding of the light absorption of OC in both the atmosphere and glaciers after deposition facilitating the estimate of the corresponding climate change caused by OC. This work reported the in-situ data of WIOC, BC and DOC concentration and deposition in the HTP for the first time, and proposed a new method

to obtain the reliable light absorption of OC.

Keywords: carbonaceous matter, concentrations, deposition rates, light absorption, precipitation, aerosol, the Himalayas and Tibetan Plateau

Acknowledgements

This research work for thesis was conducted in School of Engineering Sciences, Lappeenranta-Lahti University of Technology LUT in cooperation with the Chinese Academy of Sciences during September 2016 to February 2020. The expert research team and the enthusiasm for science made this research possible.

I am very grateful for Professor Satu-Pia Reinikainen for acting as my supervisor during the thesis preparation and writing with great patience and carefulness. I am also grateful for her comments and suggestions for further study. I appreciate her support and assistance to finalize this thesis.

I would express my sincere appreciation to Professor Mika Sillanpää who offered the opportunity to conduct this work in Lappeenranta-Lahti University of Technology LUT in the beginning. I thank for his great support and guidance in this research work.

I highly appreciate associate professor Chaoliu Li for acting as my supervisor during the whole research course for PhD thesis. He not only offered great support for this research but also very valuable and useful comments and suggestions for all the field and laboratory work and manuscript preparation. He also offered great efforts to discuss the comments from the reviewers and editors for the papers included in this thesis. I am grateful for his patient guidance and encouragement during past several years.

My sincere appreciation also expressed to Professor Shichang Kang, State Key Laboratory of Cryospheric Sciences, Chinese Academy of Sciences. I highly acknowledge his great support in the field and laboratory work. I am grateful for his profound comments in this research and patient guidance during past several years.

I express my gratitude to Professor Peter Raymond, Dr. Cenlin He, Associate professor Da Wei, Dr. Bin Qu, Dr. Kelly Aho, Dr. Shaopeng Gao, Dr. Pengfei Chen, Dr. Zhaofu Hu, Dr. Caiqing Yan, Dr. Pengling Wang, Dr. Guoshuai Zhang, Dr. Junming Guo, Dr. Xiaofei Li, Xiaoxiang Wang, Mengke Chen，Fei Wang and Duo Jie for their contributions as co-authors and/or assistance in the field work.

I sincerely acknowledge the two reviewers of this thesis for their comments. I also appreciate all the reviewers and editors of the papers included in this thesis for their constructive comments and suggestions. Acknowledgements also go to the Elsevier, Wiley and EGU publishers for their permission to include the papers in this dissertation.

I am thankful for members of the research group in Mikkeli for their assistance in my work. I also acknowledge the study programme coordinators in Lappeenranta for their instructions during the study process. I appreciate all the friends during my stay in Finland for their help and concern which made the life in Finland easy and colorful and I will keep this in mind always.

Finally, I would express gratitude to my families for their unconditional support and encouragement in my PhD study and my life.

Fangping Yan
February, 2020
Mikkeli, Finland

Contents

List of publications

This dissertation is based on the following papers. The rights have been granted by publishers to include the papers in dissertation.

I. Li, C., Yan, F., Kang, S., Chen, P., Han, X., Hu, Z., Zhang, G., Hong, Y., Gao, S., Qu, B., Zhu, Z., Li, J., Chen, B., Sillanpää, M., 2017. Re-evaluating black carbon in the Himalayas and the Tibetan Plateau: concentrations and deposition. Atmospheric Chemistry and Physics 17, 11899-11912.

II. Yan, F., He, C., Kang, S., Chen, P., Hu, Z., Han, X., Gautam, S., Yan, C., Zheng, M., Sillanpää, M., Raymond, P.A., Li, C., 2019. Deposition of organic and black carbon: direct measurements at three remote stations in the Himalayas and Tibetan Plateau. Journal of Geophysical Research: Atmospheres 124, 9702–9715.

III. Li, C., Yan, F., Kang, S., Chen, P., Hu, Z., Han, X., Zhang, G., Gao, S., Qu, B., Sillanpaa, M., 2017. Deposition and light absorption characteristics of precipitation dissolved organic carbon (DOC) at three remote stations in the Himalayas and Tibetan Plateau, China. Science Total Environment 605-606, 1039-1046.

IV. Yan, F., Wang, P., Kang, S., Chen, P., Hu, Z., Han, X., Sillanpää, M., Li, C., 2020. High particulate carbon deposition in Lhasa—a typical city in the Himalayas–Tibetan Plateau due to local contributions. Chemosphere 247, https://doi.org/10.1016/j.chemosphere. 2020. 125843.

V. Yan, F., Kang, S., Sillanpää, M., Hu, Z., Gao, S., Chen, P., Gautam, S., Reinikainen, S.-P., Li, C., 2020. A new method for extraction of methanol-soluble brown carbon: Implications for investigation of its light absorption ability. Environmental Pollution 262, https://doi.org/10.1016/j.envpol.2020.114300.

Author's contribution

Fangping Yan carried out the field campaigns, conducted the experiments, analyzed the data with co-authors and helped to prepare the first draft of paper I and III. Fangping Yan carried out the field campaigns, conducted the experiments, analyzed the data and had the main responsibility in writing paper II, IV and V.

Other related publications

I. Yan, F., Kang, S., Li, C., Zhang, Y., Qin, X., Li, Y., Zhang, X., Hu, Z., Chen, P., Li, X., Qu, B., Sillanpää, M., 2016. Concentration, sources and light absorption characteristics of dissolved organic carbon on a medium-sized valley glacier, northern Tibetan Plateau. The Cryosphere 10, 2611-2621.

II. Yan, F., Sillanpää, M., Kang, S., Aho, K.S., Qu, B., Wei, D., Li, X., Li, C., Raymond, P.A., 2018. Lakes on the Tibetan Plateau as Conduits of Greenhouse Gases to the Atmosphere. Journal of Geophysical Research: Biogeosciences 123, 2091-2103.

III. Li, C., Yan, F., Kang, S., Chen, P., Hu, Z., Gao, S., Qu, B., Sillanpää, M., 2016. Light absorption characteristics of carbonaceous aerosols in two remote stations of the southern fringe of the Tibetan Plateau, China. Atmospheric Environment 143, 79-85.

IV. Gautam, S., Yan, F., Kang, S., Han, X., Neupane, B., Chen, P., Hu, Z., Sillanpää, M., Li, C., 2019. Black carbon in surface soil of the Himalayas and Tibetan Plateau and its contribution to total black carbon deposition at glacial region. Environmental Science and Pollution Research, https://doi.org/10.1007/s11356-019-07121-7.

V. Li, C., Kang, S., Yan, F., 2018. Importance of Local Black Carbon Emissions to the Fate of Glaciers of the Third Pole. Environmental Science and Technology 52, 14027-14028.

VI. Hu, Z., Kang, S., Yan, F., Zhang, Y., Li, Y., Chen, P., Qin, X., Wang, K., Gao, S., Li, C., 2018. Dissolved organic carbon fractionation accelerates glacier-melting: A case study in the northern Tibetan Plateau. The Science of the total environment 627, 579-585.

VII. Hu, Z., Kang, S., Li, C., Yan, F., Chen, P., Gao, S., Wang, Z., Zhang, Y., Sillanpaa, M., 2017. Light absorption of biomass burning and vehicle emission-sourced carbonaceous aerosols of the Tibetan Plateau. Environmental science and pollution research 24, 15369-15378.

VIII. Hu, Z., Kang, S., He, X., Yan, F., Zhang, Y., Chen, P., Li, X., Gao, S., Li, C., 2019. Carbonaceous matter in glacier at the headwaters of the Yangtze River:

Concentration, sources and fractionation during the melting process. Journal of Environmental Sciences, 87, 389-397.

IX. Li, C., Chen, P., Kang, S., Yan, F., Tripathee, L., Wu, G., Qu, B., Sillanpää, M., Yang, D., Dittmar, T., Stubbins, A., Raymond, P.A., 2018a. Fossil Fuel Combustion Emission From South Asia Influences Precipitation Dissolved Organic Carbon Reaching the Remote Tibetan Plateau: Isotopic and Molecular Evidence. Journal of Geophysical Research: Atmospheres 123, 6248-6258.

X. Li, C., Han, X., Kang, S., Yan, F., Chen, P., Hu, Z., Yang, J., Ciren, D., Gao, S., Sillanpaa, M., Han, Y., Cui, Y., Liu, S., Smith, K.R., 2018. Heavy near-surface $PM_{2.5}$ pollution in Lhasa, China during a relatively static winter period. Chemosphere 214, 314-318.

XI. Li, Y., Kang, S., Yan, F., Chen, J., Wang, K., Paudyal, R., Liu, J., Qin, X., Sillanpää, M., 2019. Cryoconite on a glacier on the north-eastern Tibetan plateau: light-absorbing impurities, albedo and enhanced melting. Journal of Glaciology 252, 633-644.

XII. Chen, P., Kang, S., Li, C., Li, Q., Yan, F., Guo, J., Ji, Z., Zhang, Q., Hu, Z., Tripathee, L., Sillanpää, M., 2018. Source Apportionment and Risk Assessment of Atmospheric Polycyclic Aromatic Hydrocarbons in Lhasa, Tibet, China. Aerosol and Air Quality Research 18, 1294-1304.

XIII. Qu, B., Sillanpaa, M., Kang, S., Yan, F., Li, Z., Zhang, H., Li, C., 2018. Export of dissolved carbonaceous and nitrogenous substances in rivers of the "Water Tower of Asia". Journal of Environment Science (China) 65, 53-61.

XIV. Qu, B., Aho, K.S., Li, C., Kang, S., Sillanpaa, M., Yan, F., Raymond, P.A., 2017. Greenhouse gases emissions in rivers of the Tibetan Plateau. Scientific Report 7, doi:10.1038/s41598-017-16552-6.

XV. Qu, B., Sillanpaa, M., Li, C., Kang, S., Stubbins, A., Yan, F., Aho, K.S., Zhou, F., Raymond, P.A., 2017. Aged dissolved organic carbon exported from rivers of the Tibetan Plateau. PLoS One 12, e0178166.

XVI. Chen, M., Wang, C., Wang, X., Fu, J., Gong, P., Yan, J., Yu, Z., Yan, F., Nawab, J., 2019. Release of perfluoroalkyl substances from melting glacier of the Tibetan Plateau: Insights into the impact of global warming on the cycling of emerging pollutants. Journal of Geophysical Research: Atmospheres 124, 7442-7456.

Nomenclature

Abs	Light absorbance
BC	Black carbon
BrC	Brown carbon
CAM5	Community Atmosphere Model version 5
CCN	Cloud condensation nuclei
DOC	Dissolved organic carbon
HTP	The Himalayas and Tibetan Plateau
IC	Inorganic carbon
MAC	Mass absorption cross-section
MeS-OC	Methanol-soluble organic carbon
MD	Mineral dust
OC	Organic carbon
$PM_{2.5}$	Particles with an aerodynamic diameter of 2.5 μm or less
POC	Primary organic carbon
SOAs	Secondary organic aerosols
SP2	Single-particle soot photometer
TOA	Thermal-optical analysis
TC	Total carbon
TSP	Total suspended particles
VWM	Volume-weighted mean
VOCs	Volatile organic compounds
WIOC	Water-insoluble organic carbon
WSOC	Water-soluble organic carbon

1 Introduction

1.1 Significance of carbonaceous matter in the atmosphere and precipitation

Carbonaceous matter plays an important role not only in air quality but also in climate change by modifying the radiative balance in the atmosphere (Andreae and Gelencsér, 2006; Anenberg et al., 2012; Bond et al., 2013; IPCC, 2013; Ramanathan and Carmichael, 2008; Ramanathan et al., 2007). According to the chemical, thermal and optical properties, carbonaceous matter is primarily classified into two fractions: black carbon (BC, a term synonymous with element carbon, EC, in climate and air quality studies (Petzold et al., 2013)) and organic carbon (OC). The latter is further divided into water-soluble OC (WSOC) and water-insoluble OC (WIOC). BC is generally produced during the incomplete combustion processes; while OC has multiple sources besides combustion emissions, such as the natural release from plant debris, spore, pollen, soil, sea spray and the oxidation of the atmospheric volatile organic compounds (VOCs) from anthropogenic or natural processes (Seinfeld and Pankow, 2003). Although BC is a minor constituent of carbonaceous matter, the nearly inert characteristic makes it eligible for long-range transport. Thus, it has been observed in snow and ice of the remote regions, such as the Himalayas and Tibetan Plateau (HTP), Arctic and Antarctic (Bisiaux et al., 2012; Doherty et al., 2010; Dou and Xiao, 2016; Xu et al., 2009). In addition to its effect on atmospheric visibility reduction, BC is a major absorber of visible solar radiation in the atmosphere, making it the second global warming factor after carbon dioxide (Ramanathan and Carmichael, 2008). Correspondingly, OC can exert both cooling and warming effects on climate change (Andreae and Gelencsér, 2006). WSOC is also called dissolved OC (DOC) in precipitation study. Besides the role in climate forcing, precipitation DOC is also very important in global and regional carbon cycle (Pan et al., 2010; Willey et al., 2000). Moreover, when deposited on glacier surface, both BC and OC absorb solar radiation and reduce the albedo of the surface, which could accelerate the glacier retreat (as indicated in Figure 1.1) (Kang et al., 2019; Li et al., 2018b; Ming et al., 2013; Quinn et al., 2000; Xu et al., 2009).

Although the carbonaceous matter is of great significance in climate change and the cryosphere evolution (Kang et al., 2019), and the majority attention has been paid to carbonaceous matter and its environmental effects in the atmosphere at present, uncertainties exist in many aspects of its deposition (Ducret and Cachier, 1992; Sharma

et al., 2013; Yasunari et al., 2010; Zhang et al., 2015b). The factors determining the lifetime of the carbonaceous matter in the atmosphere include the concentration of ambient carbonaceous matter, the size of the particles, the duration and frequency of precipitation, and the removal rates of the particles (Ogren and Charlson, 1983). The wet deposition of carbonaceous matter is normally considered to be the significant removal process (Ogren et al., 1984), playing a crucial role in the comprehensive and better understanding of the global carbon cycle due to its potential in acting as seeds for the cloud droplets formation (Stocker et al., 2013). The wet removal of carbonaceous matter is supposed to have two processes: the rainout process where the carbonaceous mater is directly incorporated into the cloud droplets as nucleating agents or ice crystal; and the washout process where the carbonaceous matter collides with the exiting droplet or crystal in the atmosphere and is washed out by the precipitation (Ishikawa et al., 1995; Ogren et al., 1983). The two removal processes are usually determined by the hygroscopicity of carbonaceous matter, which varies largely due to its complex chemical compositions (Torres et al., 2013). For example, the freshly emitted BC is considered to be hydrophobic, however, after coated by some hygroscopic substances, its surface would be activated and become hygroscopic to be able to incorporate into the water droplets (Ogren et al., 1984); while the DOC fraction was the effective factor in cloud condensation nuclei (CCN) due to its hygroscopic nature. However, up to date, these removal mechanisms are still poorly understood because of the limited data availability from in-situ observations (Cerqueira et al., 2010; Garrett et al., 2017; Jurado et al., 2008). In addition to wet deposition, some researches indicated that dry deposition may also play an important role in particulate carbon deposition in some study regions (as presented in Figure 1.1) (Cerqueira et al., 2010; Matsuda et al., 2012; Yang et al., 2014; Zhang et al., 2015b), which is usually underestimated or failed to incorporate in carbonaceous matter deposition. Therefore, the parameters to estimate the wet and dry deposition processes, such as the deposition velocities, lifetimes of atmospheric carbonaceous matter, are variable, and large uncertainties occur when these parameters are adopted in the model simulations (Cooke, 2002; Textor et al., 2006). The discrepancies in parameters and uncertainties among different researches are important limitations in validating the global and regional aerosol models and accurately simulating the concentration, transport and deposition of the atmospheric carbonaceous matter, and thus affecting the prediction of climate change by carbonaceous matter in the atmosphere.

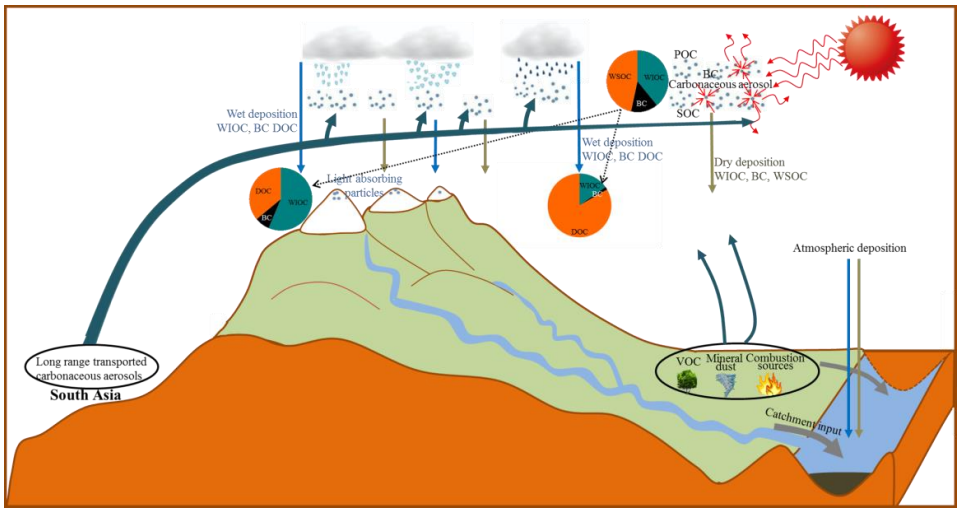

Figure 1.1: Schematic diagram of sources, wet and dry deposition of carbonaceous aerosols, and their light absorption property in the HTP. Note: the ratios of carbonaceous components were adopted from the representative remote Nam Co regions, which can be found in Figure 3.4.

1.2 Carbonaceous matter in precipitation

Currently, there are some researches focusing on particulate carbon deposition world widely despite the limited data about the carbonaceous matter in precipitation compared to those of aerosols. In a series of the earliest studies by Orgen et al., a three-step procedure was developed to separate BC from other carbon compositions (such as OC and biogenic carbon) in rainwater and a nondispersive infrared analyzer was adopted for BC measurement (Ogren et al., 1983). The wet and dry deposition mechanisms of BC were elaborated, concentrations and deposition removal rates were estimated in some urban and rural sites of the Seattle and Sweden, and the scavenging ratio was introduced in wet deposition study to simplify the complicated wet removal process (Ogren, 1982; Ogren and Charlson, 1983; Ogren et al., 1984). The first dataset of carbonaceous particles in rainwater (i.e., WIOC and BC) with long temporal series was obtained by Ducret and Cachier, 1992 directly using a two-step thermal procedure. In recent years, three studies have directly measured WIOC and BC in precipitation simultaneously using thermal-optical method, and the deposition rates and carbon isotope compositions were reported accordingly (Cerqueira et al., 2010; Huo et al., 2016; Zhang et al., 2015c). Another study measured BC concentrations directly in both rain and snow samples (Chýlek et al., 1999). Other two studies have indirectly

calculated the wet and dry deposition rates of both WIOC and BC by measuring the concentrations of the corresponding particles in the atmosphere and some influencing factors, such as wind speed, deposition velocities (Jurado et al., 2008; Matsuda et al., 2012). Meanwhile, the historical BC concentrations and deposition rates have been reconstructed in a series of studies using ice cores in mountain glacier and ice sheets (Bisiaux et al., 2012; Kaspari et al., 2011; Lavanchy et al., 1999; Ruppel et al., 2014) and lake sediment cores (Cong et al., 2013; Elmquist et al., 2007; Han et al., 2015; Husain et al., 2008; Liu et al., 2011; Ruppel et al., 2015), which provide important information on past and present climate change and the prediction of future climate. Among those studies on ice cores, Lavanchy et al. also reconstructed the WIOC concentrations in a European high-alpine glacier ice core (Lavanchy et al., 1999). Despite of the lacking of direct measurements of WIOC and BC in rainwater, the studies of BC and WIOC in snow and ice of the glacier regions deposited from the atmosphere are increasingly emerging acting as warming proxies by absorbing solar radiation and affecting the glacier retreat (Clarke and Noone, 1985; Dou and Xiao, 2016; Hagler et al., 2007; Kang et al., 2019; Kaspari et al., 2014; Ming et al., 2013; Xu et al., 2009; Xu et al., 2012).

The methods used for concentration measurement of particulate carbon of precipitation in previous studies are various, mainly including the single-particle soot photometer (SP2), UV/VIS spectrophotometer and thermal-optical analysis (TOA), and these methods were compared and evaluated (Torres et al., 2013). Although none of the three methods is perfect, the SP2 and TOA methods were truly suitable for BC measurement according to the study objectives. The SP2 is suitable for BC samples with small volume, it has low detection limit, it is fast and the result is precise and reproducible. However, this method underestimates the BC concentration. The TOA can measure WIOC and BC simultaneously; however this method requires large sample volume, the sample pyrolysis might cause uncertainty in BC concentration, and it is time-consuming (Torres et al., 2013). Nevertheless, it is feasible to adopt TOA method if we want to measure both WIOC and BC in precipitation, but further improvement of this method is required.

The DOC in precipitation which plays significant role in the global climate change and global carbon cycle (Saxena and Hildemann, 1996; Willey et al., 2000) has also been investigated. In contrast to the various methods for WIOC and BC concentration measurements, DOC concentration in precipitation was generally measured by a TOC analyzer and little uncertainty exits. The studies of DOC concentration in precipitation and wet deposition have been conducted in urban cities (Pan et al., 2010; Raymond, 2005; Siudek et al., 2015; Yan and Kim, 2012), marine sites (Gioda et al., 2011; Willey et al., 2000), coastal sites (Kieber et al., 2002), forest

sites (McDowell and Likens, 1988; Siudek et al., 2015) and a high-altitude Tibetan city (Li et al., 2016e). The reported concentration of DOC in precipitation varied largely and the global DOC deposition rate was approximately 29 kg ha^{-1} yr^{-1} (Willey et al., 2000). The carbon isotopic characterization of DOC suggested that almost all the precipitation DOC in current study regions has been influenced by fossil fuel combustion (Avery et al., 2013; Li et al., 2018a; Li et al., 2016e; Raymond, 2005). More recently, a comprehensive synthesis of atmospheric OC deposition via precipitation during the past three decades was conducted, which suggested an average OC concentration of 2.64±1.9 mg L^{-1} and an average OC deposition rate of 34±33 kg ha^{-1} yr^{-1}, providing a benchmark for the present condition of precipitation scavenged OC and for the future exploring in this research direction (Iavorivska et al., 2016). The DOC was also investigated after its deposition on glaciers and ice sheets from the atmosphere for its concentration (Antony et al., 2011; Hood et al., 2015; Singer et al., 2012), composition and ages (Spencer et al., 2014; Stubbins et al., 2012), bioavailability (Singer et al., 2012; Spencer et al., 2014) and its release through glacier runoff during glacier melting period (Hood et al., 2015; Yan et al., 2016). The process from DOC deposition to release interacts with the atmosphere and surrounding terrestrial ecosystem and poses feedbacks to the related environmental systems.

1.3 Light absorption of organic carbon in the atmosphere and precipitation

In addition to the role that precipitation OC plays in the carbon cycle, it is also an important component in the atmospheric radiative forcing studies due to the light scattering or absorption characteristics. The OC accounts for a large fraction of carbonaceous matter in the atmosphere, some of which efficiently scatters visible radiation. However, a variable fraction of OC absorbs radiation at the infrared and ultraviolet wavelengths (UV) and is relatively transparent at the visible (Vis) wavelength (Laskin et al., 2015; Yan et al., 2018). The certain OC absorbs strong UV radiation was defined as brown carbon (BrC), featured by a wavelength-dependent absorption spectrum decreasing sharply from the UV to Vis wavelength (Andreae and Gelencsér, 2006; Feng et al., 2013; Kirchstetter et al., 2004; Ramanathan et al., 2007). Currently, the well-known light-absorbing component of carbonaceous matter is BC, which is mainly produced in the combustion of fossil fuel and/or biomass (Bond et al., 2013) and absorbs solar radiation at a wide spectral wavelength range from the UV all the way to infrared. Despite the inherently complex of BC, its chemical structure and light absorption properties are well-investigated (Bond and Bergstrom, 2006; Bond et al., 2013; Ramanathan and Carmichael, 2008). However, compared to BC, BrC as a

compound is difficult to characterize its molecule compositions and to determine which molecule or molecular aggregate acts as the chromophore (Laskin et al., 2015). Therefore, the knowledge of molecule composition of BrC is poorly documented and the BrC light absorption was generally investigated by regarding OC as one substance with chromophores.

It is critical to quantify the light absorbing of BrC in accurately interpreting the radiative forcing caused by carbonaceous matter in the atmosphere. Recently, increasing attention has been focusing on BrC in both models and in-situ observation studies (Andreae and Gelencsér, 2006; Feng et al., 2013; Kirillova et al., 2016; Saleh et al., 2013). For example, it is suggested that the warming effect caused by BrC accounted for approximately 24% of that caused by combined BC and BrC (Zhang et al., 2017b). The light absorption of water-insoluble BrC has been confirmed larger than that of water-soluble BrC, and it is usually evaluated by treating the samples with organic solvents and methanol is recommended to be the one with the highest extractable OC fraction (Chen and Bond, 2010). The methanol extractable OC which includes WSOC is defined as methanol-soluble OC (MeS-OC) by assuming OC soluble in purewater can also be extracted by methanol.

Currently, the method to investigate the light absorption properties of WSOC has been well established for aerosols, and the calculation of the mass absorption cross-section (MAC) for WSOC has little uncertainty because WSOC can be accurately and easily measured by a TOC analyzer. Therefore, the light absorption properties of WSOC in aerosols have been investigated widely. For instance, studies found that the light absorption ability of WSOC of biomass combustion sourced aerosols was higher than that derived from fossil fuel combustion sourced aerosols (Cheng et al., 2011; Hu et al., 2017). The radiative forcing caused by WSOC in ambient aerosols accounted for approximately 2-10% and 3-11% of that caused by BC in heavily polluted sites of East Asia (Kirillova et al., 2014a) and urban regions of South Asia (Kirillova et al., 2014b), respectively. In addition, the corresponding radiative forcing ratio of WSOC to BC was as low as 1% in ambient aerosol of a remote Indian Ocean island due to the photobleaching of WSOC during the long distance transport (Bosch et al., 2014). Besides the studies on light characteristics of WSOC in aerosols, the related study in precipitation is also important, because the OC fraction dissolved in precipitation (i.e., DOC) represents the chemical characteristics of dissolved carbonaceous matter of the entire atmosphere column from the near surface to the cloud height, and is thus more representative for the atmospheric aerosols than those near-surface aerosols reported in the previous studies. However, the light absorption of DOC in precipitation is poorly constrained except several studies on snow and ice DOC in the glacier regions (Niu et al., 2018; Yan et al., 2016; Zhang et

al., 2019). Thus, it is necessary to investigate the light absorption of precipitation DOC to obtain information in the atmospheric process of DOC scavenging.

Contrast to the easy and accurate measurement of WSOC, the measurement of MeS-OC is complicated, because the methanol extract of OC (i.e., MeS-OC) cannot be measured in the same way with water extract (i.e., WSOC) due to the interference of organic solvent. Therefore, the indirect method to calculate MeS-OC has to be adopted (Chen and Bond, 2010; Cheng et al., 2017; Huang et al., 2018). Moreover, the method to extract MeS-OC is controversial and no consensus has been reached. Currently, there are three primary methods to extract OC with methanol to obtain the mass of MeS-OC and MAC values. Chen and Bond (2010) recommended extracting the MeS-OC by sonicating the filter sample in methanol for 1 h, keeping the extract for 20 h to reach equilibrium and sonicating the extract for another 1 h before measurement. Cheng et al., (2017) extracted the MeS-OC by only immersing aerosols in methanol for 1 h without shaking or sonication. Huang et al., (2018) extracted the MeS-OC by sonicating for 1 h in methanol. All these methods have shortcomings. For instance, the first two methods ignored the particulate carbon detached from the filter samples in calculating of MeS-OC mass, while the third method regarded the original OC of filter sample as MeS-OC by assuming that methanol completely extracted OC in original samples. Both assumptions overestimated the extractable MeS-OC and thus underestimated the MAC value of MeS-OC ($MAC_{MeS\text{-}OC}$). However, the comparison of these methods is absent. Generally, the sonication treatment increases the OC in aerosols extracted by both purewater and methanol compared to those without sonication treatment (Polidori et al., 2008). Thus the $MAC_{MeS\text{-}OC}$ should be higher for those aerosols with sonication.

Studies based on these previous methods suggested that MeS-OC represents the majority of the total OC mass in aerosol. For example, more than 92% OC of wood combustion sourced aerosols and approximately 89% OC of ambient aerosols in urban city were extracted by methanol (Chen and Bond, 2010; Cheng et al., 2017). Moreover, the light absorption ability of MeS-OC is higher than that of WSOC and the large fraction of the light absorption is produced by OC which is only extractable by methanol (i.e., WIOC) (Kirillova et al., 2016; Zhang et al., 2013). For example, the wood combustion sourced WIOC accounted for 18% of the original OC of filter samples, whereas this part of WIOC contributed 35% to 45% of the total absorbance depending on the wavelength range (Chen and Bond, 2010). The MAC value at 365 nm (MAC_{365}) of WIOC was approximately 2 times of that for WSOC in urban city of China (Cheng et al., 2017). In addition, the light absorbance of MeS-OC fraction of aerosols in the Los Angeles basin was approximately 4.2 times higher than that of WSOC (Zhang et al., 2013). This phenomenon also existed in the aerosols of the

background Himalayan regions, where the solar radiation absorption of MeS-OC relative to BC was 2.3 times higher than that for WSOC (Kirillova et al., 2016). All these results confirmed that OC plays an important role in the light absorption of aerosols. Therefore, a reliable method to measure MeS-OC and $MAC_{MeS\text{-}OC}$ was urgently required to reduce the current uncertainties and to validate further modeling studies since MAC value is the basic input data of radiative forcing model of carbonaceous particles.

1.4 Carbonaceous matter in the Himalayas and Tibetan Plateau

The HTP is known as the 'Third Pole' and 'world roof' (Qiu, 2008) with an area of 2.5×10^6 km^2 (Figure 1.2). The HTP has an average elevation about 4000 m above sea level making it the highest plateau on earth, and all the mountain peaks over 7000 m around the world are on the HTP (Yao et al., 2012b). Correspondingly, the pivotal role of this plateau is almost attributed to its high elevation, which makes it particularly cold at its altitude (Qiu, 2008). The HTP contains the largest amount of glaciers in the mid-altitude outside the Arctic and Antarctic ice sheets, vast area of alpine permafrost, and large extent of snow cover and lake ice (Yao et al., 2012a; Yao et al., 2012b). Moreover, the HTP regions are the headwaters of many Asian major rivers, such as Yangtze River, Yellow River and Lantsang River, which provides water to 1.4 billion people living downstream. Thus it is also known as the "Water Tower of Asia" (Immerzeel et al., 2010).

The environment and climate of the HTP are influenced by both Asian monsoon and westerlies (Figure 1.2), and the HTP in return exerts thermal and dynamical impact on the large scale or even global atmospheric circulation, thus affecting climate (Yanai and Wu, 2006; Zhou et al., 2009). The HTP has been experiencing significant climate change and warming since the mid-1950s (Kang et al., 2010; You et al., 2016). The temperature of the HTP has a rise of 0.3 ℃ per decade which has been going on for five decades, and this increase rate is approximately three times of global warming rate (Qiu, 2008). Moreover, approximately 82% glaciers of the HTP have retreated during past half-century, 10% permafrost has degraded in the past decade (Qiu, 2008) and 5.7% of the snow cover has decreased in last two decades (Shen et al., 2015). Therefore, the cryospheric interactions of the HTP are more sensitive to the global change than other ecosystems (Yao et al., 2012b). If the warming trend continues or even accelerates in the HTP, the problems such as natural hazards, hydrological process and atmospheric environment will emerge, which affects the sustainable development of human and ecosystems in the HTP and its downstream (Qin et al., 2017; Qiu, 2008).

The HTP has long been considered remote and pristine reflecting the global background environmental conditions from a global perspective (Cong et al., 2009; Wang et al., 2011b). However, the atmospheric information recovered from the ice cores and lake sediment cores in the HTP indicated that the atmosphere in Asia experienced a noticeable influence from the anthropogenic emissions since the 1950s (Cong et al., 2013; Kang et al., 2016; Wang et al., 2008). Surrounded by the two large regions with the intensive anthropogenic emissions, South Asia and East Asia, the HTP has been proved to be influenced by the atmospheric pollution from south Asia which transports to the HTP crossing the southern slope of the Himalayas via Indian monsoon (Lüthi et al., 2014; Ramanathan et al., 2005; Xia et al., 2011). The atmosphere of the HTP has also been influencing by the local residential combustion activities and the local emissions from vehicles (Li et al., 2018b). Additionally, the dust events from the surrounding deserts of the HTP (e.g., Taklimakan Desert and Gobi Desert) and dust emission from the arid deserts in the HTP are influencing the HTP frequently (Chen et al., 2013; Kang et al., 2019). All these local and external sourced pollutants in the HTP are influencing the environment and climate of this high-altitude plateau, especially in the glacier regions after their deposition (Xu et al., 2009).

Currently, the study on the carbonaceous matter in the HTP is a hot topic due to its important effects in the climate system and influence on the albedo of snow and ice in glacier regions after its deposition (He et al., 2015; Kaspari et al., 2011; Qian et al., 2014; Zhang et al., 2015b). To date, the studies concerning the carbonaceous matter have been conducted in this high plateau with the focus on the concentration variations and sources (Cao et al., 2011; Chen et al., 2018; Li et al., 2017; Ming et al., 2013; Xu et al., 2018; Zhang et al., 2017a), carbon isotopic compositions (Huang et al., 2010; Li et al., 2016a; Li et al., 2018a), optical properties (Chen et al., 2019; Hu et al., 2017; Li et al., 2016b; Yan et al., 2016; Zhang et al., 2019) and historical profile (Kaspari et al., 2011; Wang et al., 2008). The related results confirmed that the environment in the HTP has been influenced by the carbonaceous matter from both long-range transport and local emissions, and that the light absorbing components have important implications for the climate warming and the glacier retreat after the deposition in the HTP.

Despite a series of studies on carbonaceous matter in the HTP aforementioned, the direct measurements of its wet and dry deposition in this remote and sensitive HTP are scanty. For example, there are only two studies directly measured the concentrations and deposition rates of DOC in precipitation (Li et al., 2016e; Niu et al., 2019), and one study focused on the total DOC deposition in glacier regions (Li et al., 2016e). The primary results of these studies indicated that the concentrations and deposition rates of DOC in urban cities of the HTP were lower than those of polluted urban cities outside

the HTP (Li et al., 2016e), but higher than those in glacier regions (Li et al., 2016c). Additionally, two studies evaluated the BC deposition rate using the chemical transport models in the HTP (Bauer et al., 2013; Zhang et al., 2015b) and another two studies recovered the atmospheric BC deposition rate using the lake sediment cores in the Nam Co and Qinghai Lakes (Cong et al., 2013; Han et al., 2015) (Figure 1.2). However, the BC deposition rate from lake sediment core was approximately 30 times higher than that from modeling in the central HTP, which suggested the large uncertainties in different methods used to estimate the BC deposition rate in previous studies. The uncertainties also existed in the concentration measurements of WIOC and BC in precipitation, including those from the different measurement protocols (Chow et al., 2001), different particles size of collected samples (Zhang et al., 2015a) and the influence of carbonate carbon (inorganic carbon (IC)) (Cao et al., 2005). For example, the carbonate carbon (e.g., carbonate) in mineral dust (MD) is an important influencing factor in the measurements of WIOC and BC by the currently wide used thermal-optical analyzer, because IC can also be converted to CO_2 during this temperature increasing protocols causing overestimation of both WIOC and BC. Moreover, deserts and sand dunes were widely distributed across the HTP (Liu et al., 2005), and dust storms occur in spring and winter frequently in the HTP (Wang et al., 2005). Thus, the influence of IC on WIOC and BC measurements cannot be ignored in the HTP contrasted to that suggested in previous study (Chow and Watson, 2002). Although at present several studies on carbonaceous matter in the HTP have identified MD component, the discussion about the uncertainties caused on the measurements of WIOC and BC is missing (Cong et al., 2015; Zhao et al., 2013).

Therefore, in this work, firstly, the uncertainties in previous studies on concentration and deposition rate of carbonaceous matter are discussed, and then the BC concentration and deposition rate in the HTP are adjusted after considering the potential uncertainties (Paper I). Secondly, the in-situ WIOC, BC and DOC concentrations of precipitation are measured to estimate the more accurate deposition rates at three remote stations and an urban city in the HTP (Figure 2.1) (Paper II-IV). Lastly, the light absorption characteristics of precipitation DOC are measured at three remote stations (II), and a new method is developed to obtain reliable data of the light absorption of BrC in aerosols (V). The related content and interactions between different ecosystems and components are presented in Figure 1.1.

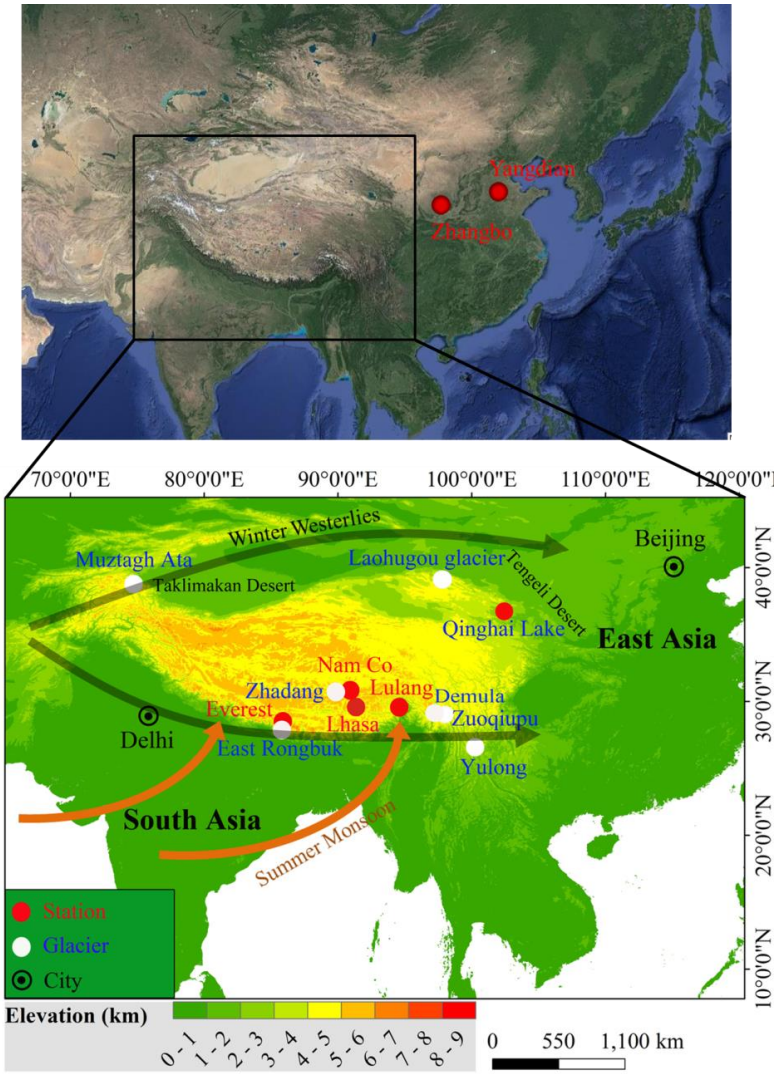

Figure 1.2: Location map of study sites including HTP stations, lakes, glaciers and two rural sites in China, and the surroundings of the HTP. Note: the maps in up and down panels are from Omap and ArcGIS 10.2, respectively.

2 Methodology

2.1 Sampling sites

2.1.1 Nam Co, Lulang and Everest stations

The Nam Co Monitoring and Research Station for Multisphere Interactions (Nam Co Station) is a typical pastoral area located on the shore of Nam Co Lake in the south-central HTP. The Nam Co basin is a transition zone of the alpine sub-humid atmosphere in the southeastern HTP and the alpine semi-arid atmosphere in the northwestern HTP. Lakes, glaciers, rivers, wetlands and mountains were widely distributed in the Nam Co basin. With the second largest Nam Co Lake (lake area of 1980 km^2) in this basin, the atmosphere at Nam Co Station is especially different from the surrounding terrestrial ecosystems. The Nam Co Station is usually considered as the representative and background site of the HTP (Cong et al., 2009). This station is influenced by the warm and humid Indian monsoon in summer, and cold and dry westerlies in other seasons, leading to the limited precipitation (You et al., 2007) (Table 2.1). The environment there is also influenced by the local pasturing and anthropogenic activities, and the tourism activities to Nam Co Lake during the warm summer season.

South-East Tibetan Plateau Station for Integrated Observation and Research of Alpine Environments (Lulang Station) is located in the sub-valley of Yarlung Tsangpo Grand Canyon in the southeastern HTP, a corridor with heavy precipitation, where the warm-humid Indian monsoon penetrates into the inner part of the HTP (Cao et al., 2011). Thus, the annual precipitation amount of this station is more than 800 mm and the vegetation coverage in this region is high (Figure 2.1). To the south of the station is located the Himalayas, which could obstruct some of the pollutants from the outside HTP, such as south Asia. There are two small villages 30-50 km away in the downwind regions of the station with some small influence on the local atmosphere (Cao et al., 2011). There is also a busy highroad in front of the station, and emissions from the passing by vehicles have important influence on the surrounding environment.

The Qomolangma Station for Atmospheric and Environmental Observation and Research (Everest Station) is located in an s-shape valley that leads directly to the northern slope of Everest in the middle Himalayas. The crests of the valley have a height of 600-800 m above ground level and are partially covered by snow and ice. The land surface of this station has sparse vegetable coverage but is covered with

sandy soil and small rocks (Figure 2.1). The Himalayan region is a representative of uplift and mountainous plateau. The high altitude makes Himalayas an ideal area for the mass and energy exchange between the free and ground atmosphere (Ma et al., 2011). The complex terrain, strong solar radiation, special atmospheric circulation and climate make the Himalayan region an ideal laboratory to study mountain atmospheric and environmental sciences in the HTP. This station is also influenced by the warm Indian monsoon in summer and cold and dry westerlies in other seasons with limited precipitation due to the rain shadow of Himalayas (Ma et al., 2011) (Table 2.1 and Figure 1.2). There is a small village approximately 3 km away from the station and a highroad only 30 m away from the station leading to Everest foothill, which indicates that local emissions including MD and anthropogenic activities influence the atmosphere of this station.

2.2.2 Lhasa city and two rural sites in China

Lhasa is located in a narrow west-east valley in the south central HTP, characterized with a wet monsoon and dry non-monsoon seasons. It is the capital and the largest city of the Tibet Autonomous Region of China with a population of 0.9 million. It is also the center of the economics and religion. During the last decades, Lhasa has experienced a profound urbanization with the economy development of China. The thriving religious activities also made contribution to the atmospheric pollution. Therefore, the atmosphere in Lhasa has been influencing by the human activities. However, compared with other seriously polluted urban cities in China, Lhasa is relatively clean except for some intensive pollution events during religious celebration (Cui et al., 2018) and static winter (Li et al., 2019). The sampling site in Lhasa is located in the Institute of Tibetan Plateau Research, China Academy of Sciences situated to the East of Lhasa city.

Zhangbo and Yangdian are two classic rural areas in Guanzhong and Huabei Plain, respectively, with serious air pollution in East China (Figure 1.2). These two regions were chosen to compare the light absorption properties of BrC with those in the remote HTP.

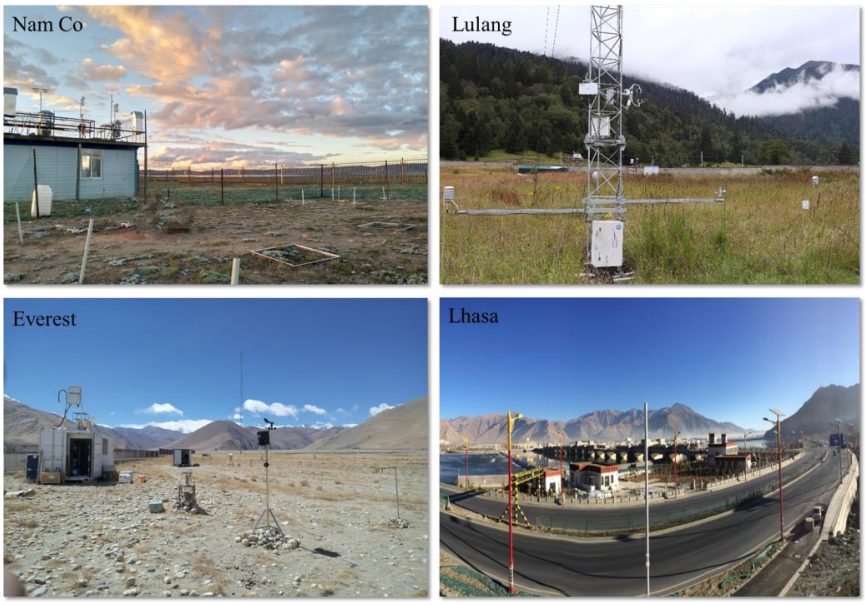

Figure 2.1: In-situ precipitation sampling sites in the HTP and their topography and geomorphology.

2.2 Sample collection and analysis

2.2.1 Aerosol

2.2.1.1 TSP

Sample collection

The total suspended particles (TSP) were collected at Nam Co and Everest stations using pre-combusted (550 ℃, 6h) quartz fiber filters (90 mm, Whatman Corp) with a vacuum pump. Four blank samples were collected at each station by exposing the blank filters in each sampler without pumping. These samples were collected to examine the influence of IC in MD on BC and total carbon (TC) concentrations, to calculate BC deposition rates based on the atmospheric BC concentrations to compare with previously reported result recovered from Nam Co Lake core, and finally to estimate the BC deposition rates in the HTP after considering the influencing factors.

To compare with the previous results, surface soil and suspended particle samples from four rivers in the Nam Co basin were collected to measure BC concentration, and

surface soil samples were collected around Everest Station for pH measurement (more details refer to paper I).

Analysis and calculation

The collected TSP samples were acidified with 37% hydrochloric acid (HCl) via a fumigation process to remove IC by exposing the subsamples to HCl for 24 h. The acidified subsamples were then dried at 60 ℃ for 2 h to vaporize any remaining acid on the filter (Bosch et al., 2014; Li et al., 2016a; Pio et al., 2007). The OC and BC concentrations of the original TSP samples and the acidified subsamples were measured by a Desert Research Institute (DRI) model 2001 thermal-optical carbon analyzer following the IMPPROVE protocol (Chow and Watson, 2002).

The BC deposition rates of Nam Co Station and Qinghai Lake basin were calculated based on the atmospheric BC concentrations and average precipitation using the following equations described in previous studies to compare with the results recovered from the lake cores (Fang et al., 2015; Jurado et al., 2008):

$$F_{BC} = F_{DD} + F_{WD} \quad (2.1)$$

$$F_{DD} = 7.78 \times 10^4 \times V_D \times C_{BC} \quad (2.2)$$

$$F_{WD} = 10^{-3} \times P_O \times W_P \times C_{BC} \quad (2.3)$$

where F_{WD} and F_{DD} are the seasonal wet and dry deposition rates (μg m^{-2}), respectively; V_D is the dry deposition velocity of aerosol (0.15 cm s^{-1}), P_0 is the precipitation amount (mm) in a given season, and W_p is the particle washout ratio (2.0×10^5) (Fang et al., 2015). C_{BC} is the BC concentrations of TSP (μg m^{-3}).

2.2.1.2 $PM_{2.5}$

Sample collection

$PM_{2.5}$ (particles with an aerodynamic diameter of 2.5 μm or less) were collected at Nam Co, Lhasa, Zhangbo and Yangdian in 2018 (Table 2.1) using pre-combusted quartz fiber filters to study the light absorption property of BrC. The $PM_{2.5}$ samples derived directly from the yak dung combustion at Nam Co Station (Chen et al., 2015), where local residents burn yak dung for cooking and heating, represented the biomass aerosols. The $PM_{2.5}$ samples collected in the ambient atmosphere of other three sites were identified as ambient aerosols. These samples were collected to develop a new method to obtain accurate light absorption of OC extracted by methanol.

Newly developed MeS-OC extraction assembly

The $PM_{2.5}$ filter samples from the urban and rural sites were acidified by fumigation with HCl (37%) to remove any IC before analysis, similar with that of TSP samples. The analytical procedure is presented in Figure 2.2. First, a subsample (punch #1) of the original filter was cut out for the initial carbon mass measurement. Second, a 3.8 cm^2 subsample (punch #2) was cut out and treated with 30 g methanol using a sandwich filter assembly we developed in Figure 2.3 to obtain the relatively reliable MAC of MeS-OC ($MAC_{MeS\text{-}OC}$) by overcoming the detachment problem of particles on filters in previous methods. In brief, the subsamples were punched and placed in a pre-combusted quartz filter (pore size: 0.45 μm, Pall TissuquartzTM) with an opening of the same area. The reassembled samples were then placed between two pre-combusted blank quartz filters with the bottom of the subsample upward. The subsequently formed three-filter sandwich was placed on the glass sand core funnel of a vacuum filtration assembly as shown in Figure 2.3. After blocking the funnel, 30 g methanol was added to the filter sandwich in three times to keep a long residence time (approximately 1 h) to ensure a high OC fraction extracted by methanol. The remaining methanol was then pumped through the filter sandwich. Thereafter, the filters were dried at 60 ℃ for two hours in glass petri dishes. Punches of 0.526 cm^2 were obtained from the center of the original filter samples, the methanol-treated subsamples and the bottom filters of the sandwich filtration assembly. OC and BC of the punched samples were measured using a thermal-optical transmittance (TOT) carbon analyzer (Sunset Laboratory, Tigard, OR, USA) following the IMPROVE protocol. The sum of the OC masses of the two punches from the sandwich filtration assembly was regarded as the methanol-insoluble OC fraction. The difference between the OC mass of the original sample and the methanol-insoluble OC is the mass of the OC dissolved in methanol, which was used in the calculation of $MAC_{MeS\text{-}OC}$. Third, a subsample (punch #3) was sonicated in purewater to obtain the $MAC_{WS\text{-}BrC}$ value (Li et al., 2016d). Lastly, another subsample (punch #4) was extracted with methanol by three previous methods and the new method in Figure 2.3 to make a comparison of four different methods (details refer to the supporting information of paper V).

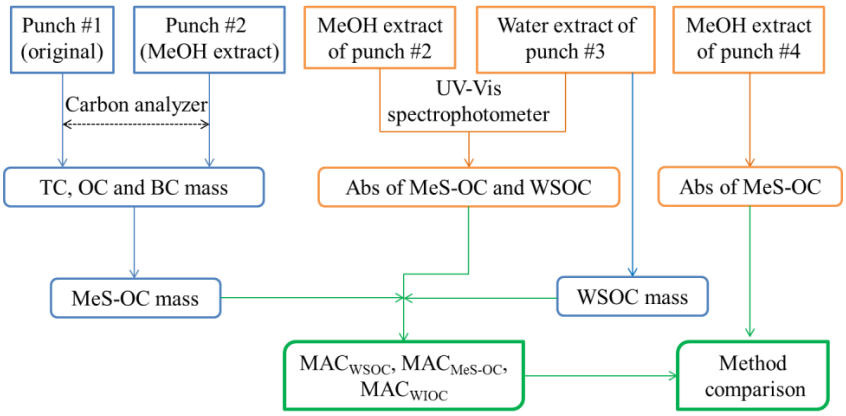

Figure 2.2: Flowchart of the measurement of light absorption of the carbonaceous aerosols.

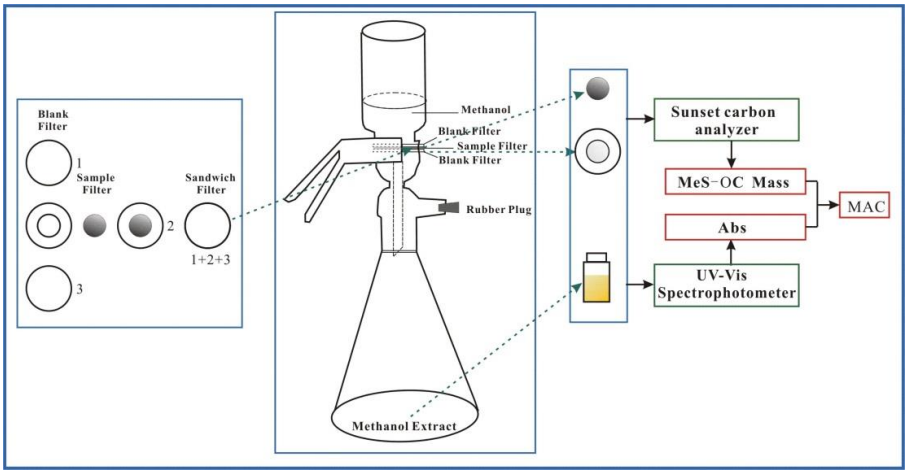

Figure 2.3: Filtration unit developed in this study to extract MeS-OC.

Analysis and calculation

The light absorption spectra of WSOC and MeS-OC were analyzed using an ultraviolet-visible (UV-Vis) absorption spectrophotometer (SpectraMax M5, USA), by scanning every 5 nm from 200-700 nm. The MAC values were calculated by the Beer-Lambert law as below (Bosch et al., 2014; Kirillova et al., 2014a):

$$\mathrm{MAC} = \frac{\mathrm{Abs}}{\mathrm{C.L}} \times \ln(10) \qquad (2.4)$$

where Abs represents the light absorbance directly from the spectrophotometer, C is

the concentration of OC dissolved in ultrapure water (WSOC) or methanol (MeS-OC), and L stands for the absorbing path length (1 cm).

The WSOC mass was measured by the TOC analyzer directly, while the MeS-OC mass was obtained through indirect calculation owing to the interference of methanol as follow:

$$\begin{aligned} \mathrm{MeS-OC} &= TC_{original} - TC_{extracted} \\ &= TC_{original} - TC_{2,sandwich} - TC_{3,sandwich} \end{aligned} \quad (2.5)$$

where $TC_{original}$ and $TC_{extracted}$ are the TC mass in original and methanol extracted filters, respectively; $TC_{2,sandwich}$ and $TC_{3,sanwich}$ are the TC mass of the middle and bottom filters extracted by methanol in the sandwich filtration assembly present in Figure 2.3.

MAC of the WIOC (MAC_{WIOC}) was calculated as the following ratio under the assumption that the OC soluble in purewater could also be extracted by methanol:

$$\mathrm{MAC_{WIOC}} = \frac{[\mathrm{Abs_{365,methanol} - Abs_{365,water}}]}{([\mathrm{MeS-OC}]-[\mathrm{WSOC}])\times \mathrm{L}} \times \ln 10 \quad (2.6)$$

where $Abs_{365,\ methanol}$ and $Abs_{365,\ water}$ are the light absorbance values measured for the methanol and water extracts at 365 nm. [MeS-OC] and [WSOC] are the concentrations of MeS-OC and WSOC.

Table 2.1: Information of the study sampling sites

	Sampling Site	Sampling Period	Latitude (N)	Longitude (E)	Elevation (m a.s.l)	Annual Precipitation (mm)
Precipitation	Nam Co	2014–2017	30°46′27″	90°57′53″	4730	313.2
	Lulang	2014–2016	29°45′59″	94°44′21″	3330	1009.5
	Everest	2014–2017	28°21′43″	86°56′59″	4276	189.8
	Lhasa	2017-2018	29°38′32″	91 °02′14″	3650	540.6
Aerosol	Nam Co	2014-2016	30°46′28″	90 °59′18″	4730	
	Nam Co yak dung	2018	30°46′28″	90 °59′18″	4730	
	Everest	2014-2016	28 °21′49″	86 °58′21″	4276	
	Lhasa	2018	29°38′32″	91 °02′14″	3650	
	Zhangbo	2018	34°26′44″	109°10′04″	359	
	Yangdian	2018	35°53′32″	116°35′40″	47	

2.2.2 Precipitation and dry deposition sample collection and analysis

2.2.2.1 Precipitation

Sampling collection

The precipitation samples were collected at three remote stations, Nam Co, Lulang and Everest, and an urban city, Lhasa (Table 2.1 and Figure 1.2 and 2.1) using a pre-washed and pre-combusted aluminum basin (550 ℃, 6h) placed on the 1.5 m high shelf. The precipitation samples for ions measurements were collected with HDPE plastic bags. The collected precipitation samples were transferred to pre-cleaned polycarbonate bottles and kept frozen until analysis. The sampling details were presented in papers II-IV. The annual precipitation amounts were 313, 1010, 190 and 541 mm at Nam Co, Lulang, Everest stations and Lhasa city, respectively, with the distinct dry and wet seasons. The precipitation amounts of the study samples at Nam Co, Lulang, Everest stations and Lhasa city accounted for 52%, 47%, 29% and 50% of the total precipitation amounts (Figure 2.4). The collected precipitation samples were used to investigate the wet deposition of WIOC, BC and DOC.

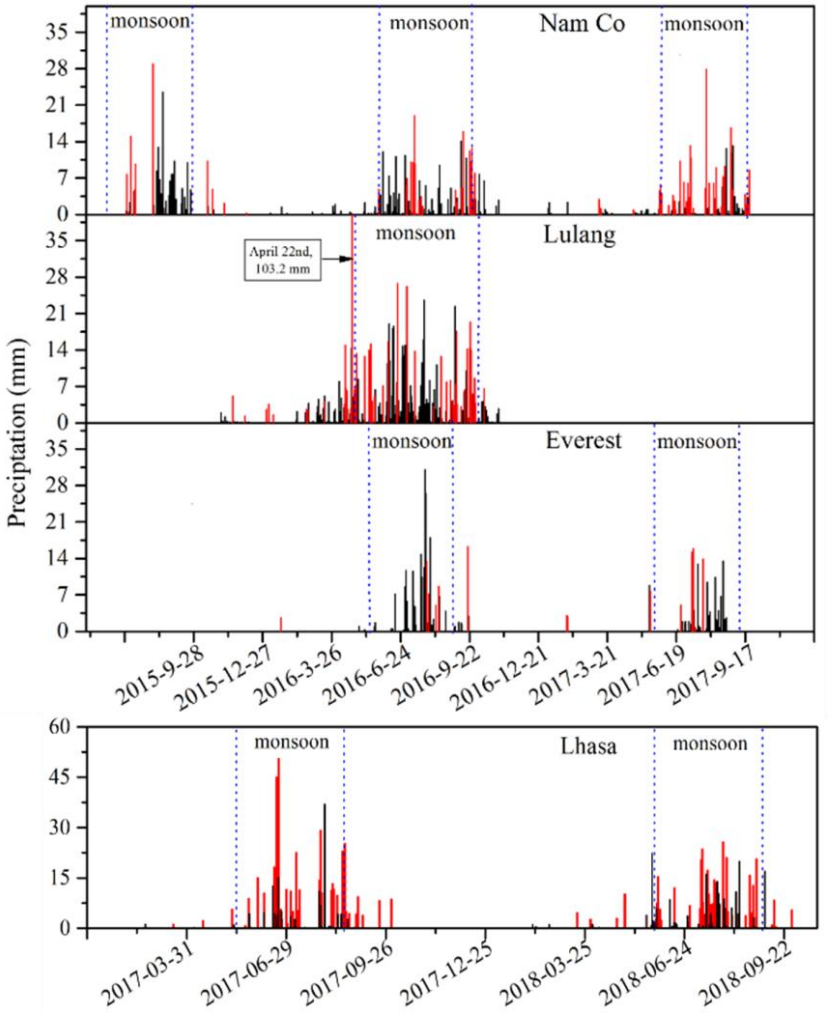

Figure 2.4: Precipitation amounts in three remote stations and Lhasa city. Note: the red columns present the collected precipitation events.

DOC and major ions analysis

The precipitation samples for DOC and major ions were filtered using PTFE membrane syringe filter with 0.45 μm pore size (Macherey-Nagle, Molecular Devices, USA). The DOC concentrations of the filtrate were measured by Shimadzu TOC-5000 total organic carbon analyzer (Shimadzu Corp, Kyoto, Japan) (Li et al., 2016e). The major anions and cations in precipitation were measured by Ion Chromatograph (Dionex-3000) and Ion Chromatograph (Dionex-6000) (Dionex, USA), respectively (Li et al., 2016e).

WIOC and BC analysis

The precipitation samples for WIOC and BC were filtered by pre-combusted quartz filters (pore size: 0.45 μm, Pall TissuquartzTM, 2500QAT-UP, USA). In order to improve the collection efficiency of carbon particle, a coagulant, $NH_4H_2PO_4$, was added to precipitation samples (1.5 g per 100 mL of samples) (Li et al., 2016a; Torres et al., 2013). The mixture was then magnetically stirred for 10 min and filtered three times through pre-combusted and equilibrated quartz filters. The IC in precipitation was acidified by adding 2 M HCl during filtration and the filter samples were washed to neutrality using purewater (Ming et al., 2008). After drying (60 ℃, 2 h) and equilibrium, the filter samples were measured by the DRI model 2001 using the same method with the collected TSP samples (Chow and Watson, 2002).

Calculation of wet deposition of WIOC, BC and DOC

The annual wet deposition rates of the WIOC, BC and DOC in precipitation were calculated using the average annual precipitation amount and the volume-weighted mean concentrations of WIOC, BC and DOC at each station as the following equations:

$$F_c = C_i \times P_i \tag{2.7}$$

$$C_i = \frac{\sum_{j=1}^{j=n} C_j \times P_j}{\sum_{j=1}^{j=n} P_j} \tag{2.8}$$

where F_c (g m^{-2} yr^{-1}) is the WIOC, BC and DOC wet deposition rate, C_i (mg L^{-1}) stands for the volume-weighted mean concentrations of WIOC, BC and DOC in precipitation at the station i, C_j (mg L^{-1}) expresses the concentration of WIOC, BC and DOC in individual precipitation sample j, P_i (mm yr^{-1}) is the average annual precipitation at station i, and P_j (mm) is the precipitation amount corresponding to the precipitation sample j.

Calculation of light absorption of precipitation DOC

The light absorption spectrum of precipitation DOC was measured by the same method as $PM_{2.5}$ samples after filtered by syringe filters and the MAC values were calculated based on the equation (2.4).

2.2.2.2 Dry deposition

Sample collection

Dry deposition samples were collected with a stainless steel bucket placed on a

shelf of 3 m in height at Nam Co Station and Lhasa city. The dry deposition bucket is similar with the barrel on the automated precipitation collector for the dry deposition but not automated (Zhang et al., 2012). The detailed sampling information refers to paper II and IV.

Dry deposition sample analysis and calculation

Each collected sample was dissolved into deionized water, transferred into polycarbonate bottles and divided into two equal parts. One part was filtered by the same process used for the precipitation samples and treated by acid following the method for sediments before BC measurement (Han et al., 2007). The detailed method information can be found in the supporting information of paper II. The other part was filtered and fumigated by 37% HCl to remove IC as TSP samples before WIOC measurement (Li et al., 2016a; Chow et al., 1993). The measurement was similar with those of precipitation filter samples.

The dry deposition rates at Nam Co Station and Lhasa city were calculated based on the monthly averaged concentrations of WIOC and BC in collected dry deposition samples. The WIOC and BC dry deposition rates at Lulang and Everest stations were estimated using equation (2.2). The total deposition rate of the study stations was calculated by summing up the dry and wet deposition rates throughout the year.

2.3 Quality control

2.3.1. Blank test

Four blank samples of precipitation samples for each station were prepared by adding 200 mL purewater to the aluminum basin. These aluminum basins were placed outside close to the precipitation sampling site for 2 h without the influence of precipitation. The blank samples were then subjected to the same treatment and analysis with those of precipitation samples. The average concentrations of WIOC, BC and DOC of these blank samples were 0.054 ± 0.002, 0.0 μg mL^{-1} and 0.05 ± 0.02, respectively. The average ion concentrations of the blanks were low (SO_4^{2-} =1.61 ng g^{-1}, Na^+= 1.77 ng g^{-1}, NH_4^+ =2.45 ng g^{-1}, Ca^{2+}, Mg^{2+}, K^+, Cl^- and NO_3^-<ng g^{-1}). Three blank samples for dry deposition sampling at each station were prepared by adding 200 mL purewater in pre-cleaned stainless steel bucket and treated using the same process with dry deposition samples. The average concentrations of WIOC and BC of these blanks were 0.036 ± 0.019 and 0 μg mL^{-1}, respectively. These low blank concentrations suggested that the sampling and analysis processes are relatively clean. All the reported results in this work were corrected by the blank values. New aluminum basins and

buckets were used in every sampling event to avoid any cross contamination.

2.3.2. Collection efficiency of precipitation particles

There are several factors influencing the collection efficiency of particulate carbon, such as the adhesion and settling of particulate carbon to the collector, evaporation of samples and the filtering efficiency. To avoid these influences and to meet the analysis volume requirement, precipitation samples were primarily collected for heavy precipitation events. In addition, the basin for precipitation collection was washed using the supernatant of each sample to reduce the particle loss. A coagulant, $NH_4H_2PO_4$, was added to precipitation samples, which could increase the filtering efficiency to approximately 95% (Torres et al., 2013).

2.3.3. BC recovery of dry deposition particles

The dry deposition particles were pretreated and analyzed following a previously published method for lake sediment samples (Han et al., 2007a). A national standard (*n*-hexane soot) was subjected to the same process with the samples, and its recoveries were estimated to be 92-105%, thus the protocols used in this work were reliable to separate BC in deposited samples (Han et al., 2007b). Additionally, a sucrose solution was analyzed by dropping on a filter paper along with the filter samples to ensure the stability of the instrument and the adopted protocols. The deviation in OC concentrations of sucrose solution was within 5%, indicating the reliable analytical process.

3 Result and discussion

3.1 Re-evaluating of BC concentration and deposition rate in the HTP

Although many studies have been conducted on the carbonaceous matter in the HTP, few of them considered the uncertainties in its concentration measurement and deposition rate estimation. Here, some influencing factors are discussed to correct the previously reported atmospheric concentration and deposition rate of BC in the HTP.

3.1.1 Influence of IC on concentrations of BC and TC

As mentioned in the introduction, there are many deserts and sand dunes across the HTP, and dust storms occur in spring and winter frequently. Thus, it is necessary to investigate the influence of IC in MD on BC and TC measurements in the HTP. The TSP samples from Nam Co and Everest stations were acid-fumigated, and then the original and acid-treated samples were measured for BC, OC and TC concentrations. The concentration ratios between BC, OC and TC of TSP samples treated with acid (BC_A, OC_A and TC_A) and the original ones (BC_O, OC_O and TC_O) were 0.48±0.35, 0.78±0.10 and 0.81±0.13, respectively, at Nam Co Station, and 0.61±0.24, 0.78±0.12 and 0.76±0.12, respectively, at Everest Station. These ratios indicated that IC has significant contribution to concentrations of BC, OC and TC in TSP samples and that the influence of IC on BC was the largest probably because the IC was more inclined to decompose under high temperature along with BC in analysis (Chow and Watson, 2002), although it can also decompose under relatively low temperature influencing the concentration of OC (Karanasiou et al., 2011). The influences of IC on BC and TC concentrations were larger in non-monsoon period than those in monsoon period at both Nam Co and Everest stations due to the heavy precipitation in monsoon period (Figure 3.1). Meanwhile, there was a clear seasonal variation of TC_A/TC_O, i.e., low TC_A/TC_O and high TC_A/TC_O in the non-monsoon period and monsoon periods, respectively, at Nam Co Station, which was consistent with the intensive occurrence of dust storms in non-monsoon period. However, no clear seasonal variation of TC_A/TC_O were observed at Everest Station, which was explained by the relatively stable seasonal variation of Ca^{2+} in TSP samples at this station (Cong et al., 2015). The different seasonal variations of TC_A/TC_O at two stations were also explained by the relative concentration ratios of MD and carbonaceous matter (CM) (Figure 3.1).

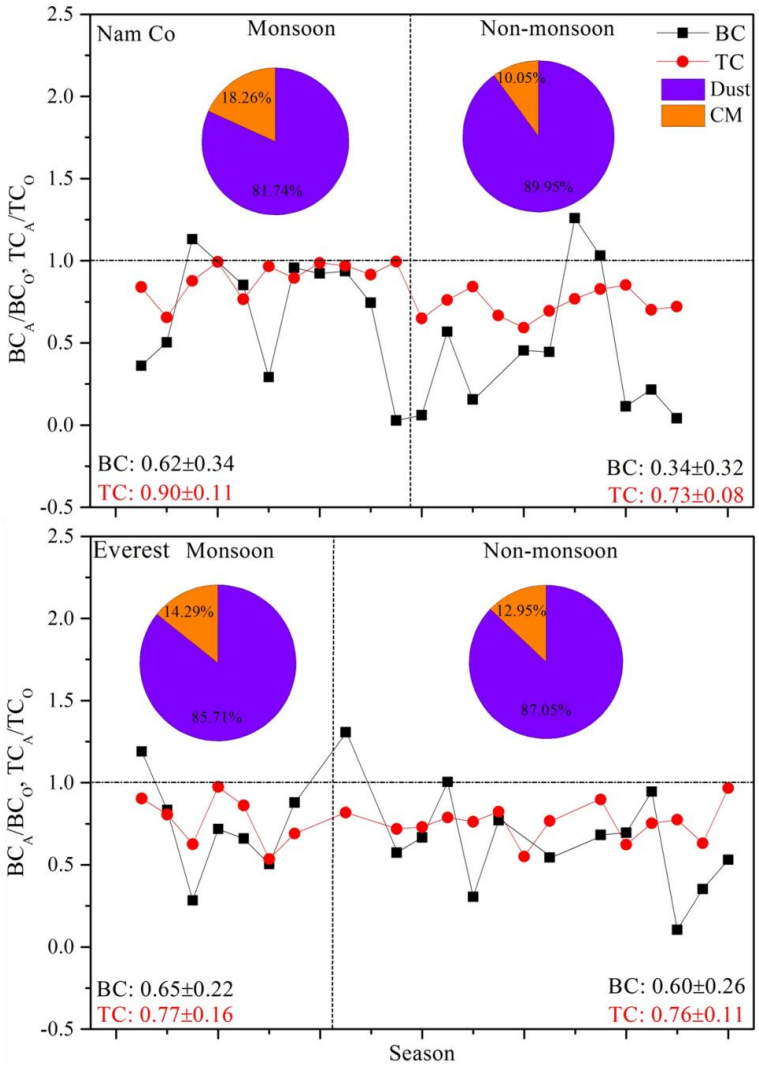

Figure 3.1: Seasonal variations of BC and TC concentrations in the acid-treated and original aerosol samples, and the relative percentages of mineral dust (Dust) and carbonaceous matter (CM) during monsoon and non-monsoon periods at Nam Co and Everest stations.

Moreover, the location of the two stations is especially important in explaining the different influences of MD. The Nam Co Station is located at a grassland region with limited locally sourced MD in monsoon period; whereas the Everest station is located in a barren site with sparse vegetation cover, thus the local derived MD from surface soil influence the aerosols considerably in monsoon period (Liu et al., 2017). Meanwhile, the precipitation amount at Nam Co Station was larger than that at Everest

Station during monsoon period because Everest Station is in the rain shadow of the Himalayas. In addition, the pH of surface soil samples collected around Nam Co and Everest stations was 8 (Li et al., 2008) and 8.2, respectively, which indicated the potentially considerable influence of IC, because it has been reported that the carbonates derived from alkaline soil in arid area cause bias in aerosol measurements (Chow and Watson, 2002). Moreover, the HTP was influenced mainly by the westerlies in non-monsoon period, which brought the MD from the arid western HTP, where distributed large deserts. In addition, the IC influence was also confirmed by a significant relationship (p<0.01) between the concentration of Ca (elements information in paper I) and IC (i.e., TC_O-TC_A) of the TSP samples at two stations (Figure 3.2). Therefore, the aerosol samples in the HTP were more influenced by the MD during non-monsoon period.

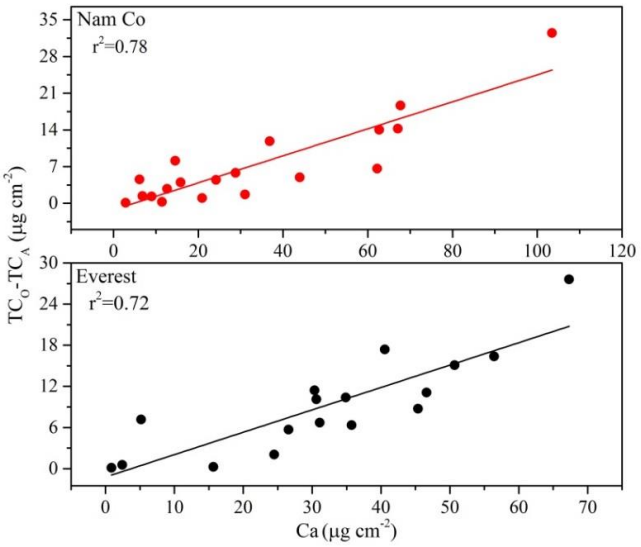

Figure 3.2: Significant correlation between IC and Ca in aerosols of Nam Co and Everest stations.

3.1.2 Adjusted BC concentrations at Nam Co and Everest stations and implications

Based on the results above, the presence of IC led to approximately 52±35% and 39±24% overestimation of BC concentrations at Nam Co and Everest stations, respectively. Therefore, the previously reported concentrations values at the two stations were higher than the actual values (Cong et al., 2015; Zhao et al., 2013). Combined with the overestimation ratios and the previously reported BC

concentrations from the same method, the adjusted BC concentrations at Nam Co and Everest stations were 61 and 154 ng m^{-3}, respectively. However, there were still some uncertainties in this correction. For example, the fumigation treatment with HCl may lead to the loss of volatile organic acid, although the influence is minor as indicated by the significant relationship between IC and Ca (Figure 3.2). This treatment may also cause the high BC concentration due to the conversion of OC to BC, which was not common at two stations since the BC_A/BC_O values were generally lower than 1 with several exceptions (Figure 3.1). Theoretically, the ratio of BC_A/BC_O should be lower than 1, thus the ratios larger than 1 were not included in the above BC concentration correction. Nevertheless, the BC_A/BC_O ratios were considered slightly overestimated due to the reason aforementioned (Jankowski et al., 2008). Moreover, the seasonal variation of BC concentration and BC_A/BC_O were not considered in this correction.

Since dust storms are more frequent in western and northern regions of the HTP, the influence of IC on BC and OC concentrations there should be more significant than that at Nam Co region and should be considered seriously. Moreover, IC in MD of the glacier regions should also have considerable influence on BC and OC concentrations, because several studies have presented that MD concentrations were much higher than that of BC in ice and snow samples of the HTP (Li et al., 2017; Qu et al., 2014; Zhang et al., 2017c); however, this influence was not considered in these studies. Therefore, the concentrations of the BC, its deposition and the corresponding radiative forcing should be corrected in further study.

3.1.3 Overestimated atmospheric BC deposition rates by lake cores in the HTP

Generally, the BC deposition rates estimated by different methods are considered consistent for a given site. For example, the BC deposition rate recovered using a lake sediment core of Chaohu in the heavily polluted eastern China (1160 mg m^{-2} a^{-1}) (Han et al., 2016) was comparable to that calculated using the atmospheric BC concentrations in northern China (1660 mg m^{-2} a^{-1}) (Fang et al., 2015) and that estimated from the in-situ observation in northern China Plain (1504-1659 mg m^{-2} a^{-1}) (Yang et al., 2014) (Table 3.1). However, this is not the case in the HTP and large discrepancies exist among the reported BC deposition rates there. For example, the BC deposition rates reconstructed by the lake core of Nam Co Lake (NMC09) in the central HTP and lake core of Qinghai Lake in the northwestern HTP were 260 and 270-290 mg m^{-2} yr^{-1}, respectively, which were much higher than those estimated by glacier ice core and snow samples of the HTP (Table 3.1). This phenomenon was probably because the lake core sediment represents not only direct atmospheric deposition but also the catchment inputs (Yang, 2015).

To investigate the contribution of the catchment inputs, BC deposition rates at Nam Co and Qinghai Lake basins were calculated based on the atmospheric BC concentrations at two regions (Cong et al., 2015; Zhao et al., 2015). As presented in Table 3.1, the BC deposition rate in Qinghai Lake constructed by the lake core was 3-4 times higher than that calculated by BC concentrations of $PM_{2.5}$ (Zhao et al., 2015). The actual discrepancy between these two estimations should be smaller than this one because atmospheric BC concentrations are higher than those in $PM_{2.5}$ samples (Li et al., 2016b). Additionally, because Qinghai Lake is located at a midpoint of an Asian "airborne dust corridor", the atmospheric dust deposition contributed approximately 56.6% of surface sediment of Qinghai Lake and the corresponding contribution of catchment input was 24.9% (Wan et al., 2012). Therefore, if the BC deposition rates from the two methods were the same, the rate from lake core was overestimated by at least 39%.

Different from Qinghai Lake, the BC deposition rate at Nam Co Lake based on the atmospheric BC was much lower than that from lake core (Table 3.1), suggesting that the catchment input was the main contributor to BC deposition in this lake sediment. Nam Co basin is covered by a large glacier area (141.88 km^2) (Figure 3.3) and large amount of glacier meltwater flows in Nam Co Lake annually (Wu et al., 2007). Those glacier runoff originated from the high-altitude glacier terminal has a steep slope facilitating the transport of allochthonous sediment to Nam Co Lake (Dobersch ütz et al., 2014). Attributed to the increasing temperature and precipitation in Nam Co region, the lake water volume of Nam Co Lake augmented with a mean annual increasing rate of 2.37×10^8 m^3 and the increased glacier meltwater accounted for approximately 50.6% of the lake water volume augment (Zhu et al., 2010). The large contribution of precipitation (63%) to water volume of Nam Co Lake also promote the transport of particles to the lake which was proved by the significant relationships between precipitation amounts and mass accumulation rates of another Nam Co lake core (NMC08-1) during the past 60 years and the significant correlation between precipitation and the grain size of lake core sediment (Figure 3.3) (Li et al., 2014; Wang et al., 2011a). Despite the different locations of the two Nam Co lake cores (Figure 3.3), the similar sediment characteristics reflected that the catchment input is common for Nam Co Lake sediment. In addition, the BC concentration of surface soil with the grain size smaller than 20 μm was 0.78 ± 0.48 mg g^{-1}, which was comparable with the BC concentration of Nam Co Lake core sediment (0.74 mg g^{-1}) (Cong et al., 2013). Therefore, the atmospheric BC deposition is minor in Nam Co Lake compared to the contribution of catchment input.

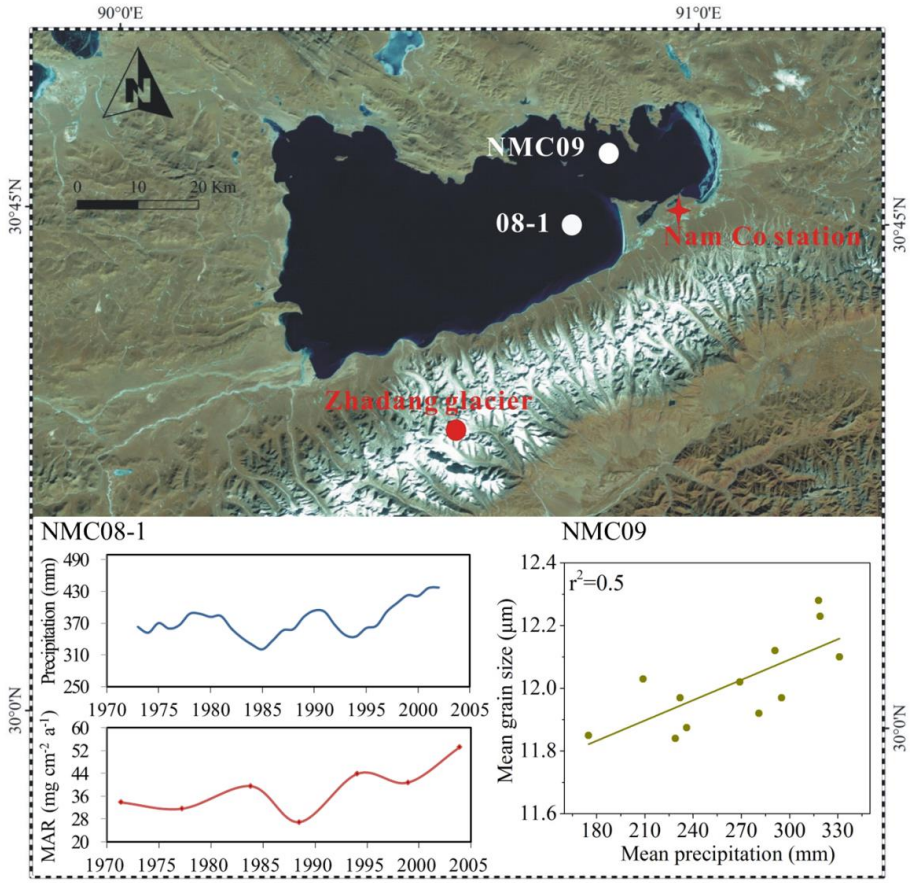

Figure 3.3: Significant relationship between mean precipitation and mean grain size (Li et al., 2014), and similar variations of precipitation and mass accumulation rate (MAR) of Nam Co lake cores (Wang et al., 2011a).

Table 3.1: BC deposition rates (mg m^{-2} yr^{-1}) monitored or recovered in the HTP and other regions of the world.

Region	Sites	Deposition rate	Period	References
HTP	Zuoqiupu glacier	12	1970-2005	1
	Muztagh Ata	18	1970-2005	1
	East Rongbuk ice core	10.2	1995-2002	2
	Laohugou glacier	25	2013-2014	3,4
	Tanggula glacier	21.2	2013-2014	3,4
	Zhadang glacier	22.8	2013-2014	3,4
	Demula glacier	14.4	2013-2014	3,4
	Yulong glacier	20.3	2013-2014	3,4
	Model results of central TP	9	2013-2014	5
	Aerosol of Nam Co station	10.5	2005-2007	This study
	Aerosol of Qinghai Lake	92.7	2011-2012	This study
	Nam Co Lake core	260	1960-2009	6
	Qinghai Lake core	270-390	1770s-2011	7
East China	Chaohu lake core, East China	1160	1980-2012	8
	Northern China	1660	Around 2010	9
	Northern China Plain	1500	2008-2009	10

Note: 1: (Bauer et al., 2013); 2: BC concentration and snow accumulation were derived from (Ming et al., 2008) and (Li et al., 2016c), respectively. 3: (Li et al., 2016c); 4: (Li et al., 2016a); 5: (Zhang et al., 2015b); 6: (Cong et al., 2013); 7: (Han et al., 2015); 8: (Han et al., 2016); 9: (Fang et al., 2015); 10: (Yang et al., 2014).

3.1.4 Atmospheric BC deposition in glacier regions of the HTP

It is suggested that BC deposition rates derived from ice cores and snow pits are more representative than those from lake cores. The ice core and snow pit are generally obtained in the accumulation zone of a glacier recording the relatively actual atmospheric information. The BC deposition rates estimated by snow pit samples at Yulong, Demula, Zhadang, Tanggula and Laohugou glaciers were 20.3, 14.4, 22.8, 21.2 and 25 mg m^{-2} yr^{-1}, respectively (Table 3.1), which was in the same order of magnitude, reflecting a relatively homogeneous distribution of BC deposition in the HTP. Meanwhile, the BC deposition rates from the ice cores of Zuoqiupu glacier in the southeastern HTP, Muztagh Ata in the western HTP (Bauer et al., 2013) and East Rongbuk glacier in the southern HTP (Li et al., 2016c; Ming et al., 2008) were 12, 18 and 10.2 mg m^{-2} yr^{-1}, respectively (Table 3.1). The BC deposition rate of the central HTP from an atmosphere model was also similar to the aforementioned deposition

rates (Zhang et al., 2015b). Therefore, we proposed that the BC atmospheric deposition rate in the glacier regions of the HTP was 17.9±5.3 mg m^{-2} yr^{-1}, despite the uncertainties existed in the previously reported data.

3.2 In-situ investigation of wet and dry deposition of carbonaceous matter

Although some of the potential influencing factors in evaluating the concentration and deposition of carbonaceous matter have been discussed in section 3.1, the corrected results based on the previous studies still have uncertainties. Therefore, in-situ investigations are necessary to obtain the reliable concentration and deposition rate and to provide basic dataset to further related studies. In this section the in-situ concentrations of carbonaceous matter (WIOC, BC and DOC) in precipitation of three remote stations and urban Lhasa city of the HTP were measured and the corresponding wet and dry deposition rates were evaluated.

3.2.1 WIOC, BC and DOC concentrations in precipitation

The volume-weighted mean (VWM) concentrations of WIOC and BC after the precipitation filter samples being acidified were 192±258.6 and 18.5±33.7, 327±258 and 34.3±35.3, 248±210 and 13.5±14.5, and 314±382 and 35.8±34.2 μg L^{-1} at three remote Nam Co, Lulang and Everest stations and an urban Lhasa city, respectively (Table 3.2). Generally, the WIOC and BC concentrations at the study stations of the HTP were expected to be lower than those in megacities, such as Paris (851 and 333 μg L^{-1} for WIOC and BC) (Ducret and Cachier, 1992) and Tokyo (657 and 78.9 μg L^{-1}) (Huo et al., 2016), but comparable to those at mountain (145 and 5.2 μg L^{-1}) and remote (274 and 26 μg L^{-1}) sites in other regions (Table 3.2) because of the relatively clean atmosphere at the study stations. Although the sampling site of Lhasa is located in the urban city, the concentration of WIOC and BC were still comparable to those of Lulang Station, which suggested that on the one hand the atmosphere in Lhasa is relatively clean despite of some pollution in static winter and religious activities (Cui et al., 2018; Li et al., 2019), on the other hand Lulang Station was also influenced by some pollution as the average OC concentration in the atmosphere of Lulang (4280 μg m^{-3}) (Zhao et al., 2013) was as high as that of Lhasa city (4740 μg m^{-3}) (Li et al., 2016b). The VWM concentrations of WIOC and BC at Lulang and Everest stations were higher than the values of the adjacent Demula and East Rongbuk glaciers, respectively. Whereas, the corresponding values at Nam Co Station were lower than those of the adjacent Zhadang glacier, this was probably because Zhadang glacier is a

small valley glacier which is easily influenced by the surrounding environment and experiencing a strong melting during the ablation season, leading to the enrichment of WIOC and BC, and thus the high concentration values (Li et al., 2018c; Ming et al., 2013). The BC concentration in this study was 2.3 times higher than that reported in previous study at Nam Co Station (Ming et al., 2010), which was probably attributed to the shorter sampling period in monsoon season during which the atmospheric concentration was low and the relatively lower particle collection efficiency in previous study compared to those in this study.

The VWM concentrations of DOC were 1.05±1.01, 0.83±0.85, 0.86±0.91 and 1.17±1.02 mg L^{-1} at Nam Co, Lulang and Everest stations and Lhasa city, respectively. These values in the HTP were lower than those in urban cities, such as Beijing and Tokyo in Asia and Araraquara in Brazil (Coelho et al., 2008; Huo et al., 2016; Pan et al., 2010), but comparable to those of remote sites such as New Zealand (Kieber et al., 2002) and Sado in Japan (Huo et al., 2016). Meanwhile, the DOC concentrations at Nam Co, Lulang and Everest stations were higher than those of adjacent Zhadang glacier (0.19 mg L^{-1}), Demula glacier (0.17 mg L^{-1}) and East Rongbuk glacier (0.09 mg L^{-1}) (Table 3.2). Seasonally, the concentrations of WIOC, BC and DOC were higher in non-monsoon period than those in monsoon period at four study stations.

Table 3.2: WIOC, BC and DOC concentrations (μg L^{-1}) in precipitation at study sites in the HTP and other study regions in the world.

Sampling Site	Site Type	WIOC	BC	DOC	Reference
Nam Co	HTP	192±258.6	18.5±33.7	1169±1020	This study
Lulang	HTP	327±258	34.3±35.3	830±850	This study
Everest	HTP	248±210	13.5±14.5	860±910	This study
Lhasa	HTP	314±382	35.8±34.2	1169±1021	This study
Nam Co	HTP	476±565	8±7		1
Zhadang glacier	HTP	290	37.9	190	2,3
Demula glacier	HTP	198.5	17.2	170	2,3
East Rongbuk	HTP	82.9	10.4	90	2,3
Tokyo, Japan	Urban	657	78.9	1425	4
Paris, France	Urban	851	333		5
Sado, Japan	Remote	274	26	1125	4
Schauinsland, Germany	Mountain	205±266	28±38	1492	6
Sonnbick, Austria	Mountain	145	5.2		6
Aveiro, Portugal	Rural	98±56	14±13	442	6
K-Puszta, Hungary	Rural	358	24	1352	6
Beijing, China	urban			3900±800	7
New Zealand	Remote			700	8

Note. 1: (Ming et al., 2010); 2: (Li et al., 2016a); 3: (Li et al., 2016c); 4: (Huo et al., 2016); 5: (Ducret and Cachier, 1992); 6:(Cerqueira et al., 2010); 7: (Pan et al., 2010) 8: (Kieber et al., 2002).

3.2.2 Relative ratios of WIOC, BC and DOC in precipitation

The relative ratios of WIOC, BC and DOC in precipitation can provide insights in the sources and removal of carbonaceous matter in the atmosphere (Custodio et al., 2014). Therefore, the relative contribution of WIOC, BC and DOC in the atmosphere (before removal) and precipitation (wet removal) of three remote stations and an urban city, and the adjacent snow pits of glaciers (after dry and wet removal) were presented in Figure 3.4 and the removal processes were in Figure 1.1, which indicated that BC is the smallest fraction of carbonaceous matter at all study sites. The ratios of WIOC and BC were higher in snow pit than those in precipitation, which indicated that the wet deposition was not the only way to remove the atmospheric particles, dry deposition also made important contribution to the carbonaceous matter of snow pits. The removal of DOC by precipitation was much more efficient than WIOC and BC resulting in the highest DOC ratios in precipitation. Meanwhile, the WIOC/BC ratios in precipitation

samples were higher than those in aerosol samples at four study stations, suggesting that WIOC was more liable to be removed by precipitation compared to BC due to its relatively hydrophilic characteristics. Moreover, the average WIOC/DOC ratio of precipitation of the HTP was 0.28, which was comparable to those of rural sites in Europe, such as K-Puszta in Hungary (0.27) and Aveiro in Portugal (0.22) (Cerqueira et al., 2010), and the remote site in Japan (0.24) (Huo et al., 2016). However, this ratio was lower than that in urban cities, such as Tokyo in Japan (0.46) (Huo et al., 2016), which was probably because the atmospheric carbonaceous matter in the HTP was originated from both the long-range transported pollutions in the heavily polluted South Asia (Lüthi et al., 2014; Li et al., 2016a) and the local emissions of HTP itself (Li et al., 2018b); while the carbonaceous matter in urban cities were mainly contributed by local emissions. The carbonaceous matter becomes aged and more hydrophilic with the conversion of WIOC to DOC during the long-range transport, and thus, leading to a relatively low ratio of WIOC/DOC at study stations of the HTP.

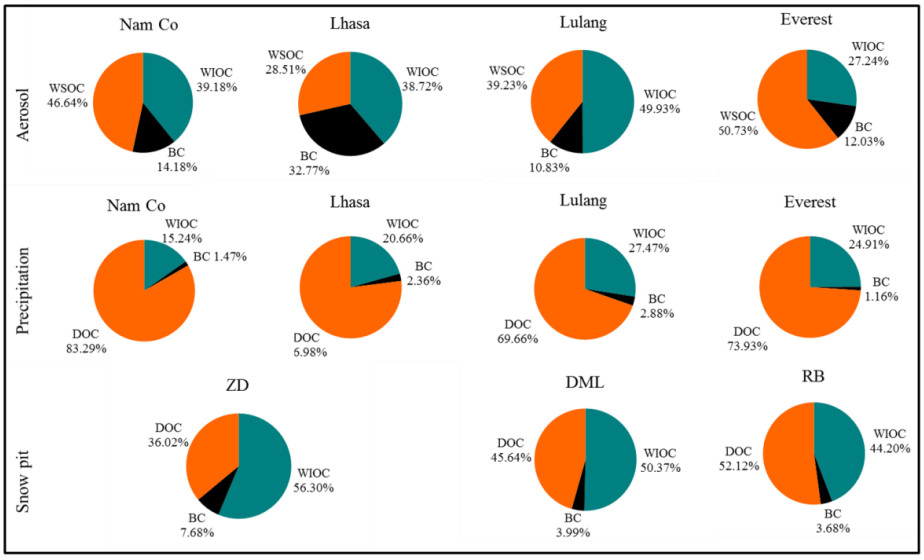

Figure 3.4: Percentages of WIOC, BC and DOC in precipitation and aerosols of three remote stations and an urban city, and the nearby snow pits in the study glacier regions of the HTP. Note: the concentrations of WIOC, BC and DOC in the three snow pits were from Li et al., (2016b). The concentrations of WIOC, BC (after considering the influence of IC) and DOC in the Everest aerosols were from Cong et al., (2015); the WIOC and BC concentrations in Lulang aerosols were from Zhao et al., (2013); the DOC concentration in the Lulang aerosols was calculated from Zhao et al., (2013) and Li et al., (2016c).

3.2.3 Deposition mechanisms and rates of carbonaceous matter

3.2.3.1 Deposition mechanisms

The carbonaceous particles could be removed from the atmosphere by both wet and dry deposition. The wet deposition rates are relatively easy to estimate and could be obtained from the measurements of the particles in precipitation samples. The dry deposition rate is more complicated and could be achieved by exposing a clean sampler to the atmosphere without the influence of precipitation (Ogren, 1982). The mechanisms of the wet and dry deposition are intricate due to the various influencing factors. Generally, dry deposition is primarily controlled by the metrological factors (wind speed and temperature lapse rate) and the vertical distribution of the carbonaceous particles. The particle transfer through the layers in the high level of the atmosphere might be the limiting step of the dry deposition rate, which is usually

influenced by the dynamical process in the atmosphere. However, the major influence of the dry deposition is within the near surface layer, including the gravitational settling, Brownian diffusion and the nature of the surface to which the particles deposited (Ogren et al., 1983).

There are two scavenging processes in wet deposition of carbonaceous particles: the washout process in which the particles collide with the existing crystal or droplets, and the rainout process in which the particles act as the nucleating agents in the formation of ice crystals or cloud droplets. The collision of carbonaceous particles with existing cloud and precipitation droplets is affected by some of the similar factors that control the dry deposition process; whereas, the formation of nucleating agents strongly depends on the chemical and physical characteristics of the particles. Additionally, the ability of carbonaceous particles acting as the CCN primarily depends on the chemical nature of the particle surface and their sizes. The freshly emitted particles with the hydrophobic nature and small particle size are not likely to act as CCN. However, after coagulating with the other particles, such as the sulfuric acid and ammonium sulfate in adequate time, the properties of particles are controlled by the coated mixture, which may be facilitating the formation of CCN. Generally, the washout and rainout processes co-exist in a precipitation event, and the washout process plays an important role in the beginning of the event, while rainout process is predominant from the middle to the end of the event (Ishikawa et al., 1995). A reverse correlation generally existed between the precipitation amounts and the concentrations of the carbonaceous particles in previous studies, which was partly explained by the influence of the washout process (Prado-Fiedler, 1990). This correlation was not presented at three remote stations but existed at urban Lhasa city in the HTP (Figure 3.5), which was consistent with the studies conducted in other urban and remote sites (Ducret and Cachier, 1992; Huo et al., 2016). Thus, it is generally considered that washout process plays a dominant role in particle removal at urban sites where the atmospheric loading of particles is high, whereas rainout process is important at remote sites where the atmosphere is relatively clean.

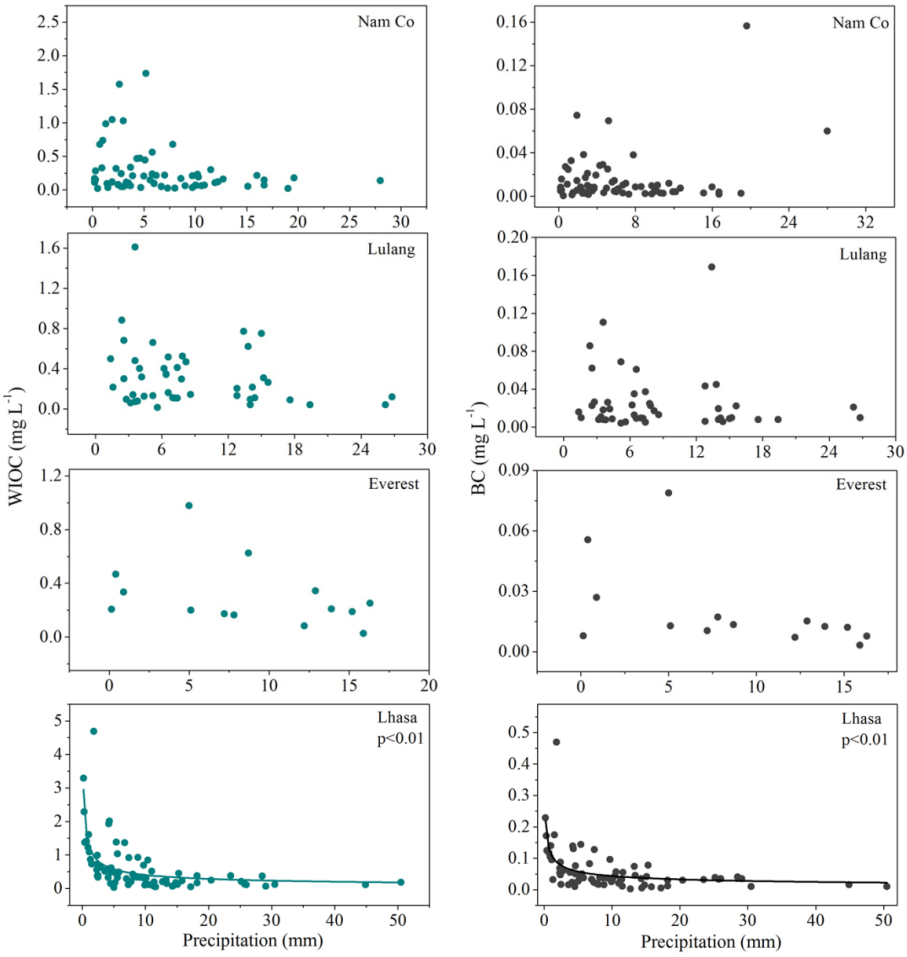

Figure 3.5: The relationships between WIOC and BC concentrations in precipitation and precipitation amounts at four study stations.

3.2.3.2 Scavenging ratios of WIOC and BC

The frequently used parameter for calculating and modeling the wet deposition rate of carbonaceous particles is the scavenging ratio (Fang et al., 2015; Sandnes, 1993), which is defined as the ratio of mass concentration of a particle in precipitation and its average mass concentration in the atmosphere. This scavenging ratio is a simplification of the complexities of the involved mechanisms and processes in wet deposition. Although this ratio cannot explicitly explain the aforementioned properties incorporated in wet deposition (Harrison and Allen, 1991), it does provide a way to estimate the wet deposition rates.

The scavenging ratios of WIOC and BC at three remote stations of the HTP were estimated and the results indicated that the scavenging ratios of WIOC (0.91×10^6, 0.14×10^6 and 0.72×10^6 at Nam Co, Lulang and Everest respectively) were higher than those of BC (0.24×10^6, 0.07×10^6 and 0.09×10^6, respectively). Thus, it is clear that WIOC is more hydrophilic and preferentially removed by precipitation than BC. This result has also been reported by many other studies. For instance, the scavenging ratios of WIOC and BC at a remote site in Japan were 1.24×10^6 and 0.08×10^6, respectively (Huo et al., 2016); the scavenging ratios of WIOC and BC at European background sites were 0.06×10^6–0.63×10^6 and 0.02×10^6–0.18×10^6, respectively (Cerqueira et al., 2010). On this basis, the scavenging ratios of WIOC and BC have large spatial variations, which have significant implications in the observation and modeling studies of the atmospheric carbonaceous particles. For instance, a 3.5 times increase in BC wet deposition scavenging ratio could cause a 30-40% decrease in the modeled BC concentration at the remote areas of Scandinavia (Tsyro et al., 2007).

Because of the assumption of the uniform distribution of atmospheric particles, the scavenging ratios of WIOC and BC are expected large in high mountains (Cerqueira et al., 2010). The large scavenging ratios at Nam Co Station were in accordance with this expectation, which also could be attributed to the aged aerosols from South Asia by long-range transport (Lüthi et al., 2014; Li et al., 2016a). However, the scavenging ratios of WIOC and BC were relatively lower at Lulang and Everest stations compared to those at Nam Co Station probably because the atmospheric concentrations of WIOC and BC were much higher at the two former stations attributed to the large local emissions (Chen et al., 2018; Li et al., 2018b; Wang et al., 2018); whereas the WIOC and BC concentrations in precipitation of the two stations were comparable or slightly higher than those at Nam Co Station (Table 3.2). It should be acknowledged that there are some uncertainties and limitations in this approach. For example, the reported scavenging ratios were estimated based on the concentrations of the near-surface atmosphere, which differed from those at the cloud formation altitude. Additionally, the sampling date and time of the atmospheric and precipitation WIOC and BC are usually difficult to keep exactly consistent and the average concentrations were adopted in the calculation.

3.2.3.3 Deposition rates of WIOC, BC and DOC

Among four study stations, the largest wet deposition rates were observed at Lulang Station because the annual precipitation amount at this station is the largest and the pollutants from the severely polluted south Asia could be transported via the Yarlung Zangbo Grand Canyon to this station (Zhao et al., 2013). The similar phenomenon was reported in the study concerning wet deposition of major ions at this

station (Liu et al., 2013). Additionally, a recent research about the sources of atmospheric BC has found that emissions from the local vehicles and anthropogenic activities is contributing to BC at Lulang Station (Wang et al., 2018). Thus, the local emissions may account for some part of the wet deposition of WIOC, BC and DOC at this station. These additional local emissions are probably the reason that the concentrations of atmospheric OC and BC were the highest among three remote stations despite its largest precipitation amount (supporting information of paper II,). Consequently, the total BC deposition rate (58.9 mg m^{-2} yr^{-1}) at Lulang Station was around four times higher than that at Nam Co Station. Although Everest Station is also experiencing the influence of the local emissions (Chen et al., 2018; Li et al., 2018b), the wet deposition rates of WIOC, BC and DOC were the lowest among four study stations because of the limited precipitation amount. Moreover, the wet deposition rates of WIOC, BC and DOC at Lhasa city were also lower than those at Lulang Station because the concentrations of three components at the two sites were comparable, whereas the precipitation at Lulang Station was approximately two times higher than that at Lhasa city, implying that precipitation amount was the dominant factor in wet deposition of carbonaceous matter in the HTP.

Seasonally, the deposition rates of WIOC, BC and DOC during monsoon period were higher than those during non-monsoon period at both three remote stations and an urban city, which was similar with the precipitation seasonal variation (Figure 3.6). The variations in both deposition rates and precipitation could also imply the potential sources of these carbonaceous components. For example, the wet deposition rates of WIOC and BC in August were lower than those in July and September despite of the largest precipitation amount in August at Nam Co Station (Figure 3.6), implying the dilution and washout effects of pollutants from the long-range transport before reaching this remote station. The largest wet deposition rates of WIOC, BC and DOC at Lulang Station appeared in April, which was also a severely polluted period in South Asia (Bonasoni et al., 2010). Correspondingly, the higher deposition rates of WIOC and BC in August than those in July at Lhasa city indicated the influence of local emissions because the precipitation amounts were almost similar in the two months (Figure 3.6), but the local emissions in August were enhanced due to one of the traditional Tibetan festival and the rapidly increased tourists.

The wet deposition rates of WIOC and BC at study stations of the HTP were overall lower than those at urban sites but comparable to those at rural (Cerqueira et al., 2010), remote (Huo et al., 2016) and mountain (Cerqueira et al., 2010) sites around the world (Table 3.3). It is noticeable that dry deposition of carbonaceous particles contributes significantly to the total deposition in the HTP, especially during non-monsoon period when the precipitation is limited, because of the unique location

and atmospheric circulation system. For instance, the annual dry deposition rate of BC at Lhasa city was approximately 8.5 times higher than the corresponding wet deposition rate due to the locally emitted fresh particles, local mineral dust from dust storm and other construction activities. The dry deposition rates of BC at Nam Co and Everest stations were around two times higher than their wet deposition rates (Table 3.3). Regarding the adjacent glaciers of these study stations, the BC total deposition rates at Nam Co Station (15.3 mg m^{-2} yr^{-1}) and Zhadang glacier (20 mg m^{-2} yr^{-1}) were comparable, which were also consistent with those obtained in Svalbard, an Arctic site (6-26 mg m^{-2} yr^{-1}) (Ruppel et al., 2014), but much lower than that reconstructed by the lake sediment core from the nearby Nam Co Lake due to the reasons discussed in section 3.1. Because of the heavy precipitation at Lulang Station (1010 mm), the dry deposition rates of WIOC and BC were comparable with the corresponding wet deposition rates. Meanwhile, with the limited precipitation and the contribution of the local emissions, the total BC deposition rate at Everest Station was also higher than that in snow pit of East Rongbuk Glacier although the calculated dry deposition rates based on the atmospheric concentrations could cause underestimation.

Table 3.3: Annual deposition rates (mg m^{-2} yr^{-1}) of WIOC, BC and DOC at four study stations in the HTP and other sites.

Sampling Site	Sampling Period	Wet DOC	Wet (Total) WIOC	Wet (Total) BC	Reference
Nam Co, HTP	2015–2017	340	60.2 (329.2)	5.8 (15.3)	This study
Lulang, HTP	2015–2016	840	330 (530)	34.6 (58.9)	This study
Everest, HTP	2015–2017	160	47.0 (99.1)	2.6 (9.7)	This study
Lhasa, HTP	2017-2018	632	169.6	19.4 (185.1)	This study
Zhadang glacier HTP	2013–2014	100	(153.0)	(20.0)	1,2
Demula glacier, HTP	2013–2014	150	(167.1)	(14.5)	1,2
East Rongbuk, HTP	2013–2014	50	(41.5)	(5.2)	1,2
Nam Co Lake core, HTP	1857–2009			(260)	3
Qinghai Lake core, HTP	1770–2011			(270–390)	4
WDC06A ice core, Antarctic	1850–2000			$((16 \pm 2.7)*10^{-3})$	5
DSSW19K ice core, Antarctic	1850–2000			$((13.5 \pm 2.7)*10^{-3})$	5
Holtedahlfonna ice core, Arctic	1700–2004			(6–26)	6
Tokyo, Japan, Urban	2011–2012	1444	676	59.8	7
Sado, Japan, Remote	2011–2012	1029	314	26.3	7
Aveiro, Portugal, Rural	2003–2004	442	61	7.5	8
Schauinsland, Germany, Mountain	2003–2004	1492	378	38	8

1. (Li et al., 2016a); 2. (Li et al., 2016b); 3. (Cong et al., 2013); 4. (Han et al., 2015); 5. (Bisiaux et al., 2012); 6. (Ruppel et al., 2014); 7. (Huo et al., 2016); 8. (Cerqueira et al., 2010).

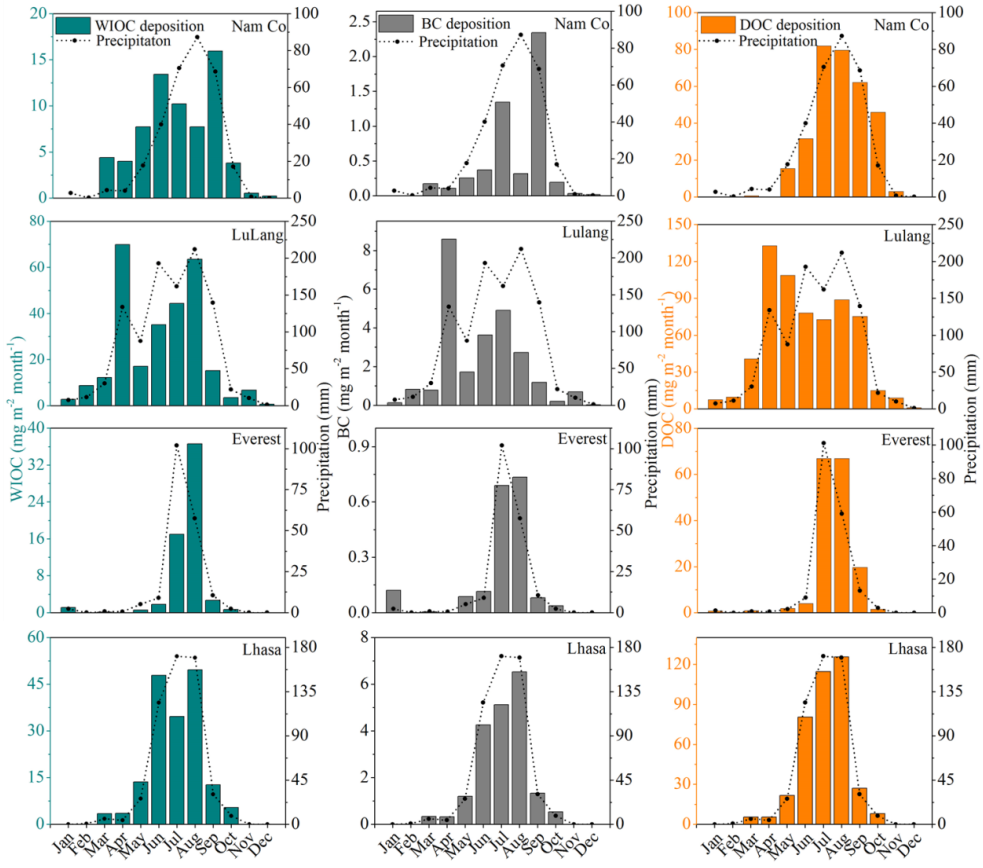

Figure 3.6: Seasonal variations of precipitation and wet deposition rates of WIOC, BC and DOC at Nam Co, Lulang, and Everest stations and Lhasa city.

3.2.3.4 Comparisons of BC deposition rates from different methods

It is true that WIOC and BC dry deposition rates in the HTP make significant contribution to the total deposition rates, especially in non-monsoon period with sparse precipitation (Figure 3.7). Besides the in-situ observation of the dry deposition rates of BC at Nam Co and Lhasa stations, the BC deposition rate in the HTP was also estimated by a Community Atmosphere Model version 5 (CAM5) (Zhang et al., 2015b) and empirical algorithms, i.e., the empirical calculation presented as formula (1)-(3) in section 3.1. The in-situ average ratios of BC dry and wet deposition rates were 1.6 and 8.5 at Nam Co Station and Lhasa city, respectively, which were much higher than the ratio simulated by CAM5 model (with the ratio of ~0.1) in the central HTP (Zhang et al., 2015b). Meanwhile, the in-situ BC total, wet and dry deposition rates were 1.7, 0.7

and 11 times the corresponding deposition rates by CAM5 model, respectively, at Nam Co station (Zhang et al., 2015b). Thus, CAM5 model probably underestimated the BC dry deposition rate and overestimated its wet deposition rate in Nam Co region compared to the values from in-situ observation. There were several reasons accounted for these differences. The most important reason was supposed to be that this model primarily considered BC derived from combustion emissions but ignored BC from local MD in the HTP, although this model did consider the internal mixing of fine-mode dust and BC. In addition, our in-situ deposition rates were based on the given sites, while the data from model represented the average values in the grid box at a grid mean elevation of 1.9 °×2.5 ° (Zhang et al., 2015b); meanwhile, the in-situ and modeling studies were conducted in different years.

The important contribution of MD to the carbonaceous particles in the HTP has been investigated by several previous studies (Cao et al., 2009; Kang et al., 2016; Li et al., 2007; Liu et al., 2017). BC is widely existed in soil dust (i.e., MD) due to its inert property. The BC concentrations in the surface soil were 1.3 and 2.0 mg g^{-1} in the northeastern (Zhan et al., 2015) and mid-western HTP (Gautam et al., 2020), respectively. Meanwhile, the contribution of MD to aerosols is common in the HTP, especially in non-monsoon period when dust storm happens (Dong et al., 2016), during which the aerosol particle size increases rapidly (Cong et al., 2009). Furthermore, the dry deposition velocity augments significantly with the increasing particle size when the size is larger than 2 μm (Zhang et al., 2001). For instance, the dry deposition velocity is as high as 3.0 cm s^{-1} when the particle size increases to 3.8 μm, which is much higher than that used in the calculation of dry deposition rate based on the aerosol data (0.15 cm s^{-1}) (Fang et al., 2015). Moreover, the modal sizes of the volume-size distribution of the local MD and the long-range transported eolian dust in the HTP were 39.8-48.3 and 11.5-13.4 μm, respectively. Thus, the BC total deposition rate calculated at Nam Co (10.5 mg m^{-2} a^{-1}) in paper I was underestimated, which was proved by the in-situ observation result (15.3 mg m^{-2} a^{-1}) (paper II). The underestimation also existed in Lhasa city as the BC dry deposition rate from in-situ observation (165.7 mg m^{-2} a^{-1}) was much higher than that from empirical calculation (27.0 mg m^{-2} a^{-1}). Accordingly, the dry deposition rate at Everest Station should be higher than the one we calculated in paper II. Although the dry deposition data at Everest Station were not investigated in situ, it is supposed that dry deposition has larger contribution at this station than Nam Co Station due to its lighter precipitation, which is consistent with the fact the Everest Station is more influenced by local fine particles than Nam Co Station (Liu et al., 2017). Therefore, the emission inventories for the modeling and the constants used in empirical calculation should all be improved based on the reference data from the in-situ observation.

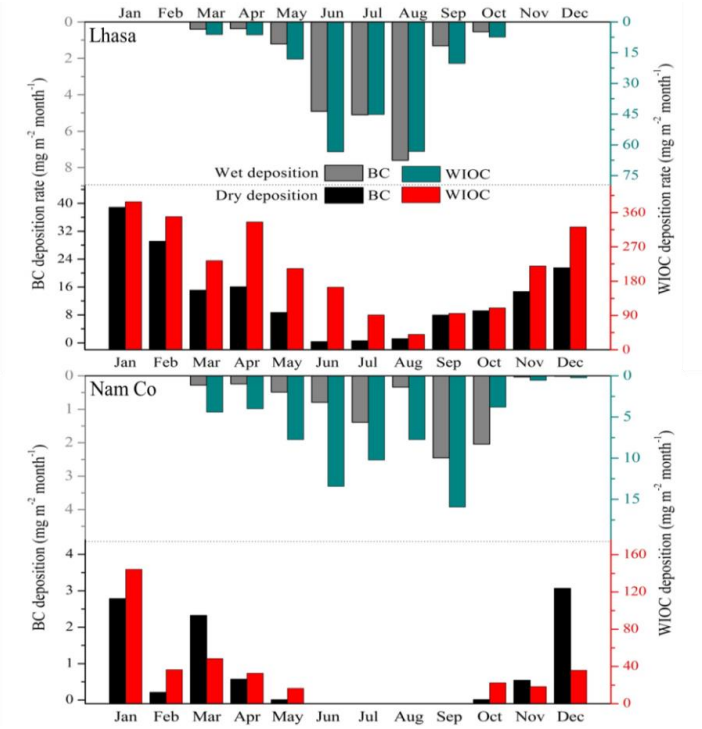

Figure 3.7: Monthly average variations in in-situ wet and dry deposition rates of WIOC and BC at Lhasa city and Nam Co Station. Note: The dry deposition samples were not collected from June to September at Nam Co Station due to the frequent precipitation events during this period.

3.2.4 Potential sources of carbonaceous matter in the HTP

In this work, we focus on the sources of precipitation DOC. Combined with our previously reported data on carbon isotopes of precipitation DOC (Li et al., 2018a), and isotopes on atmospheric and snow pit BC (Li et al., 2016a), the potential source regions of the carbonaceous matter in the HTP are discussed.

Precipitation DOC is produced via multiple sources including primary organic aerosols, such as biomass and fossil fuel combusted aerosols, secondary organic aerosols from the organic gases and gaseous precursors and MD (May et al., 2013). The potential DOC sources were preliminarily investigated by analyzing its relationship with major dissolved ions in precipitation in this study. The precipitation DOC at Nam Co Station was significantly correlated with NO_3^- (p<0.01) (Figure 3.8), which is an indicator of anthropogenic source in the remote HTP (Liu et al., 2015).

Meanwhile, it has proved that pollutants in South Asia could across the Himalayas and transport to this station (Lüthi et al., 2014), and the local emissions have also been detected at this station (Chen et al., 2015; Li et al., 2018b; Li et al., 2007). Thus, the precipitation DOC at Nam Co Station was primarily influenced by combustion emissions from South Asia and local activities. The precipitation DOC at Lulang Station displayed significant relationships with Na^+ and K^+ (Figure 3.8), and Na^+ presented a significant relationship with Cl^-, which indicated the Indian Ocean source of precipitation DOC because this station is located in the Yarlung Tsangpo Grand Canyon where Indian monsoon penetrates the HTP. The much higher ratio of K^+/Na^+ (0.49) in precipitation of Lulang than that of sea salt (0.04) indicated the additional contribution from biomass burning because K^+ typically acts as a biomass burning tracer (Szidat et al., 2006). South Asia is known as a large biomass burning region and the pollutants there could transport to Lulang Station by Indian monsoon (Bond et al., 2007; Gustafsson et al., 2009). The precipitation DOC at Everest Station was significantly correlated with Ca^{2+} and Mg^{2+} (Figure 3.8), suggesting the MD source because the Everest Station is situated in a valley of the southern Himalayas with arid environment and wide distribution of barren deserts.

The previous study on isotopic compositions of precipitation DOC at Nam Co Station suggested that 15±6% DOC was contributed by fossil fuel combustion, which was mainly originated and transported from South Asia (Li et al., 2018a). Meanwhile, the isotopic compositions of BC in aerosols across the Himalayas and snow pits across the Tibetan Plateau were comprehensively investigated and the results confirmed that the Himalayas (the southern HTP) is approximately equally influenced by biomass and fossil fuel combustion sources primarily from Indo-Gangetic Plain, South Asia; the northern HTP is primarily influenced by fossil fuel combustion from China, and the inland HTP (such as Nam Co region) is also influenced by the additional local emissions (such as Yak dung combustion and local MD) which are previously overlooked besides the pollution transported from South Asia (Li et al., 2016a).

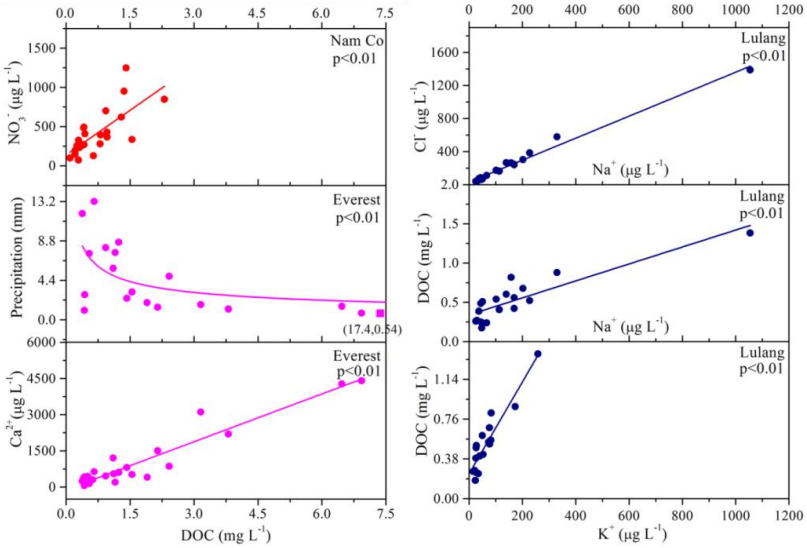

Figure 3.8: Significant relationships between DOC and Ca^{2+}, DOC and precipitation amounts at Everest Station and between the DOC and NO_3^- at Nam Co Station, and significant relationships between the DOC and K^+, DOC and Na^+, and Na^+ and Cl^- of precipitation samples at Lulang Station.

3.3 Light absorption of organic carbon

3.3.1 Light absorption of precipitation DOC

The WSOC fraction (i.e., DOC fraction) accounts for a large part of OC in the atmosphere, and some fractions of WSOC have strong light absorption in UV spectral range. Precipitation is an effective way to scavenge OC from the atmosphere and it contains the carbonaceous aerosol information of the entire atmospheric column from the high altitude to the near-surface. Thus, the light absorption study of the precipitation DOC may provide more comprehensive information in understanding the light absorbing DOC in the entire atmospheric column and in investigating the scavenging process of this light absorbing DOC.

The average MAC_{DOC} values were 0.48 ± 0.47, 0.25 ± 0.15 and 0.64 ± 0.49 $m^2\ g^{-1}$ at Nam Co, Lulang and Everest stations, respectively. The lowest value at Lulang Station was probably because this station is located in the forest region and a large amount of VOCs, which has low light absorption ability, were emitted there (Zhang et al., 2011). The precipitation DOC from South Asia may also contribute to this low value at Lulang Station because some part of DOC experienced photo/chemical bleaching

during the long-range transport in the atmosphere leading to the low light absorption of DOC (Forrister et al., 2015; Li et al., 2016d). The highest MAC_{DOC} at Everest Station was probably caused by the DOC from local MD. For example, the MAC_{DOC} of local MD at Everest Station was as high as 1.7 ± 0.5 m^2 g^{-1} (Li et al., 2016d).

It is interesting that the average MAC_{DOC} values of precipitation were significantly lower than the corresponding average MAC_{WSOC} values of aerosols at the three remote stations (p<0.01) (Figure 3.9), suggesting that the precipitation DOC has low light absorbing ability, which was probably because the DOC in precipitation was primarily consisted of VOCs and secondary organic aerosols (SOAs), two types of compounds with low light absorption ability (Lambe et al., 2013; Zhang et al., 2011). Similarly, the MAC_{DOC} of precipitation (0.84 ± 0.45 m^2 g^{-1}) was lower than MAC_{WSOC} of aerosols in East Asia (1.54 ± 0.16 m^2 g^{-1}) (Yan et al., 2015). This common phenomenon at both remote and urban regions indicated that the OC with low light-absorbing ability (such as VOCs and SOAs) was easier to be scavenged by precipitation than the OC with high light-absorbing ability, and thus, the remaining WSOC in the atmosphere generally has a large ability in absorbing light, which may pose a positive effect on the climate forcing. Therefore, the more comprehensive scavenging process of WSOC from the atmosphere by precipitation should be investigated to better understand the influence of precipitation on the aerosol forcing in the both remote and urban atmosphere.

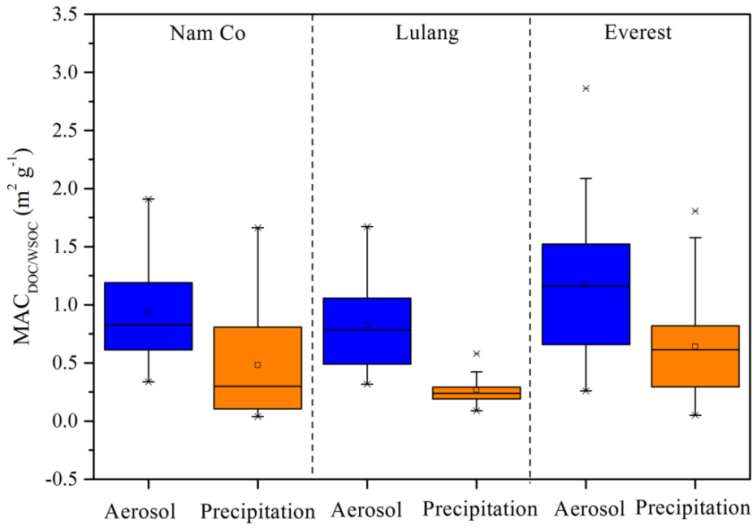

Figure 3.9: Significantly lower MAC_{DOC} values for precipitation samples relative to MAC_{WSOC} values for the aerosol samples at the three remote stations.

3.3.2 Light absorption of methanol-soluble OC in aerosol

The BrC is an important component of organic aerosols, which has strong light absorption in UV wavelength (Laskin et al., 2015) and has increasingly become a hotspot in the recently atmospheric solar radiation studies. Currently, the most commonly used solvent to extract BrC is purewater (Hecobian et al., 2010; Kirillova et al., 2014a) partly because this fraction of BrC can be readily quantified as WSOC (or DOC, as discussed in 3.3.1). However, WSOC represents a large range of BrC, for instance, the fraction of WSOC can be as low as 20% in an urban site (Miyazaki et al., 2006) but as high as 80% at some nonurban sites (Pio et al., 2007). To enhance the extractable fraction of OC, organic solvents were introduced and methanol was considered as the representative due to the high extraction efficiency (larger than 92% for the wood combustion aerosols) (Chen and Bond, 2010). However, in this case, the OC extracted by methanol (i.e., MeS-OC) cannot be determined directly using the extracts. Thus, the previous studies (Table 3.4) using MeS-OC as BrC surrogate typically assumed either that methanol extracted all the BrC in aerosols or that particles detached from the filters during the methanol extraction could be ignored. To solve this problem, we developed a new method (extraction assembly in section 2.2.1.2, Figure 2.2 and 2.3) to quantitatively measure MeS-OC mass, and thus obtaining a reliable $MAC_{MeS\text{-}OC}$ value.

3.3.2.1 Evaluation of three previous methods

Herein, the general information of three previous extraction methods was presented in Table 3.4. It is acknowledged that the particle detachment from the filters in the methanol extraction caused the underestimate of $MAC_{MeS\text{-}OC}$ in previous studies (Chen and Bond, 2010; Kirillova et al., 2016). To investigate the influence of the particle detachment, the $PM_{2.5}$ samples were extracted with methanol using the third method in Table 3.4. The extracts were measured for the light absorbance at wavelength of 365 nm (Abs_{365}) before and after filtration. The results suggested that the Abs_{365} values of unfiltered methanol extracts were much higher than those of filtered extracts (Figure 3.10a), proving that the particulate carbon detachment does exist in previous methods. In addition, the influence of particulate carbon detachment on Abs_{365} was larger for ambient aerosols than biomass aerosols, and the corresponding Abs_{365} increases of unfiltered extracts were approximately 101% and 45%, respectively, compared to the filtered extracts (Figure 3.10a). Moreover, if we assume methanol can completely extract OC of aerosol samples as method 2 listed in Table 3.4, the MAC_{365} values can be underestimated by 10% and 43% for the extracts of biomass and ambient aerosols, respectively (Figure 3.10c). The large discrepancy between two types of aerosols might be because the MeS-OC fraction of ambient aerosols was smaller than

that of biomass aerosols and the particle size from biomass combustion was finer and easier to adhere to filter than ambient particles. Thus, the particle detachment from the filter samples should be taken into consideration during the methanol extraction to study its reliable light absorption property

Table 3.4: Information and comparison of three previous extraction methods and the one in this work.

Method	Extraction process	Calculation of MeS-OC	Potential problems of previous methods	Reference
Method 1	Filter samples were immersed in methanol for 1 h without shaking or sonication	MeS-OC=OC of original filter−OC remaining on methanol extracted filter	The methanol insoluble particulate carbon detachment was ignored	(Cheng et al., 2017)
Method 2	Filter samples were sonicated for 1 h in methanol	MeS-OC=OC of original filter	The OC of original filter samples was assumed to be completely extracted by methanol	(Huang et al., 2018)
Method 3	Filter samples were sonicated in methanol for 1 h, the solution was kept at room temperature for 20 h, then it was sonicated for another 1 h	MeS-OC=OC of original filter − OC remaining on methanol extracted filter	The methanol insoluble particulate carbon detachment was ignored	(Chen and Bond, 2010)
New method	Filter samples were placed in the middle of a sandwich filtration assembly as presented in Figure 2.3, and extracted with methanol by three times. The total residence time of methanol on filters is 1 h	MeS-OC=TC of original filter−TC remaining on middle and bottom methanol extracted filters in sandwich filtration assembly, i.e., equation (2.5)		This study

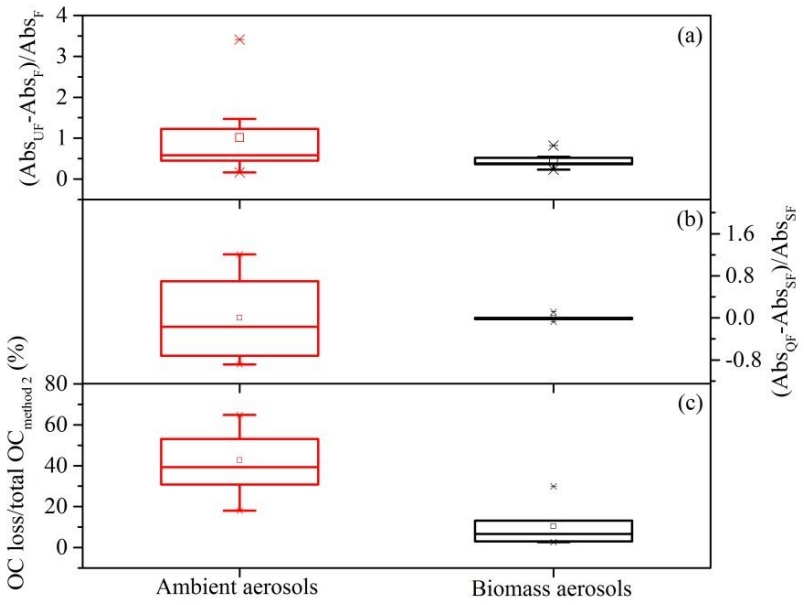

Figure 3.10: The increase ratios of Abs_{365} of the unfiltered (Abs_{UF}) methanol extracts compared to those of Abs_{365} of the filtered extracts (Abs_F) (a), the increase ratios of Abs_{365} of the extracts filtered by a quartz filter (Abs_{QF}) compared to those of Abs_{365} of the extracts filtered a by syringe filter (Abs_{SF}) (b), and the ratio of OC loss to total OC of original filter samples using method 2 in Table 3.4.

3.3.2.2 Abs of MeS-OC from four different methods

The Abs_{365} values were measured for the ambient and biomass aerosols using three previous methods and the one we developed in this research (section 2.2.1.2, extraction assembly in Figure 2.3). The average Abs_{365} values of MeS-OC using the new method lie between the first two methods but lower than that from third method (Figure 3.11). Meanwhile, the differences of Abs_{365} from these four methods were statistically insignificant (p>0.05, N=33) for both ambient and biomass aerosols. The different filtration filters also have insignificant influence on the Abs values (Figure 3.10b). Thus, it is proposed that the sonication and longer residence time cannot significantly enhance the OC extraction. Considering the relatively high extraction efficiency and the function to prevent particle loss from filter during methanol extraction, the newly developed method is recommended to investigate the light absorption of MeS-OC quantitatively. However, it should be acknowledged that the theoretical MAC_{365} of MeS-OC from the third method is the highest among the four

methods because of the elevated Abs_{365} values by the sonication treatment despite its insignificance.

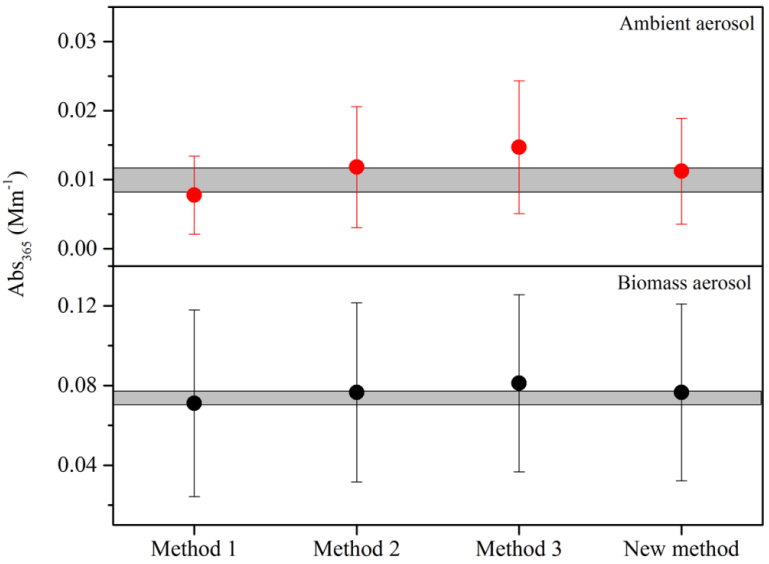

Figure 3.11: Normalized light absorbance of the methanol-extracted OC by four different extraction methods. Note: the large standard deviation (SD) values were attributed to the large variation in the particulate carbon mass of each collected sample.

3.3.2.3 WSOC versus MeS-OC and their light absorption properties

The OC fractions extracted by purewater were 63.3±13.3% and 55.2±29.1% for the biomass and ambient aerosols, respectively, which were consistent with the previous studies (Chen and Bond, 2010; Graham et al., 2002; Kirillova et al., 2016) because the extraction and measurement of WSOC in aerosols are well established with little uncertainties. The OC fraction of biomass aerosols extracted by methanol was approximately 93.0±3.8%, which was likely the low bond value of the previously reported data of the wood combustion aerosols (92-98%) (Chen and Bond, 2010); while the fraction of ambient aerosols was approximately 79.3±10.0%, which was lower than that of ambient aerosols in Beijing (89%) (Cheng et al., 2017). This discrepancy of methanol extracted fractions of OC was possibly because the aerosol sources in different studies were diverse and the previous two studies failed to take account of the particle detachment during methanol extraction. Therefore, the assumption that methanol extracts almost all OC on filter samples in previous studies does lead to the overestimation of MeS-BrC mass, and thus underestimation of

$MAC_{MeS\text{-}OC}$, especially for those ambient aerosols.

The MAC_{365} values of MeS-OC ($MAC_{MeS\text{-}OC,365}$) in biomass and ambient aerosols we collected were 1.55±0.43 m^2 g^{-1} (1.07-2.44 m^2 g^{-1}) and 1.14±0.50 m^2 g^{-1} (0.55-1.51 m^2 g^{-1}), respectively, using the newly developed method. It is obvious that average $MAC_{MeS\text{-}OC,365}$ of biomass combustion aerosols was higher than that of ambient aerosols (Figure 3.12); meanwhile $MAC_{MeS\text{-}OC,365}$ of aerosols in Lhasa was lower than those of the other two rural sites due to the influence of fossil fuel combustion in Lhasa, which was also reflected by the lower OC/BC ratios in Lhasa (3.4 in Lhasa, 7.1 and 7.3 in the other two rural sites) as presented in previous studies (Li et al., 2016b). The MeS-OC has higher MAC values than WS-BrC across the near UV wavelength, which was in accordance with the previous results (Chen and Bond, 2010; Kirchstetter et al., 2004; Zhang et al., 2013) (Figure 3.13).

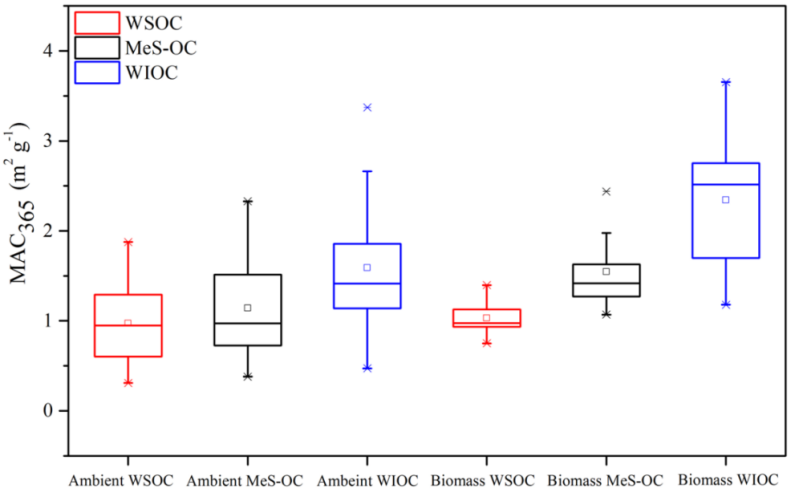

Figure 3.12: Average MAC_{365} of the water and methanol extracts of ambient and the biomass aerosols.

The OC only extractable by methanol was supposed to be more light-absorbing than WSOC (Figure 3.12), and it was defined as WIOC. The average MAC_{WIOC} values at 365 nm for biomass and ambient aerosols were 2.34±0.78 and 1.59±0.76 m^2 g^{-1}, approximately 2.3 and 1.6 times of the corresponding MAC_{WSOC} values. This strong light-absorbing component was suggested to be large molecular weighted PAHs or large molecules with conjugated aromatic rings which have low water-solubility (Apicella et al., 2004; Chen and Bond, 2010; Zhang et al., 2013). These molecules

could be produced in biomass and fossil fuel combustion under the flaming and smoldering combustion status (Evans and Milne, 1987; Schauer et al., 2001). Whereas, the less light-absorbing WSOC was identified as the humic-like or protein-like substances (Sun et al., 2007; Wu et al., 2019). Moreover, as a proxy of light absorption, Abs_{365} of WIOC presented a strong correlation with WIOC mass for both biomass and ambient aerosols besides the significant correlations between WSOC and its Abs values (p<0.01, supporting Figure S4 of paper V), which further indicated that a larger fraction of WIOC was BrC chromophores. Therefore, it is significantly necessary to incorporate the MeS-OC in light absorption study to better understand its role in the climate forcing using this more accurate and quantitative method developed in our study.

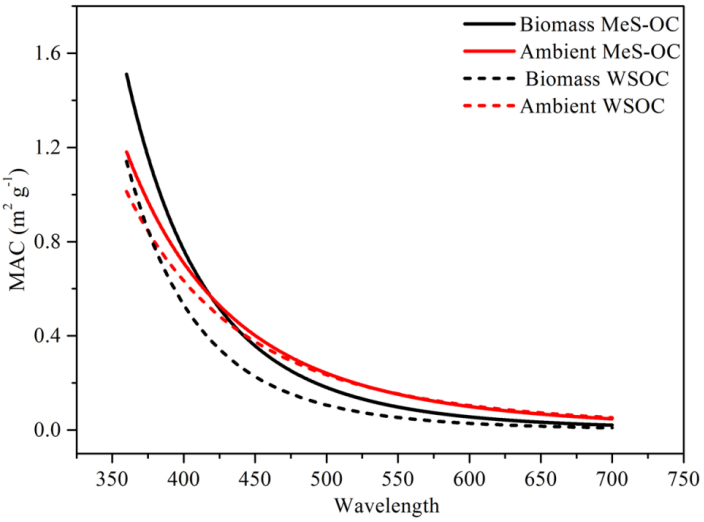

Figure 3.13: Average mass absorption cross-section spectra of WSOC and MeS-OC in the ambient and biomass aerosols.

4 Conclusions and prospectives

1. Concentration and deposition rates of BC in the HTP were re-investigated to estimate the potential uncertainties in previously reported results. The findings suggested that inorganic carbon in mineral dust caused approximately 52±35% and 39±24% overestimation in the previously reported BC concentrations at two remote stations - Nam Co and Everest- because of the wide distribution of arid and desert regions in the HTP. Thus, BC concentrations were corrected by these overestimation rates. The BC deposition rates from previous lake cores did not represent the actual atmospheric BC deposition due to the large catchment input. Correspondingly, the relatively consistent BC deposition rates derived from snow pits and ice cores were considered more reliable, and BC deposition rate of 17.9±5.3 mg m^{-2} yr^{-1} was proposed for the glacier regions of the HTP. This work provides improved methods and data references for the future related research in the HTP and other regions.

2. To further investigate concentration and deposition of carbonaceous matter in the HTP, the in-situ observations were conducted at three remote stations and an urban site in the HTP. The results indicated that the concentrations and deposition rates of carbonaceous matter in the HTP were lower than those of urban cities, but comparable to those of remote, mountain and rural sites. The scavenging mechanisms of both wet and dry deposition are complex with various influencing factors. Generally, the wet deposition mechanism includes two processes, washout and rainout. For the urban Lhasa city, the main scavenging process was washout, while for the remote stations the dominated scavenging process was rainout in the HTP. This phenomenon was attributed to the different atmospheric particle loadings. By comparing the research results, this study emphasizes that dry deposition has a more important or equally important role with wet deposition in the total particulate carbon deposition at study stations of the HTP, which has been greatly underestimated in the previous modeling studies. This should be a common phenomenon in most parts of the HTP (especially in the northwest part) due to its unique location and atmospheric circulation. Therefore, the in-situ results provide the basic input data to improve the modeling and related deposition studies in the HTP. In addition, the in-situ observation of carbonaceous matter should also be conducted in other regions of the HTP since the concentrations and deposition rates of carbonaceous matter have large spatial and temporal variations.

3. Besides the important role in carbon cycle, DOC also has a significant role in the atmospheric forcing and glacier melting after deposition due to its light-absorbing properties. The light absorption of precipitation DOC presents general information of light-absorbing carbonaceous matter scavenging process from the atmosphere. Meanwhile, the light absorption of DOC in precipitation was consistently lower than the corresponding value in the atmosphere (i.e., light absorption of WSOC in the atmosphere). Different from the easy and reliable method to measure the light absorption of DOC (or WSOC), the light absorption measurement of WIOC is more complicated due to the controversial extraction methods despite of its stronger light absorption compared to WSOC. After comparing the previous methods to investigate the light absorption property of WIOC by extracting OC with methanol, the existed uncertainties were comprehensively discussed, then a newly developed method was introduced to overcome the previous problems to obtain reliable light absorption of this strong light absorbing methanol extracted OC. Moreover, this new method can be applied to all the other regions in the world to better constrain the light absorption ability of OC both in the atmosphere and in glacier regions.

References

Andreae, M., Gelencsér, A., 2006. Black carbon or brown carbon? The nature of light-absorbing carbonaceous aerosols. Atmospheric Chemistry and Physics 6, 3131-3148.

Anenberg, S.C., Schwartz, J., Shindell, D., Amann, M., Faluvegi, G., Klimont, Z., Janssens-Maenhout, G., Pozzoli, L., Van Dingenen, R., Vignati, E., 2012. Global air quality and health co-benefits of mitigating near-term climate change through methane and black carbon emission controls. Environmental Health Perspectives 120, 831-839.

Antony, R., Mahalinganathan, K., Thamban, M., Nair, S., 2011. Organic carbon in Antarctic snow: spatial trends and possible sources. Environmental Science & Technology 45, 9944-9950.

Apicella, B., Alfe, M., Barbella, R., Tregrossi, A., Ciajolo, A., 2004. Aromatic structures of carbonaceous materials and soot inferred by spectroscopic analysis. Carbon 42, 1583-1589.

Avery, G.B., Biswas, K.F., Mead, R., Southwell, M., Willey, J.D., Kieber, R.J., Mullaugh, K.M., 2013. Carbon isotopic characterization of hydrophobic dissolved organic carbon in rainwater. Atmospheric Environment 68, 230-234.

Bauer, S.E., Bausch, A., Nazarenko, L., Tsigaridis, K., Xu, B., Edwards, R., Bisiaux, M., McConnell, J., 2013. Historical and future black carbon deposition on the three ice caps: Ice core measurements and model simulations from 1850 to 2100. Journal of Geophysical Research: Atmospheres 118, 7948-7961.

Bisiaux, M.M., Edwards, R., McConnell, J.R., Curran, M.A.J., Van Ommen, T.D., Smith, A.M., Neumann, T.A., Pasteris, D.R., Penner, J.E., Taylor, K., 2012. Changes in black carbon deposition to Antarctica from two high-resolution ice core records, 1850–2000 AD. Atmospheric Chemistry and Physics 12, 4107-4115.

Bonasoni, P., Laj, P., Marinoni, A., Sprenger, M., Angelini, F., Arduini, J., Bonafè, U., Calzolari, F., Colombo, T., Decesari, S., 2010. Atmospheric Brown Clouds in the Himalayas: first two years of continuous observations at the Nepal Climate Observatory-Pyramid (5079 m). Atmospheric Chemistry and Physics 10, 7515-7531.

Bond, T.C., Bergstrom, R.W., 2006. Light absorption by carbonaceous particles: An investigative review. Aerosol Science and Technology 40, 27-67.

Bond, T.C., Bhardwaj, E., Dong, R., Jogani, R., Jung, S., Roden, C., Streets, D.G., Trautmann, N.M., 2007. Historical emissions of black and organic carbon aerosol from energy‐related combustion, 1850–2000. Global biogeochemical cycles 21, doi: 10.1029/2006GB002840.

Bond, T.C., Doherty, S.J., Fahey, D.W., Forster, P.M., Berntsen, T., DeAngelo, B.J.,

Flanner, M.G., Ghan, S., Kärcher, B., Koch, D., Kinne, S., Kondo, Y., Quinn, P.K., Sarofim, M.C., Schultz, M.G., Schulz, M., Venkataraman, C., Zhang, H., Zhang, S., Bellouin, N., Guttikunda, S.K., Hopke, P.K., Jacobson, M.Z., Kaiser, J.W., Klimont, Z., Lohmann, U., Schwarz, J.P., Shindell, D., Storelvmo, T., Warren, S.G., Zender, C.S., 2013. Bounding the role of black carbon in the climate system: A scientific assessment. Journal of Geophysical Research: Atmospheres 118, 5380-5552.

Bosch, C., Andersson, A., Kirillova, E.N., Budhavant, K., Tiwari, S., Praveen, P., Russell, L.M., Beres, N.D., Ramanathan, V., Gustafsson, Ö., 2014. Source‐diagnostic dual‐isotope composition and optical properties of water‐soluble organic carbon and elemental carbon in the South Asian outflow intercepted over the Indian Ocean. Journal of Geophysical Research: Atmospheres 119, 11,743-711,759.

Cao, J.-J., Xu, B.-Q., He, J.-Q., Liu, X.-Q., Han, Y.-M., Wang, G.-h., Zhu, C.-s., 2009. Concentrations, seasonal variations, and transport of carbonaceous aerosols at a remote Mountainous region in western China. Atmospheric Environment 43, 4444-4452.

Cao, J., Lee, S., Zhang, X., Chow, J.C., An, Z., Ho, K., Watson, J.G., Fung, K., Wang, Y., Shen, Z., 2005. Characterization of airborne carbonate over a site near Asian dust source regions during spring 2002 and its climatic and environmental significance. Journal of Geophysical Research: Atmospheres 110, doi:10.1029/2004JD005244.

Cao, J., Tie, X., Xu, B., Zhao, Z., Zhu, C., Li, G., Liu, S., 2011. Measuring and modeling black carbon (BC) contamination in the SE Tibetan Plateau. Journal of Atmospheric Chemistry 67, 45-60.

Cerqueira, M., Pio, C., Legrand, M., Puxbaum, H., Kasper-Giebl, A., Afonso, J., Preunkert, S., Gelencsér, A., Fialho, P., 2010. Particulate carbon in precipitation at European background sites. Journal of Aerosol Science 41, 51-61.

Chýlek, P., Kou, L., Johnson, B., Boudala, F., Lesins, G., 1999. Black carbon concentrations in precipitation and near surface air in and near Halifax, Nova Scotia. Atmospheric Environment 33, 2269-2277.

Chen, P., Kang, S., Bai, J., Sillanpää, M., Li, C., 2015. Yak dung combustion aerosols in the Tibetan Plateau: Chemical characteristics and influence on the local atmospheric environment. Atmospheric Research 156, 58-66.

Chen, P., Kang, S., Li, C., Zhang, Q., Guo, J., Tripathee, L., Zhang, Y., Li, G., Gul, C., Cong, Z., Wan, X., Niu, H., Panday, A.K., Rupakheti, M., Ji, Z., 2019. Carbonaceous aerosol characteristics on the Third Pole: A primary study based on the Atmospheric Pollution and Cryospheric Change (APCC) network. Environ Pollut 253, 49-60.

Chen, S., Huang, J., Zhao, C., Qian, Y., Leung, L.R., Yang, B., 2013. Modeling the transport and radiative forcing of Taklimakan dust over the Tibetan Plateau: A case study in the summer of 2006. Journal of Geophysical Research: Atmospheres 118, 797-812.

Chen, X., Kang, S., Cong, Z., Yang, J., Ma, Y., 2018. Concentration, temporal variation, and sources of black carbon in the Mt. Everest region retrieved by real-time observation and simulation. Atmospheric Chemistry and Physics 18, 12859-12875.

Chen, Y., Bond, T.C., 2010. Light absorption by organic carbon from wood combustion. Atmospheric Chemistry and Physics 10, 1773-1787.

Cheng, Y., He, K.-B., Engling, G., Weber, R., Liu, J.-M., Du, Z.-Y., Dong, S.-P., 2017. Brown and black carbon in Beijing aerosol: Implications for the effects of brown coating on light absorption by black carbon. Science of the Total Environment 599, 1047-1055.

Cheng, Y., He, K.-B., Zheng, M., Duan, F.-K., Du, Z.-Y., Ma, Y.-L., Tan, J.-H., Yang, F.-M., Liu, J.-M., Zhang, X.-L., 2011. Mass absorption efficiency of elemental carbon and water-soluble organic carbon in Beijing, China. Atmospheric Chemistry and Physics 11, 11497-11510.

Chow, J.C., Watson, J.G., 2002. $PM_{2.5}$ carbonate concentrations at regionally representative Interagency Monitoring of Protected Visual Environment sites. Journal of Geophysical Research: Atmospheres 107, ICC 6-1-ICC 6-9.

Chow, J.C., Watson, J.G., Crow, D., Lowenthal, D.H., Merrifield, T., 2001. Comparison of IMPROVE and NIOSH carbon measurements. Aerosol Science & Technology 34, 23-34.

Clarke, A.D., Noone, K.J., 1985. Soot in the Arctic snowpack: A cause for perturbations in radiative transfer. Atmospheric Environment (1967) 19, 2045-2053.

Coelho, C., Francisco, J., Nogueira, R.F.P., Campos, M., 2008. Dissolved organic carbon in rainwater from areas heavily impacted by sugar cane burning. Atmospheric Environment 42, 7115-7121.

Cong, Z., Kang, S., Gao, S., Zhang, Y., Li, Q., Kawamura, K., 2013. Historical trends of atmospheric black carbon on tibetan plateau as reconstructed from a 150-year lake sediment record. Environmental Science & Technology 47, 2579-2586.

Cong, Z., Kang, S., Kawamura, K., Liu, B., Wan, X., Wang, Z., Gao, S., Fu, P., 2015. Carbonaceous aerosols on the south edge of the Tibetan Plateau: concentrations, seasonality and sources. Atmospheric Chemistry and Physics 15, 1573-1584.

Cong, Z., Kang, S., Smirnov, A., Holben, B., 2009. Aerosol optical properties at Nam Co, a remote site in central Tibetan Plateau. Atmospheric Research 92, 42-48.

Cooke, W.F., 2002. A general circulation model study of the global carbonaceous

aerosol distribution. Journal of Geophysical Research 107, doi: 10.1029/2001JD 001274.

Cui, Y.Y., Liu, S., Bai, Z., Bian, J., Li, D., Fan, K., McKeen, S.A., Watts, L.A., Ciciora, S.J., Gao, R.-S., 2018. Religious burning as a potential major source of atmospheric fine aerosols in summertime Lhasa on the Tibetan Plateau. Atmospheric Environment 181, 186-191.

Custodio, D., Cerqueira, M., Fialho, P., Nunes, T., Pio, C., Henriques, D., 2014. Wet deposition of particulate carbon to the Central North Atlantic Ocean. Science of the Total Environment 496, 92-99.

Dobersch ütz, S., Frenzel, P., Haberzettl, T., Kasper, T., Wang, J., Zhu, L., Daut, G., Schwalb, A., Mńusbacher, R., 2014. Monsoonal forcing of Holocene paleoenvironmental change on the central Tibetan Plateau inferred using a sediment record from Lake Nam Co (Xizang, China). Journal of Paleolimnology 51, 253-266.

Doherty, S., Warren, S., Grenfell, T., Clarke, A., Brandt, R., 2010. Light-absorbing impurities in Arctic snow. Atmospheric Chemistry and Physics 10, 11647-11680.

Dong, Z., Qin, D., Kang, S., Liu, Y., Li, Y., Huang, J., Qin, X., 2016. Individual particles of cryoconite deposited on the mountain glaciers of the Tibetan Plateau: Insights into chemical composition and sources. Atmospheric Environment 138, 114-124.

Dou, T.F., Xiao, C.D., 2016. An overview of black carbon deposition and its radiative forcing over the Arctic. Advances in Climate Change Research 7, 115-122.

Ducret, J., Cachier, H., 1992. Particulate carbon content in rain at various temperate and tropical locations. Journal of Atmospheric Chemistry 15, 55-67.

Elmquist, M., Zencak, Z., Gustafsson, Ö., 2007. A 700 year sediment record of black carbon and polycyclic aromatic hydrocarbons near the EMEP air monitoring station in Aspvreten, Sweden. Environmental Science & Technology 41, 6926-6932.

Evans, R.J., Milne, T.A., 1987. Molecular characterization of the pyrolysis of biomass. Energy & Fuels 1, 123-137.

Fang, Y., Chen, Y., Tian, C., Lin, T., Hu, L., Huang, G., Tang, J., Li, J., Zhang, G., 2015. Flux and budget of BC in the continental shelf seas adjacent to Chinese high BC emission source regions. Global biogeochemical cycles 29, 957-972.

Feng, Y., Ramanathan, V., Kotamarthi, V.R., 2013. Brown carbon: a significant atmospheric absorber of solar radiation? Atmospheric Chemistry and Physics 13, 8607-8621.

Forrister, H., Liu, J., Scheuer, E., Dibb, J., Ziemba, L., Thornhill, K.L., Anderson, B., Diskin, G., Perring, A.E., Schwarz, J.P., 2015. Evolution of brown carbon in wildfire plumes. Geophysical Research Letters 42, 4623-4630.

Garrett, T., Zhao, C., Novelli, P., 2017. Assessing the relative contributions of transport efficiency and scavenging to seasonal variability in Arctic aerosol. Tellus B: Chemical and Physical Meteorology 62, 190-196.

Gautam, S., Yan, F., Kang, S., Han, X., Neupane, B., Chen, P., Hu, Z., Sillanpää, M., Li, C., 2020. Black carbon in surface soil of the Himalayas and Tibetan Plateau and its contribution to total black carbon deposition at glacial region. Environmental Science and Pollution Research 27, 2670-2676.

Gioda, A., Reyes‐Rodríguez, G.J., Santos‐Figueroa, G., Collett Jr, J.L., Decesari, S., Ramos, M.d.C.K., Bezerra Netto, H.J., de Aquino Neto, F.R., Mayol‐Bracero, O.L., 2011. Speciation of water‐soluble inorganic, organic, and total nitrogen in a background marine environment: Cloud water, rainwater, and aerosol particles. Journal of Geophysical Research: Atmospheres 116, doi: 10.1029/2010JD015010.

Graham, B., Mayol‐Bracero, O.L., Guyon, P., Roberts, G.C., Decesari, S., Facchini, M.C., Artaxo, P., Maenhaut, W., Köll, P., Andreae, M.O., 2002. Water‐soluble organic compounds in biomass burning aerosols over Amazonia 1. Characterization by NMR and GC‐MS. Journal of Geophysical Research: Atmospheres 107, LBA 14-11-LBA 14-16.

Gustafsson, Ö., Kruså, M., Zencak, Z., Sheesley, R.J., Granat, L., Engström, E., Praveen, P., Rao, P., Leck, C., Rodhe, H., 2009. Brown clouds over South Asia: biomass or fossil fuel combustion? Science 323, 495-498.

Hagler, G.S., Bergin, M.H., Smith, E.A., Dibb, J.E., Anderson, C., Steig, E.J., 2007. Particulate and water‐soluble carbon measured in recent snow at Summit, Greenland. Geophysical Research Letters 34, doi: 10.1029/2007GL030110.

Han, Y., Cao, J., An, Z., Chow, J.C., Watson, J.G., Jin, Z., Fung, K., Liu, S., 2007. Evaluation of the thermal/optical reflectance method for quantification of elemental carbon in sediments. Chemosphere 69, 526-533.

Han, Y.M., Wei, C., Bandowe, B.A., Wilcke, W., Cao, J.J., Xu, B.Q., Gao, S.P., Tie, X.X., Li, G.H., Jin, Z.D., An, Z.S., 2015. Elemental carbon and polycyclic aromatic compounds in a 150-year sediment core from Lake Qinghai, Tibetan Plateau, China: influence of regional and local sources and transport pathways. Environmental Science & Technology 49, 4176-4183.

Han, Y.M., Wei, C., Huang, R.J., Bandowe, B.A., Ho, S.S., Cao, J.J., Jin, Z.D., Xu, B.Q., Gao, S.P., Tie, X.X., An, Z.S., Wilcke, W., 2016. Reconstruction of atmospheric soot history in inland regions from lake sediments over the past 150 years. Scientific reports 6, 19151.

Harrison, R.M., Allen, A.G., 1991. Scavenging ratios and deposition of sulphur, nitrogen and chlorine species in eastern England. Atmospheric Environment. Part A. General Topics 25, 1719-1723.

He, C., Li, Q., Liou, K.N., Takano, Y., Gu, Y., Qi, L., Mao, Y., Leung, L.R., 2015.

Black carbon radiative forcing over the Tibetan Plateau. Geophysical Research Letters 41, 7806-7813.

Hecobian, A., Zhang, X., Zheng, M., Frank, N., Edgerton, E.S., Weber, R.J., 2010. Water-Soluble Organic Aerosol material and the light-absorption characteristics of aqueous extracts measured over the Southeastern United States. Atmospheric Chemistry and Physics 10, 5965-5977.

Hood, E., Battin, T.J., Fellman, J., O'neel, S., Spencer, R.G., 2015. Storage and release of organic carbon from glaciers and ice sheets. Nature Geoscience 8, doi: 10.1038/NGEO2331.

Hu, Z., Kang, S., Li, C., Yan, F., Chen, P., Gao, S., Wang, Z., Zhang, Y., Sillanpää, M., 2017. Light absorption of biomass burning and vehicle emission-sourced carbonaceous aerosols of the Tibetan Plateau. Environmental Science and Pollution Research 24, 15369-15378.

Huang, J., Kang, S., Shen, C., Cong, Z., Liu, K., Wang, W., Liu, L., 2010. Seasonal variations and sources of ambient fossil and biogenic-derived carbonaceous aerosols based on ^{14}C measurements in Lhasa, Tibet. Atmospheric Research 96, 553-559.

Huang, R.-J., Yang, L., Cao, J., Chen, Y., Chen, Q., Li, Y., Duan, J., Zhu, C., Dai, W., Wang, K., 2018. Brown carbon aerosol in urban Xi'an, northwest China: The composition and light absorption properties. Environmental Science & Technology 52, 6825-6833.

Huo, M.Q., Sato, K., Ohizumi, T., Akimoto, H., Takahashi, K., 2016. Characteristics of carbonaceous components in precipitation and atmospheric particle at Japanese sites. Atmospheric Environment 146, 164-173.

Husain, L., Khan, A., Ahmed, T., Swami, K., Bari, A., Webber, J.S., Li, J., 2008. Trends in atmospheric elemental carbon concentrations from 1835 to 2005. Journal of Geophysical Research: Atmospheres 113.

Iavorivska, L., Boyer, E.W., DeWalle, D.R., 2016. Atmospheric deposition of organic carbon via precipitation. Atmospheric Environment 146, 153-163.

Immerzeel, W.W., Van Beek, L.P., Bierkens, M.F., 2010. Climate change will affect the Asian water towers. Science 328, 1382-1385.

IPCC, 2013. IPCC Climate Change. The Physical Science Basis. Contribution of Working Group I to the Fifth Assessment Report of the Intergovernmental Panel on Climate Change. 2013. Cambridge Univeristy. Press, Cambridge, U. K., and New York, 33-118.

Ishikawa, Y., Murakami, H., Sekine, T., Yoshihara, K., 1995. Precipitation scavenging studies of radionuclides in air using cosmogenic ^{7}Be. Journal of Environmental Radioactivity 26, 19-36.

Jankowski, N., Schmidl, C., Marr, I.L., Bauer, H., Puxbaum, H., 2008. Comparison of

methods for the quantification of carbonate carbon in atmospheric PM_{10} aerosol samples. Atmospheric Environment 42, 8055-8064.

Jurado, E., Dachs, J., Duarte, C., Simó, R., 2008. Atmospheric deposition of organic and black carbon to the global oceans.

Kang, S., Chen, P., Li, C., Liu, B., Cong, Z., 2016. Atmospheric aerosol elements over the inland Tibetan Plateau: Concentration, seasonality, and transport. Aerosol and Air Quality Research 16, 789-800.

Kang, S., Xu, Y., You, Q., Flügel, W.-A., Pepin, N., Yao, T., 2010. Review of climate and cryospheric change in the Tibetan Plateau. Environmental Research Letters 5, doi: 10.1088/1748-9326/1085/1081/015101.

Kang, S., Zhang, Q., Qian, Y., Ji, Z., Li, C., Cong, Z., Zhang, Y., Guo, J., Du, W., Huang, J., 2019. Linking Atmospheric Pollution to Cryospheric Change in the Third Pole Region: Current Progresses and Future Prospects. National Science Review 6, 796–809.

Karanasiou, A., Diapouli, E., Cavalli, F., Eleftheriadis, K., Viana, M., Alastuey, A., Querol, X., Reche, C., 2011. On the quantification of atmospheric carbonate carbon by thermal/optical analysis protocols. Atmospheric Measurement Techniques 4, 2409-2419.

Kaspari, S., Painter, T.H., Gysel, M., Skiles, S., Schwikowski, M., 2014. Seasonal and elevational variations of black carbon and dust in snow and ice in the Solu-Khumbu, Nepal and estimated radiative forcings. Atmospheric Chemistry and Physics 14, 8089-8103.

Kaspari, S.D., Schwikowski, M., Gysel, M., Flanner, M.G., Kang, S., Hou, S., Mayewski, P.A., 2011. Recent increase in black carbon concentrations from a Mt. Everest ice core spanning 1860-2000 AD. Geophysical Research Letters 38, doi: 10.1029/2010GL046096.

Kieber, R.J., Peake, B., Willey, J.D., Avery, G.B., 2002. Dissolved organic carbon and organic acids in coastal New Zealand rainwater. Atmospheric Environment 36, 3557-3563.

Kirchstetter, T.W., Novakov, T., Hobbs, P.V., 2004. Evidence that the spectral dependence of light absorption by aerosols is affected by organic carbon. Journal of Geophysical Research: Atmospheres 109, doi: 10.1029/2004JD004999.

Kirillova, E.N., Andersson, A., Han, J., Lee, M., Gustafsson, Ö., 2014a. Sources and light absorption of water-soluble organic carbon aerosols in the outflow from northern China. Atmospheric Chemistry and Physics 14, 1413-1422.

Kirillova, E.N., Andersson, A., Tiwari, S., Srivastava, A.K., Bisht, D.S., Gustafsson, Ö., 2014b. Water-soluble organic carbon aerosols during a full New Delhi winter: Isotope-based source apportionment and optical properties. Journal of Geophysical Research: Atmospheres 119, 3476-3485.

Kirillova, E.N., Marinoni, A., Bonasoni, P., Vuillermoz, E., Facchini, M.C., Fuzzi, S., Decesari, S., 2016. Light absorption properties of brown carbon in the high Himalayas. Journal of Geophysical Research: Atmospheres 121, 9621-9639.

Lüthi, Z.L., Škerlak, B., Kim, S.W., Lauer, A., Mues, A., Rupakheti, M., Kang, S., 2014. Atmospheric brown clouds reach the Tibetan Plateau by crossing the Himalayas. Atmospheric Chemistry and Physics Discussions 14, 28105-28146.

Lambe, A.T., Cappa, C.D., Massoli, P., Onasch, T.B., Forestieri, S.D., Martin, A.T., Cummings, M.J., Croasdale, D.R., Brune, W.H., Worsnop, D.R., 2013. Relationship between oxidation level and optical properties of secondary organic aerosol. Environmental Science & Technology 47, 6349-6357.

Laskin, A., Laskin, J., Nizkorodov, S.A., 2015. Chemistry of atmospheric brown carbon. Chem Rev 115, 4335-4382.

Lavanchy, V., G äggeler, H., Schotterer, U., Schwikowski, M., Baltensperger, U., 1999. Historical record of carbonaceous particle concentrations from a European high - alpine glacier (Colle Gnifetti, Switzerland). Journal of Geophysical Research: Atmospheres 104, 21227-21236.

Li, C., Bosch, C., Kang, S., Andersson, A., Chen, P., Zhang, Q., Cong, Z., Chen, B., Qin, D., Gustafsson, O., 2016a. Sources of black carbon to the Himalayan-Tibetan Plateau glaciers. Nat Commun 7, 12574, doi: 12510.11038/ncomms12574.

Li, C., Chen, P., Kang, S., Yan, F., Hu, Z., Qu, B., Sillanp ää, M., 2016b. Concentrations and light absorption characteristics of carbonaceous aerosol in $PM_{2.5}$ and PM_{10} of Lhasa city, the Tibetan Plateau. Atmospheric Environment 127, 340-346.

Li, C., Chen, P., Kang, S., Yan, F., Li, X., Qu, B., Sillanp ää, M., 2016c. Carbonaceous matter deposition in the high glacial regions of the Tibetan Plateau. Atmospheric Environment 141, 203-208.

Li, C., Chen, P., Kang, S., Yan, F., Tripathee, L., Wu, G., Qu, B., Sillanp ää, M., Yang, D., Dittmar, T., Stubbins, A., Raymond, P.A., 2018a. Fossil Fuel Combustion Emission From South Asia Influences Precipitation Dissolved Organic Carbon Reaching the Remote Tibetan Plateau: Isotopic and Molecular Evidence. Journal of Geophysical Research: Atmospheres 123, 6248-6258.

Li, C., Han, X., Kang, S., Yan, F., Chen, P., Hu, Z., Yang, J., Ciren, D., Gao, S., Sillanp ää, M., 2019. Heavy near-surface $PM_{2.5}$ pollution in Lhasa, China during a relatively static winter period. Chemosphere 214, 314-318.

Li, C., Kang, S., Wang, X., Ajmone-Marsan, F., Zhang, Q., 2008. Heavy metals and rare earth elements (REEs) in soil from the Nam Co Basin, Tibetan Plateau. Environmental Geology 53, 1433-1440.

Li, C., Kang, S., Yan, F., 2018b. Importance of Local Black Carbon Emissions to the Fate of Glaciers of the Third Pole. Environmental Science & Technology 52, 14027-14028.

Li, C., Kang, S., Zhang, Q., Kaspari, S., 2007. Major ionic composition of precipitation in the Nam Co region, Central Tibetan Plateau. Atmospheric Research 85, 351-360.

Li, C., Yan, F., Kang, S., Chen, P., Hu, Z., Gao, S., Qu, B., Sillanp ää, M., 2016d. Light absorption characteristics of carbonaceous aerosols in two remote stations of the southern fringe of the Tibetan Plateau, China. Atmospheric Environment 143, 79-85.

Li, C., Yan, F., Kang, S., Chen, P., Qu, B., Hu, Z., Sillanpaa, M., 2016e. Concentration, sources, and flux of dissolved organic carbon of precipitation at Lhasa city, the Tibetan Plateau. Environmental Science and Pollution Research 23, 12915-12921.

Li, Q., Kang, S., Zhang, Q., Huang, J., Guo, J., Wang, K., Wang, J., 2014. A 150 year climate change history reconstructed by lake sediment of Nam Co, Tibetan Plateau. Acta Sedimentologica Sinica 32, 669-676.

Li, X., Kang, S., He, X., Qu, B., Tripathee, L., Jing, Z., Paudyal, R., Li, Y., Zhang, Y., Yan, F., Li, G., Li, C., 2017. Light-absorbing impurities accelerate glacier melt in the Central Tibetan Plateau. Science of the Total Environment 587-588, 482-490.

Li, X., Kang, S., Zhang, G., Qu, B., Tripathee, L., Paudyal, R., Jing, Z., Zhang, Y., Yan, F., Li, G., Cui, X., Xu, R., Hu, Z., Li, C., 2018c. Light-absorbing impurities in a southern Tibetan Plateau glacier: Variations and potential impact on snow albedo and radiative forcing. Atmospheric Research 200, 77-87.

Liu, B., Cong, Z., Wang, Y., Xin, J., Wan, X., Pan, Y., Liu, Z., Wang, Y., Zhang, G., Wang, Z., 2017. Background aerosol over the Himalayas and Tibetan Plateau: observed characteristics of aerosol mass loading. Atmospheric Chemistry & Physics 17, 449-463.

Liu, B., Kang, S., Sun, J., Zhang, Y., Xu, R., Wang, Y., Liu, Y., Cong, Z., 2013. Wet precipitation chemistry at a high-altitude site (3,326 m asl) in the southeastern Tibetan Plateau. Environmental Science and Pollution Research 20, 5013-5027.

Liu, X., Xu, L., Sun, L., Liu, F., Wang, Y., Yan, H., Liu, Y., Luo, Y., Huang, J., 2011. A 400-year record of black carbon flux in the Xisha archipelago, South China Sea and its implication. Marine pollution bulletin 62, 2205-2212.

Liu, Y., Dong, G., Li, S., Dong, Y., 2005. Status, causes and combating suggestions of sandy desertification in Qinghai-Tibet Plateau. Chinese geographical science 15, 289-296.

Liu, Y., Wang, Y., Pan, Y., Piao, S., 2015. Wet deposition of atmospheric inorganic nitrogen at five remote sites in the Tibetan Plateau. Atmospheric Chemistry and Physics 15, 11683-11700.

Ma, Y., Wang, Y., Zhong, L., Wu, R., Wang, S., Li, M., 2011. The characteristics of atmospheric turbulence and radiation energy transfer and the structure of atmospheric boundary layer over the northern slope area of Himalaya. Journal of

the Meteorological Society of Japan. Ser. II 89, 345-353.

Matsuda, K., Sase, H., Murao, N., Fukazawa, T., Khoomsub, K., Chanonmuang, P., Visaratana, T., Khummongkol, P., 2012. Dry and wet deposition of elemental carbon on a tropical forest in Thailand. Atmospheric Environment 54, 282-287.

May, B., Wagenbach, D., Hoffmann, H., Legrand, M., Preunkert, S., Steier, P., 2013. Constraints on the major sources of dissolved organic carbon in Alpine ice cores from radiocarbon analysis over the bomb - peak period. Journal of Geophysical Research: Atmospheres 118, 3319-3327.

McDowell, W.H., Likens, G.E., 1988. Origin, composition, and flux of dissolved organic carbon in the Hubbard Brook Valley. Ecological Monographs 58, 177-195.

Ming, J., Cachier, H., Xiao, C., Qin, D., Kang, S., Hou, S., Xu, J., 2008. Black carbon record based on a shallow Himalayan ice core and its climatic implications. Atmospheric Chemistry and Physics 8, 1343-1352.

Ming, J., Xiao, C., Du, Z., Yang, X., 2013. An overview of black carbon deposition in High Asia glaciers and its impacts on radiation balance. Advances in Water Resources 55, 80-87.

Ming, J., Xiao, C., Sun, J., Kang, S., Bonasoni, P., 2010. Carbonaceous particles in the atmosphere and precipitation of the Nam Co region, central Tibet. Journal of Environmental Sciences 22, 1748-1756.

Miyazaki, Y., Kondo, Y., Takegawa, N., Komazaki, Y., Fukuda, M., Kawamura, K., Mochida, M., Okuzawa, K., Weber, R., 2006. Time-resolved measurements of water-soluble organic carbon in Tokyo. Journal of Geophysical Research: Atmospheres 111, doi: 10.1029/2006JD007125.

Niu, H., Kang, S., Lu, X., Shi, X., 2018. Distributions and light absorption property of water soluble organic carbon in a typical temperate glacier, southeastern Tibetan Plateau. Tellus B: Chemical and Physical Meteorology 70, 1-15.

Niu, H., Kang, S., Shi, X., Zhang, G., Wang, S., Pu, T., 2019. Dissolved organic carbon in summer precipitation and its wet deposition flux in the Mt. Yulong region, southeastern Tibetan Plateau. Journal of Atmospheric Chemistry 76, 1-20.

Ogren, J., 1982. Deposition of particulate elemental carbon from the atmosphere, Particulate Carbon. Springer, pp. 379-391.

Ogren, J., Charlson, R., 1983. Elemental carbon in the atmosphere: cycle and lifetime. Tellus B 35, 241-254.

Ogren, J., Groblicki, P., Charlson, R., 1984. Measurement of the removal rate of elemental carbon from the atmosphere. Science of the Total Environment 36, 329-338.

Ogren, J.A., Charlson, R.J., Groblicki, P.J., 1983. Determination of elemental carbon in rainwater. Analytical chemistry 55, 1569-1572.

Pan, Y., Wang, Y., Xin, J., Tang, G., Song, T., Wang, Y., Li, X., Wu, F., 2010. Study on dissolved organic carbon in precipitation in Northern China. Atmospheric Environment 44, 2350-2357.

Petzold, A., Ogren, J.A., Fiebig, M., Laj, P., Li, S.M., Baltensperger, U., Holzer-Popp, T., Kinne, S., Pappalardo, G., Sugimoto, N., Wehrli, C., Wiedensohler, A., Zhang, X.Y., 2013. Recommendations for reporting "black carbon" measurements. Atmospheric Chemistry and Physics 13, 8365-8379.

Pio, C.A., Legrand, M., Oliveira, T., Afonso, J., Santos, C., Caseiro, A., Fialho, P., Barata, F., Puxbaum, H., Sanchez-Ochoa, A., Kasper-Giebl, A., Gelencsér, A., Preunkert, S., Schock, M., 2007. Climatology of aerosol composition (organic versus inorganic) at nonurban sites on a west-east transect across Europe. Journal of Geophysical Research 112, doi: 10.1029/2006JD008038.

Polidori, A., Turpin, B.J., Davidson, C.I., Rodenburg, L.A., Maimone, F., 2008. Organic $PM_{2.5}$: Fractionation by Polarity, FTIR Spectroscopy, and OM/OC Ratio for the Pittsburgh Aerosol. Aerosol Science and Technology 42, 233-246.

Prado-Fiedler, R., 1990. On the relationship between precipitation amount and wet deposition of nitrate and ammonium. Atmospheric Environment. Part A. General Topics 24, 3061-3065.

Qian, Y., Yasunari, T.J., Doherty, S.J., Flanner, M.G., Lau, W.K.M., Ming, J., Wang, H., Wang, M., Warren, S.G., Zhang, R., 2014. Light-absorbing particles in snow and ice: Measurement and modeling of climatic and hydrological impact. Advances in Atmospheric Sciences 32, 64-91.

Qin, D., Ding, Y., Xiao, C., Kang, S., Ren, J., Yang, J., Zhang, S., 2017. Cryospheric Science: research framework and disciplinary system. National Science Review 5, 255-268.

Qiu, J., 2008. China: the third pole. Nature News 454, 393-396.

Qu, B., Ming, J., Kang, S., Zhang, G., Li, Y., Li, C., Zhao, S., Ji, Z., Cao, J., 2014. The decreasing albedo of the Zhadang glacier on western Nyainqentanglha and the role of light-absorbing impurities. Atmospheric Chemistry and Physics 14, 11117-11128.

Quinn, P., Stohl, A., Arneth, A., Berntsen, T., Burkhart, J., Christensen, J., Flanner, M., Kupiainen, K., Lihavainen, H., Shepherd, M., 2000. The impact of black carbon on Arctic climate. Arctic Monitoring and Assessment Programme, Oslo. 72 pp. ISBN – 978-82-7971-069-1.

Ramanathan, V., Carmichael, G., 2008. Global and regional climate changes due to black carbon. Nature Geoscience 1, 221-227.

Ramanathan, V., Chung, C., Kim, D., Bettge, T., Buja, L., Kiehl, J.T., Washington, W.M., Fu, Q., Sikka, D.R., Wild, M., 2005. Atmospheric brown clouds: impacts on South Asian climate and hydrological cycle. Proceedings of the National

Academy of Sciences of the USA 102, 5326-5333.

Ramanathan, V., Ramana, M.V., Roberts, G., Kim, D., Corrigan, C., Chung, C., Winker, D., 2007. Warming trends in Asia amplified by brown cloud solar absorption. Nature 448, 575.

Raymond, P.A., 2005. The composition and transport of organic carbon in rainfall: Insights from the natural (^{13}C and ^{14}C) isotopes of carbon. Geophysical Research Letters 32, L14402, doi:14410.11029/12005GL022879.

Ruppel, M.M., Gustafsson, O.r., Rose, N.L., Pesonen, A., Yang, H., Weckström, J., Palonen, V., Oinonen, M.J., Korhola, A., 2015. Spatial and temporal patterns in black carbon deposition to dated Fennoscandian Arctic lake sediments from 1830 to 2010. Environmental Science & Technology 49, 13954-13963.

Ruppel, M.M., Isaksson, I., Ström, J., Beaudon, E., Svensson, J., Pedersen, C.A., Korhola, A., 2014. Increase in elemental carbon values between 1970 and 2004 observed in a 300-year ice core from Holtedahlfonna (Svalbard). Atmospheric Chemistry and Physics 14, 11447-11460.

Saleh, R., Hennigan, C.J., McMeeking, G.R., Chuang, W.K., Robinson, E.S., Coe, H., Donahue, N.M., Robinson, A.L., 2013. Absorptivity of brown carbon in fresh and photo-chemically aged biomass-burning emissions. Atmospheric Chemistry and Physics 13, 7683-7693.

Sandnes, H., 1993. Calculated budgets for airborne acidifying components in Europe, 1985, 1987, 1988, 1989, 1990, 1991 and 1992. EMEP/MSC-W Report 1/92, MSC-W, Oslo, Norway.

Saxena, P., Hildemann, L.M., 1996. Water-soluble organics in atmospheric particles: A critical review of the literature and application of thermodynamics to identify candidate compounds. Journal of Atmospheric Chemistry 24, 57-109.

Schauer, J.J., Kleeman, M.J., Cass, G.R., Simoneit, B.R., 2001. Measurement of emissions from air pollution sources. 3. C1−C29 organic compounds from fireplace combustion of wood. Environmental Science & Technology 35, 1716-1728.

Seinfeld, J.H., Pankow, J.F., 2003. Organic atmospheric particulate material. Annual Review of Physical Chemistry 54, 121-140.

Sharma, S., Ishizawa, M., Chan, D., Lavoué, D., Andrews, E., Eleftheriadis, K., Maksyutov, S., 2013. 16-year simulation of Arctic black carbon: Transport, source contribution, and sensitivity analysis on deposition. Journal of Geophysical Research: Atmospheres 118, 943-964.

Shen, S.S., Yao, R., Ngo, J., Basist, A.M., Thomas, N., Yao, T., 2015. Characteristics of the Tibetan Plateau snow cover variations based on daily data during 1997–2011. Theoretical and Applied Climatology 120, 445-453.

Singer, G.A., Fasching, C., Wilhelm, L., Niggemann, J., Steier, P., Dittmar, T., Battin,

T.J., 2012. Biogeochemically diverse organic matter in Alpine glaciers and its downstream fate. Nature Geoscience 5, 710.

Siudek, P., Frankowski, M., Siepak, J., 2015. Seasonal variations of dissolved organic carbon in precipitation over urban and forest sites in central Poland. Environmental Science and Pollution Research 22, 11087-11096.

Spencer, R.G., Guo, W., Raymond, P.A., Dittmar, T., Hood, E., Fellman, J., Stubbins, A., 2014. Source and biolability of ancient dissolved organic matter in glacier and lake ecosystems on the Tibetan Plateau. Geochimica et Cosmochimica Acta 142, 64-74.

Stocker, T.F., Qin, D., Plattner, G., Tignor, M., Allen, S., Boschung, J., Nauels, A., Xia, Y., Bex, V., Midgley, P., 2013. Climate change 2013: the physical science basis. Intergovernmental panel on climate change, working group I contribution to the IPCC fifth assessment report (AR5). New York.

Stubbins, A., Hood, E., Raymond, P.A., Aiken, G.R., Sleighter, R.L., Hernes, P.J., Butman, D., Hatcher, P.G., Striegl, R.G., Schuster, P., 2012. Anthropogenic aerosols as a source of ancient dissolved organic matter in glaciers. Nature Geoscience 5, doi: 10.1038/NGEO1403.

Sun, H., Biedermann, L., Bond, T.C., 2007. Color of brown carbon: A model for ultraviolet and visible light absorption by organic carbon aerosol. Geophysical Research Letters 34, doi: 10.1029/2007GL029797.

Szidat, S., Jenk, T.M., Synal, H.A., Kalberer, M., Wacker, L., Hajdas, I., Kasper‐Giebl, A., Baltensperger, U., 2006. Contributions of fossil fuel, biomass‐burning, and biogenic emissions to carbonaceous aerosols in Zurich as traced by ^{14}C. Journal of Geophysical Research: Atmospheres 111, doi: 10.1029/2005JD006590.

Textor, C., Schulz, M., Guibert, S., Kinne, S., Balkanski, Y., Bauer, S., Berntsen, T., Berglen, T., Boucher, O., Chin, M., 2006. Analysis and quantification of the diversities of aerosol life cycles within AeroCom. Atmospheric Chemistry & Physics 5, 8331-8420.

Torres, A., Bond, T.C., Lehmann, C.M.B., Subramanian, R., Hadley, O.L., 2013. Measuring Organic Carbon and Black Carbon in Rainwater: Evaluation of Methods. Aerosol Science and Technology 48, 239-250.

Tsyro, S., Simpson, D., Tarrasón, L., Klimont, Z., Kupiainen, K., Pio, C., Yttri, K.E., 2007. Modeling of elemental carbon over Europe. Journal of Geophysical Research 112, doi: 10.1029/2006JD008164.

Wan, D., Jin, Z., Wang, Y., 2012. Geochemistry of eolian dust and its elemental contribution to Lake Qinghai sediment. Applied geochemistry 27, 1546-1555.

Wang, J., Zhu, L., Wang, Y., Gao, S., Daut, G., 2011a. Spatial variability of recent sedimentation rate and variations in the past 60 years in Nam Co, Tibetan Palteau, China. Quaternary Sciences 31, 535-543.

Wang, Q., Cao, J., Han, Y., Tian, J., Zhu, C., Zhang, Y., Zhang, N., Shen, Z., Ni, H., Zhao, S., 2018. Sources and physicochemical characteristics of black carbon aerosol from the southeastern Tibetan Plateau: internal mixing enhances light absorption. Atmospheric Chemistry and Physics 18, 4639-4656.

Wang, S., Wang, J., Zhou, Z., Shang, K., 2005. Regional characteristics of three kinds of dust storm events in China. Atmospheric Environment 39, 509-520.

Wang, X., Xu, B., Kang, S., Cong, Z., Yao, T., 2008. The historical residue trends of DDT, hexachlorocyclohexanes and polycyclic aromatic hydrocarbons in an ice core from Mt. Everest, central Himalayas, China. Atmospheric Environment 42, 6699-6709.

Wang, Y., Xin, J., Li, Z., Wang, S., Wang, P., Hao, W.M., Nordgren, B.L., Chen, H., Wang, L., Sun, Y., 2011b. Seasonal variations in aerosol optical properties over China. Journal of Geophysical Research: Atmospheres 116, doi: 10.1029/2010JD015376.

Willey, J.D., Kieber, R.J., Eyman, M.S., Avery Jr, G.B., 2000. Rainwater dissolved organic carbon: concentrations and global flux. Global biogeochemical cycles 14, 139-148.

Wu, G., Ram, K., Fu, P., Wang, W., Zhang, Y., Liu, X., Stone, E.A., Pradhan, B.B., Dangol, P.M., Panday, A.K., 2019. Water-Soluble Brown Carbon in Atmospheric Aerosols from Godavari (Nepal), a Regional Representative of South Asia. Environmental Science & Technology 53, 3471-3479.

Wu, Y., Zhu, L., Ye, Q., Wang, L., 2007. The response of lake-glacier area change to climate variations in Namco Basin, Central Tibetan Plateau, during the last three decades. ACTA GEOGRAPHICA SINICA-CHINESE EDITION- 62, 311.

Xia, X., Zong, X., Cong, Z., Chen, H., Kang, S., Wang, P., 2011. Baseline continental aerosol over the central Tibetan plateau and a case study of aerosol transport from South Asia. Atmospheric Environment 45, 7370-7378.

Xu, B., Cao, J., Hansen, J., Yao, T., Joswia, D.R., Wang, N., Wu, G., Wang, M., Zhao, H., Yang, W., 2009. Black soot and the survival of Tibetan glaciers. Proceedings of the National Academy of Sciences 106, 22114-22118.

Xu, B., Cao, J., Joswiak, D.R., Liu, X., Zhao, H., He, J., 2012. Post-depositional enrichment of black soot in snow-pack and accelerated melting of Tibetan glaciers. Environmental Research Letters 7, doi: 10.1088/1748-9326/1087/1081/014022.

Xu, J., Zhang, Q., Shi, J., Ge, X., Xie, C., Wang, J., Kang, S., Zhang, R., Wang, Y., 2018. Chemical characteristics of submicron particles at the central Tibetan Plateau: insights from aerosol mass spectrometry. Atmospheric Chemistry and Physics 18, 427-443.

Yan, C., Zheng, M., Sullivan, A.P., Bosch, C., Desyaterik, Y., Andersson, A., Li, X., Guo, X., Zhou, T., Gustafsson, Ö., 2015. Chemical characteristics and

light-absorbing property of water-soluble organic carbon in Beijing: Biomass burning contributions. Atmospheric Environment 121, 4-12.

Yan, F., Kang, S., Li, C., Zhang, Y., Qin, X., Li, Y., Zhang, X., Hu, Z., Chen, P., Li, X., Qu, B., Sillanpää, M., 2016. Concentration, sources and light absorption characteristics of dissolved organic carbon on a medium-sized valley glacier, northern Tibetan Plateau. The Cryosphere 10, 2611-2621.

Yan, G., Kim, G., 2012. Dissolved organic carbon in the precipitation of Seoul, Korea: Implications for global wet depositional flux of fossil-fuel derived organic carbon. Atmospheric Environment 59, 117-124.

Yan, J., Wang, X., Gong, P., Wang, C., Cong, Z., 2018. Review of brown carbon aerosols: Recent progress and perspectives. Science of the Total Environment 634, 1475-1485.

Yanai, M., Wu, G.-X., 2006. Effects of the tibetan plateau, The Asian Monsoon. Springer, pp. 513-549.

Yang, H., 2015. Lake Sediments May Not Faithfully Record Decline of Atmospheric Pollutant Deposition. Environmental Science & Technology 49, 12607-12608.

Yang, T., Guilin, H., Zhifang, X., 2014. Atmospheric Black Carbon Deposit in Beijing and Zhangbei, China. Procedia Earth and Planetary Science 10, 383-387.

Yao, T., Thompson, L., Yang, W., Yu, W., Gao, Y., Guo, X., Yang, X., Duan, K., Zhao, H., Xu, B., 2012a. Different glacier status with atmospheric circulations in Tibetan Plateau and surroundings. Nature Climate Change 2, doi: 10.1038/NCLIMATE1580.

Yao, T., Thompson, L.G., Mosbrugger, V., Zhang, F., Ma, Y., Luo, T., Xu, B., Yang, X., Joswiak, D.R., Wang, W., Joswiak, M.E., Devkota, L.P., Tayal, S., Jilani, R., Fayziev, R., 2012b. Third Pole Environment (TPE). Environmental Development 3, 52-64.

Yasunari, T.J., Bonasoni, P., Laj, P., Fujita, K., Vuillermoz, E., Marinoni, A., Cristofanelli, P., Duchi, R., Tartari, G., Lau, K.M., 2010. Estimated impact of black carbon deposition during pre-monsoon season from Nepal Climate Observatory – Pyramid data and snow albedo changes over Himalayan glaciers. Atmospheric Chemistry and Physics 10, 6603-6615.

You, Q., Kang, S., Li, C., Li, M., Liu, J., 2007. Variation Features of Meteorological Elements at Namco Station, Tibetan Plateau. Meteorological 33, 54-60.

You, Q., Min, J., Kang, S., 2016. Rapid warming in the Tibetan Plateau from observations and CMIP5 models in recent decades. International Journal of Climatology 36, 2660-2670.

Zhan, C., Cao, J., Han, Y., Wang, P., Huang, R., Wei, C., Hu, W., Zhang, J., 2015. Spatial patterns, storages and sources of black carbon in soils from the catchment of Q inghai L ake, C hina. European Journal of Soil Science 66, 525-534.

Zhang, L., Gong, S., Padro, J., Barrie, L., 2001. A size-segregated particle dry deposition scheme for an atmospheric aerosol module. Atmospheric Environment 35, 549-560.

Zhang, Q., Shen, Z., Cao, J., Zhang, R., Zhang, L., Huang, R.-J., Zheng, C., Wang, L., Liu, S., Xu, H., 2015a. Variations in $PM_{2.5}$, TSP, BC, and trace gases (NO_2, SO_2, and O_3) between haze and non-haze episodes in winter over Xi'an, China. Atmospheric Environment 112, 64-71.

Zhang, R., Wang, H., Qian, Y., Rasch, P.J., Easter, R.C., Ma, P.-L., Singh, B., Huang, J., Fu, Q., 2015b. Quantifying sources, transport, deposition, and radiative forcing of black carbon over the Himalayas and Tibetan Plateau. Atmospheric Chemistry and Physics 15, 6205-6223.

Zhang, X., Lin, Y.H., Surratt, J.D., Weber, R.J., 2013. Sources, composition and absorption Angstrom exponent of light-absorbing organic components in aerosol extracts from the Los Angeles Basin. Environmental Science & Technology 47, 3685-3693.

Zhang, X., Lin, Y.H., Surratt, J.D., Zotter, P., Prévôt, A.S., Weber, R.J., 2011. Light-absorbing soluble organic aerosol in Los Angeles and Atlanta: A contrast in secondary organic aerosol. Geophysical Research Letters 38, doi: 10.1029/2011GL049385.

Zhang, X., Ming, J., Li, Z., Wang, F., Zhang, G., 2017a. The online measured black carbon aerosol and source orientations in the Nam Co region, Tibet. Environmental Science and Pollution Research 24, 25021-25033.

Zhang, Y.-L., Cerqueira, M., Salazar, G., Zotter, P., Hueglin, C., Zellweger, C., Pio, C., Prévôt, A.S., Szidat, S., 2015c. Wet deposition of fossil and non-fossil derived particulate carbon: Insights from radiocarbon measurement. Atmospheric Environment 115, 257-262.

Zhang, Y., Forrister, H., Liu, J., Dibb, J., Anderson, B., Schwarz, J.P., Perring, A.E., Jimenez, J.L., Campuzano-Jost, P., Wang, Y., Nenes, A., Weber, R.J., 2017b. Top-of-atmosphere radiative forcing affected by brown carbon in the upper troposphere. Nature Geoscience 10, 486-489.

Zhang, Y., Kang, S., Cong, Z., Schmale, J., Sprenger, M., Li, C., Yang, W., Gao, T., Sillanpää, M., Li, X., 2017c. Light-absorbing impurities enhance glacier albedo reduction in the southeastern Tibetan plateau. Journal of Geophysical Research: Atmospheres 122, 6915-6933.

Zhang, Y., Kang, S., Gao, T., Schmale, J., Liu, Y., Zhang, W., Guo, J., Du, W., Hu, Z., Cui, X., Sillanpaa, M., 2019. Dissolved organic carbon in snow cover of the Chinese Altai Mountains, Central Asia: Concentrations, sources and light-absorption properties. Science of the Total Environment 647, 1385-1397.

Zhang, Y., Kang, S., Li, C., Cong, Z., Zhang, Q., 2012. Wet deposition of precipitation

chemistry during 2005–2009 at a remote site (Nam Co Station) in central Tibetan Plateau. Journal of Atmospheric Chemistry 69, 187-200.

Zhao, Z., Cao, J., Shen, Z., Huang, R.-J., Hu, T., Wang, P., Zhang, T., Liu, S., 2015. Chemical composition of $PM_{2.5}$ at a high–altitude regional background site over Northeast of Tibet Plateau. Atmospheric Pollution Research 6, 815-823.

Zhao, Z., Cao, J., Shen, Z., Xu, B., Zhu, C., Chen, L.W.A., Su, X., Liu, S., Han, Y., Wang, G., Ho, K., 2013. Aerosol particles at a high-altitude site on the Southeast Tibetan Plateau, China: Implications for pollution transport from South Asia. Journal of Geophysical Research: Atmospheres 118, 11,360-311,375.

Zhou, X., Zhao, P., Chen, J., Chen, L., Li, W., 2009. Impacts of thermodynamic processes over the Tibetan Plateau on the Northern Hemispheric climate. Science in China Series D: Earth Sciences 52, 1679-1693.

Zhu, L., Xie, M., Wu, Y., 2010. Quantitative analysis of lake area variations and the influence factors from 1971 to 2004 in the Nam Co basin of the Tibetan Plateau. Chinese Science Bulletin 55, 1294-1303.

Publication I

Li, C., Yan, F., Kang, S., Chen, P., Han, X., Hu, Z., Zhang, G., Hong, Y., Gao, S., Qu, B., Zhu, Z., Li, J., Chen, B., Sillanpää, M.

Re-evaluating black carbon in the Himalayas and the Tibetan Plateau: concentrations and deposition

Reprinted with permission from
Atmospheric Chemistry and Physics
Vol. 17, pp. 11899-11912, 2017

Atmos. Chem. Phys., 17, 11899–11912, 2017
https://doi.org/10.5194/acp-17-11899-2017

Atmospheric Chemistry and Physics
Open Access
EGU

Re-evaluating black carbon in the Himalayas and the Tibetan Plateau: concentrations and deposition

Chaoliu Li[1,3,4], Fangping Yan[3], Shichang Kang[2,4], Pengfei Chen[2], Xiaowen Han[1,5], Zhaofu Hu[2,5], Guoshuai Zhang[1], Ye Hong[6], Shaopeng Gao[1], Bin Qu[3], Zhejing Zhu[7], Jiwei Li[7], Bing Chen[7], and Mika Sillanpää[3,8]

[1]Key Laboratory of Tibetan Environment Changes and Land Surface Processes, Institute of Tibetan Plateau Research, Chinese Academy of Sciences, Beijing 100101, China
[2]State Key Laboratory of Cryospheric Sciences, Northwest Institute of Eco-Environment and Resources, Chinese Academy of Sciences, Lanzhou 730000, China
[3]Laboratory of Green Chemistry, Lappeenranta University of Technology, Sammonkatu 12, 50130 Mikkeli, Finland
[4]CAS Center for Excellence in Tibetan Plateau Earth Sciences, Beijing 100101, China
[5]University of Chinese Academy of Sciences, Beijing 100049, China
[6]Institute of Atmospheric Environment, China Meteorological Administration, Shenyang 110166, China
[7]Environmental Research Institute, Shandong University, Jinan 250100, China
[8]Department of Civil and Environmental Engineering, Florida International University, Miami, FL 33174, USA

Correspondence to: Chaoliu Li (lichaoliu@itpcas.ac.cn)

Received: 7 March 2017 – Discussion started: 3 April 2017
Revised: 29 August 2017 – Accepted: 1 September 2017 – Published: 9 October 2017

Abstract. Black carbon (BC) is the second most important warming component in the atmosphere after CO_2. The BC in the Himalayas and the Tibetan Plateau (HTP) has influenced the Indian monsoon and accelerated the retreat of glaciers, resulting in serious consequences for billions of Asian residents. Although a number of related studies have been conducted in this region, the BC concentrations and deposition rates remain poorly constrained. Because of the presence of arid environments and the potential influence of carbonates in mineral dust (MD), the reported BC concentrations in the HTP are overestimated. In addition, large discrepancies have been reported among the BC deposition derived from lake cores, ice cores, snow pits and models. Therefore, the actual BC concentration and deposition values in this sensitive region must be determined. A comparison between the BC concentrations in acid (HCl)-treated and untreated total suspected particle samples from the HTP showed that the BC concentrations previously reported for the Nam Co station (central part of the HTP) and the Everest station (northern slope of the central Himalayas) were overestimated by approximately 52 ± 35 and 39 ± 24 %, respectively, because of the influence of carbonates in MD. Additionally, the organic carbon (OC) levels were overestimated by approximately 22 ± 10 and 22 ± 12 % for the same reason. Based on previously reported values from the study region, we propose that the actual BC concentrations at the Nam Co and Everest stations are 61 and 154 ng m^{-3}, respectively. Furthermore, a comprehensive comparison of the BC deposition rates obtained via different methods indicated that the deposition of BC in HTP lake cores was mainly related to river sediment transport from the lake basin as a result of climate change (e.g., increases in temperature and precipitation) and that relatively little BC deposition occurred via atmospheric deposition. Therefore, previously reported BC deposition rates from lake cores overestimated the atmospheric deposition of BC in the HTP. Correspondingly, BC deposition derived from snow pits and ice cores agreed well with that derived from models, implying that the BC depositions of these two methods reflect the actual values in the HTP. Therefore, based on reported values from snow pits and ice cores, we propose that the BC deposition in the HTP is 17.9 ± 5.3 mg m^{-2} a^{-1}, with higher and lower values appearing along the fringes and central areas of the HTP, respectively. These adjusted BC concentrations and deposition values in the HTP are critical for performing accurate evalua-

Published by Copernicus Publications on behalf of the European Geosciences Union.

tions of other BC factors, such as atmospheric distribution, radiative forcing and chemical transport in the HTP.

1 Introduction

The Himalayas and the Tibetan Plateau (HTP) region is the highest mountain–plateau system in the world and is the source of approximately 10 large rivers in Asia. This region is also sensitive to climate change (Bolch et al., 2012; Kang et al., 2010; You et al., 2010). Black carbon (BC) in and around the HTP has been found to play key roles in climate change patterns in the HTP and Asia, including causing atmospheric warming (Xu et al., 2016; Ramanathan and Carmichael, 2008; Lau et al., 2010; Ji et al., 2015), promoting HTP glacial retreat (Xu et al., 2009; Qu et al., 2014; Li et al., 2017; Zhang et al., 2017b; Ming et al., 2009, 2013), altering monsoon system evolution (Bollasina et al., 2008) and affecting the fresh water supplies of billions of residents across Asia. To date, numerous studies have been conducted on the BC concentrations in the atmosphere (Zhao et al., 2013b; Ming et al., 2010; Cong et al., 2015; Marinoni et al., 2010; Wan et al., 2015) and atmospheric BC deposition as determined from lake core sediments (Han et al., 2015; Cong et al., 2013). However, all of these studies exhibit limitations because of certain special environmental factors in the HTP (e.g., high concentrations of mineral dust (MD) in aerosols and catchment inputs to lake core sediment). Therefore, the above studies should be reinvestigated to better define the actual BC values in the HTP. Therefore, in this article, we discussed the actual concentrations and deposition of BC in the HTP based on data of aerosols collected at two remote stations and previously reported BC deposition data.

At present, the thermal–optical method is a widely used method for measuring BC concentrations in aerosols from the HTP (Zhao et al., 2013b; Ming et al., 2010; Cong et al., 2015; Li et al., 2016d). An important factor influencing the accurate measurement of BC concentrations via this method is the presence of carbonates (inorganic carbon – IC) in MD. IC can also emit CO_2 in response to increasing temperature during measurements, thus causing an overestimation of the total carbon (TC) in carbonaceous aerosols (CAs) (Karanasiou et al., 2011). Hence, IC is generally excluded in CA studies (Bond et al., 2013). However, few studies of the HTP have considered the contributions of IC to TC and BC because one study concluded that IC can be neglected in studies of the TC and BC in midlatitude aerosols because the IC exists at far lower concentrations relative to TC and BC (Chow and Watson, 2002).

This conclusion cannot be blindly applied to other areas because of the complexities of midlatitude environments around the world (e.g., arid areas and deserts with intense dust storm events). For example, previous studies in Xi'an, midwestern and northeastern China showed that IC accounts for approximately 8 % (Cao et al., 2005) to 10 % (Ho et al., 2011) of the TC in particles with diameters less than 2.5 µm ($PM_{2.5}$) during dust storm events. Similar phenomena have also been found for both $PM_{2.5}$ and total suspended particle (TSP) samples in southern Europe (Sillanpää et al., 2005; Perrone et al., 2011). Because TSP samples contain more MD and carbonates than $PM_{2.5}$, they should have higher concentrations of IC.

The above phenomenon should also be taken into consideration in the study of CAs of the HTP. Similar to northern China, large sand dunes and deserts are widely distributed across the western HTP (Liu et al., 2005), and dust storms occur frequently in winter and spring (Wang et al., 2005). Thus, IC may account for a large portion of the CAs in the HTP. Unfortunately, the potential contributions of IC to the TC and BC in HTP aerosols have been overlooked (Cao et al., 2010; Cong et al., 2015; Li et al., 2016b; Ming et al., 2010; Wan et al., 2015; Zhao et al., 2013b). Additionally, IC contributions may be high because almost all of the reported data on CAs are based on the TSP content, which includes large volumes of coarse particles derived directly from MD. Therefore, the TC and BC concentrations in the HTP are likely overestimated. In fact, some published articles on aerosols collected from remote areas of the HTP have identified MD components (Cong et al., 2015; Zhao et al., 2013b), although neither of these two studies have directly discussed this issue or evaluated the effects of IC.

Because MD has lower influences on light than BC in the atmosphere (Clarke et al., 2004; Bond and Bergstrom, 2006) and on glacier surfaces (Qu et al., 2014), considering IC as BC will overestimate the BC-driven climate forcing. Organic carbon (OC) is generally considered to scatter sunlight. However, some components of OC also absorb sunlight and warm the atmosphere (Andreae and Gelencser, 2006). Therefore, the contributions of IC to the OC and BC values in HTP aerosols must be quantitatively evaluated. In this study, TSP samples from two remote stations in the HTP were collected to evaluate the contributions of IC to the TC and BC. Additionally, seasonal variations in the extent of the overestimations of TC and BC and possible causes were also examined. Finally, previously published TC and BC concentrations at these two stations were adjusted (Cong et al., 2015; Zhao et al., 2013a).

BC deposition is closely related to the BC transport processes, lifetime and radiative forcing. Depositional value can be measured from historical media, such as sediments (Gustafsson and Gschwend, 1998; Han et al., 2016) and ice cores (Ming et al., 2007; Ruppel et al., 2014), estimated from BC concentrations in the atmosphere (Jurado et al., 2008) or calculated using models (Zhang et al., 2015). At present, the BC deposition process remains poorly quantified in the HTP because of its complex terrain and dynamic regimes (Bond et al., 2013; Bauer et al., 2013). Thus far, only three studies have directly reported on BC deposition in the HTP. One model indicated that the BC deposition in the central HTP

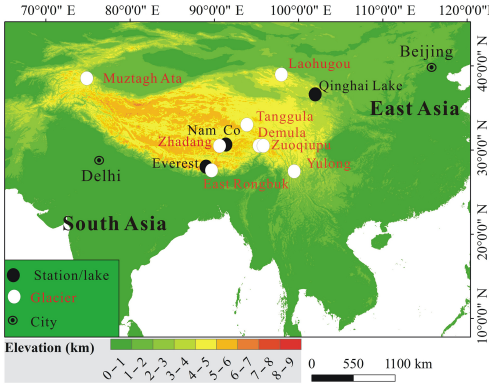

Figure 1. Selected study sites, including the HTP stations, lakes and glaciers.

was 9 mg m^{-2} a^{-1} (Zhang et al., 2015), which is approximately 30 times lower than the values measured in lake cores at Nam Co and Qinghai lakes (270–390 mg m^{-2} a^{-1}) (Fig. 1) (Cong et al., 2013; Han et al., 2011). Although considerable uncertainties exist in atmospheric BC deposition estimated from models (Koch et al., 2009; Bond et al., 2013) and lake core sediments (Yang, 2015; Cohen, 2003), these large differences need to be thoroughly investigated.

For instance, although the influence of sediment focusing on BC deposition in lake cores has been noted in other areas (Yang, 2015; Blais and Kalff, 1995), it has not been pointed out and evaluated in the HTP. Consequently, correcting for this process might result in incorrect data and explanations. Therefore, additional studies must be performed to provide more reliable BC deposition values. For instance, other researchers have reported BC concentrations and water accumulation rates in ice cores and snow pits from the HTP (Fig. 1) (Xu et al., 2009; Li et al., 2016a, c; Ming et al., 2008). Although these studies did not report BC deposition values directly, BC deposition rates could be easily calculated from the data reported in those articles. Because the cols of glaciers where the snow and ice samples were collected are generally located at the highest altitudes of a given region, BC is only deposited via wet and dry deposition from the atmosphere. Therefore, these data need to be comprehensively evaluated.

Notably, some uncertainties exist in the comparison of BC data among different studies. Despite recent technological achievements, accurately measuring BC concentrations in ambient samples remains a challenge in atmospheric chemistry research (Andreae and Gelencser, 2006; Bond et al., 2013; Lim et al., 2014). Because the methods used to measure BC concentrations and determine BC deposition levels are not the same, uncertainties will be introduced when directly comparing the results from different studies. For instance, different thermal–optical methods with different temperature increase protocols (e.g., NIOSH vs. IMPROVE vs. EUSAAR_2) will produce different BC concentrations for the same sample (Karanasiou et al., 2015; Andreae and Gelencser, 2006). In general, BC concentrations derived from the IMPROVE method are 1.2–1.5 times higher than those derived from the NIOSH method (Chow et al., 2001; Reisinger et al., 2008), and BC concentrations from the EUSAAR_2 temperature protocol are approximately twice as high as those derived from the NIOSH protocol (Cavalli et al., 2010). Furthermore, lake core samples need to be pretreated with HCl and hydrofluoric acid (HF) several times prior to measurements with the thermal–optical methods (Han et al., 2015). However, because of the complex chemical properties of ambient samples, the "best" thermal–optical protocol has not been identified (Karanasiou et al., 2015), and an exact ratio for BC produced from different methods is difficult to determine. Therefore, although the direct comparison of BC concentrations and deposition levels across different studies presents certain uncertainties in this study, the comparison between data of lake core and snow pit is still reliable because BC deposition of the former was much higher (approximately 20 times) than that of the latter, up to 7 times more among different methods (Watson et al., 2005). For instance, although large uncertainties exist for BC concentrations within the same environmental matrix (Watson et al., 2005; Hammes et al., 2007; Han et al., 2011), the similarity of the BC deposition values among different glaciers (Table 1) in different studies implies that comparing BC deposition data is feasible for the glacial region in the HTP. In addition, because BC concentrations measured via the SP2 method are far lower than those measured via thermal–optical methods (Lim et al., 2014) (the former can only measure BC in grain sizes finer than 500 nm; Kaspari et al., 2011), SP2-based BC data were avoided in this study.

2 Methods

2.1 Collection of aerosols, surface soils and river sediments

TSP samples were collected from the Nam Co Monitoring and Research Station for Multisphere Interactions and the Qomolangma Atmospheric and Environmental Observation and Research Station (Everest station) (Fig. 1) from 2014 to 2016. The Nam Co station is located in the center of the HTP. The Everest station is located on the northern slopes of the Himalayas. Both of these two stations are generally considered to be located in remote areas of the HTP that receive BC transported over long distances from south Asia, and several BC studies have been conducted there (Chen et al., 2015; Cong et al., 2015; Ming et al., 2010; Li et al., 2016a). In detail, TSP samples were collected using 90 mm pre-combusted

Table 1. Monitored or recovered BC deposition ($mg\,m^{-2}\,a^{-1}$) from the HTP and other regions of the world.

Region	Sites	Deposition	Period	References
Tibet	Zuoqiupu glacier	12	1970–2005	1
	Muztagh Ata	18	1970–2005	1
	East Rongbuk ice core	10.2	1995–2002	2
	Laohugou glacier	25	2013–2014	3, 4
	Tanggula glacier	21.2	2013–2014	3, 4
	Zhangdang glacier	22.8	2013–2014	3, 4
	Demula glacier	14.4	2013–2014	3, 4
	Yulong glacier	20.3	2013–2014	3, 4
	Model results of central Tibetan Plateau	9	2013–2014	5
	Nam Co Lake core	260	1960–2009	6
	Qinghai Lake core	270–390	1770 s–2011	7
	Aerosol of Nam Co station	10.5	2005–2007	8
	Aerosol of Qinghai Lake	92.7	2011–2012	8
East China	Chaohu lake core, East China	1160	1980–2012	9
	Northern China	1660	Around 2010	10
	North China Plain	1500	2008–2009	11

Note: 1: Bauer et al. (2013); 2: BC concentration ($20.3\,ng\,g^{-1}$) and snow accumulation (500 mm) were adopted from Ming et al. (2008) and Li et al. (2016c), respectively; 3: Li et al. (2016c); 4: Li et al. (2016a); 5: Zhang et al. (2015); 6: Cong et al. (2013); 7: Han et al. (2015); 8: calculated in this study; 9: Han et al., (2016); 10: Fang et al. (2015); 11: Tang et al. (2014).

Table 2. Precipitation (mm) and BC concentration ($ng\,m^{-3}$) values used for the BC deposition calculations for Nam Co Lake and Qinghai Lake.

	Nam Co Lake precipitation	BC concentration	Qinghai Lake precipitation	BC concentration
Spring	29.65	135.86	77.51	1000
Summer	190.05	90.97	244.02	530
Autumn	79.72	86.58	89.78	690
Winter	2.95	93.55	3.81	1050

(550 °C, 6 h) quartz fiber filters (Whatman Corp) with a vacuum pump (VT 4.8, Germany). Because the pump was not equipped with a flow meter, the air volumes passing through each filter could not be determined (Li et al., 2016d); however, this did not influence the objectives of this study (e.g., relative concentrations of TC and BC in the original and acid-treated samples). Four field blank filters were also collected from each station by exposing the filters in each sampler without pumping.

To compare the BC concentrations of the Nam Co Lake cores, two surface soil samples and four suspended particle samples from four rivers in the Nam Co Basin were collected during a period of peak river flow in 2015. The $< 20\,\mu m$ fraction of these samples was extracted (Li et al., 2009) and treated (Han et al., 2015) to measure the BC concentrations. In addition, 10 surface soil samples around the Everest station were collected to study the pH values.

2.2 Measurement of BC and elemental concentrations

The carbonates of the collected aerosol samples were removed via a fumigation process involving exposing a subset of samples to a vapor of 37 % hydrochloric acid (HCl) for 24 h. Then, the treated samples were held at 60 °C for over 1 h to remove any acid remaining on the filter (Li et al., 2016a; Pio et al., 2007; Chen et al., 2013; Bosch et al., 2014). The OC and elemental carbon (EC, the common chemical/mass definition of BC) concentrations of both the original and treated samples were measured using a Desert Research Institute (DRI) model 2001 thermal–optical carbon analyzer (Atmoslytic Inc., Calabasas, CA, USA) following the IMPROVE-A protocol (Chow and Watson, 2002). The OC and BC concentrations were determined based on varying transmission signals. To investigate the BC concentration measured by different methods, 16 acid-fumigated aerosol samples were measured following the EUSAAR_2 and NIOSH protocols for comparison with the results of the IMPROVE protocol. The results showed that the TC concentrations of three methods for the

same sample were similar, as suggested by previous research (Chow et al., 2001). The ratios of $BC_{(IMPROVE)}/BC_{(NIOSH)}$ and $BC_{(EUSAAR_2)}/BC_{(NIOSH)}$ for the studied samples were 1.36 ± 0.35 and 1.88 ± 0.60, respectively, both of which agreed with the previously proposed ratios of 1.2–1.5 (Chow et al., 2001; Reisinger et al., 2008) and 2 (Cavalli et al., 2010), respectively. To evaluate the concentrations of MD, the concentrations of Ca, Fe, Al and Ti in the aerosol samples were measured by inductively coupled plasma optical emission spectroscopy (ICP-OES) following the method of Li et al. (2009). All the reported values in this study were corrected based on the values of the blanks. The contributions of MD (Maenhaut et al., 2002) and CA (Ram et al., 2010) of the collected samples were calculated using the following equations:

$$\mathrm{MD} = (1.41 \times \mathrm{Ca} + 2.09 \times \mathrm{Fe} + 1.9 \times \mathrm{Al} + 2.15 \times \mathrm{Si} + 1.67 \times \mathrm{Ti}) \times 1.16, \quad (1)$$

where Si is calculated from Al assuming an average ratio of Si/Al is 2.5 (Carrico et al., 2003), and

$$\mathrm{CA} = \mathrm{OC} \times 1.6 + \mathrm{BC}. \quad (2)$$

2.3 Adoption and calculation of BC deposition data

To determine the actual BC deposition in the HTP, previously reported data were compiled and evaluated (Table 1). In addition, BC deposition rates from the Nam Co station and Qinghai Lake basin were estimated from the average BC concentrations in the atmosphere and average precipitation levels using the method described in detail in other studies (Jurado et al., 2008; Fang et al., 2015) (Table 2). In brief, the annual atmospheric deposition rate of BC ($\mu g\,m^{-2}\,a^{-1}$) was calculated as follows:

$$F_{BC} = F_{DD} + F_{WD} \quad (3)$$

$$F_{DD} = 7.78 \times 10^4 \cdot V_D \cdot C_{BC-TSP} \quad (4)$$

$$F_{WD} = 10^{-3} \cdot P_0 \cdot W_p \cdot C_{BC-TSP}, \quad (5)$$

where F_{DD} and F_{WD} are the seasonal dry and wet deposition ($\mu g\,m^{-2}$), respectively; V_D, P_0 and W_p are the dry deposition velocity of aerosol ($0.15\,cm\,s^{-1}$), the precipitation amount (mm) in a given season and the particle washout ratio (2.0×10^5), respectively (Fang et al., 2015); and C_{BC-TSP} is the BC concentration of the TSPs ($\mu g\,m^{-3}$). The seasonal BC concentrations at the Nam Co station were monitored with an AE-31, and the average precipitation levels at the station were recorded from 2014–2015. The BC concentrations in Qinghai Lake are reported in Zhao et al. (2015), and the average 1961–2010 precipitation levels recorded by the China Meteorological Administration from the Huangyuan station in the lake basin were used. The values used in the BC deposition calculations for these two areas are shown in Table 2.

3 Results and discussion

3.1 Actual BC concentrations in the atmosphere over the HTP

3.1.1 Contribution of carbonate carbon to both TC and BC

In this study, it was shown that carbonate carbon significantly contributes to the BC, TC and OC concentrations of the TSP samples of Nam Co and Everest stations after comparing BC and OC concentrations between original and acid-treated samples. The ratios of the TC, OC and BC levels of the aerosols treated with acid (TC_A, OC_A and BC_A) to those of the original samples (TC_O, OC_O and BC_O) were 0.81 ± 0.13, 0.78 ± 0.10 and 0.48 ± 0.35, respectively, for the Nam Co station and 0.76 ± 0.12, 0.78 ± 0.12 and 0.61 ± 0.24, respectively, for the Everest station. Meanwhile, because of heavy precipitation during monsoon period, influences of IC to both BC and TC during this time were lower than those of non-monsoon period at two studied stations (Fig. 2). As proposed in previous work (Chow and Watson, 2002), BC concentrations are more heavily influenced than OC and TC concentrations because carbonates are more prone to decompose at high temperatures along with BC during analyses. The OC concentrations in the treated samples used in this study also decreased, indicating that carbonates can also decompose at low temperatures (Karanasiou et al., 2011). Clear seasonal variations, i.e., low TC_A/TC_o ratios during non-monsoon periods and high TC_A/TC_o ratios during monsoon periods, were observed in the aerosols at the Nam Co station (Fig. 2). This pattern is consistent with the intense dust storms that occur during non-monsoon periods. However, clear seasonal patterns in the TC_A/TC_o ratio at the Everest station were not observed, in accordance with the relatively stable seasonal variations in the Ca^{2+} content in aerosols recorded at this station (Cong et al., 2015). To evaluate the relative ratio of MD and CA, MD/(MD + CA) values were calculated (Fig. 3). The MD/(MD + CA) levels recorded at the Nam Co station during non-monsoon periods were significantly higher than those recorded during monsoon periods ($p < 0.01$), whereas the corresponding values at the Everest station were not significantly different between the two periods ($p > 0.05$) (Fig. 3). Compared with those of other areas, the MD/(MD + CA) values recorded at the two stations were higher than those recorded at the NCO-P station (27.95° N, 86.82° E; 5079 m.a.s.l) (70 and 73 % for the premonsoon and monsoon periods, respectively) located on the southern slope of the Himalayas (Decesari et al., 2010). This difference may be related to the serious levels of south Asian pollutants at the NCO-P station and the relative ease with which polluted clouds are transported to this station. However, because the measured particle size (PM_{10}) and the measurement methods of Ca, Mg and EC at the NCO-P station

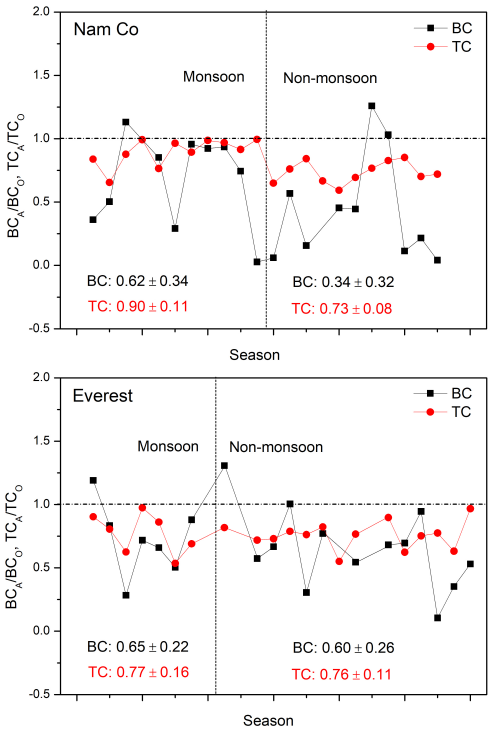

Figure 2. Seasonal variations in the BC and TC concentrations in the original and acid-treated aerosol samples collected at the Nam Co and Everest stations.

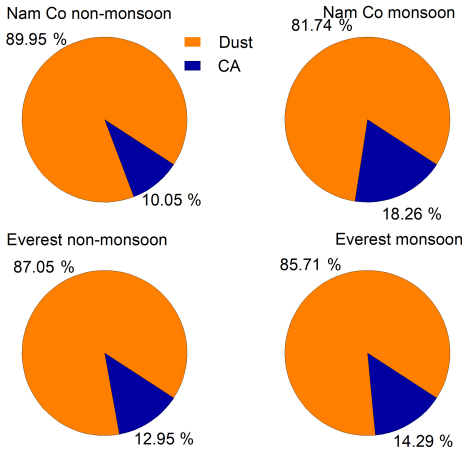

Figure 3. Percentage of MD and CA relative to their sum during both non-monsoon and monsoon periods at the Nam Co and Everest stations.

differed from those in this study, uncertainties exist in such a direct comparison.

The Everest station is located in a dry river valley with sparse vegetation cover (a typical barren site), and the MD derived from the local surface soil contributes considerably to aerosols collected during monsoon periods (Liu et al., 2017). However, the Nam Co station is located in a typical grassland region with limited amounts of locally sourced dust during monsoon periods. Additionally, the Everest station is located in the rain shadow of the Himalayas; thus, the precipitation level recorded at the Everest station (172 mm during the monsoon period between 2014 and 2015) is much lower than that at the Nam Co station (258 mm), causing high MD concentrations in the atmosphere of the Everest station during that period. Potential carbonate-induced biasing of aerosol samples has been proposed to occur in arid areas with alkaline soils (Chow and Watson, 2002). Because of the dry weather conditions, the pH values of the soil around the Nam Co and Everest stations are as high as 8 (Li et al., 2008) and 8.3, respectively, implying considerable carbonate contributions. During non-monsoon periods, MD is mainly transported by westerlies from the arid western HTP, where MD is distributed across large deserts with sand dunes; thus, the aerosol samples were influenced by MD with high concentrations of carbonates. Finally, the significant positive relationship ($p < 0.01$) between Ca and IC (TC_O–TC_A) for the aerosols of these two stations further demonstrated the contributions of $CaCO_3$ to aerosol IC (Fig. 4). The ratio of Ca/IC was higher in the Everest station samples than that of Nam Co station, possibly reflecting different types of carbonate at these two stations.

3.1.2 Actual BC concentrations at the two stations and implications

In summary, we clearly showed that the presence of carbonates in MD led the TC levels in TSP samples in the HTP to be overestimated by approximately 19 ± 13 and 24 ± 12 % at the Nam Co and Everest stations, respectively. These overestimates were higher than the corresponding value of 10 % found for coarse particles in the central Mediterranean region of Europe (Perrone et al., 2011). In addition, the related BC values were overestimated by approximately 52 ± 35 and 39 ± 24 %, respectively, thus implying that the actual BC concentrations at these two stations were lower than previously reported values. Although fumigation with HCl can cause the loss of volatile organic acids in treated samples (Chow et al., 1993), this potential influence is not important because of the significant relationship between TC_O–TC_A and Ca (Fig. 4). Moreover, because of the large variations in the above val-

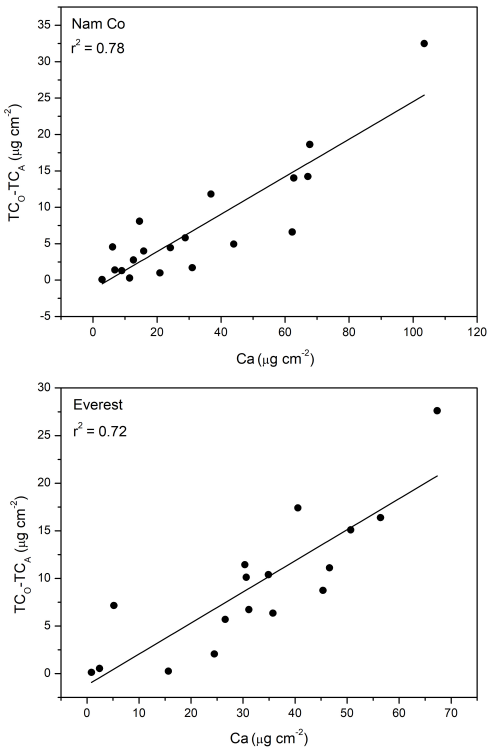

Figure 4. Relationship between aerosol IC and Ca at the Nam Co and Everest stations.

ues, the corrected BC concentrations at the two stations have large uncertainties. Therefore, based on previously reported BC concentrations measured via the same method as in this study (Zhao et al., 2013a; Cong et al., 2015), the actual BC concentrations at the Nam Co and Everest stations were estimated to be 61 and 154 ng m^{-3}, respectively.

Carbonates can decompose at relatively low temperatures during measurement, leading to overestimation of both BC and OC concentrations (Karanasiou et al., 2011). In addition, sometimes the acid-treated ambient samples transfer some components of OC to BC, leading to higher BC concentrations (Jankowski et al., 2008). However, this phenomenon was not common in the aerosol samples examined in this study, although several samples from both stations showed higher BC concentrations in the acid-treated samples (Fig. 2). Because BC_A cannot be higher than BC_O, the samples with BC_A / BC_O values greater than 1 were not included in the above calculations. Nevertheless, the ratio of BC_A / BC_O was considered to be slightly overestimated, as some portion of OC was considered BC in the acid-treated samples (Jankowski et al., 2008).

Since the influence of carbonate carbon on TC has been observed in $PM_{2.5}$ samples from Qinghai Lake, northwest China (Zhao et al., 2015), this phenomenon should be obvious in the TSP samples in this study. Because dust storms in the northern and western parts of the HTP are more severe than those near the two studied stations during the non-monsoon periods, the effect of carbonates on the concentrations of OC and BC should be more pronounced in such areas and must be seriously considered in future studies. Therefore, the overestimation of BC values is likely greater in the northern and western parts of the HTP than near Nam Co, as we noted previously. MD concentrations have been shown to be much higher than BC concentrations in snow and ice core samples from the HTP (Qu et al., 2014; Li et al., 2017). However, numerous studies have measured BC concentrations without using an acid pretreatment step (Qu et al., 2014; Li et al., 2017; Zhang et al., 2017b). Therefore, the contribution of carbonates in MD to the BC concentrations in snow and ice core samples is likely considerable and needs to be quantitatively evaluated in a future study. Similarly, related HTP studies on other issues, such as BC radiative forcing and atmospheric transport models, based on in situ BC concentrations must be adjusted.

3.2 Actual BC deposition in the HTP

3.2.1 Overestimated BC deposition in lake cores from the HTP

In general, the BC deposition levels measured via different methods should be consistent for a given region. For instance, in the severely polluted region of eastern China (Chen et al., 2013; Yan et al., 2015), the BC deposition rate recovered from a Chaohu lake core was 1660 mg m^{-2} a^{-1} (Han et al., 2016), which was close to the values of northern China calculated from the BC concentrations in aerosols (Fang et al., 2015) and determined via in situ monitoring on the North China Plain (Tang et al., 2014) (Table 1). However, this consistency was not the case in the HTP, where large discrepancies were found among the reported HTP BC deposition values. Catchment inputs have been shown to significantly influence the chemical deposition values reconstructed from lake cores (Yang, 2015). For instance, BC deposition rates derived from lake cores of Nam Co Lake (NMC09) and Qinghai Lake were 260 and 270–390 mg m^{-2} a^{-1}, respectively, which were much higher than those derived from ice core and snow pit samples from the HTP (Table 1). We proposed that the BC deposition in the lake cores of Qinghai Lake mainly reflected atmospheric deposition followed by catchment inputs. However, the NMC09 value of Nam Co Lake was mainly influenced by catchment inputs.

Lake-core-derived BC deposition in Qinghai Lake was only 2–3 times higher than that estimated from the BC con-

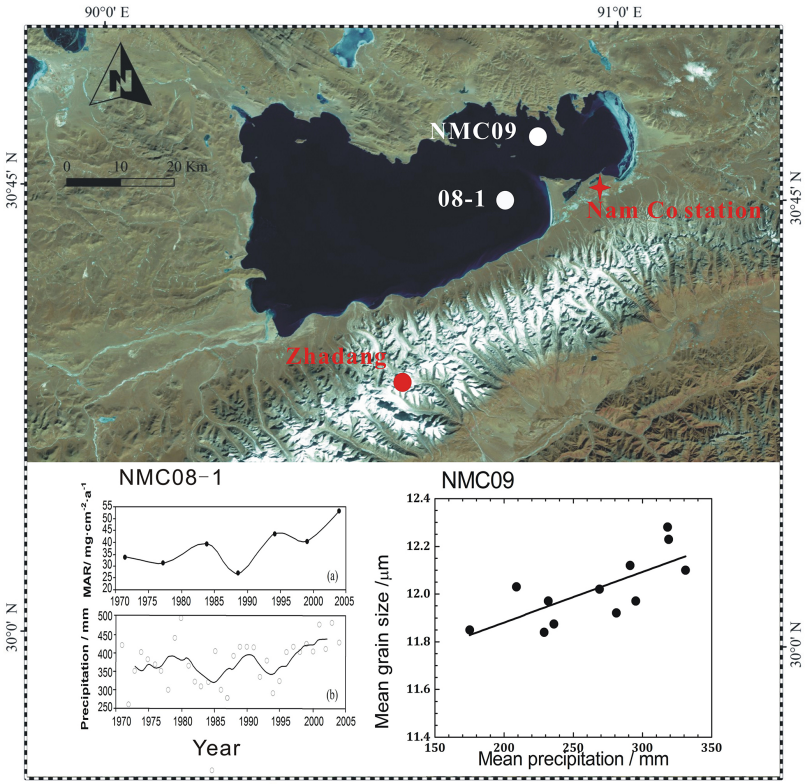

Figure 5. Similar variations in precipitation and mass accumulation rates **(a)** (Wang et al., 2011) and significant relationships between mean precipitation and mean grain size **(b)** (Li et al., 2014) in the Nam Co Lake cores.

centrations of $PM_{2.5}$ in the atmosphere (Zhao et al., 2015). Because $PM_{2.5}$ does not include all particles in the atmosphere, the actual BC concentration in the atmosphere should be higher than that of $PM_{2.5}$ (Li et al., 2016b; Viidanoja et al., 2002); therefore, the atmospheric BC deposition should be more similar to that of a lake core. In addition, a previous study showed that approximately 65 and 22 % of the surface sediments in Qinghai Lake resulted from atmospheric deposition and catchment inputs (Wan et al., 2012), respectively, further demonstrating the significant effects of atmospheric deposition on lake core sediments. Therefore, if the BC deposition from atmospheric particles and that of the lake core are the same, then the atmospheric BC deposition based on Qinghai Lake core data is overestimated by approximately 35 %.

Correspondingly, catchment inputs account for a large proportion of the NMC09 samples. BC is widely distributed throughout environmental materials (e.g., soil and river sediments) because of its inert characteristics (Cornelissen et al., 2005; Bucheli et al., 2004). Therefore, river inputs contribute sediments as well as BC to lakes. For instance, in the Nam Co Basin, BC concentrations within the $< 20\,\mu m$ fraction of surface soil and sediment reach $0.78 \pm 0.48\,mg\,g^{-1}$, which is close to the Nam Co Lake core concentration of $0.74\,mg\,g^{-1}$ (Cong et al., 2013). In addition, several findings have demonstrated the contributions of catchment inputs to Nam Co Lake cores because of the focusing factor, which was shown in the following sections.

First, a large glacial area ($141.88\,km^2$) is present within the Nam Co Basin (Fig. 5), and large volumes of glacier meltwater and sediment flow into the lake annually (Wu et al., 2007). Due to recent increasing temperatures and precipitation in the Nam Co Basin, glacier meltwater accounts for approximately 50.6 % of the lake's volume, which has

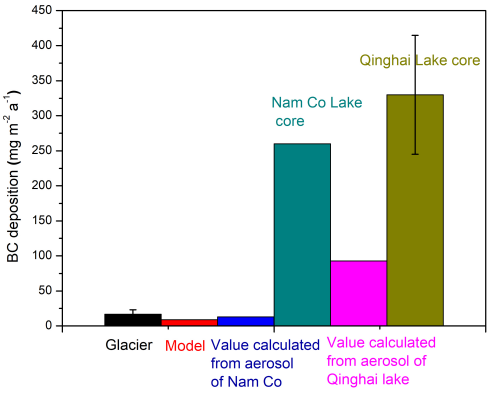

Figure 6. Comparison of atmospheric BC deposition rates derived from the glacial region, models, lake cores and values calculated from BC concentrations in the aerosols of the HTP.

increased over the last 30 years (Zhu et al., 2010). Originating at high-elevation glacier terminal, these rivers flow are at a steep angle, and large volumes of suspended allochthonous sediments are transported into Nam Co Lake annually (Doberschütz et al., 2014). A similar phenomenon was also observed in lake cores of a glacier-fed lake as a result of glacier meltwater effects (Bogdal et al., 2011). Second, previous studies on the accumulation rates in lake cores have revealed significant contributions of riverine particles. The accumulation rates in a Nam Co Lake core (NMC 08-1) are consistent with the precipitation variations recorded in the Nam Co Basin during the last 60 years (Fig. 5a) (Wang et al., 2011), indicating that heavy precipitation promotes the transport of large riverine particles to the lake, thus increasing the accumulation rates in the lake cores. Interestingly, the mean grain size of the lake core (NMC09) that reported BC atmospheric deposition showed a significant positive relationship with precipitation (Fig. 5b), thus reflecting the same relationship between catchment inputs and lake core accumulation rates (Li et al., 2014). Because these two lake cores were drilled from different sites (Fig. 5), their similar catchment input characteristics reflect a common feature of Nam Co sediment. As shown above, the BC concentrations in the fine fraction of the river sediments are nearly equivalent to those in the lake cores; thus, additional catchment inputs will increase the BC deposition rates within lake cores. Third, the atmospheric BC deposition rate calculated from BC concentrations in the atmosphere is much lower than the BC deposition rate recorded in the Nam Co Lake cores (Fig. 6), further reflecting the dominant contributions of catchment inputs relative to atmospheric inputs in lake cores.

The above evidence demonstrates that variations in the BC deposition in Nam Co Lake mainly reflect variations in catchment inputs rather than in atmospheric inputs; thus, atmospheric deposition plays a minor role relative to catchment inputs. Because most lakes in the HTP have increased in area over the last 20 years (Zhang et al., 2017a), this phenomenon likely occurs in many other lakes in the HTP.

3.2.2 Actual atmospheric BC deposition and potential uncertainties

BC deposition rates derived from ice cores and snow pits are proposed to be closer to the actual atmospheric values in the HTP. This hypothesis is supported by two lines of evidence. First, BC deposition levels in the snow pits of different glaciers are consistent. For example, the estimated BC deposition rates of Laohugou, Tanggula, Zhadang, Demula and Yulong are 25, 21.3, 20, 14.5 and 20.2 $\mathrm{mg\,m^{-2}\,a^{-1}}$, respectively (Table 1), which reflects a homogeneous spatial distribution in BC deposition. The above values are also similar to those of ice cores described in other articles (e.g., 18, 12 and 10.1 $\mathrm{mg\,m^{-2}\,a^{-1}}$ for the Muztagh Ata, Zuoqiupu and east Rongbuk glaciers, respectively (Xu et al., 2009; Bauer et al., 2013; Ming et al., 2008) (Table 1). Second, these values are nearly equivalent to those of atmospheric BC deposition rates derived from completely different methods (e.g., Community Atmosphere Model version 5 (Zhang et al., 2015) and other models (Bauer et al., 2013) (Table 1). In summary, despite some uncertainties associated with the remote study area, the atmospheric BC deposition rate of $17.9 \pm 5.3\ \mathrm{mg\,m^{-2}\,a^{-1}}$ in the glacial region of the HTP is proposed.

4 Conclusions

The BC concentration and deposition in the HTP region, which features the largest glacial area in the middle latitudes, were investigated and re-evaluated in this article. Our findings indicated that carbonate carbon contributions from MD have led to overestimations of approximately 52 ± 35 and 39 ± 24 % in previously reported BC concentrations in TSP samples at the remote Nam Co and Everest stations, respectively, in the central and southern HTP. After omitting the contributions of carbonate carbon, the actual BC concentrations at the Nam Co and Everest stations should be 61 and $154\ \mathrm{ng\,m^{-3}}$, respectively. In addition, the levels of OC and TC in TSP samples were also overestimated by 22 ± 10 and 19 ± 13 %, respectively, at the Nam Co station and by 22 ± 12 and 24 ± 12 %, respectively, at the Everest station. These values of TC were close to those of a study in the western HTP (Cao et al., 2009). Large arid areas that receive little precipitation are distributed across the western and northern HTP; thus, the effects of carbonates on BC measurements are expected to be greater in these areas and must be considered in future related studies. In addition, TSP samples must be treated with acid to eliminate the effects of carbonates prior to measuring BC. A comparison among BC deposition val-

ues based on different methods and materials showed that, because of catchment inputs, the BC deposition rates derived from HTP lake cores were higher than the actual atmospheric deposition values. Correspondingly, the BC deposition values measured from snow pits and ice cores in glacial regions were similar to those obtained via models; thus, these data reflect the actual atmospheric BC deposition values. Although the HTP is located adjacent to seriously polluted regions in south Asia and east China, the HTP BC deposition rates are relatively low because of the high elevation. Finally, our results indicate that the atmospheric BC deposition rate in the HTP is approximately $17.9 \pm 5.3\,\mathrm{mg\,m^{-2}\,a^{-1}}$, with lower and higher values appearing in the central and peripheral areas of the HTP, respectively.

Data availability. All the data reported in this article are available upon request. Please contact the corresponding author (Chaoliu Li, lichaoliu@itpcas.ac.cn).

Competing interests. The authors declare that they have no conflict of interest.

Special issue statement. This article is part of the special issue "Atmospheric pollution in the Himalayan foothills: the SusKat-ABC international air pollution measurement campaign". It is not associated with a conference.

Acknowledgements. This study was supported by the NSFC (41630754, 41675130), the State Key Laboratory of Cryospheric Science (SKLCS-ZZ-2017) and the China Postdoctoral Science Foundation (2016M602897). This study is part of a framework across the HTP: atmospheric Pollution and Cryospheric Change (APCC). Additionally, the authors thank the staff of the Nam Co and Everest stations for collecting samples and providing precipitation data.

Edited by: Ernest Weingartner
Reviewed by: two anonymous referees

References

Andreae, M. O. and Gelencser, A.: Black carbon or brown carbon? The nature of light-absorbing carbonaceous aerosols, Atmos. Chem. Phys., 6, 3131–3148, https://doi.org/10.5194/acp-6-3131-2006, 2006.

Bauer, S. E., Bausch, A., Nazarenko, L., Tsigaridis, K., Xu, B., Edwards, R., Bisiaux, M., and McConnell, J.: Historical and future black carbon deposition on the three ice caps: ice core measurements and model simulations from 1850 to 2100, J. Geophys. Res.-Atmos., 118, 7948–7961, 2013.

Blais, J. M. and Kalff, J.: The influence of lake morphometry on sediment focusing, Limnol. Oceanogr., 40, 582–588, 1995.

Bogdal, C., Bucheli, T. D., Agarwal, T., Anselmetti, F. S., Blum, F., Hungerbühler, K., Kohler, M., Schmid, P., Scheringer, M., and Sobek, A.: Contrasting temporal trends and relationships of total organic carbon, black carbon, and polycyclic aromatic hydrocarbons in rural low-altitude and remote high-altitude lakes, J. Environ. Monitor., 13, 1316–1326, 2011.

Bolch, T., Kulkarni, A., Kääb, A., Huggel, C., Paul, F., Cogley, J. G., Frey, H., Kargel, J. S., Fujita, K., and Scheel, M.: The state and fate of Himalayan glaciers, Science, 336, 310–314, 2012.

Bollasina, M., Nigam, S., and Lau, K. M.: Absorbing aerosols and summer monsoon evolution over South Asia: an observational portrayal, J. Clim., 21, 3221–3239, https://doi.org/10.1175/2007jcli2094.1, 2008.

Bond, T. C. and Bergstrom, R. W.: Light absorption by carbonaceous particles: an investigative review, Aerosol Sci. Tech., 40, 27–67, 2006.

Bond, T. C., Doherty, S. J., Fahey, D. W., Forster, P. M., Berntsen, T., DeAngelo, B. J., Flanner, M. G., Ghan, S., Kaercher, B., Koch, D., Kinne, S., Kondo, Y., Quinn, P. K., Sarofim, M. C., Schultz, M. G., Schulz, M., Venkataraman, C., Zhang, H., Zhang, S., Bellouin, N., Guttikunda, S. K., Hopke, P. K., Jacobson, M. Z., Kaiser, J. W., Klimont, Z., Lohmann, U., Schwarz, J. P., Shindell, D., Storelvmo, T., Warren, S. G., and Zender, C. S.: Bounding the role of black carbon in the climate system: a scientific assessment, J. Geophys. Res.-Atmos., 118, 5380–5552, https://doi.org/10.1002/jgrd.50171, 2013.

Bosch, C., Andersson, A., Kirillova, E. N., Budhavant, K., Tiwari, S., Praveen, P., Russell, L. M., Beres, N. D., Ramanathan, V., and Gustafsson, Ö.: Source-diagnostic dual-isotope composition and optical properties of water-soluble organic carbon and elemental carbon in the South Asian outflow intercepted over the Indian Ocean, J. Geophys. Res.-Atmos., 119, 11743–711759, 2014.

Bucheli, T. D., Blum, F., Desaules, A., and Gustafsson, Ö.: Polycyclic aromatic hydrocarbons, black carbon, and molecular markers in soils of Switzerland, Chemosphere, 56, 1061–1076, 2004.

Cao, J. J., Lee, S. C., Zhang, X. Y., Chow, J. C., An, Z. S., Ho, K. F., Watson, J. G., Fung, K., Wang, Y. Q., and Shen, Z. X.: Characterization of airborne carbonate over a site near Asian dust source regions during spring 2002 and its climatic and environmental significance, J. Geophys. Res.-Atmos., 110, D03203, https://doi.org/10.1029/2004jd005244, 2005.

Cao, J.-J., Xu, B.-Q., He, J.-Q., Liu, X.-Q., Han, Y.-M., Wang, G.-H., and Zhu, C.-S.: Concentrations, seasonal variations, and transport of carbonaceous aerosols at a remote Mountainous region in western China, Atmos. Environ., 43, 4444–4452, https://doi.org/10.1016/j.atmosenv.2009.06.023, 2009.

Cao, J., Tie, X., Xu, B., Zhao, Z., Zhu, C., Li, G., and Liu, S.: Measuring and modeling black carbon (BC) contamination in the SE Tibetan Plateau, J. Atmos. Chem., 67, 45–60, https://doi.org/10.1007/s10874-011-9202-5, 2010.

Carrico, C. M., Bergin, M. H., Shrestha, A. B., Dibb, J. E., Gomes, L., and Harris, J. M.: The importance of carbon and mineral dust to seasonal aerosol properties in the Nepal Himalaya, Atmos. Environ., 37, 2811–2824, https://doi.org/10.1016/S1352-2310(03)00197-3, 2003.

Cavalli, F., Viana, M., Yttri, K. E., Genberg, J., and Putaud, J. P.: Toward a standardised thermal-optical protocol for measuring atmospheric organic and elemental carbon: the EUSAAR protocol, Atmos. Meas. Tech., 3, 79–89, https://doi.org/10.5194/amt-3-79-2010, 2010.

Chen, B., Andersson, A., Lee, M., Kirillova, E. N., Xiao, Q., Krusa, M., Shi, M., Hu, K., Lu, Z., Streets, D. G., Du, K., and Gustafsson, O.: Source forensics of black carbon aerosols from China, Environ. Sci. Technol., 47, 9102–9108, https://doi.org/10.1021/es401599r, 2013.

Chen, P., Kang, S., Bai, J., Sillanpää, M., and Li, C.: Yak dung combustion aerosols in the Tibetan Plateau: chemical characteristics and influence on the local atmospheric environment, Atmos. Res., 156, 58–66, https://doi.org/10.1016/j.atmosres.2015.01.001, 2015.

Chow, J. C. and Watson, J. G.: $PM_{2.5}$ carbonate concentrations at regionally representative interagency monitoring of protected visual environment sites, J. Geophys. Res.-Atmos., 107, 8344, https://doi.org/10.1029/2001jd000574, 2002.

Chow, J. C., Watson, J. G., Pritchett, L. C., Pierson, W. R., Frazier, C. A., and Purcell, R. G.: The dri thermal/optical reflectance carbon analysis system: description, evaluation and applications in US Air quality studies, Atmos. Environ. A.-Gen., 27, 1185–1201, https://doi.org/10.1016/0960-1686(93)90245-t, 1993.

Chow, J. C., Watson, J. G., Crow, D., Lowenthal, D. H., and Merrifield, T.: Comparison of IMPROVE and NIOSH carbon measurements, Aerosol Sci. Tech., 34, 23–34, https://doi.org/10.1080/027868201300081923, 2001.

Clarke, A. D., Shinozuka, Y., Kapustin, V. N., Howell, S., Huebert, B., Doherty, S., Anderson, T., Covert, D., Anderson, J., Hua, X., Moore, K. G., McNaughton, C., Carmichael, G., and Weber, R.: Size distributions and mixtures of dust and black carbon aerosol in Asian outflow: physiochemistry and optical properties, J. Geophys. Res.-Atmos., 109, D15S09, https://doi.org/10.1029/2003jd004378, 2004.

Cohen, A. S.: Paleolimnology: The History and Evolution of Lake Systems, Oxford University Press, 2003.

Cong, Z., Kang, S., Gao, S., Zhang, Y., Li, Q., and Kawamura, K.: Historical trends of atmospheric black carbon on Tibetan Plateau as reconstructed from a 150 year lake sediment record, Environ. Sci. Technol., 47, 2579–2586, 2013.

Cong, Z., Kang, S., Kawamura, K., Liu, B., Wan, X., Wang, Z., Gao, S., and Fu, P.: Carbonaceous aerosols on the south edge of the Tibetan Plateau: concentrations, seasonality and sources, Atmos. Chem. Phys., 15, 1573–1584, https://doi.org/10.5194/acp-15-1573-2015, 2015.

Cornelissen, G., Gustafsson, Ö., Bucheli, T. D., Jonker, M. T., Koelmans, A. A., and van Noort, P. C.: Extensive sorption of organic compounds to black carbon, coal, and kerogen in sediments and soils: mechanisms and consequences for distribution, bioaccumulation, and biodegradation, Environ. Sci. Technol., 39, 6881–6895, 2005.

Decesari, S., Facchini, M. C., Carbone, C., Giulianelli, L., Rinaldi, M., Finessi, E., Fuzzi, S., Marinoni, A., Cristofanelli, P., and Duchi, R.: Chemical composition of PM_{10} and PM_1 at the high-altitude Himalayan station Nepal Climate Observatory-Pyramid (NCO-P) (5079 m a.s.l.), Atmos. Chem. Phys., 10, 4583–4596, https://doi.org/10.5194/acp-10-4583-2010, 2010.

Doberschütz, S., Frenzel, P., Haberzettl, T., Kasper, T., Wang, J., Zhu, L., Daut, G., Schwalb, A., and Mäusbacher, R.: Monsoonal forcing of Holocene paleoenvironmental change on the central Tibetan Plateau inferred using a sediment record from Lake Nam Co (Xizang, China), J. Paleolimnol., 51, 253–266, https://doi.org/10.1007/s10933-013-9702-1, 2014.

Fang, Y., Chen, Y., Tian, C., Lin, T., Hu, L., Huang, G., Tang, J., Li, J., and Zhang, G.: Flux and budget of BC in the continental shelf seas adjacent to Chinese high BC emission source regions, Global Biogeochem. Cy., 29, 957–972, https://doi.org/10.1002/2014gb004985, 2015.

Gustafsson, Ö. and Gschwend, P. M.: The flux of black carbon to surface sediments on the New England continental shelf, Geochim. Cosmochim. Ac., 62, 465–472, 1998.

Hammes, K., Schmidt, M. W. I., Smernik, R. J., Currie, L. A., Ball, W. P., Nguyen, T. H., Louchouarn, P., Houel, S., Gustafsson, O., Elmquist, M., Cornelissen, G., Skjemstad, J. O., Masiello, C. A., Song, J., Peng, P. a., Mitra, S., Dunn, J. C., Hatcher, P. G., Hockaday, W. C., Smith, D. M., Hartkopf-Froeder, C., Boehmer, A., Lueer, B., Huebert, B. J., Amelung, W., Brodowski, S., Huang, L., Zhang, W., Gschwend, P. M., Flores-Cervantes, D. X., largeau, C., Rouzaud, J.-N., Rumpel, C., Guggenberger, G., Kaiser, K., Rodionov, A., Gonzalez-Vila, F. J., Gonzalez-Perez, J. A., de la Rosa, J. M., Manning, D. A. C., Lopez-Capel, E., and Ding, L.: Comparison of quantification methods to measure fire-derived (black/elemental) carbon in soils and sediments using reference materials from soil, water, sediment and the atmosphere, Global Biogeochem. Cy., 21, GB3016, https://doi.org/10.1029/2006gb002914, 2007.

Han, Y. M., Cao, J. J., Yan, B. Z., Kenna, T. C., Jin, Z. D., Cheng, Y., Chow, J. C., and An, Z. S.: Comparison of elemental carbon in lake sediments measured by three different methods and 150 year pollution history in eastern China, Environ. Sci. Technol., 45, 5287–5293, 2011.

Han, Y., Wei, C., Bandowe, B., Wilcke, W., Cao, J., Xu, B., Gao, S., Tie, X., Li, G., and Jin, Z.: Elemental carbon and polycyclic aromatic compounds in a 150 year sediment core from Lake Qinghai, Tibetan Plateau, China: influence of regional and local sources and transport pathways, Environ. Sci. Technol., 49, 4176–4183, 2015.

Han, Y. M., Wei, C., Huang, R. J., Bandowe, B. A. M., Ho, S. S. H., Cao, J. J., Jin, Z. D., Xu, B. Q., Gao, S. P., Tie, X. X., An, Z. S., and Wilcke, W.: Reconstruction of atmospheric soot history in inland regions from lake sediments over the past 150 years, Sci. Rep.-UK, 6, 19151, https://doi.org/10.1038/srep19151, 2016.

Ho, K. F., Zhang, R. J., Lee, S. C., Ho, S. S. H., Liu, S. X., Fung, K., Cao, J. J., Shen, Z. X., and Xu, H. M.: Characteristics of carbonate carbon in $PM_{2.5}$ in a typical semi-arid area of Northeastern China, Atmos. Environ., 45, 1268–1274, https://doi.org/10.1016/j.atmosenv.2010.12.007, 2011.

Jankowski, N., Schmidl, C., Marr, I. L., Bauer, H., and Puxbaum, H.: Comparison of methods for the quantification of carbonate carbon in atmospheric PM_{10} aerosol samples, Atmos. Environ., 42, 8055–8064, https://doi.org/10.1016/j.atmosenv.2008.06.012, 2008.

Ji, Z., Kang, S., Cong, Z., Zhang, Q., and Yao, T.: Simulation of carbonaceous aerosols over the Third Pole and adjacent regions: distribution, transportation, deposition, and climatic effects, Clim.

Dynam., 45, 2831–2846, https://doi.org/10.1007/s00382-015-2509-1, 2015.

Jurado, E., Dachs, J., Duarte, C. M., and Simo, R.: Atmospheric deposition of organic and black carbon to the global oceans, Atmos. Environ., 42, 7931–7939, 2008.

Kang, S., Xu, Y., You, Q., Flügel, W.-A., Pepin, N., and Yao, T.: Review of climate and cryospheric change in the Tibetan Plateau, Environ. Res. Lett., 5, 015101, https://doi.org/10.1088/1748-9326/5/1/015101, 2010.

Karanasiou, A., Diapouli, E., Cavalli, F., Eleftheriadis, K., Viana, M., Alastuey, A., Querol, X., and Reche, C.: On the quantification of atmospheric carbonate carbon by thermal/optical analysis protocols, Atmos. Meas. Tech., 4, 2409–2419, https://doi.org/10.5194/amt-4-2409-2011, 2011.

Karanasiou, A., Minguillón, M. C., Viana, M., Alastuey, A., Putaud, J. P., Maenhaut, W., Panteliadis, P., Močnik, G., Favez, O., and Kuhlbusch, T. A. J.: Thermal-optical analysis for the measurement of elemental carbon (EC) and organic carbon (OC) in ambient air a literature review, Atmos. Meas. Tech. Discuss., 8, 9649–9712, https://doi.org/10.5194/amtd-8-9649-2015, 2015.

Kaspari, S. D., Schwikowski, M., Gysel, M., Flanner, M. G., Kang, S., Hou, S., and Mayewski, P. A.: Recent increase in black carbon concentrations from a Mt. Everest ice core spanning 1860–2000 AD, Geophys. Res. Lett., 38, L04703, https://doi.org/10.1029/2010gl046096, 2011.

Koch, D., Schulz, M., Kinne, S., McNaughton, C., Spackman, J. R., Balkanski, Y., Bauer, S., Berntsen, T., Bond, T. C., Boucher, O., Chin, M., Clarke, A., De Luca, N., Dentener, F., Diehl, T., Dubovik, O., Easter, R., Fahey, D. W., Feichter, J., Fillmore, D., Freitag, S., Ghan, S., Ginoux, P., Gong, S., Horowitz, L., Iversen, T., Kirkevag, A., Klimont, Z., Kondo, Y., Krol, M., Liu, X., Miller, R., Montanaro, V., Moteki, N., Myhre, G., Penner, J. E., Perlwitz, J., Pitari, G., Reddy, S., Sahu, L., Sakamoto, H., Schuster, G., Schwarz, J. P., Seland, O., Stier, P., Takegawa, N., Takemura, T., Textor, C., van Aardenne, J. A., and Zhao, Y.: Evaluation of black carbon estimations in global aerosol models, Atmos. Chem. Phys., 9, 9001–9026, https://doi.org/10.5194/acp-9-9001-2009, 2009.

Lau, W. K. M., Kim, M.-K., Kim, K.-M., and Lee, W.-S.: Enhanced surface warming and accelerated snow melt in the Himalayas and Tibetan Plateau induced by absorbing aerosols, Environ. Res. Lett., 5, 025204, https://doi.org/10.1088/1748-9326/5/2/025204, 2010.

Li, C., Kang, S., Wang, X., Ajmone-Marsan, F., and Zhang, Q.: Heavy metals and rare earth elements (REEs) in soil from the Nam Co Basin, Tibetan Plateau, Environ. Geol., 53, 1433–1440, https://doi.org/10.1007/s00254-007-0752-4, 2008.

Li, C., Kang, S., Zhang, Q., and Wang, F.: Rare earth elements in the surface sediments of the Yarlung Tsangbo (Upper Brahmaputra River) sediments, southern Tibetan Plateau, Quatern. Int., 208, 151–157, 2009.

Li, Q., Kang, S., Zhang, Q., Huang, J., guo, J., Wang, K., and Wang, J.: A 150 year climate change history reconstructed by lake sediment of Nam Co, Tibetan Plateau (in Chinese), Acta Sedimentologica Sinica, 32, 669–676, 2014.

Li, C., Bosch, C., Kang, S., Andersson, A., Chen, P., Zhang, Q., Cong, Z., Chen, B., Qin, D., and Gustafsson, Ö.: Sources of black carbon to the Himalayan–Tibetan Plateau glaciers, Nat. Commun., 7, 12574, https://doi.org/10.1038/ncomms12574, 2016a.

Li, C., Chen, P., Kang, S., Yan, F., Hu, Z., Qu, B., and Sillanpää, M.: Concentrations and light absorption characteristics of carbonaceous aerosol in $PM_{2.5}$ and PM_{10} of Lhasa city, the Tibetan Plateau, Atmos. Environ., 127, 340–346, https://doi.org/10.1016/j.atmosenv.2015.12.059, 2016b.

Li, C., Chen, P., Kang, S., Yan, F., Li, X., Qu, B., and Sillanpää, M.: Carbonaceous matter deposition in the high glacial regions of the Tibetan Plateau, Atmos. Environ., 141, 203–208, https://doi.org/10.1016/j.atmosenv.2016.06.064, 2016c.

Li, C., Yan, F., Kang, S., Chen, P., Hu, Z., Gao, S., Qu, B., and Sillanpää, M.: Light absorption characteristics of carbonaceous aerosols in two remote stations of the southern fringe of the Tibetan Plateau, China, Atmos. Environ., 143, 79–85, https://doi.org/10.1016/j.atmosenv.2016.08.042, 2016d.

Li, X., Kang, S., He, X., Qu, B., Tripathee, L., Jing, Z., Paudyal, R., Li, Y., Zhang, Y., Yan, F., Li, G., and Li, C.: Light-absorbing impurities accelerate glacier melt in the Central Tibetan Plateau, Sci. Total Environ., 587, 482–490, https://doi.org/10.1016/j.scitotenv.2017.02.169, 2017.

Lim, S., Faïn, X., Zanatta, M., Cozic, J., Jaffrezo, J. L., Ginot, P., and Laj, P.: Refractory black carbon mass concentrations in snow and ice: method evaluation and inter-comparison with elemental carbon measurement, Atmos. Meas. Tech., 7, 3307–3324, https://doi.org/10.5194/amt-7-3307-2014, 2014.

Liu, B., Cong, Z., Wang, Y., Xin, J., Wan, X., Pan, Y., Liu, Z., Wang, Y., Zhang, G., Wang, Z., Wang, Y., and Kang, S.: Background aerosol over the Himalayas and Tibetan Plateau: observed characteristics of aerosol mass loading, Atmos. Chem. Phys., 17, 449–463, https://doi.org/10.5194/acp-17-449-2017, 2017.

Liu, Y.-H., Dong, G.-R., Li, S., and Dong, Y.-X.: Status, causes and combating suggestions of sandy desertification in qinghai-tibet plateau, Chinese Geogr. Sci., 15, 289–296, https://doi.org/10.1007/s11769-005-0015-9, 2005.

Maenhaut, W., Schwarz, J., Cafmeyer, J., and Chi, X.: Aerosol chemical mass closure during the EUROTRAC-2 AEROSOL Intercomparison 2000, Nucl. Instrum. Meth. B, 189, 233–237, https://doi.org/10.1016/S0168-583X(01)01048-5, 2002.

Marinoni, A., Cristofanelli, P., Laj, P., Duchi, R., Calzolari, F., Decesari, S., Sellegri, K., Vuillermoz, E., Verza, G. P., Villani, P., and Bonasoni, P.: Aerosol mass and black carbon concentrations, a two year record at NCO-P (5079 m, Southern Himalayas), Atmos. Chem. Phys., 10, 8551–8562, https://doi.org/10.5194/acp-10-8551-2010, 2010.

Ming, J., Zhang, D., Kang, S., and Tian, W.: Aerosol and fresh snow chemistry in the East Rongbuk Glacier on the northern slope of Mt. Qomolangma (Everest), J. Geophys. Res., 112, D15307, https://doi.org/10.1029/2007JD008618, 2007.

Ming, J., Cachier, H., Xiao, C., Qin, D., Kang, S., Hou, S., and Xu, J.: Black carbon record based on a shallow Himalayan ice core and its climatic implications, Atmos. Chem. Phys., 8, 1343–1352, https://doi.org/10.5194/acp-8-1343-2008, 2008.

Ming, J., Xiao, C., Cachier, H., Qin, D., Qin, X., Li, Z., and Pu, J.: Black carbon (BC) in the snow of glaciers in west China and its potential effects on albedos, Atmos. Res., 92, 114–123, 2009.

Ming, J., Xiao, C., Sun, J., Kang, S., and Bonasoni, P.: Carbonaceous particles in the atmosphere and precipitation of the

Nam Co region, Central Tibet, J. Environ. Sci., 22, 1748–1756, 2010.

Ming, J., Xiao, C., Du, Z., and Yang, X.: An overview of black carbon deposition in High Asia glaciers and its impacts on radiation balance, Adv. Water Resour., 55, 80–87, https://doi.org/10.1016/j.advwatres.2012.05.015, 2013.

Perrone, M. R., Piazzalunga, A., Prato, M., and Carofalo, I.: Composition of fine and coarse particles in a coastal site of the central Mediterranean: carbonaceous species contributions, Atmos. Environ., 45, 7470–7477, 2011.

Pio, C. A., Legrand, M., Oliveira, T., Afonso, J., Santos, C., Caseiro, A., Fialho, P., Barata, F., Puxbaum, H., Sanchez-Ochoa, A., Kasper-Giebl, A., Gelencser, A., Preunkert, S., and Schock, M.: Climatology of aerosol composition (organic versus inorganic) at nonurban sites on a west–east transect across Europe, J. Geophys. Res.-Atmos., 112, D23S02, https://doi.org/10.1029/2006jd008038, 2007.

Qu, B., Ming, J., Kang, S. C., Zhang, G. S., Li, Y. W., Li, C. D., Zhao, S. Y., Ji, Z. M., and Cao, J. J.: The decreasing albedo of the Zhadang glacier on western Nyainqentanglha and the role of light-absorbing impurities, Atmos. Chem. Phys., 14, 11117–11128, https://doi.org/10.5194/acp-14-11117-2014, 2014.

Ram, K., Sarin, M. M., and Tripathi, S. N.: A 1 year record of carbonaceous aerosols from an urban site in the Indo-Gangetic Plain: characterization, sources, and temporal variability, J. Geophys. Res., 115, 9–12, 2010.

Ramanathan, V. and Carmichael, G.: Global and regional climate changes due to black carbon, Nat. Geosci., 1, 221–227, 2008.

Reisinger, P., Wonaschütz, A., Hitzenberger, R., Petzold, A., Bauer, H., Jankowski, N., Puxbaum, H., Chi, X., and Maenhaut, W.: Intercomparison of measurement techniques for black or elemental carbon under urban background conditions in wintertime: influence of biomass combustion, Environ. Sci. Technol., 42, 884–889, https://doi.org/10.1021/es0715041, 2008.

Ruppel, M. M., Isaksson, E., Ström, J., Beaudon, E., Svensson, J., Pedersen, C. A., and Korhola, A.: Increase in elemental carbon values between 1970 and 2004 observed in a 300 year ice core from Holtedahlfonna (Svalbard), Atmos. Chem. Phys., 14, 11447–11460, https://doi.org/10.5194/acp-14-11447-2014, 2014.

Sillanpää, M., Frey, A., Hillamo, R., Pennanen, A. S., and Salonen, R. O.: Organic, elemental and inorganic carbon in particulate matter of six urban environments in Europe, Atmos. Chem. Phys., 5, 2869–2879, https://doi.org/10.5194/acp-5-2869-2005, 2005.

Tang, Y., Han, G. L., and Xu, Z. F.: Atmospheric black carbon deposit in Beijing and Zhangbei, China, in: Geochemistry of the Earth's Surface Ges-10, edited by: Gaillardet, J., Procedia Earth and Planetary Science, 383–387, 2014.

Viidanoja, J., Sillanpaa, M., Laakia, J., Kerminen, V. M., Hillamo, R., Aarnio, P., and Koskentalo, T.: Organic and black carbon in $PM_{2.5}$ and PM_{10}: 1 year of data from an urban site in Helsinki, Finland, Atmos. Environ., 36, 3183–3193, https://doi.org/10.1016/s1352-2310(02)00205-4, 2002.

Wan, D. J., Jin, Z. D., and Wang, Y. X.: Geochemistry of eolian dust and its elemental contribution to Lake Qinghai sediment, Appl. Geochem., 27, 1546–1555, https://doi.org/10.1016/j.apgeochem.2012.03.009, 2012.

Wan, X., Kang, S., Wang, Y., Xin, J., Liu, B., Guo, Y., Wen, T., Zhang, G., and Cong, Z.: Size distribution of carbonaceous aerosols at a high-altitude site on the central Tibetan Plateau (Nam Co Station, 4730 m a.s.l.), Atmos. Res., 153, 155–164, https://doi.org/10.1016/j.atmosres.2014.08.008, 2015.

Wang, S., Wang, J., Zhou, Z., and Shang, K.: Regional characteristics of three kinds of dust storm events in China, Atmos. Environ., 39, 509–520, https://doi.org/10.1016/j.atmosenv.2004.09.033, 2005.

Wang, J., Zhu, L., Wang, Y., Gao, S., and Daut, G.: Spatial variability of recent sedimentation rate and variations in the past 60 years in Nam Co, Tibetan Palteau, China (in Chinese), Quaternary Sci. Rev., 31, 535–543, 2011.

Watson, J. G., Chow, J. C., and Chen, L. W. A.: Summary of organic and elemental carbon/black carbon analysis methods and intercomparisons, Aerosol Air Qual. Res., 5, 65–102, 2005.

Wu, Y., Zhu, L., Ye, Q., and Wang, L.: The response of lake-glacier area change to climate variations in Namco Basin, Central Tibetan Plateau, during the last three decades (in Chinese), Acta Geographica Sinica, 62, 301–311, 2007.

Xu, B., Cao, J., Hansen, J., Yao, T., Joswia, D. R., Wang, N., Wu, G., Wang, M., Zhao, H., and Yang, W.: Black soot and the survival of Tibetan glaciers, P. Natl. Acad. Sci. USA, 106, 22114–22118, 2009.

Xu, Y., Ramanathan, V., and Washington, W. M.: Observed high-altitude warming and snow cover retreat over Tibet and the Himalayas enhanced by black carbon aerosols, Atmos. Chem. Phys., 16, 1303–1315, https://doi.org/10.5194/acp-16-1303-2016, 2016.

Yan, C., Zheng, M., Sullivan, A. P., Bosch, C., Desyaterik, Y., Andersson, A., Li, X., Guo, X., Zhou, T., Gustafsson, Ö., and Collett Jr, J. L.: Chemical characteristics and light-absorbing property of water-soluble organic carbon in Beijing: biomass burning contributions, Atmos. Environ., 121, 4–12, https://doi.org/10.1016/j.atmosenv.2015.05.005, 2015.

Yang, H.: Lake sediments may not faithfully record decline of atmospheric pollutant deposition, Environ. Sci. Technol., 49, 12607–12608, https://doi.org/10.1021/acs.est.5b04386, 2015.

You, Q., Kang, S., Pepin, N., Fluegel, W.-A., Yan, Y., Behrawan, H., and Huang, J.: Relationship between temperature trend magnitude, elevation and mean temperature in the Tibetan Plateau from homogenized surface stations and reanalysis data, Glob. Planet. Change, 71, 124–133, https://doi.org/10.1016/j.gloplacha.2010.01.020, 2010.

Zhang, G., Yao, T., Piao, S., Bolch, T., Xie, H., Chen, D., Gao, Y., O'Reilly, C. M., Shum, C. K., Yang, K., Yi, S., Lei, Y., Wang, W., He, Y., Shang, K., Yang, X., and Zhang, H.: Extensive and drastically different alpine lake changes on Asia's high plateaus during the past four decades, Geophys. Res. Lett., 44, 252–260, https://doi.org/10.1002/2016gl072033, 2017a.

Zhang, R., Wang, H., Qian, Y., Rasch, P. J., Easter, R. C., Ma, P. L., Singh, B., Huang, J., and Fu, Q.: Quantifying sources, transport, deposition, and radiative forcing of black carbon over the Himalayas and Tibetan Plateau, Atmos. Chem. Phys., 15, 6205–6223, https://doi.org/10.5194/acp-15-6205-2015, 2015.

Zhang, Y., Kang, S., Cong, Z., Schmale, J., Sprenger, M., Li, C., Yang, W., Gao, T., Sillanpää, M., and Li, X.: Light-absorbing impurities enhance glacier albedo reduction in the southeastern Tibetan Plateau, J. Geophys. Res.-Atmos., 122, 6915–6933, 2017b.

Zhao, S., Ming, J., Sun, J., and Xiao, C.: Observation of carbonaceous aerosols during 2006–2009 in Nyainqntanglha Mountains and the implications for glaciers, Environ. Sci. Pollut. R., 20, 5827–5838, https://doi.org/10.1007/s11356-013-1548-6, 2013a.

Zhao, Z., Cao, J., Shen, Z., Xu, B., Zhu, C., Chen, L. W. A., Su, X., Liu, S., Han, Y., Wang, G., and Ho, K.: Aerosol particles at a high-altitude site on the Southeast Tibetan Plateau, China: implications for pollution transport from South Asia, J. Geophys. Res.-Atmos., 118, 11360–11375, https://doi.org/10.1002/jgrd.50599, 2013b.

Zhao, Z. Z., Cao, J. J., Shen, Z. X., Huang, R. J., Hu, T. F., Wang, P., Zhang, T., and Liu, S. X.: Chemical composition of $PM_{2.5}$ at a high-altitude regional background site over Northeast of Tibet Plateau, Atmos. Pollut. Res., 6, 815–823, https://doi.org/10.5094/apr.2015.090, 2015.

Zhu, L., Xie, M., and Wu, Y.: Quantitative analysis of lake area variations and the influence factors from 1971 to 2004 in the Nam Co basin of the Tibetan Plateau, Chinese Sci. Bull., 55, 1294–1303, 2010.

Publication II

Yan, F., He, C., Kang, S., Chen, P., Hu, Z., Han, X., Gautam, S., Yan, C., Zheng, M., Sillanpää, M., Raymond, P.A., Li, C.

Deposition of organic and black carbon: direct measurements at three remote stations in the Himalayas and Tibetan Plateau

Reprinted with permission from
Journal of Geophysical Research: Atmospheres
Vol. 124, pp. 9702–9715, 2019

Publication III

Li, C., Yan, F., Kang, S., Chen, P., Hu, Z., Han, X., Zhang, G., Gao, S., Qu, B., Sillanpaa, M.

Deposition and light absorption characteristics of precipitation dissolved organic carbon (DOC) at three remote stations in the Himalayas and Tibetan Plateau

Reprinted with permission from
Science of the Total Environment
Vol. 605–606, pp. 1039-1046, 2017

Science of the Total Environment 605–606 (2017) 1039–1046

Contents lists available at ScienceDirect

Science of the Total Environment

journal homepage: www.elsevier.com/locate/scitotenv

Deposition and light absorption characteristics of precipitation dissolved organic carbon (DOC) at three remote stations in the Himalayas and Tibetan Plateau, China

Chaoliu Li [a,c,d,*], Fangping Yan [c], Shichang Kang [b,d,e], Pengfei Chen [b], Zhaofu Hu [b,e], Xiaowen Han [a,e], Guoshuai Zhang [a], Shaopeng Gao [a], Bin Qu [c], Mika Sillanpää [c,f]

[a] Key Laboratory of Tibetan Environment Changes and Land Surface Processes, Institute of Tibetan Plateau Research, Chinese Academy of Sciences, Beijing 100101, China
[b] State Key Laboratory of Cryospheric Sciences, Northwest Institute of Eco-Environment and Resources, Chinese Academy of Sciences, Lanzhou 730000, China
[c] Laboratory of Green Chemistry, Lappeenranta University of Technology, Sammonkatu 12, Mikkeli 50130, Finland
[d] CAS Center for Excellence in Tibetan Plateau Earth Sciences, Beijing 100101, China
[e] University of Chinese Academy of Sciences, Beijing 100049, China
[f] Department of Civil and Environmental Engineering, Florida International University, Miami, FL 33174, USA

HIGHLIGHTS

- Precipitation DOC characteristics at three remote stations on the HTP were studied.
- Precipitation DOC contents in this study were lower than those of urban cities.
- Annual precipitation DOC deposition of the HTP was estimated of 0.94 ± 0.87 Tg C.
- MAC_{DOC} values were lower than those of near surface aerosols.

GRAPHICAL ABSTRACT

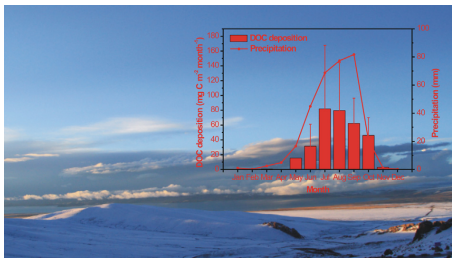

ARTICLE INFO

Article history:
Received 9 May 2017
Received in revised form 25 June 2017
Accepted 26 June 2017
Available online xxxx

Editor: Jay Gan

Keywords:
Dissolved organic carbon
The Third Pole
Deposition
Light absorption

ABSTRACT

The concentrations, depositions and optical properties of precipitation DOC at three remote stations (Nam Co, Lulang and Everest) were investigated in the Himalayas and Tibetan Plateau (HTP). The results showed that their volume-weighted mean DOC concentrations were 1.05 ± 1.01 mg C L^{-1}, 0.83 ± 0.85 mg C L^{-1} and 0.86 ± 0.91 mg C L^{-1}, respectively, close to those of other remote areas in the world and lower than those of typical polluted urban cities. Combined with precipitation amounts, the DOC depositions at these three stations were calculated to be 0.34 ± 0.32 g C m^{-2} yr^{-1}, 0.84 ± 0.86 g C m^{-2} yr^{-1} and 0.16 ± 0.17 g C m^{-2} yr^{-1}, respectively. The annual DOC deposition in the HTP was approximately 0.94 ± 0.87 Tg C, the highest and lowest values appeared in the southeastern and northwestern plateau, respectively. The sources of DOC in the precipitation at these three stations were remarkably different, indicating large spatial heterogeneity in the sources of precipitation DOC over the HTP. Nam Co presented combustion sources from South Asia and local residents, Lulang showed biomass combustion source from South Asia, and Everest was mainly influenced by local mineral dust. The values of the MAC_{DOC} at 365 nm were 0.48 ± 0.47 m^2 g^{-1}, 0.25 ± 0.15 m^2 g^{-1}, and 0.64 ± 0.49 m^2 g^{-1}, respectively, for the precipitation at the three stations. All of these values were significantly lower than those

* Corresponding author at: Key Laboratory of Tibetan Environment Changes and Land Surface Processes, Institute of Tibetan Plateau Research, Chinese Academy of Sciences, Beijing 100101, China.
E-mail address: lichaoliu@itpcas.ac.cn (C. Li).

http://dx.doi.org/10.1016/j.scitotenv.2017.06.232

of corresponding near-surface aerosol samples because precipitation DOC contains more secondary organic aerosol with low light absorption abilities. Additionally, this phenomenon was also observed in seriously polluted urban areas, implying it is universal in the atmosphere. Because precipitation DOC contains information for both particle-bound and gaseous components from the near surface up to the altitude of clouds where precipitation occurs, the MAC_{DOC} of precipitation is more representative than that of near-surface aerosols for a given region.

1. Introduction

Carbonaceous aerosol (CA) is a key component affecting climate change. CA contains black carbon (BC) and organic carbon (OC). The latter can be further divided into water insoluble organic carbon (WIOC) and water soluble organic carbon (WSOC). WSOC is called dissolved organic carbon (DOC) during carbon studies in precipitation (Andreae and Gelencser, 2006; Bond et al., 2013). Precipitation DOC plays an important role in the global climate system (Saxena and Hildemann, 1996; Willey et al., 2000). For instance, precipitation DOC deposition is an important input data for study of global carbon cycle (Bond et al., 2013; Pan et al., 2010; Yan and Kim, 2012). It has been estimated that precipitation DOC deposition in the world was approximately 430 Tg C yr^{-1} ($1Tg = 10^{12}$ g) (Willey et al., 2000). Additional studies have since been conducted in urban areas such as North America (Avery et al., 2013; Raymond, 2005), Europe (Siudek et al., 2015) and Asia (Pan et al., 2010; Yan and Kim, 2012), enriching the database of concentration and deposition of precipitation DOC in the world.

In addition to the role that precipitation DOC plays in the carbon cycle, the presence of precipitation DOC may be an important component in atmospheric radiative forcing studies due to its role in the scattering of sunlight that reaches the earth's surface (Kieber et al., 2006). Meanwhile, some components of DOC strongly absorb sunlight at ultraviolet and blue wavelengths. Those components of DOC that can absorb sunlight are generally termed water soluble brown carbon (WS-BrC). The light absorption characteristics of WS-BrC have been widely investigated around the world. For instance, it was found that the overall light absorption abilities of WS-BrC that originate from biomass combustion were higher than that sourced from fossil burning (Cheng et al., 2011; Hu et al., 2017). Studies on ambient aerosols have found that the direct radiative forcing caused by WSOC was approximately 2–10% and 3–11% higher than that caused by BC in seriously polluted areas of East Asia (Kirillova et al., 2014a) and urban areas of South Asia (Kirillova et al., 2014b), respectively. Because of the photobleaching of WSOC during the long-distance transport of aerosols, the corresponding value was found to be as low as 1% for aerosols at a remote island in the Indian Ocean (Bosch et al., 2014). Despite the above studies on the WSOC of aerosols, little knowledge is available on the light absorption characteristics of precipitation DOC (Yan et al., 2016), which includes the chemical characteristics of the entire atmospheric column from the cloud height to the surface and is more representative of atmosphere aerosols than of near-surface aerosols.

At present, studies on the deposition and light absorption characteristics of precipitation DOC are still limited to a small fraction of the world's environments. Remote areas such as the Himalayas and Tibetan Plateau (HTP), the largest and highest plateau in the world, need further study. As the HTP are adjacent to two seriously polluted regions in the world (i.e., East China and South Asia), the HTP receive long-distance transported carbonaceous matter (e.g., BC) from these two regions, as suggested by both atmospheric transport models (Lu et al., 2012; Zhang et al., 2015) and geochemical evidence (Kaspari et al., 2011; Li et al., 2016a; Ming et al., 2010), influencing precipitation chemistry of the HTP. For example, it was shown that emissions from the combustion activities of both local residents and South Asia contributed to major ions in the precipitation at Nam Co Station in the central HTP (Fig. 1) (Li et al., 2007; Zhang et al., 2012). Similarly, pollutants derived from South Asia showed a large influence on the precipitation chemistry at another remote area (Lulang Station) located in the southeastern HTP (Liu et al., 2013) (Fig. 1). Based on these studies, it was further proposed that NO_3^--N and NH_4^+-N in the precipitation in the HTP, were mainly influenced by anthropogenic emissions outside of the HTP (Liu et al., 2015). However, only few studies to date were conducted on precipitation DOC (Li et al., 2016c, 2016e; Yan et al., 2016). The primary results of the above studies showed that although the precipitation DOC concentrations of urban areas in the HTP were lower than those of other seriously polluted cities of Asia (Li et al., 2016e), they were still much higher than those of glacial areas (Li et al., 2016c; Yan et al., 2016). However, knowledge concerning precipitation DOC concentrations and deposition over the platform that accounts for a large part of the area of the HTP is limited, particularly regarding its light absorption characteristics. This limited knowledge inhibits a total understanding of the deposition of precipitation DOC and its potential climate forcing attributes.

Therefore, in this study, precipitation DOC was investigated at three remote stations (Nam Co, Lulang and Everest) in the HTP that belong to the Tibetan Observation and Research Platform (TORP) network (Ma et al., 2008). The innovation of this study is that for the first time, the deposition of precipitation DOC in the HTP was estimated, and its light absorption ability was evaluated. Although these two research directions are independent, the deposition rates and light absorption abilities of precipitation DOC are important research topics because they are related to the carbon cycle and the radiative forcing of carbonaceous matter in the atmosphere, respectively. The aims of this study were (1) to quantitatively estimate the concentrations and deposition of precipitation DOC at the studied stations in the HTP and (2) to characterize the light absorption characteristics of precipitation DOC at the studied stations.

2. Methodology

2.1. Study area and sampling site

The precipitation samples were collected at the Nam Co Monitoring and Research Station for Multisphere Interactions (Nam Co Station) (30°46′23.80″N, 90°57′48.88″E, 4747 m a.s.l.), the Southeast Tibet Station for Alpine Environment Observation and research in Lulang (Lulang Station) (29°45′58.77″N, 94°44′17.68″E, 3330 m a.s.l.) and the Qomolangma Station for Atmospheric and Environmental Observation and Research (Everest Station) (28°21′40.52″N, 86°56′55.67″E, 4276 m a.s.l.) (Fig. 1, Table 1). Nam Co Station is located in a typical pastoral area in the central HTP. The average annual precipitation at this station is approximately 320 mm, which mainly occurs during the period from July to September (i.e., the monsoon period). Previous studies have shown that Nam Co is influenced by both long-range transported (Luthi et al., 2015) and locally emitted pollutants (Li et al., 2007). Lulang Station is located in a subvalley of the Yarlung Tsangpo Grand Canyon, which is a corridor for warm-humid Indian monsoon to penetrate the inner part of the HTP. Therefore, the annual precipitation amount at this station is high (1010 mm). Everest Station is located on the northern slope of the middle Himalayas. Because of the blocking effect of the height of the Himalayas, the annual precipitation amount at this station is only approximately 190 mm and is concentrated between July and August (Fig. 2). These three stations are far from urban areas or

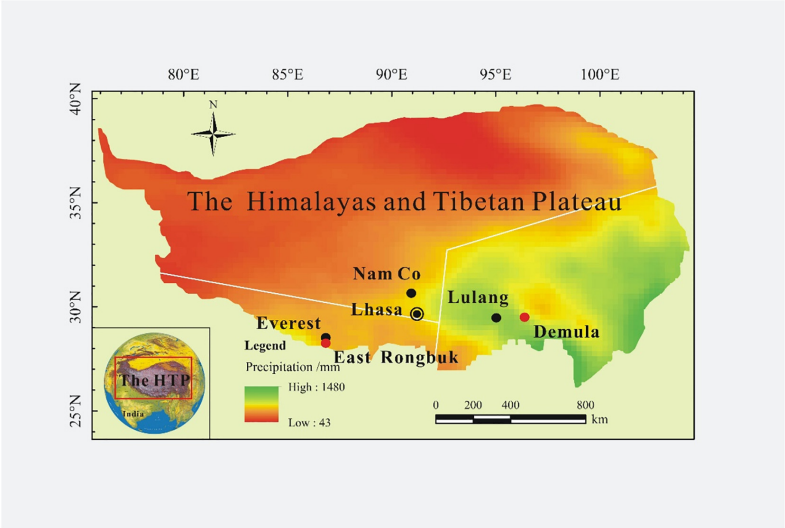

Fig. 1. Location map of the three studied stations (black points) and related sites (red points) in the HTP. The white lines are used to divide the HTP into three individual subareas. The background image represents the spatial distribution of precipitation amounts that are adopted from (Qi et al., 2013). (For interpretation of the references to color in this figure legend, the reader is referred to the web version of this article.)

industry centers and are considered as typical remote areas. A large amount of atmospheric research has been conducted at these sites (e.g., Cao et al., 2010; Cong et al., 2015; Lüthi et al., 2014). In addition, 10 and 14 precipitation samples were collected from the city of Lhasa in the summer and from East China in the winter of 2015 to investigate the light absorption abilities of precipitation DOC in seriously polluted urban areas and to compare the light absorption abilities of precipitation DOC to those of aerosols in the same areas.

A total of 54, 59 and 45 precipitation samples were collected at Nam Co, Lulang and Everest, respectively, from 2014 to 2016. Samples of DOC were collected in prebaked aluminum basins (450 °C, 6 h) that were placed on a 1.5 m high shelf. Meanwhile, precipitation samples of ions (Ca^{2+}, Mg^{2+}, Na^{+}, K^{+}, NH_4^{+}, Cl^{-}, NO_3^{-} and SO_4^{2-}) were also collected with HDPE plastic bags (Li et al., 2016e). Not all of the samples were measured for their ion contents due to an insufficient number of samples. During the field work, basins and bags were put out when precipitation events started. The collected samples were then transferred into precleaned polycarbonate bottles after the precipitation events finished and were kept frozen until analysis. Four blank samples for DOC and ions were prepared and subjected to the same processes as those of the samples from each station. Precipitation amounts were monitored simultaneously with automatic weather stations set up at the studied stations. For a comparison of the light absorption of precipitation DOC with the WSOC of near-surface aerosols, total suspended particle (TSP) samples were also collected for a whole year at these three stations. Data of carbonaceous matter at Lulang and Everest has been reported previously (Li et al., 2016d). All the samples were filtered with PTFE membrane filter with 0.45 μm pore size (Macherey-Nagel, Molecular Devices, USA) before analysis. The measurements of DOC and major ions followed the same methods described in our previous work (Li et al., 2016e). The average DOC concentration of the blanks was 0.05 ± 0.02 mg L^{-1}. The average ion concentrations of the blanks were low (SO_4^{2-} = 1.61 ng g^{-1}, Na^{+} = 1.77 ng g^{-1}, NH_4^{+} = 2.45 ng g^{-1}, Ca^{2+}, Mg^{2+}, K^{+}, Cl^{-} and NO_3^{-} < 1 ng g^{-1}). All the reported concentrations in this study were subduced by those of the blanks.

Table 1
Comparison of volume-weighted mean (VWM) DOC concentrations (mg C L^{-1}) and wet deposition fluxes (g C m^{-2} yr^{-1}) between the studied stations and other regions.

	Sites	Year	DOC concentration	DOC deposition	Reference
Urban area	Lhasa, China	2013	1.10	0.63	1
	Beijing, China	2007–2008	3.9	2.7	2
Glacier	Zhadang, HTP	2013–2014	0.19	0.1	3
	Demula, HTP	2013–2014	0.17	0.15	3
	Everest, HTP	2013–2014	0.09	0.05	3
	Col du Dôme, Alps	1970–1976	0.32	0.79	4
Remote area	Enewetak Atoll, Marshall Islands	1979	1.44	0.59	5
	New Zealand	1999–2000	0.70	–	6
	Nam Co, HTP	2014–2015	1.05	0.34	This study
	Lulang, HTP	2014–2015	0.83	0.84	This study
	Everest, HTP	2014–2015	0.86	0.16	This study

1: (Li et al., 2016e); 2: (Pan et al., 2010); 3: (Li et al., 2016c); 4: (Legrand et al., 2007); 5: (Zafiriou et al., 1985); 6: (Kieber et al., 2002).

2.2. DOC deposition estimation

The annual wet deposition of precipitation DOC was calculated using the following equation (Zhang et al., 2012):

$$F_c = 0.001 \times \sum_{i=1}^{i=n} C_i \times P_i \quad (1)$$

where F_c (g C m^{-2} yr^{-1}) expresses the wet deposition of precipitation DOC, C_i (mg L^{-1}) represents the DOC concentration in an individual precipitation sample i, and P_i (mm) stands for the precipitation amount corresponding to the precipitation sample i. Not all precipitation sample was collected from the three stations, and thus, the total DOC deposition for a given station was estimated based on the ratio between the precipitation amounts of the studied samples and the total value.

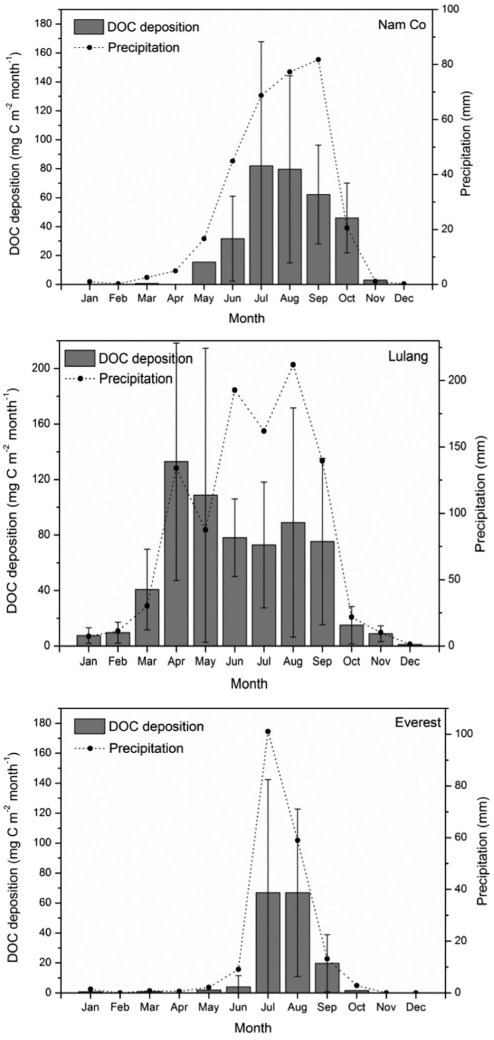

Fig. 2. Similar monthly variations of DOC wet deposition and precipitation amounts among the three studied stations.

The DOC deposition throughout the whole HTP was calculated using the volume-weighted mean (VWM) DOC concentration and annual precipitation amount. Precipitation totals for the HTP have been monitored for decades at many stations, and it is relatively easy to extend these data to the whole HTP. Based on the three studied stations and variations in the precipitation amount distribution, the HTP was divided into three subareas: the northern slope of the Himalayas along the Yarlung Tsangpo valley where Everest Station is located and low precipitation is recorded, the southeastern part of the HTP with heavy precipitation and large forested areas where Lulang Station is located, and the middle and northern part of the HTP that is mainly covered by grassland and barren desert where Nam Co Station is located (Fig. 1). Then, these three subareas were further subdivided into small cells of 0.25 × 0.25°, and the precipitation amounts of these cells were estimated based on the corresponding values of the monitoring stations (Qi et al., 2013).

The wet deposition of atmospheric C was calculated by Eq. (2):

$$C_{wet} = 0.001 \times \sum_{i=1}^{i=n} C_i \times P_i \quad (2)$$

where C_{wet} (g C yr^{-1}) is the total wet DOC deposition in the HTP, C_i (mg L^{-1}) is the DOC VWM concentration of an individual cell i, and P_i (mm) stands for the precipitation amount of a cell i. It need to point out that because only three stations were selected due to the harsh environment, the estimation of DOC deposition for the whole HTP in this study has some uncertainties.

2.3. Light absorption of DOC

The mass absorption cross-section (MAC) is an important parameter that characterizes the light absorption properties of precipitation DOC, which is the same as the absorption per mass (α/ρ). The light absorption spectra of the DOC were measured with a UV–Visible Spectrophotometer (SpectraMax M5, Molecular Devices, USA) between wavelengths of 200 nm and 800 nm with a precision of 5 nm. Each spectrum was determined relative to that of Milli-Q water. The value of MAC_{DOC} can be calculated by the following equation:

$$MAC_{DOC} = \frac{A}{c \cdot L} \times \ln(10) \quad (3)$$

where A (absorbance) is derived directly from the spectrophotometer at 365 nm, L is the absorbing path length, and c is the DOC concentration (Cheng et al., 2011).

3. Results and discussion

3.1. DOC concentration and deposition

The precipitation DOC concentrations at the studied stations and other related sites were listed in Table 1. The VWM DOC concentrations at Nam Co, Lulang and Everest were 1.05 ± 1.01 mg C L^{-1}, 0.83 ± 0.85 mg C L^{-1} and 0.86 ± 0.91 mg C L^{-1}, respectively, which were comparable to those of other remote areas such as the Marshall Islands and New Zealand (Table 1). The DOC concentrations at Lulang and Everest were lower than that of Lhasa, a typical urban area in the HTP (Li et al., 2016e), and of Beijing, a heavily polluted megacity in East China, reflecting a clean atmosphere at these two stations (Cong et al., 2015; Liu et al., 2013). Meanwhile, the average DOC concentrations at these two stations were significantly higher than those of adjacent glacial regions, such as East Rongbuk (0.09 mg C L^{-1}) and Demula (0.17 mg C L^{-1}) (Fig. 1, Table 1). The average DOC concentration at Nam Co Station was the highest of all of the three studied stations, which is mainly because this station is located in the middle part of the TP and receives more local emissions and pollutants that have been transported from South Asia (Li et al., 2007). Seasonally, the DOC concentrations at these three stations during the non-monsoon period were higher than those of the monsoon period, mainly due to low precipitation amounts and high aerosol concentrations during the non-monsoon period (Kang et al., 2016).

Combined with the precipitation amounts, it was estimated that the DOC depositions at Nam Co, Lulang and Everest were 0.34 ± 0.32 g C m^{-2} yr^{-1}, 0.84 ± 0.86 g C m^{-2} yr^{-1} and 0.16 ± 0.17 g C m^{-2} yr^{-1} during the studied period, respectively, which were lower than those of urban areas (e.g., Beijing) because of the low DOC concentrations at the studied stations. The highest value at Lulang reflects the mostly high observed precipitation amount at this station. Seasonally, the high DOC depositions at Nam Co and Everest also

appeared during the period from July to September during the peak monsoon period, which is strongly in accordance with variations of their precipitation amounts (Fig. 2). Based on the DOC concentrations at the studied stations and the distribution of the precipitation amounts across the HTP (Qi et al., 2013), it was calculated that the annual DOC wet deposition of the HTP was 0.94 ± 0.87 Tg C, which is approximately 0.27% and 169 times the global value (Willey et al., 2000) and the glacial regions of the HTP (Li et al., 2016c), respectively, with the high and low values appearing at its southeastern and northwestern parts, respectively. This was similar to the spatial variation of precipitation amounts, indicating that the precipitation amount is the most important factor influencing the deposition of DOC throughout the HTP.

3.2. DOC sources

Precipitation DOC is derived from multiple sources, such as mineral dust, combustion emission, and secondary organic aerosols (SOAs) from various gaseous precursors and organic gases (May et al., 2013). The exact sources of DOC for these three stations were investigated in the following section by comparing its relationship with major ions.

The precipitation DOC of Nam Co Station was transported from both local combustion sources and pollutants from South Asia. The DOC of this station was significantly correlated with NO_3^- (Fig. 3) and showed no relationship with Ca^{2+} ($p > 0.01$). Because NO_3^- in the precipitation of the remote HTP is mainly derived from anthropogenic sources (Liu et al., 2015), it is assumed that the DOC of Nam Co Station was derived mainly from combustion emissions from both South Asia and local residents (Li et al., 2007). For instance, pollutants from South Asia can be transported to this station directly at high levels (Lüthi et al., 2014). Meanwhile, the influence of emissions from local residential combustion activities on the atmosphere outside of the HTP has also been detected in other studies (Chen et al., 2015; Li et al., 2007). Lulang Station is located in the Yarlung Tsangpo Grand Canyon where Indian monsoon penetrates the HTP (Fig. 1), and thus, its precipitation chemistry reflects the characteristics of the Indian Ocean and South Asia, which were discovered by previous research on precipitation ions (Liu et al., 2013). For example, Cl^- and Na^+ showed a significant correlation (Fig. 4), reflecting their common source of the Ocean. Additionally, both Na^+ and K^+ displayed a positive relationship with DOC (Fig. 4). Meanwhile, the average ratio of K^+/Na^+ (0.49 ± 0.14) was approximately 10 times higher than the value of sea salt (0.04) (Pilson, 1998) at Lulang, implying that more K^+ entered the atmosphere during atmospheric mass transport from South Asia to Lulang. Because K^+ is a typical biomass burning tracer (Szidat et al., 2006) and South Asia is known to burn large amounts of biomass fuel annually (Bond et al., 2007; Gustafsson et al., 2009), it is proposed that the precipitation DOC of Lulang Station was mainly transported from South Asia. It is clear that the precipitation DOC at Everest Station was significantly negatively correlated with precipitation amounts (Fig. 3). This phenomenon was also found at other urban areas (Li et al., 2016e; Pan et al., 2010), indicating that the DOC was effectively washed out from the atmosphere by below-cloud scavenging within the initial period of precipitation (Pan et al., 2010). Meanwhile, the DOC and Ca^{2+} were positively related, reflecting their common mineral dust source. In addition, Mg^{2+} and DOC also showed a significant relationship ($r^2 = 0.78$, $p < 0.01$). Therefore, the DOC at Everest Station was dominantly derived from mineral dust, which is in accordance with the fact that Everest Station is located in the rain shadow area of the Himalayas with an arid environment and a widely distributed barren desert along the Yarlung Tsangpo valley.

Based on the above analysis, we hypothesize that the contribution from local sources to the precipitation DOC becomes increasingly larger when precipitation is transported from outside of the HTP to its inner area. On the other hand, the precipitation DOC of the three studied stations were derived from almost completely different sources, indicating an obvious spatial heterogeneity in their precipitation chemistry (Liu et al., 2015) and even in the atmospheric chemistry of the HTP.

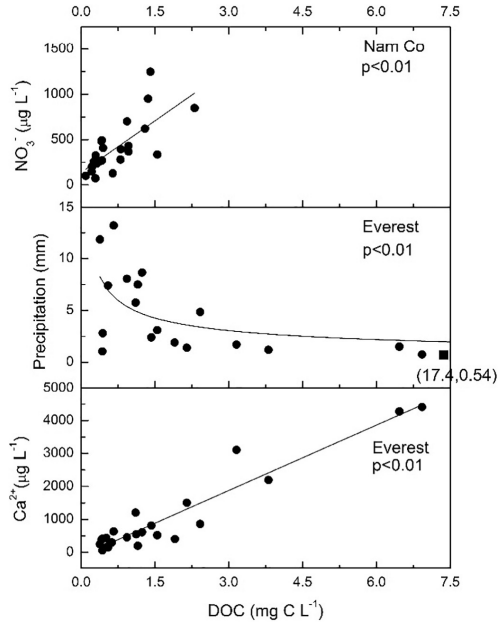

Fig. 3. Significant relationships between the DOC and Ca^{2+}, DOC and precipitation amounts at Everest Station and between the DOC and NO_3^- at Nam Co Station.

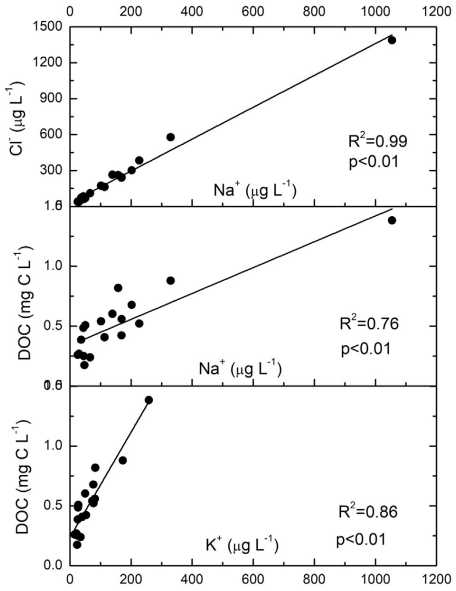

Fig. 4. Significant relationships between the DOC and K^+, DOC and Na^+, and Na^+ and Cl^- of precipitation samples at Lulang Station.

3.3. Light absorption characteristics of DOC

The average MAC_{DOC} values of Nam Co, Lulang and Everest were 0.48 ± 0.47 $m^2 g^{-1}$, 0.25 ± 0.15 $m^2 g^{-1}$, and 0.64 ± 0.49 $m^2 g^{-1}$, respectively. The lowest MAC_{DOC} value appeared at Lulang Station and agree with the fact that the precipitation DOC at this station was mainly derived from South Asia. The light absorption ability of WS-BrC decreased after being exposed to sunlight because some part of the light-absorbing components will be destroyed during transport in the atmosphere (Forrister et al., 2015). This phenomenon has been observed in prior studies on seasonal variations of the MAC_{WSOC} of aerosols at this station (Li et al., 2016d). In addition, Lulang Station is located in a forested region where the living biomass emits a large amount of volatile organic compounds (VOCs) with weak light absorption abilities (Zhang et al., 2011), which also contributed to the low MAC_{DOC} value in this region. The maximum observed value at Everest Station was mainly caused by contributions of DOC from natural mineral dust. For instance, the MAC_{DOC} value of local mineral dust at Everest Station was 1.7 ± 0.5 $m^2 g^{-1}$, which is even higher than that of aerosols at Everest station (1.18 ± 0.64 $m^2 g^{-1}$) (Li et al., 2016d). The MAC_{DOC} values of the three stations showed no relationship with precipitation DOC concentrations, indicating that the variations of the MAC_{DOC} in the remote areas of the HTP are independent of the precipitation DOC concentration. This relationship is different with those for the seriously polluted urban areas of Lhasa and Beijing (Fig. 5). It is assumed that the precipitation DOC concentrations of seriously polluted areas were mainly contributed from particle-bound components located at low levels in the atmosphere. In contrast, because of the much lower near-surface aerosol concentrations at remote stations, the precipitation DOC values at the studied stations were mainly caused by large amounts of other sources (e.g., biogenic VOCs) in addition to near-surface aerosols.

Another obvious issue is that the mean MAC_{DOC} values for each of the three studied stations were significantly lower than the MAC_{WSOC} values of aerosols ($p < 0.01$) (Fig. 6), indicating that precipitation DOC contains more SOAs that experience strong light bleaching processes (Lambe et al., 2013) and biogenic VOCs than surface aerosols. SOAs are formed when the atmospheric oxidation products of volatile organic compounds (VOCs) undergo gas-particle transfer (Hallquist et al., 2009). Previous studies have shown that, because of the lack of enough light absorption components, the light absorption abilities of SOAs are relatively low (Lambe et al., 2013). Similarly, the MAC_{DOC} of the precipitation samples collected from the seriously polluted region of East Asia was 0.84 ± 0.45 $m^2 g^{-1}$, which was also significantly lower than the MAC_{WSOC} of aerosols collected during this period of 1.54 ± 0.16 $m^2 g^{-1}$ (Yan et al., 2015) or 1.26 $m^2 g^{-1}$ (Du et al., 2014). Meanwhile, the MAC_{DOC} of Lhasa was 0.38 ± 0.24 $m^2 g^{-1}$, which was much lower than that of aerosols of 0.78 ± 0.21 $m^2 g^{-1}$ (Li et al., 2016b). Therefore, the general phenomenon wherein the MAC_{DOC} of precipitation is lower than the MAC_{WSOC} of surface aerosols for both remote areas and seriously polluted urban cities occurs mainly because of two reasons. First, larger amounts of biogenic VOCs exist in precipitation DOC. For instance, previous in situ measurements studied for two different urban cities (Zhang et al., 2011) showed that the optical properties of biogenic VOCs had lower light absorption abilities than that of particle-bound WSOC. Second, precipitation DOC experience stronger oxidation in the atmosphere than aerosolized WSOC. Previous studies also showed that oxidized low light-absorption water-soluble carbonyls with low molecular weights are more easily dissolved into precipitation (Ervens et al., 2011), resulting in low MAC_{DOC} values. Other studies further indicated that vapor phase VOCs are more susceptible to oxidation in the atmosphere than those associated with porous, carbonaceous particles such as soot or fly ash (Maliszewska-Kordybach, 1999).

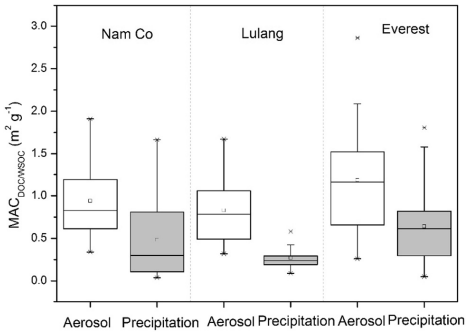

Fig. 6. Significantly lower MAC_{DOC} values for the precipitation samples relative to MAC_{WSOC} values for the aerosol samples at the three studied stations.

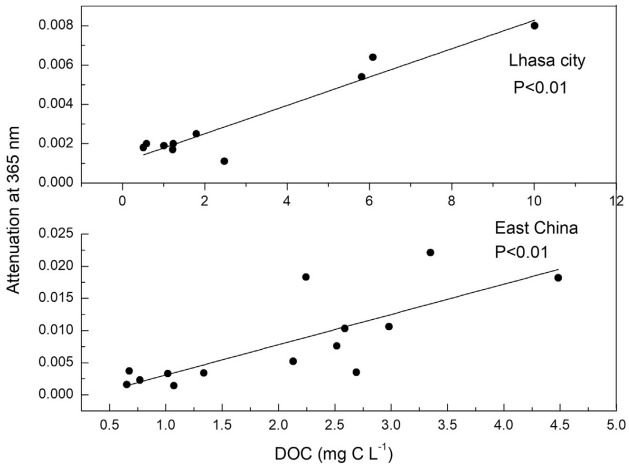

Fig. 5. Relationships between the DOC concentration and attenuation at 365 nm at Lhasa and East China.

Because precipitation is an effective way of scavenging impurities from the atmosphere (Textor et al., 2007; Vignati et al., 2010), the majority of DOC (including both particle-bound and gaseous components) can be removed from the atmosphere. Calculation of the radiative forcing of atmospheric impurities considers the entire atmospheric column. Meanwhile, the aerosol characteristics at different altitude are different. Because precipitation contains aerosol information of both the near surface and high altitude, it is proposed that the value of the MAC_{DOC} of precipitation is representative of a given region than that of near-surface aerosols. Therefore, despite a number of studies that have investigated the MAC_{WSOC} of surface aerosols (e.g., Bosch et al., 2014; Cheng et al., 2011; Hecobian et al., 2010; Li et al., 2016d), the reported data were higher than the actual value of the entire atmospheric column.

4. Conclusions

This study showed that the VWM DOC concentrations at three remote stations (Nam Co, Lulang and Everest) in the HTP were 1.05 ± 1.01 mg C L^{-1}, 0.83 ± 0.85 mg C L^{-1} and 0.86 ± 0.91 mg C L^{-1}, respectively. Due to the high altitudes and sparse local populations of the studied stations, all of these values were lower than those of urban areas with heavy air pollution. The precipitation DOC of Nam Co was mainly influenced by combustion emissions from South Asia and local Tibetan residents. Lulang Station is located in the corridor whereby Indian monsoon penetrates into the HTP, and thus, the precipitation DOC at this station reflected contributions from both South Asia emissions and ocean evaporation. Although it is located along the southern part of the HTP, Everest Station is also located in the rain shadow of the Himalayas with light precipitation, and thus, the precipitation DOC at this station was mainly contributed by mineral dust. Therefore, the precipitation DOC values at different remote areas of the HTP were largely different, reflecting multiple influencing factors of precipitation DOC over the HTP. The precipitation DOC depositions at the three studied stations were 0.34 ± 0.32 g C m^{-2} yr^{-1}, 0.84 ± 0.86 g C m^{-2} yr^{-1} and 0.16 ± 0.17 g C m^{-2} yr^{-1}, respectively. The annual and seasonal variations of DOC deposition were strongly controlled by the precipitation amounts at the studied stations. Accordingly, the deposition of precipitation DOC in the HTP decreased from the southeast to the northwest, with a total annual value of 0.94 ± 0.87 Tg annually. It should be noted that the estimation of wet deposition of DOC for the HTP might have large uncertainties since data from only three stations were used. However, due to the harsh environment and sparsity of stations on the HTP, this is the best estimation to date that can be achieved on the HTP. Meanwhile, because Lhasa and the glacial regions only account for a small fraction of the area (~2%) of the total HTP, the deposition of DOC in the HTP is estimated based on the data of the studied stations. The average MAC_{DOC} values at 365 nm of the three studied stations were 0.48 ± 0.47 m^2 g^{-1}, 0.25 ± 0.15 m^2 g^{-1}, and 0.64 ± 0.49 m^2 g^{-1}, respectively, all of which were significantly lower than those of corresponding near-surface aerosol samples. In addition, this phenomenon was also found at typical urban areas, implying that this is a general occurrence for both pristine and seriously polluted areas. Therefore, it is proposed that the radiative forcing caused by WS-BrC that achieved from near surface aerosols, is higher than those at high altitudes and cannot be simply applied to the entire atmospheric column, which includes both particle-bound and vaporous WS-BrC.

Acknowledgements

This study was supported by the NSFC (41675130, 41630754), China Postdoctoral Science Foundation (2016M602897), State Key Laboratory of Cryospheric Science (SKLCS-ZZ-2017). The authors acknowledge the staff of Lulang, Nam Co and Everest station for sample collection. The authors also appreciate these three stations for providing precipitation data.

References

Andreae, M.O., Gelencser, A., 2006. Black carbon or brown carbon? The nature of light-absorbing carbonaceous aerosols. Atmos. Chem. Phys. 6, 3131–3148.
Avery, G.B., Biswas, K.F., Mead, R., Southwell, M., Willey, J.D., Kieber, R.J., Mullaugh, K.M., 2013. Carbon isotopic characterization of hydrophobic dissolved organic carbon in rainwater. Atmos. Environ. 68, 230–234.
Bond, T.C., Bhardwaj, E., Dong, R., Jogani, R., Jung, S., Roden, C., Streets, D.G., Trautmann, N.M., 2007. Historical emissions of black and organic carbon aerosol from energy-related combustion, 1850–2000. Glob. Biogeochem. Cycles 21, GB2018.
Bond, T.C., Doherty, S.J., Fahey, D.W., Forster, P.M., Berntsen, T., DeAngelo, B.J., Flanner, M.G., Ghan, S., Kaercher, B., Koch, D., Kinne, S., Kondo, Y., Quinn, P.K., Sarofim, M.C., Schultz, M.G., Schulz, M., Venkataraman, C., Zhang, H., Zhang, S., Bellouin, N., Guttikunda, S.K., Hopke, P.K., Jacobson, M.Z., Kaiser, J.W., Klimont, Z., Lohmann, U., Schwarz, J.P., Shindell, D., Storelvmo, T., Warren, S.G., Zender, C.S., 2013. Bounding the role of black carbon in the climate system: a scientific assessment. J. Geophys. Res.-Atmos. 118, 5380–5552.
Bosch, C., Andersson, A., Kirillova, E.N., Budhavant, K., Tiwari, S., Praveen, P., Russell, L.M., Beres, N.D., Ramanathan, V., Gustafsson, Ö., 2014. Source-diagnostic dual-isotope composition and optical properties of water-soluble organic carbon and elemental carbon in the South Asian outflow intercepted over the Indian Ocean. J. Geophys. Res. Atmos. 119, 11,743–711,759.
Cao, J., Tie, X., Xu, B., Zhao, Z., Zhu, C., Li, G., Liu, S., 2010. Measuring and modeling black carbon (BC) contamination in the SE Tibetan Plateau. J. Atmos. Chem. 67, 45–60.
Chen, P., Kang, S., Bai, J., Sillanpää, M., Li, C., 2015. Yak dung combustion aerosols in the Tibetan Plateau: chemical characteristics and influence on the local atmospheric environment. Atmos. Res. 156, 58–66.
Cheng, Y., He, K.-B., Zheng, M., Duan, F.-K., Du, Z.-Y., Ma, Y.-L., Tan, J.-H., Yang, F.-M., Liu, J.-M., Zhang, X.-L., 2011. Mass absorption efficiency of elemental carbon and water-soluble organic carbon in Beijing, China. Atmos. Chem. Phys. 11, 11497–11510.
Cong, Z., Kang, S., Kawamura, K., Liu, B., Wan, X., Wang, Z., Gao, S., Fu, P., 2015. Carbonaceous aerosols on the south edge of the Tibetan Plateau: concentrations, seasonality and sources. Atmos. Chem. Phys. 15, 1573–1584.
Du, Z., He, K., Cheng, Y., Duan, F., Ma, Y., Liu, J., Zhang, X., Zheng, M., Weber, R., 2014. A yearlong study of water-soluble organic carbon in Beijing II: light absorption properties. Atmos. Environ. 89, 235–241.
Ervens, B., Turpin, B.J., Weber, R.J., 2011. Secondary organic aerosol formation in cloud droplets and aqueous particles (aqSOA): a review of laboratory, field and model studies. Atmos. Chem. Phys. 11, 11069–11102.
Forrister, H., Liu, J., Scheuer, E., Dibb, J., Ziemba, L., Thornhill, K.L., Anderson, B., Diskin, G., Perring, A.E., Schwarz, J.P., 2015. Evolution of brown carbon in wildfire plumes. Geophys. Res. Lett. 42, 4623–4630.
Gustafsson, Ö., Kruså, M., Zencak, Z., Sheesley, R.J., Granat, L., Engström, E., Praveen, P.S., Rao, P.S.P., Leck, C., Rodhe, H., 2009. Brown clouds over South Asia: biomass or fossil fuel combustion? Science 323, 495–498.
Hallquist, M., Wenger, J.C., Baltensperger, U., Rudich, Y., Simpson, D., Claeys, M., Dommen, J., Donahue, N.M., George, C., Goldstein, A.H., Hamilton, J.F., Herrmann, H., Hoffmann, T., Iinuma, Y., Jang, M., Jenkin, M.E., Jimenez, J.L., Kiendler-Scharr, A., Maenhaut, W., McFiggans, G., Mentel, T.F., Monod, A., Prevot, A.S.H., Seinfeld, J.H., Surratt, J.D., Szmigielski, R., Wildt, J., 2009. The formation, properties and impact of secondary organic aerosol: current and emerging issues. Atmos. Chem. Phys. 9, 5155–5236.
Hecobian, A., Zhang, X., Zheng, M., Frank, N., Edgerton, E.S., Weber, R.J., 2010. Water-soluble organic aerosol material and the light-absorption characteristics of aqueous extracts measured over the Southeastern United States. Atmos. Chem. Phys. 10, 5965–5977.
Hu, Z., Kang, S., Li, C., Yan, F., Chen, P., Gao, S., Wang, Z., Zhang, Y., Sillanpaa, M., 2017. Light absorption of biomass burning and vehicle emission-sourced carbonaceous aerosols of the Tibetan Plateau. Environ. Sci. Pollut. Res. Int. http://dx.doi.org/10.1007/s11356-017-9077-3.
Kang, S., Chen, P., Li, C., Liu, B., Cong, Z., 2016. Atmospheric aerosol elements over the inland Tibetan Plateau: concentration, seasonality, and transport. Aerosol Air Qual. Res. 16, 789–800.
Kaspari, S.D., Schwikowski, M., Gysel, M., Flanner, M.G., Kang, S., Hou, S., Mayewski, P.A., 2011. Recent increase in black carbon concentrations from a Mt. Everest ice core spanning 1860–2000 AD. Geophys. Res. Lett. 38.
Kieber, R.J., Peake, B., Willey, J.D., Avery, G.B., 2002. Dissolved organic carbon and organic acids in coastal New Zealand rainwater. Atmos. Environ. 36, 3557–3563.
Kieber, R.J., Whitehead, R.F., Reid, S.N., Willey, J.D., Seaton, P.J., 2006. Chromophoric dissolved organic matter (CDOM) in rainwater, southeastern North Carolina, USA. J. Atmos. Chem. 54, 21–41.
Kirillova, E.N., Andersson, A., Han, J., Lee, M., Gustafsson, Ö., 2014a. Sources and light absorption of water-soluble organic carbon aerosols in the outflow from northern China. Atmos. Chem. Phys. 14, 1413–1422.
Kirillova, E.N., Andersson, A., Tiwari, S., Srivastava, A.K., Bisht, D.S., Gustafsson, O., 2014b. Water-soluble organic carbon aerosols during a full New Delhi winter: isotope-based source apportionment and optical properties. J. Geophys. Res.-Atmos. 119, 3476–3485.
Lambe, A.T., Cappa, C.D., Massoli, P., Onasch, T.B., Forestieri, S.D., Martin, A.T., Cummings, M.J., Croasdale, D.R., Brune, W.H., Worsnop, D.R., Davidovits, P., 2013. Relationship between oxidation level and optical properties of secondary organic aerosol. Environ. Sci. Technol. 47, 6349–6357.
Legrand, M., Preunkert, S., Schock, M., Cerqueira, M., Kasper-Giebl, A., Afonso, J., Pio, C., Gelencser, A., Dombrowski-Etchevers, I., 2007. Major 20th century changes of carbonaceous aerosol components (EC, WinOC, DOC, HULIS, carboxylic acids, and cellulose) derived from Alpine ice cores. J. Geophys. Res.-Atmos. 112.
Li, C., Kang, S., Zhang, Q., Kaspari, S., 2007. Major ionic composition of precipitation in the Nam Co region, Central Tibetan Plateau. Atmos. Res. 85, 351–360.
Li, C., Bosch, C., Kang, S., Andersson, A., Chen, P., Zhang, Q., Cong, Z., Chen, B., Qin, D., Gustafsson, Ö., 2016a. Sources of black carbon to the Himalayan–Tibetan Plateau glaciers. Nat. Commun. 7, 12574.

Li, C., Chen, P., Kang, S., Yan, F., Hu, Z., Qu, B., Sillanpää, M., 2016b. Concentrations and light absorption characteristics of carbonaceous aerosol in PM2.5 and PM10 of Lhasa city, the Tibetan Plateau. Atmos. Environ. 127, 340–346.
Li, C., Chen, P., Kang, S., Yan, F., Li, X., Qu, B., Sillanpää, M., 2016c. Carbonaceous matter deposition in the high glacial regions of the Tibetan Plateau. Atmos. Environ. 141, 203–208.
Li, C., Yan, F., Kang, S., Chen, P., Hu, Z., Gao, S., Qu, B., Sillanpää, M., 2016d. Light absorption characteristics of carbonaceous aerosols in two remote stations of the southern fringe of the Tibetan Plateau, China. Atmos. Environ. 79–85.
Li, C., Yan, F., Kang, S., Chen, P., Qu, B., Hu, Z., Sillanpää, M., 2016e. Concentration, sources, and flux of dissolved organic carbon of precipitation at Lhasa city, the Tibetan Plateau. Environ. Sci. Pollut. Res. 23, 12915–12921.
Liu, B., Kang, S., Sun, J., Zhang, Y., Xu, R., Wang, Y., Liu, Y., Cong, Z., 2013. Wet precipitation chemistry at a high-altitude site (3,326 m a.s.l.) in the southeastern Tibetan Plateau. Environ. Sci. Pollut. Res. 20, 5013–5027.
Liu, Y.W., Xu, R., Wang, Y.S., Pan, Y.P., Piao, S.L., 2015. Wet deposition of atmospheric inorganic nitrogen at five remote sites in the Tibetan Plateau. Atmos. Chem. Phys. 15, 11683–11700.
Lu, Z., Streets, D.G., Zhang, Q., Wang, S., 2012. A novel back-trajectory analysis of the origin of black carbon transported to the Himalayas and Tibetan Plateau during 1996–2010. Geophys. Res. Lett. 39, L01809.
Lüthi, Z.L., Kerlak, B., Kim, S.-W., Lauer, A., Mues, A., Rupakheti, M., Kang, S., 2014. Atmospheric brown clouds reach the Tibetan Plateau by crossing the Himalayas. Atmos. Chem. Phys. Discuss. 14, 28105–28146.
Luthi, Z.L., Skerlak, B., Kim, S.W., Lauer, A., Mues, A., Rupakheti, M., Kang, S., 2015. Atmospheric brown clouds reach the Tibetan Plateau by crossing the Himalayas. Atmos. Chem. Phys. 15, 6007–6021.
Ma, Y., Kang, S., Zhu, L., Xu, B., Tian, L., Yao, T., 2008. Tibetan Observation and Research Platform atmosphere-land interaction over a heterogeneous landscape. Bull. Am. Meteorol. Soc. 89 (1487-+).
Maliszewska-Kordybach, B., 1999. Sources, concentrations, fate and effects of polycyclic aromatic hydrocarbons (PAHs) in the environment. Part A: PAHs in air. Pol. J. Environ. Stud. 8, 131–136.
May, B., Wagenbach, D., Hoffmann, H., Legrand, M., Preunkert, S., Steier, P., 2013. Constraints on the major sources of dissolved organic carbon in Alpine ice cores from radiocarbon analysis over the bomb-peak period. J. Geophys. Res. Atmos. 118, 3319–3327.
Ming, J., Xiao, C., Sun, J., Kang, S., Bonasoni, P., 2010. Carbonaceous particles in the atmosphere and precipitation of the Nam Co region, central Tibet. J. Environ. Sci. 22, 1748–1756.
Pan, Y., Wang, Y., Xin, J., Tang, G., Song, T., Wang, Y., Li, X., Wu, F., 2010. Study on dissolved organic carbon in precipitation in Northern China. Atmos. Environ. 44, 2350–2357.
Pilson, M.E.Q., 1998. An Introduction to the Chemistry of the Sea. American Society for Microbiology (ASM).
Qi, W., Zhang, B., Pang, Y., Zhao, F., Zhang, S., 2013. TRMM-data-based spatial and seasonal patterns of precipitation in the Qinghai-Tibet Plateau. Sci. Geogr. Sin. 33, 999–1005.
Raymond, P.A., 2005. The composition and transport of organic carbon in rainfall: insights from the natural (^{13}C and ^{14}C) isotopes of carbon. Geophys. Res. Lett. 32, L14402.
Saxena, P., Hildemann, L.M., 1996. Water-soluble organics in atmospheric particles: a critical review of the literature and application of thermodynamics to identify candidate compounds. J. Atmos. Chem. 24, 57–109.
Siudek, P., Frankowski, M., Siepak, J., 2015. Seasonal variations of dissolved organic carbon in precipitation over urban and forest sites in central Poland. Environ. Sci. Pollut. Res. 22, 11087–11096.
Szidat, S., Jenk, T.M., Synal, H.-A., Kalberer, M., Wacker, L., Hajdas, I., Kasper-Giebl, A., Baltensperger, U., 2006. Contributions of fossil fuel, biomass-burning, and biogenic emissions to carbonaceous aerosols in Zurich as traced by ^{14}C. J. Geophys. Res. Atmos. 111 (1984–2012).
Textor, C., Schulz, M., Guibert, S., Kinne, S., Balkanski, Y., Bauer, S., Berntsen, T., Berglen, T., Boucher, O., Chin, M., Dentener, F., Diehl, T., Feichter, J., Fillmore, D., Ginoux, P., Gong, S., Grini, A., Hendricks, J., Horowitz, L., Huang, P., Isaksen, I.S.A., Iversen, T., Kloster, S., Koch, D., Kirkevag, A., Kristjansson, J.E., Krol, M., Lauer, A., Lamarque, J.F., Liu, X., Montanaro, V., Myhre, G., Penner, J.E., Pitari, G., Reddy, M.S., Seland, O., Stier, P., Takemura, T., Tie, X., 2007. The effect of harmonized emissions on aerosol properties in global models – an AeroCom experiment. Atmos. Chem. Phys. 7, 4489–4501.
Vignati, E., Karl, M., Krol, M., Wilson, J., Stier, P., Cavalli, F., 2010. Sources of uncertainties in modelling black carbon at the global scale. Atmos. Chem. Phys. 10, 2595–2611.
Willey, J.D., Kieber, R.J., Eyman, M.S., Avery Jr., G.B., 2000. Rainwater dissolved organic carbon: concentrations and global flux. Glob. Biogeochem. Cycles 14, 139–148.
Yan, G., Kim, G., 2012. Dissolved organic carbon in the precipitation of Seoul, Korea: implications for global wet depositional flux of fossil-fuel derived organic carbon. Atmos. Environ. 59, 117–124.
Yan, C., Zheng, M., Sullivan, A.P., Bosch, C., Desyaterik, Y., Andersson, A., Li, X., Guo, X., Zhou, T., Gustafsson, Ö., Collett Jr., J.L., 2015. Chemical characteristics and light-absorbing property of water-soluble organic carbon in Beijing: biomass burning contributions. Atmos. Environ. 121, 4–12.
Yan, F., Kang, S., Li, C., Zhang, Y., Qin, X., Li, Y., Zhang, X., Hu, Z., Chen, P., Li, X., Qu, B., Sillanpää, M., 2016. Concentration, sources and light absorption characteristics of dissolved organic carbon on a medium-sized valley glacier, northern Tibetan Plateau. Cryosphere 10, 2611–2621.
Zafiriou, O.C., Gagosian, R.B., Peltzer, E.T., Alford, J.B., Loder, T., 1985. Air-to-sea fluxes of lipids at Enewetak atoll. J. Geophys. Res.-Atmos. 90, 2409–2423.
Zhang, X., Lin, Y.-H., Surratt, J.D., Zotter, P., Prévôt, A.S.H., Weber, R.J., 2011. Light-absorbing soluble organic aerosol in Los Angeles and Atlanta: a contrast in secondary organic aerosol. Geophys. Res. Lett. 38 (n/a-n/a).
Zhang, Y., Kang, S., Li, C., Cong, Z., Zhang, Q., 2012. Wet deposition of precipitation chemistry during 2005–2009 at a remote site (Nam Co Station) in central Tibetan Plateau. J. Atmos. Chem. 69, 187–200.
Zhang, R., Wang, H., Qian, Y., Rasch, P.J., Easter, R.C., Ma, P.L., Singh, B., Huang, J., Fu, Q., 2015. Quantifying sources, transport, deposition, and radiative forcing of black carbon over the Himalayas and Tibetan Plateau. Atmos. Chem. Phys. 15, 6205–6223.

Publication IV

Yan, F., Wang, P., Kang, S., Chen, P., Hu, Z., Han, X., Sillanpää, M., Li, C.
High particulate carbon deposition in Lhasa—a typical city in the Himalayas–Tibetan Plateau due to local contributions

Reprinted with permission from
Chemosphere
Vol. 247, 2020

Chemosphere 247 (2020) 125843

Contents lists available at ScienceDirect

Chemosphere

journal homepage: www.elsevier.com/locate/chemosphere

High particulate carbon deposition in Lhasa—a typical city in the Himalayan–Tibetan Plateau due to local contributions

Fangping Yan [a, b, d], Pengling Wang [c], Shichang Kang [d, e, f], Pengfei Chen [d], Zhaofu Hu [d, f], Xiaowen Han [b, f], Mika Sillanpää [a], Chaoliu Li [b, e, *]

[a] Department of Green Chemistry, LUT University, Sammonkatu 12, FI-50130, Mikkeli, Finland
[b] Key Laboratory of Tibetan Environment Changes and Land Surface Processes, Institute of Tibetan Plateau Research, Chinese Academy of Sciences, Beijing, 100101, China
[c] National Climate Center, China Meteorological Administration, Beijing, 100081, China
[d] State Key Laboratory of Cryospheric Sciences, Northwest Institute of Eco-Environment and Resources, Chinese Academy of Sciences, Lanzhou, 730000, China
[e] CAS Center for Excellence in Tibetan Plateau Earth Sciences, Chinese Academy of Sciences, Beijing, 100085, PR China
[f] University of Chinese Academy of Sciences, Beijing, 100049, China

HIGHLIGHTS

- High in-situ black and organic carbon deposition rates were reported in Lhasa.
- High deposition rates were mainly resulted from local emissions in Lhasa.
- Dry deposition is more important than wet deposition in Lhasa particle scavenging.

GRAPHICAL ABSTRACT

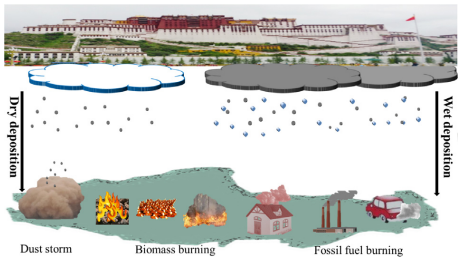

ARTICLE INFO

Article history:
Received 26 August 2019
Received in revised form
30 December 2019
Accepted 3 January 2020
Available online 6 January 2020

Handling editor: R Ebinghaus

Keywords:
Black carbon
Organic carbon
Lhasa
Dry and wet deposition

ABSTRACT

The Himalayan–Tibetan Plateau is a typical remote region with sparse air pollution. However, air pollution in cites of the inner Himalayan–Tibetan Plateau is relatively serious due to emissions from local residents. Carbonaceous aerosols are not only an important component of air pollutants that affect the health of local residents but also an important trigger of climate change. In this study, the annual wet and dry deposition rates of carbonaceous particles were investigated in Lhasa—a typical city in the Himalayan–Tibetan Plateau, by collecting precipitation and dry deposition samples and analyzing with a thermal-optical measurement protocol. The results showed that the in-situ annual wet deposition rates of water-insoluble organic carbon (WIOC) and black carbon (BC) were 169.6 and 19.4 mg m^{-2} yr^{-1}, respectively, with the highest and lowest values occurring in the monsoon and non-monsoon periods, respectively. Both precipitation amounts and concentrations of WIOC and BC contributed to wet deposition rates. The dry deposition rates of WIOC and BC in Lhasa had an opposite seasonal variation to that of wet deposition, with annual average deposition rates of 2563.9 and 165.7 mg m^{-2} yr^{-1}, respectively,

* Corresponding author. Key Laboratory of Tibetan Environment Changes and Land Surface Processes, Institute of Tibetan Plateau Research, Chinese Academy of Sciences, Beijing, 100101, China.
E-mail address: lichaoliu@itpcas.ac.cn (C. Li).

https://doi.org/10.1016/j.chemosphere.2020.125843

which were much higher than those of the nearby glacier region and remote area. These values were also much higher than the results from modeling and empirical calculations, indicating that Lhasa is a high pollution point that cannot capture by models. The results in this study have significant implications for the transport of local emissions in Lhasa to the nearby remote and glacier regions.

1. Introduction

Carbonaceous matter is an important component of atmospheric aerosols, which generally consist of black carbon (BC) and organic carbon (OC). BC is a primary species derived from the incomplete combustion of either fossil fuel or biomass combustion. OC has both primary and secondary origins. Primary OC is mainly derived from combustion processes as submicron particles and some mechanical processes (e.g., release of plant spores and pollen, spread of soil organic matter, decomposition of vegetation debris) as coarse particles. Secondary OC is mainly formed by the conversion of gas to particles of volatile organic compounds (Seinfeld and Pankow, 2003). OC is a complex mixture of organic matter. According to its water solubility, OC is divided into water-soluble OC (i.e., DOC) and water-insoluble OC (WIOC). Both BC and OC influence the radiation budget in the atmosphere and climate forcing. For example, BC is considered the second agent after carbon dioxide on the climate warming effect in the present atmosphere (Jacobson, 2000; Bond et al., 2013), while OC can exert both warming and cooling effects (Andreae and Gelencsér, 2006). Therefore, atmospheric BC and OC have been investigated at many sites worldwide due to their significant local and global climate impacts. However, current knowledge on the atmospheric removal of BC and OC is still incomplete due to the poor documentation of one of its key aspects, wet deposition, which is regarded as an important removal process of particulate carbon from the atmosphere (Jurado et al., 2008; Custodio et al., 2014; Zhang et al., 2015a; Iavorivska et al., 2016; Sorokina and Soier, 2016; Qi et al., 2017a, 2017b). Meanwhile, recent studies also suggest that dry deposition may play an equally or more important role in BC and OC scavenging as wet deposition in some regions (Cerqueira et al., 2010; Matsuda et al., 2012; Yang et al., 2014; Yan et al., 2019). Nevertheless, related studies are scarce, especially in remote regions, such as the Himalayan–Tibetan Plateau (Kang et al., 2019; Yan et al., 2019), hindering the ability of global and regional models to adequately simulate the concentration and transport of particulate carbon in the atmosphere and consequently introducing large uncertainties in the simulated climate forcing.

The Himalayan–Tibetan Plateau is generally considered one of the most remote and pristine regions in the world. Lhasa is the largest city and the capital of the Tibetan Autonomous Region of China. Lhasa is also one of the economic and cultural centers of the Himalayan–Tibetan Plateau. The total population of this city is approximately 0.9 million. In recent years, Lhasa has witnessed dramatic urbanization and economic growth (Huang et al., 2010). As the holy land of Buddhism, thousands of tourists rush to Lhasa, boosting energy consumption, construction and religious activities, which all contribute to the deteriorating atmosphere of Lhasa (Chen et al., 2018; Cui et al., 2018; Li et al., 2018b). Moreover, due to the high elevation, incomplete fuel combustion in the low-oxygen atmosphere may aggravate the air pollution in Lhasa. The unique location, energy consumption structure and religious activities make Lhasa a unique city compared to other urban cities in the world and a subject of scientific concern and interest (Zhang et al., 2001; Huang et al., 2010; Cong et al., 2011).

So far, most efforts have been focused on investigating atmospheric chemistry in the ambient atmosphere (Huang et al., 2010; Cong et al., 2011; Li et al., 2016b; Wan et al., 2016; Chen et al., 2019a, 2019b) and the near surface atmosphere in Lhasa (Hu et al., 2017; Cui et al., 2018; Li et al., 2018b), which suggests that despite relatively clean compared to other large cities in China, the atmosphere in Lhasa is significantly influenced by local emissions, and pollution events are particularly common in static winter conditions (Li et al., 2018b). However, chemical deposition studies in Lhasa have merely investigated mercury (Huang et al., 2013), trace elements (Guo et al., 2015) and DOC in precipitation (Li et al., 2016d). To our knowledge, there has been no study dedicated to both the dry and the wet deposition rates of WIOC and BC in Lhasa. Thus, we investigated dry and wet deposition rates of WIOC and BC during 2017 and 2018 in Lhasa. This work is the continuation of our previous study on the wet deposition rate of precipitation DOC in Lhasa (Li et al., 2016d). The aims are to determine the concentrations and deposition rates of WIOC and BC and their removal and lifetime characteristics in this typical urban city of the Himalayan–Tibetan Plateau and to provide reference data for other studies, such as modeling in the high-elevation cities of the Himalayan–Tibetan Plateau.

2. Methodology

2.1. Sampling site

Lhasa is located in a narrow west-east valley in the southern Himalayan–Tibetan Plateau (Fig. 1). It is characterized by a dry non-monsoon season and a wet monsoon season (May to September, Fig. 2). During the monsoon season, the low pressure over the Himalayan–Tibetan Plateau brings warm and moist air masses from the Indian Ocean, contributing to the intense precipitation. During the non-monsoon seasons, the atmospheric circulation patterns are dominated by westerly air flows with limited precipitation. The average annual precipitation in Lhasa was 540.6 mm during the study period, and most of this precipitation occurred during the monsoon season (93%).

2.2. Sample collection and analysis

A total of 81 precipitation samples were collected in a prebaked aluminum basin (550 °C, 6 h) on top of the 15-m-high office building of Lhasa station at the Institute of Tibetan Plateau Research, Chinese Academy of Sciences, from 2017 to 2018 (Fig. 1) (Li et al., 2016d). This sampling site is situated in the western part of the city. It is considered as a typical urban location which does not have obvious emission sources nearby but is primarily influenced by emissions from Lhasa city such as industries, vehicular traffic and local residents (Cong et al., 2011; Gong et al., 2011; Huang et al., 2013). The majority of collected samples represented the heavy precipitation events, and the amount of precipitation that was analyzed for carbonaceous particles accounted for approximately 75% of the total amount of precipitation during the study period. In this case, a large volume of precipitation could be collected in a

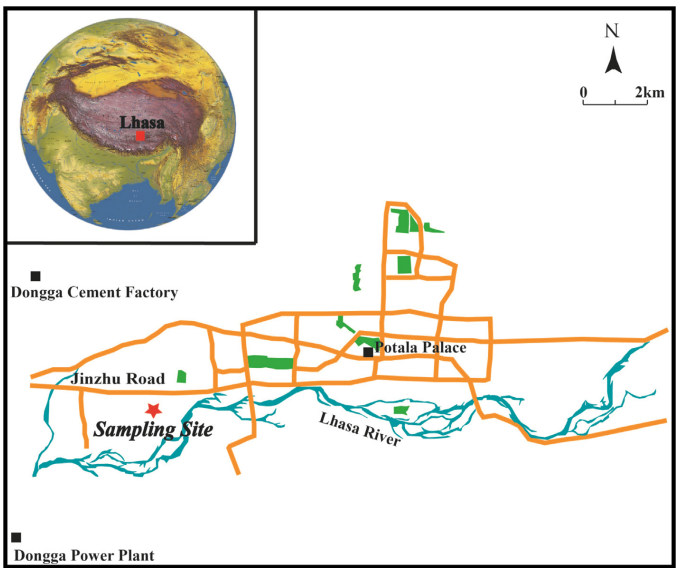

Fig. 1. Location map of the sampling site of Lhasa in the Himalayan–Tibetan Plateau.

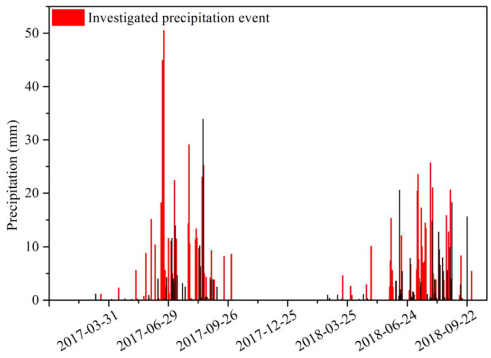

Fig. 2. Precipitation amount during the sampling period in Lhasa during 2017–2018.

short period, which not only met the analytical requirement but also avoided interference of dry deposition, evaporation and adhesion of particles to the collector. The collected samples were then well shaken and transferred to precleaned polycarbonate bottles when the precipitation ended and were kept frozen until analysis (Raymond, 2005). The precipitation amounts during the study period were obtained from the China Meteorological Administration in Lhasa (approximately 10 km east of the sampling site) (Fig. 2).

A coagulant, $NH_4H_2PO_4$, was added to the collected samples to improve the BC collection efficiency (Torres et al., 2013; Li et al., 2016a). In detail, $NH_4H_2PO_4$ (1.5 g per 100 mL of samples) was added to the melted precipitation samples, and the mixture was then magnetically stirred for 10 min, after which samples were filtered three times through prebaked and equilibrated quartz filters (pore size: 0.45 μm, Pall Tissuquartz™, 2500QAT-UP, USA). To reduce the potential contribution of carbonate carbon from mineral dust, the filtered samples were acidified with 2 M HCl (Ming et al., 2009; Yan et al., 2019).

A total of 12 dry deposition samples were collected monthly during 2017 and 2018 in a stainless-steel bucket using the same method provided in Yan et al. (2019). Each collected sample was dissolved in ultrapure water, transferred into polycarbonate bottles and divided into two equal parts. One part was filtered with the same method used for the precipitation samples and treated in acid following the protocol used for BC sediments (Han et al., 2007a; Yan et al., 2019). The other part was filtered and fumigated by 12 M HCl to remove carbonate carbon (Chow et al., 1993; Li et al., 2016a; Yan et al., 2019) before WIOC measurement. New aluminum basins and buckets for wet and dry deposition samples were used for every sampling event. To eliminate the influence of precipitation, the dry deposition rates of WIOC and BC were obtained by subtracting the wet deposition rates in those months with precipitation events.

After filtration and consequent dry and equilibrium of the filter samples (Torres et al., 2013), the concentrations of WIOC and BC in the treated wet and dry deposition samples were analyzed using a thermal-optical reflectance (TOR) carbon analyzer (Sunset Laboratory, Tigard, OR, USA) following the Interagency Monitoring of Protected Visual Environments (IMPROVE) protocol. A national standard (*n*-hexane) and a sucrose standard were subjected to the pretreatment process of the dry deposition samples and measurement process of the filter samples, respectively (Han et al., 2007b; Chen et al., 2013). The DOC concentration was determined by a Shimadzu TOC-5000 total organic carbon analyzer (Shimadzu Corp, Kyoto, Japan) after being filtered through a membrane of 0.45 μm pore size (PTFE, Macherey–Nagel) (Li et al., 2016d; Yan et al., 2016). The blank concentrations for WIOC, BC and DOC

during the wet deposition collection and analysis processes were 0.062 ± 0.004, 0.0 and 0.05 ± 0.02 μg mL^{-1}, respectively. The corresponding values were 0.048 ± 0.016, 0.0 and 0.05 ± 0.01 μg mL^{-1}, respectively, for the dry deposition collection and analysis processes.

2.3. Deposition rates of WIOC, BC and DOC

The annual wet deposition rates of WIOC, BC and DOC in precipitation were calculated using the volume-weighted mean concentrations and the average annual precipitation amount in Lhasa because not every precipitation event was sampled. The wet deposition rate was calculated based on the following equations:

$$Fc = C \times P \quad (1)$$

$$C = \frac{\sum_{i=1}^{i=n} Ci \times Pi}{\sum_{i=1}^{i=n} Pi} \quad (2)$$

where Fc (mg C m^{-2} yr^{-1}) expresses the WIOC, BC or DOC wet deposition rate, C (mg L^{-1}) represents the volume-weighted mean concentrations of WIOC, BC or DOC in precipitation, Ci (mg L^{-1}) stands for the concentration of WIOC, BC or DOC in individual precipitation sample i, Pi (mm) is the precipitation amount corresponding to precipitation sample i, and P (mm yr^{-1}) is the average annual precipitation.

Dry deposition rates were calculated by measuring average concentrations of WIOC and BC in every monthly collected deposition sample. The total deposition rate was calculated by counting the dry and wet deposition rates throughout the year.

3. Results and discussion

3.1. WIOC, BC and DOC concentrations in precipitation

The annual volume-weighted mean concentrations of WIOC, BC and DOC in the precipitation of Lhasa during the study period were 314 ± 382, 35.8 ± 34.2 and 1169 ± 1021 μg L^{-1}, respectively. These values were slightly underestimated because the samples were mainly collected during heavy precipitation event. Nevertheless, the concentrations of WIOC and BC in Lhasa were comparable to those in remote sites, such as Sado in Japan (Huo et al., 2016) and rural sites in Europe, such as K-Puszta in Hungary (Cerqueira et al., 2010). However, these concentrations in Lhasa were lower than those in megacities such as Tokyo (Huo et al., 2016) and Paris (Ducret and Cachier, 1992) (Table 1), indicating that despite some relatively heavy pollution (Cui et al., 2018; Li et al., 2018b), the atmosphere in Lhasa is relatively clean. Moreover, the concentrations of WIOC and BC in Lhasa were lower than those of the nearby Zhadang glacier, which was probably attributed to the additional dry deposition of carbonaceous matter on this glacier (Table 1). The annual volume-weighted mean DOC concentration of this study was almost the same as the concentration we reported in 2013 (Li et al., 2016d), reflecting the consistent atmospheric conditions in Lhasa.

Seasonally, the highest concentrations of WIOC and BC occurred in the non-monsoon period, while the lowest concentrations existed in the monsoon period (Fig. 3), which was similar to the concentration variation in total carbon in the atmosphere (Huang et al., 2010) and to the concentration variations in DOC (Li et al., 2016d), mercury (Huang et al., 2013) and trace elements (Guo et al., 2015) in precipitation of Lhasa, reflecting that this is a general phenomenon of pollutant variation in Lhasa. The low concentrations of WIOC and BC in precipitation during the monsoon season were mainly attributed to the relatively large precipitation amount and the flourishing vegetation and high mixing height of the atmosphere. In contrast, high concentrations of WIOC and BC in precipitation in the non-monsoon season were primarily caused by the minimal precipitation amount and the high concentration of particulate carbon in the atmosphere because of the enhanced combustion activities and dust suspension during this period (Penduo et al., 2008). The peaks of the WIOC and BC concentrations appeared in April and were mainly caused by both dust loading from dust storms and construction activities. There was a statistically significant relationship between WIOC and BC concentrations ($p < 0.01$), indicating their common sources and consistent variations.

The concentrations of WIOC and BC in precipitation were also influenced by the diversity of local emissions. For instance, despite the similar precipitation amounts in July and August, the concentrations of WIOC and BC in August were higher than those in July (Fig. 3) because of the increased local carbonaceous particle emissions in August. One of the important traditional festivals for Tibetan residents—the Sho Dun Festival—occurs every year in August or early September for approximately one week. People gather together during this festival to organize activities such as a Buddha exhibition and Tibetan Opera. A similar phenomenon was also observed in the monthly concentration variation in polycyclic aromatic hydrocarbons and other particulate air pollutants in Lhasa (Gong et al., 2011). In addition, a large number of tourists come to Lhasa in August because of the summer holiday, resulting in more anthropogenic emissions in this month.

3.2. Relative ratios of WIOC, BC and DOC

The relative ratios of the three components of carbonaceous matter (WIOC, BC and DOC) can provide information on their sources and removal process from the atmosphere (Cerqueira et al., 2010; Huo et al., 2016). It is obvious that BC was a minor component of total carbon mass in precipitation at both Lhasa and other study sites (Table 1, Fig. 4), which reflected a lower incorporation of BC into precipitation or a relatively higher input of WIOC to the atmosphere of Lhasa. The ratio of WIOC to DOC in Lhasa (0.27) was comparable to that in a rural site (0.26) but higher than that in a mountain site (0.14) of Europe (Table 1), which was because the relatively high ratio in Lhasa was mainly attributed to the primary emissions from this city itself (Li et al., 2016b; Hu et al., 2017); In contrast, the low ratios in remote and mountain sites were primarily influenced by the long-range transported emissions with large fraction of secondary organic aerosols that can easily dissolve in precipitation (Li et al., 2017b). The ratio of WIOC to BC in aerosol samples (1.2) was approximately 7.4 times lower than that in precipitation samples (8.8) (Fig. 4), indicating that compared to BC, WIOC was more easily removed by the wet deposition process.

3.3. Two scavenge processes in wet deposition of particulate carbon

There are two processes for the wet deposition of particulate carbon in the atmosphere: “below-cloud” scavenging (the washout process), where the particles are directly removed by precipitation; and “in-cloud” scavenging (rainout process), where the particles are incorporated into cloud droplets. The chemical nature of the surface of particulate carbon in the atmosphere is an important determining factor for the scavenging process. If the surface is hydrophilic, the particles could be activated and incorporated into water droplets, acting as cloud condensation nuclei (CCN). However, if the surface is hydrophobic, the particles may be inactivated and removed more by the washout process (Ducret and Cachier, 1992). Generally, both processes are involved in different periods

Table 1
Concentrations and deposition rates of WIOC, BC and DOC in precipitation of Lhasa and other study sites.

Sampling site	Site type	Period	WIOC (μg L^{-1})	BC (μg L^{-1})	DOC (μg L^{-1})	Annual precipitation (mm)	Annual wet WIOC deposition (mg m^{-2} yr^{-1})	Annual wet (total) BC deposition (mg m^{-2} yr^{-1})	Method	Reference
Lhasa	HTP	2017–2018	314 ± 382	35.8 ± 34.2	1169 ± 1021	540.6	169.6	19.4 (185.1)	TOR	This study
Nam Co Station	HTP	2005–2007				302.4		(10.5)	TOT	1
Zhadang glacier	HTP	2013–2014	578	78.9	370	527.5	167	(22.8)	TOT	1,2
Nam Co Station	HTP	2015–2017	192 ± 258.6	18.5 ± 33.7	105	313.2	60.2	5.8 (15.3)	TOR	3, 4
Lulang Station	HTP	2015–2016	327 ± 258	34.3 ± 35.3	830	1009.5	330.0	34.6 (58.9)	TOR	3,4
Everest Station	HTP	2015–2017	248 ± 210	13.5 ± 14.5	860	189.8	47.0	2.6 (9.7)	TOR	3,4
Azores, Portugal	Marine	2003–2004	113 ± 78	2.8 ± 4.3	210 ± 110	1132	114	5 (5.3)	Thermal-optical method	5
Schauinsland, Germany	Mountain	2003–2004	205 ± 266	28 ± 38	1492 ± 1291	1574	378	38 (40.2)	Thermal-optical method	5
Sonnblick, Austria	Mountain	2003–2004	145 ± 174	5.2 ± 3.7		2082	234	10 (11.1)	Thermal-optical method	5
K-Puszta, Hungary	Rural	2003–2004	358 ± 194	24 ± 24	1352 ± 666	595	219	9.5 (18.6)	Thermal-optical method	5
Aveiro, Portugal	Rural	2003–2004	98 ± 56	14 ± 13	442 ± 185	729	61	7.5 (15.4)	Thermal-optical method	5
Sado, Japan	Remote	2011–2012	274	26	1125	1087	314	26.3	TOR	6
Tokyo, Japan	Urban	2011–2012	657	78.9	1425	1438	676	59.8	TOR	6
Paris, France	Urban	1988–1990	851	330					Two-step Thermal process	7

1. (Li et al., 2017a); 2. (Li et al., 2016c); 3. (Li et al., 2017b); 4. (Yan et al., 2019); 5. (Cerqueira et al., 2010); 6. (Huo et al., 2016); 7. (Ducret and Cachier, 1992). Note: the concentrations of WIOC, BC and DOC are mean ± standard deviation.

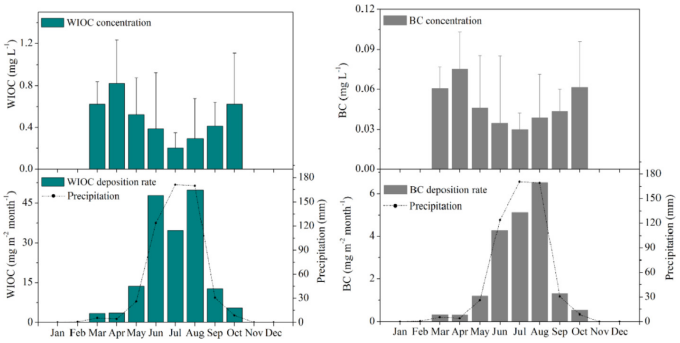

Fig. 3. Monthly average concentrations and wet deposition rates of WIOC and BC in precipitation of Lhasa during 2017–2018.

of a precipitation occurrence (Ishikawa et al., 1995), but it is rather difficult to clearly distinguish the contribution of the two scavenging processes. In previous studies, an inverse relationship between concentration and precipitation as presented in Fig. 5 was usually explained by the effect of the washout process, which suggested that the particles were washed out from the atmosphere during the early stage of the precipitation occurrence, resulting in low precipitation concentrations at the later stage (Seymour and Stout, 1983; Prado-Fiedler, 1990). However, this inverse relationship may be contributed by rainout process simultaneously as suggested by Prado-Fiedler (1990). This phenomenon was also consistent with a pictorial model proposed by Ishikawa et al. (1995), in which the washout and rainout processes play important role in the scavenging of particles at different precipitation stages.

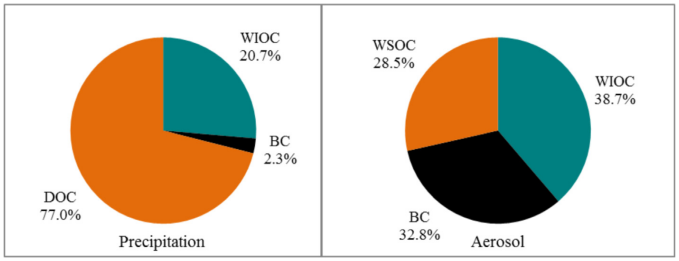

Fig. 4. Relative ratios of average WIOC, BC and DOC in precipitation during 2017–2018 and in aerosols of Lhasa. *Note:* the aerosol data were adopted from Li et al. (2016b).

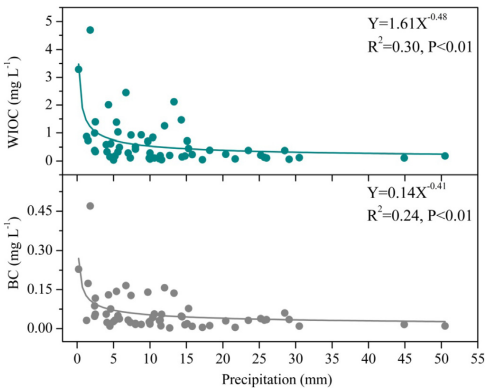

Fig. 5. Concentrations of WIOC and BC versus precipitation amounts in individual precipitation events in Lhasa during 2017–2018.

3.4. Discussion of deposition rates of WIOC and BC

The annual wet deposition rates of WIOC and BC in Lhasa were 169.6 and 19.4 mg m^{-2} yr^{-1}, respectively, with a high wet deposition rate in the monsoon season and a low wet deposition rate in the non-monsoon season (Fig. 3), indicating that the precipitation amount fundamentally influenced the wet depositions of WIOC and BC. Conversely, the high dry deposition rates of WIOC and BC occurred in the non-monsoon period (Fig. 6). In addition, annual dry deposition rates of WIOC and BC in Lhasa were 2563.9 and 165.7 mg m^{-2} yr^{-1}, respectively, approximately 15 and 8.5 times higher than the corresponding wet deposition rates, implying the more important role of dry deposition in total carbon deposition in Lhasa, especially during the non-monsoon period when precipitation is rare (Fig. 6). The much higher WIOC and BC dry than wet deposition rate in Lhasa could be attributed to the locally emitted fresh particles that were not easily incorporated into precipitation, the enhanced emissions during non-monsoon period, as well as due to the mineral dust sourced from dust storms, construction and other activities. Lhasa is located in a river valley, and dust storms are common during the non-monsoon period, especially in spring.

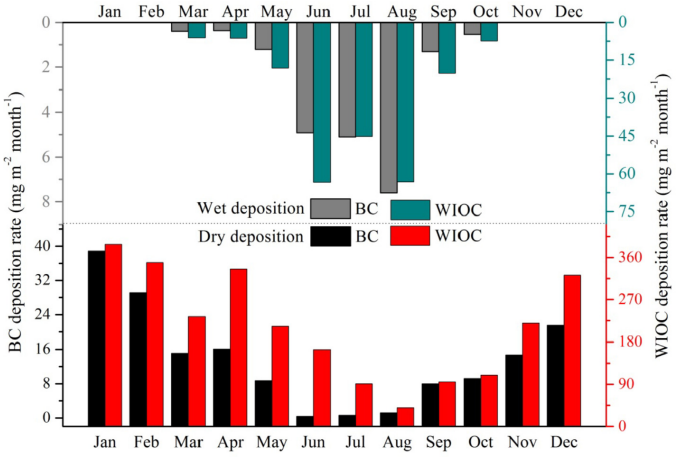

Fig. 6. Monthly average variations in wet and dry deposition rates of WIOC and BC in Lhasa during 2017–2018.

Many construction activities have occurred in Lhasa in recent years. The average BC concentration in dry deposition samples was 7.2 mg g^{-1} in Lhasa, higher than those in surface soil (e.g., 1.3 mg g^{-1} and 2.2 ± 1.6 mg g^{-1} in the northern and western parts of the Himalayan–Tibetan Plateau, respectively (Zhan et al., 2015; Gautam et al., 2019)). Because the grain size of mineral dust is much larger than that of particles from combustion sources (Pósfai et al., 2003; Dong et al., 2016), the deposition speed of mineral dust is much faster than that of the latter, causing the high dry deposition of WIOC and BC in Lhasa during the non-monsoon seasons with limited precipitation.

The wet deposition rates of WIOC and BC in Lhasa were lower than those in the urban city of Tokyo and in a mountain region in Germany due to either the large precipitation amounts or high WIOC and BC concentrations. However, they were higher than those in rural and marine sites in Europe (Table 1). The total deposition rate of BC (185.1 mg m^{-2} yr^{-1}) in Lhasa was much lower than that recovered from the sediment core of Lake Chaohu in seriously polluted southeastern China during the last 30 years (1660 mg m^{-2} yr^{-1}) (Han et al., 2016) and that from atmospheric dust deposition in Beijing (1659 mg m^{-2} yr^{-1}) (Yang et al., 2014). However, this total BC deposition rate in Lhasa was much higher than that in the nearby Zhadang glacier (22.8 mg m^{-2} yr^{-1}) (Li et al., 2016c), nearby Nam Co observation station (10.5 mg m^{-2} yr^{-1} (Li et al., 2017a) and 15.3 mg m^{-2} yr^{-1} (Yan et al., 2019)), and the other two remote observation stations (9.7 and 58.9 mg m^{-2} yr^{-1}) (Yan et al., 2019), indicating that Lhasa was mainly influenced by local emissions.

Large differences were found between in-situ data and those of models or empirical calculations in the Himalayan and Tibetan Plateau. For instance, the wet/(wet + dry) of BC in Lhasa was 0.12, much lower than that modeled by CAM5 (>0.8) (Zhang et al., 2015b), suggesting the underestimated BC dry deposition and/or overestimated BC wet deposition by this model. Therefore, the populated areas in the Himalayan–Tibetan Plateau, such as Lhasa, should be considered separately when using the model to simulate the concentrations and deposition of WIOC and BC in the atmosphere. Meanwhile, the parameters used in models should be optimized to improve their accuracy. The BC dry deposition rate (27.0 mg m^{-2} yr^{-1}) based on the empirical calculation from Fang et al. (2015) was also lower than that of the in-situ observation in this study, which indicated that the empirical calculation underestimated BC dry deposition rate. By contrast, compared to our in-situ wet deposition result, the BC wet deposition rate (249.8 mg m^{-2} yr^{-1}) from the empirical calculation was overestimated. The large discrepancy between the in-situ result and the other modeling or empirical estimates could be caused by the different approaches adopted because the models are usually based on emission inventories, and empirical calculations use the constant dry deposition velocity and wet scavenging ratio ignoring the temporal (e.g., the seasonal BC dry and wet deposition rates in Fig. 6) and spatial variability in dry deposition (Jurado et al., 2008; Cerqueira et al., 2010).

4. Conclusion and implications

This study is the first to report the in-situ WIOC and BC concentrations in precipitation and their wet and dry deposition rates in Lhasa, the largest city with relatively heavy air pollution in the southern Himalayan–Tibetan Plateau. We found that the WIOC and BC concentrations in precipitation of Lhasa were similar to those in some rural and remote sites in Europe and Asia but higher than those in mountain and marine sites in Europe, reflecting moderate air pollution in Lhasa. Seasonally, wet deposition rates of BC and WIOC peaked in summer and were mainly affected by the precipitation amount and emission strength of carbonaceous matter. BC was a minor component of the total carbonaceous matter in precipitation. With a relatively high WIOC/DOC ratio, the atmosphere in Lhasa seems to be influenced by local hydrophobic and fresh emissions. Additionally, the dry deposition rate showed reverse seasonal variation characteristics and had a high value during the non-monsoon period. In addition to the combustion sources of carbonaceous particles from local residents, mineral dust derived from dust storms, construction activities and other sources was also an important contributor to the BC and WIOC total deposition rate. Due to the long dry season and heavy mineral dust in the atmosphere, annual dry deposition rates of WIOC and BC were much higher than wet deposition rates, which is a special characteristic of the Himalayan–Tibetan Plateau and different from the normal phenomena at other sites. The in-situ deposition rates further suggested that the model and empirical calculations in previous studies probably underestimated the dry deposition and overestimated the wet deposition of carbonaceous matter in the Himalayan–Tibetan Plateau. Therefore, the results in this study provide significant implications and reference data for future modeling studies, especially in those regions significantly influenced by local anthropogenic activities.

Lhasa is closer to the glaciers of the Himalayan–Tibetan Plateau than other pollution sites. The carbonaceous matter in Lhasa is easily transported to remote areas and glacier surfaces, especially during the non-monsoon season when air pollution is relatively serious. It has been assumed that BC deposited on the nearby Zhadang glacier is influenced by emissions from Lhasa (Ming et al., 2009). Similar evidence was also found in precipitation DOC at Nam Co Station because precipitation air masses passing through Lhasa before reaching Nam Co showed high fossil contributions (Li et al., 2018a). As the largest city in the southern Himalayan–Tibetan Plateau, Lhasa can be viewed as a special pollution point that needs to be treated differently from other remote areas in pollution studies such as modeling. Therefore, pollution in Lhasa not only adversely influences the environment and health of local residents but can also be transported to other remote areas such as glacier regions, contributing to glacier melting. More researches on carbon isotopic and molecular compositions of carbonaceous particles in Lhasa and snow samples of glaciers at its downwind need to be conducted in the future to quantitatively evaluate contributions of pollutants from Lhasa to glaciers of the Himalayan–Tibetan Plateau.

Declaration of competing interest

The authors declare that they have no known competing financial interests or personal relationships that could have appeared to influence the work reported in this paper.

CRediT authorship contribution statement

Fangping Yan: Conceptualization, Methodology, Investigation, Resources, Writing - original draft, Visualization, Writing - review & editing. **Pengling Wang:** Investigation, Resources. **Shichang Kang:** Validation, Writing - review & editing, Supervision, Project administration, Funding acquisition. **Pengfei Chen:** Resources, Writing - review & editing. **Zhaofu Hu:** Investigation, Writing - review & editing. **Xiaowen Han:** Investigation, Resources. **Mika Sillanpää:** Writing - review & editing. **Chaoliu Li:** Conceptualization, Methodology, Validation, Data curation, Writing - review & editing, Supervision, Project administration, Funding acquisition.

Acknowledgments

This study was supported by the second Tibetan Plateau Scientific Expedition and Research Program (STEP) (2019QZKK0605), the NSFC (41971096, 41675130, 41630754, and 41705132), the Strategic Priority Research Program of the Chinese Academy of Sciences, Pan-Third Pole Environment Study for a Green Silk Road (Pan-TPE) (XDA20040501) and the State Key Laboratory of Cryospheric Science (SKLCS-ZZ-2017). This study is part of a framework across the HTP: Atmospheric Pollution and Cryospheric Change (APCC).

References

Andreae, M., Gelencsér, A., 2006. Black carbon or brown carbon? The nature of light-absorbing carbonaceous aerosols. Atmos. Chem. Phys. 6, 3131–3148.
Bond, T.C., Doherty, S.J., Fahey, D.W., Forster, P.M., Berntsen, T., DeAngelo, B.J., Flanner, M.G., Ghan, S., Kärcher, B., Koch, D., Kinne, S., Kondo, Y., Quinn, P.K., Sarofim, M.C., Schultz, M.G., Schulz, M., Venkataraman, C., Zhang, H., Zhang, S., Bellouin, N., Guttikunda, S.K., Hopke, P.K., Jacobson, M.Z., Kaiser, J.W., Klimont, Z., Lohmann, U., Schwarz, J.P., Shindell, D., Storelvmo, T., Warren, S.G., Zender, C.S., 2013. Bounding the role of black carbon in the climate system: a scientific assessment. J. Geophys. Res.: Atmosphere 118, 5380–5552.
Cerqueira, M., Pio, C., Legrand, M., Puxbaum, H., Kasper-Giebl, A., Afonso, J., Preunkert, S., Gelencsér, A., Fialho, P., 2010. Particulate carbon in precipitation at European background sites. J. Aerosol Sci. 41, 51–61.
Chen, B., Andersson, A., Lee, M., Kirillova, E.N., Xiao, Q., Krusa, M., Shi, M., Hu, K., Lu, Z., Streets, D.G., 2013. Source forensics of black carbon aerosols from China. Environ. Sci. Technol. 47, 9102–9108.
Chen, P., Kang, S., Li, C., Li, Q., Yan, F., Guo, J., Ji, Z., Zhang, Q., Hu, Z., Tripathee, L., Sillanpää, M., 2018. Source apportionment and risk assessment of atmospheric polycyclic aromatic hydrocarbons in Lhasa, tibet, China. Aerosol and Air Quality Research 18, 1294–1304.
Chen, P., Kang, S., Li, C., Zhang, Q., Guo, J., Tripathee, L., Zhang, Y., Li, G., Gul, C., Cong, Z., Wan, X., Niu, H., Panday, A.K., Rupakheti, M., Ji, Z., 2019a. Carbonaceous aerosol characteristics on the Third Pole: a primary study based on the Atmospheric Pollution and Cryospheric Change (APCC) network. Environ. Pollut. 253, 49–60.
Chen, P., Yang, J., Pu, T., Li, C., Guo, J., Tripathee, L., Kang, S., 2019b. Spatial and temporal variations of gaseous and particulate pollutants in six sites in tibet, China, during 2016–2017. Aerosol and Air Quality Research 19, 516–527.
Chow, J.C., Watson, J.G., Pritchett, L.C., Pierson, W.R., Frazier, C.A., Purcell, R.G., 1993. The DRI thermal/optical reflectance carbon analysis system: description, evaluation and applications in US air quality studies. Atmos. Environ. Part A. General Topics 27, 1185–1201.
Cong, Z., Kang, S., Luo, C., Li, Q., Huang, J., Gao, S., Li, X., 2011. Trace elements and lead isotopic composition of PM_{10} in Lhasa, Tibet. Atmos. Environ. 45, 6210–6215.
Cui, Y.Y., Liu, S., Bai, Z., Bian, J., Li, D., Fan, K., McKeen, S.A., Watts, L.A., Ciciora, S.J., Gao, R.-S., 2018. Religious burning as a potential major source of atmospheric fine aerosols in summertime Lhasa on the Tibetan Plateau. Atmos. Environ. 181, 186–191.
Custodio, D., Cerqueira, M., Fialho, P., Nunes, T., Pio, C., Henriques, D., 2014. Wet deposition of particulate carbon to the central north atlantic ocean. Sci. Total Environ. 496, 92–99.
Dong, Z., Kang, S., Qin, D., Li, Y., Wang, X., Ren, J., Li, X., Yang, J., Qin, X., 2016. Provenance of cryoconite deposited on the glaciers of the Tibetan Plateau: new insights from Nd-Sr isotopic composition and size distribution. J. Geophys. Res.: Atmosphere 121, 7371–7382.
Ducret, J., Cachier, H., 1992. Particulate carbon content in rain at various temperate and tropical locations. J. Atmos. Chem. 15, 55–67.
Fang, Y., Chen, Y., Tian, C., Lin, T., Hu, L., Huang, G., Tang, J., Li, J., Zhang, G., 2015. Flux and budget of BC in the continental shelf seas adjacent to Chinese high BC emission source regions. Glob. Biogeochem. Cycles 29, 957–972.
Gautam, S., Yan, F., Kang, S., Han, X., Neupane, B., Chen, P., Hu, Z., Sillanpää, M., Li, C., 2019. Black carbon in surface soil of the Himalayas and Tibetan Plateau and its contribution to total black carbon deposition at glacial region. Environ. Sci. Pollut. Control Ser. https://doi.org/10.1007/s11356-11019-07121-11357.
Gong, P., Wang, X., Yao, T., 2011. Ambient distribution of particulate- and gas-phase n-alkanes and polycyclic aromatic hydrocarbons in the Tibetan Plateau. Environmental Earth Sciences 64, 1703–1711.
Guo, J., Kang, S., Huang, J., Zhang, Q., Tripathee, L., Sillanpää, M., 2015. Seasonal variations of trace elements in precipitation at the largest city in Tibet, Lhasa. Atmos. Res. 153, 87–97.
Han, Y., Cao, J., An, Z., Chow, J.C., Watson, J.G., Jin, Z., Fung, K., Liu, S., 2007a. Evaluation of the thermal/optical reflectance method for quantification of elemental carbon in sediments. Chemosphere 69, 526–533.
Han, Y., Cao, J., Chow, J.C., Watson, J.G., An, Z., Jin, Z., Fung, K., Liu, S., 2007b. Evaluation of the thermal/optical reflectance method for discrimination between char-and soot-EC. Chemosphere 69, 569–574.
Han, Y.M., Wei, C., Huang, R.J., Bandowe, B.A., Ho, S.S., Cao, J.J., Jin, Z.D., Xu, B.Q., Gao, S.P., Tie, X.X., An, Z.S., Wilcke, W., 2016. Reconstruction of atmospheric soot history in inland regions from lake sediments over the past 150 years. Sci. Rep. 6, 19151.
Hu, Z., Kang, S., Li, C., Yan, F., Chen, P., Gao, S., Wang, Z., Zhang, Y., Sillanpaa, M., 2017. Light absorption of biomass burning and vehicle emission-sourced carbonaceous aerosols of the Tibetan Plateau. Environ. Sci. Pollut. Res. Int. 24, 15369–15378.
Huang, J., Kang, S., Shen, C., Cong, Z., Liu, K., Wang, W., Liu, L., 2010. Seasonal variations and sources of ambient fossil and biogenic-derived carbonaceous aerosols based on ^{14}C measurements in Lhasa, Tibet. Atmos. Res. 96, 553–559.
Huang, J., Kang, S., Wang, S., Wang, L., Zhang, Q., Guo, J., Wang, K., Zhang, G., Tripathee, L., 2013. Wet deposition of mercury at Lhasa, the capital city of Tibet. Sci. Total Environ. 447, 123–132.
Huo, M.Q., Sato, K., Ohizumi, T., Akimoto, H., Takahashi, K., 2016. Characteristics of carbonaceous components in precipitation and atmospheric particle at Japanese sites. Atmos. Environ. 146, 164–173.
Iavorivska, L., Boyer, E.W., DeWalle, D.R., 2016. Atmospheric deposition of organic carbon via precipitation. Atmos. Environ. 146, 153–163.
Ishikawa, Y., Murakami, H., Sekine, T., Yoshihara, K., 1995. Precipitation scavenging studies of radionuclides in air using cosmogenic ^{7}Be. J. Environ. Radioact. 26, 19–36.
Jacobson, M.Z., 2000. A physically-based treatment of elemental carbon optics: implications for global direct forcing of aerosols. Geophys. Res. Lett. 27, 217–220.
Jurado, E., Dachs, J., Duarte, C.M., Simo, R., 2008. Atmospheric deposition of organic and black carbon to the global oceans. Atmos. Environ. 42, 7931–7939.
Kang, S., Zhang, Q., Qian, Y., Ji, Z., Li, C., Cong, Z., Zhang, Y., Guo, J., Du, W., Huang, J., 2019. Linking atmospheric pollution to cryospheric Change in the third Pole region: current progresses and future prospects. National Science Review 6, 796–809.
Li, C., Bosch, C., Kang, S., Andersson, A., Chen, P., Zhang, Q., Cong, Z., Chen, B., Qin, D., Gustafsson, O., 2016a. Sources of black carbon to the Himalayan-Tibetan Plateau glaciers. Nat. Commun. 7, 12574.
Li, C., Chen, P., Kang, S., Yan, F., Hu, Z., Qu, B., Sillanpää, M., 2016b. Concentrations and light absorption characteristics of carbonaceous aerosol in $PM_{2.5}$ and PM_{10} of Lhasa city, the Tibetan Plateau. Atmos. Environ. 127, 340–346.
Li, C., Chen, P., Kang, S., Yan, F., Li, X., Qu, B., Sillanpää, M., 2016c. Carbonaceous matter deposition in the high glacial regions of the Tibetan Plateau. Atmos. Environ. 141, 203–208.
Li, C., Chen, P., Kang, S., Yan, F., Tripathee, L., Wu, G., Qu, B., Sillanpää, M., Yang, D., Dittmar, T., Stubbins, A., Raymond, P.A., 2018a. Fossil fuel combustion emission from south Asia influences precipitation dissolved organic carbon reaching the remote Tibetan plateau: isotopic and molecular evidence. J. Geophys. Res.: Atmosphere 123, 6248–6258.
Li, C., Han, X., Kang, S., Yan, F., Chen, P., Hu, Z., Yang, J., Ciren, D., Gao, S., Sillanpaa, M., Han, Y., Cui, Y., Liu, S., Smith, K.R., 2018b. Heavy near-surface $PM_{2.5}$ pollution in Lhasa, China during a relatively static winter period. Chemosphere 214, 314–318.
Li, C., Yan, F., Kang, S., Chen, P., Han, X., Hu, Z., Zhang, G., Hong, Y., Gao, S., Qu, B., Zhu, Z., Li, J., Chen, B., Sillanpää, M., 2017a. Re-evaluating black carbon in the Himalayas and the Tibetan Plateau: concentrations and deposition. Atmos. Chem. Phys. 17, 11899–11912.
Li, C., Yan, F., Kang, S., Chen, P., Hu, Z., Han, X., Zhang, G., Gao, S., Qu, B., Sillanpaa, M., 2017b. Deposition and light absorption characteristics of precipitation dissolved organic carbon (DOC) at three remote stations in the Himalayas and Tibetan Plateau, China. Sci. Total Environ. 605–606, 1039–1046.
Li, C., Yan, F., Kang, S., Chen, P., Qu, B., Hu, Z., Sillanpaa, M., 2016d. Concentration, sources, and flux of dissolved organic carbon of precipitation at Lhasa city, the Tibetan Plateau. Environ. Sci. Pollut. Res. Int. 23, 12915–12921.
Matsuda, K., Sase, H., Murao, N., Fukazawa, T., Khoomsub, K., Chanonmuang, P., Visaratana, T., Khummongkol, P., 2012. Dry and wet deposition of elemental carbon on a tropical forest in Thailand. Atmos. Environ. 54, 282–287.
Ming, J., Xiao, C., Cachier, H., Qin, D., Qin, X., Li, Z., Pu, J., 2009. Black Carbon (BC) in the snow of glaciers in west China and its potential effects on albedos. Atmos. Res. 92, 114–123.
Pósfai, M., Simonics, R., Li, J., Hobbs, P.V., Buseck, P.R., 2003. Individual aerosol particles from biomass burning in southern Africa: 1. Compositions and size distributions of carbonaceous particles. J. Geophys. Res.: Atmosphere 108, 8483, 8410.1029/2002JD002291.
Penduo, D., Norbu, D., Mima, T., 2008. Correlative analysis on relationship between changes of several main contaminations and some meteorological elements in Lhasa urban area. J. Tibet Univ 23, 7–11.
Prado-Fiedler, R., 1990. On the relationship between precipitation amount and wet deposition of nitrate and ammonium. Atmos. Environ. Part A. General Topics 24, 3061–3065.
Qi, L., Li, Q., He, C., Wang, X., Huang, J., 2017a. Effects of the Wegener-Bergeron-Findeisen process on global black carbon distribution. Atmos. Chem. Phys. 17, 7459–7479.
Qi, L., Li, Q., Li, Y., He, C., 2017b. Factors controlling black carbon distribution in the Arctic. Atmos. Chem. Phys. 17, 1037–1059.
Raymond, P.A., 2005. The composition and transport of organic carbon in rainfall: insights from the natural (^{13}C and ^{14}C) isotopes of carbon. Geophys. Res. Lett. 32, L14402, 14410.11029/12005GL022879.
Seinfeld, J.H., Pankow, J.F., 2003. Organic atmospheric particulate material. Annu.

Rev. Phys. Chem. 54, 121–140.
Seymour, M.D., Stout, T., 1983. Observations on the chemical composition of rain using short sampling times during a single event. Atmos. Environ. 17, 1483–1487, 1967.
Sorokina, V.V., Soier, V.G., 2016. Dry and wet atmospheric deposition of organic carbon in coastal and water areas of the northeastern part of the Sea of Azov. Oceanology 56, 733–741.
Torres, A., Bond, T.C., Lehmann, C.M.B., Subramanian, R., Hadley, O.L., 2013. Measuring organic carbon and black carbon in rainwater: evaluation of methods. Aerosol Sci. Technol. 48, 239–250.
Wan, X., Kang, S., Xin, J., Liu, B., Wen, T., Wang, P., Wang, Y., Cong, Z., 2016. Chemical composition of size-segregated aerosols in Lhasa city, Tibetan Plateau. Atmos. Res. 174–175, 142–150.
Yan, F., He, C., Kang, S., Chen, P., Hu, Z., Han, X., Gautam, S., Yan, C., Zheng, M., Sillanpää, M., Raymond, P.A., Li, C., 2019. Deposition of organic and black carbon: direct measurements at three remote stations in the himalayas and Tibetan plateau. J. Geophys. Res.: Atmosphere 124, 9702–9715.
Yan, F., Kang, S., Li, C., Zhang, Y., Qin, X., Li, Y., Zhang, X., Hu, Z., Chen, P., Li, X., Qu, B., Sillanpää, M., 2016. Concentration, sources and light absorption characteristics of dissolved organic carbon on a medium-sized valley glacier, northern Tibetan Plateau. Cryosphere 10, 2611–2621.
Yang, T., Guilin, H., Zhifang, X., 2014. Atmospheric black carbon deposit in beijing and zhangbei, China. Procedia Earth and Planetary Science 10, 383–387.
Zhan, C.L., Cao, J.J., Han, Y.M., Wang, P., Huang, R.J., Wei, C., Hu, W.G., Zhang, J.Q., 2015. Spatial patterns, storages and sources of black carbon in soils from the catchment of Qinghai Lake, China. Eur. J. Soil Sci. 66, 525–534.
Zhang, Cerqueira, M., Salazar, G., Zotter, P., Hueglin, C., Zellweger, C., Pio, C., Prevot, A.S.H., Szidat, S., 2015a. Wet deposition of fossil and non-fossil derived particulate carbon: insights from radiocarbon measurement. Atmos. Environ. 115, 257–262.
Zhang, Wang, H., Qian, Y., Rasch, P.J., Easter, R.C., Ma, P.-L., Singh, B., Huang, J., Fu, Q., 2015b. Quantifying sources, transport, deposition, and radiative forcing of black carbon over the Himalayas and Tibetan Plateau. Atmos. Chem. Phys. 15, 6205–6223.
Zhang, D., Iwasaka, Y., Shi, G., 2001. Soot particles and their impacts on the mass cycle in the Tibetan atmosphere. Atmos. Environ. 35, 5883–5894.

Publication V

Yan, F., Kang, S., Sillanpää, M., Hu, Z., Gao, S., Chen, P., Gautam. S., Reinikainen, S.-P., Li, C.

A new method for extraction of methanol-soluble brown carbon: Implications for investigation of its light absorption ability

Reprinted with permission from
Environmental Pollution
Vol. 262, 2020

Environmental Pollution 262 (2020) 114300

Contents lists available at ScienceDirect

Environmental Pollution

journal homepage: www.elsevier.com/locate/envpol

A new method for extraction of methanol-soluble brown carbon: Implications for investigation of its light absorption ability☆

Fangping Yan [a, b, c], Shichang Kang [c, d, e], Mika Sillanpää [f], Zhaofu Hu [c, e], Shaopeng Gao [a], Pengfei Chen [c], Sangita Gautam [a, e], Satu-Pia Reinikainen [b], Chaoliu Li [a, d, *]

[a] Key Laboratory of Tibetan Environment Changes and Land Surface Processes, Institute of Tibetan Plateau Research, Chinese Academy of Sciences, Beijing, 100101, China
[b] LUT School of Engineering Science, Lappeenranta University of Technology, P.O. Box 20, 53851, Lappeenranta, Finland
[c] State Key Laboratory of Cryospheric Sciences, Northwest Institute of Eco-Environment and Resources, Chinese Academy of Sciences, Lanzhou, 730000, China
[d] CAS Center for Excellence in Tibetan Plateau Earth Sciences, Chinese Academy of Sciences, Beijing, 100085, PR China
[e] University of Chinese Academy of Sciences, Beijing, 100049, China
[f] Department of Civil and Environmental Engineering, Floride International University, Miami, FI, USA

ARTICLE INFO

Article history:
Received 15 October 2019
Received in revised form
28 February 2020
Accepted 28 February 2020
Available online 2 March 2020

Keywords:
Methanol-soluble brown carbon
MAC
Biomass aerosol
Ambient aerosol

ABSTRACT

As an important component of organic carbon (OC), brown carbon (BrC) plays a significant role in radiative forcing in the atmosphere. Water-insoluble OC (WIOC) generally has higher light absorption ability than water-soluble OC (WSOC). The mass absorption cross-section (MAC) of WIOC is normally investigated by dissolving OC in methanol. However, all the current methods have shortcomings due to neglecting the methanol insoluble particulate carbon that is detached from the filter and suspended in methanol extracts, which results in MAC uncertainties of the methanol-soluble BrC and its climate warming estimation. In this study, by investigating typical biomass combustion sourced aerosols from the Tibetan Plateau and ambient aerosols from rural and urban areas in China, we evaluated the light absorption of extractable OC fraction for the existing methods. Moreover, a new method was developed to overcome the methanol insoluble particulate carbon detachment problem to achieve more reliable MAC values. We found that OC can be dissolved in methanol in a short time (e.g., 1 h) and ultrasonic treatment and long-term soaking do not significantly increase the extractable OC fraction. Additionally, we proved that methanol insoluble particulate carbon detachment in methanol does exist in previous methods, causing overestimation of the BrC mass extracted by methanol and thus the underestimation of MAC values. We therefore recommend the newly developed extraction method in this study to be utilized in future related studies to quantitatively obtain the light absorption property of methanol-soluble BrC.

1. Introduction

Aerosol particles are among the largest sources of uncertainties in estimating radiative climate forcing (Anderson et al., 2003). As an important part of aerosol particles, organic carbon (OC) plays an important role in solar radiation absorbing in addition to its solar radiation scattering, especially in the ultraviolet (UV) wavelength range (Laskin et al., 2015; Yan et al., 2018). Recently, increasing attention has been focused on those OC fractions that absorb solar radiation, i.e., brown carbon (BrC), in both models and in situ observation studies (Andreae and Gelencsér, 2006; Kirillova et al., 2014; Lin et al., 2014; Saleh et al., 2013; Shamjad et al., 2015; Xie et al., 2019). For instance, it is estimated that BrC accounts for approximately 24% of the combined black carbon (BC) and BrC warming effects at the tropopause (Zhang et al., 2017). BrC is generally divided into water-soluble brown carbon (WS-BrC) and water-insoluble brown carbon. Light absorption of the latter carbon fraction is generally evaluated by treating the sample with methanol (Chen and Bond, 2010). Therefore, this BrC fraction is called methanol-soluble brown carbon (MeS-BrC). To date, the method for

☆ This paper has been recommended for acceptance by Charles Wong.

* Corresponding author. Building 3, Yard 16, Lincui road, Chaoyang district, Beijing, 100101, China.
E-mail address: lichaoliu@itpcas.ac.cn (C. Li).

https://doi.org/10.1016/j.envpol.2020.114300
0269-7491/

Table 1
Information and comparison of three previous extraction methods and the one in this study.

Method	Extraction process	Calculation of MeS-BrC	Potential problems of previous methods	Reference
Method 1	Filter samples were immersed in methanol for 1 h without shaking or sonication	MeS-BrC=OC of original filter−OC remaining on methanol extracted filter	The methanol insoluble particulate carbon detachment was ignored	Cheng et al. (2017)
Method 2	Filter samples were sonicated for 1 h in methanol	MeS-BrC=OC of original filter	The OC of original filter samples was assumed to be completely extracted by methanol	Huang et al. (2018)
Method 3	Filter samples were sonicated in methanol for 1 h, the solution was kept at room temperature for 20 h, then it was sonicated for another 1 h	MeS-BrC=OC of original filter−OC remaining on methanol extracted filter	The methanol insoluble particulate carbon detachment was ignored	Chen and Bond (2010)
New method	Filter samples were placed in the middle of a sandwich filtration assembly as presented in Fig. 1, and extracted with methanol by three times. The total residence time of methanol on filters is 1 h	MeS-BrC=OC of original filter−OC remaining on middle and bottom methanol extracted filters in sandwich filtration assembly, i.e., equation (2)		This study

investigating the light absorption of WS-BrC in aerosol samples has been well established, and little uncertainty exists regarding the value of the mass absorption cross-section of WS-BrC ($MAC_{WS\text{-}BrC}$) because OC dissolved in water can be easily and accurately measured by a TOC analyzer after filtering the extracts (Li et al., 2016b). However, OC dissolved in methanol (i.e., MeS-BrC) cannot be directly measured by this method due to the interference of organic solvent, so that indirect calculations have to be adopted (Chen and Bond, 2010; Cheng et al., 2017; Huang et al., 2018). Moreover, the treatment of samples with methanol is still a complicated issue, and no consensus has been reached. To date, aerosol samples are treated with methanol using multiple methods (e.g., different treatment times, with or without sonication) (method details and comparison are provided in Table 1). However, all existing methods have shortcomings. For example, the methanol insoluble particulate carbon detaching from the filter and entering into the methanol cannot be quantitatively measured, thus the indirect calculation of MeS-BrC in previous studies was conducted by assuming either OC of original filter samples could be completely extracted by methanol or the methanol insoluble particulate carbon detachment is ignorable (Table 1), which caused the overestimation of MeS-BrC and accordingly the underestimation of the mass absorption cross-section of MeS-BrC ($MAC_{MeS\text{-}BrC}$) (Chen and Bond, 2010; Cheng et al., 2016). In addition, sonication treatment generally increases the extractable fraction of carbon compared to other methods without sonication treatment (Polidori et al., 2008); thus, both $MAC_{MeS\text{-}BrC}$ and $MAC_{WS\text{-}BrC}$ values of the samples treated by sonication should be higher than those without sonication. Currently, a comparison of methanol extractable OC fraction by the three existing methods presented in Table 1 is still lacking. Because mass absorption cross-section of BrC (MAC_{BrC}) data are the basic input of radiative models of aerosol particles, the aforementioned limitations and uncertainties will ultimately be propagated to climate forcing estimation. Therefore, it is urgent to establish a reliable method for MAC_{BrC} to better evaluate the radiative forcing of carbonaceous particles.

Normally, the BrC derived from biomass combustion sourced aerosols is more easily dissolved in water and methanol than that derived from fossil-sourced and ambient aerosols (Chen and Bond, 2010). In this study, $PM_{2.5}$ samples (particulate matter with a diameter smaller than 2.5 μm) originated from yak dung combustion, from a typical urban city on the Tibetan Plateau and from rural areas in East China (which is seriously polluted) were collected (Table S1). The collected samples were treated with methanol by the previous three methods to investigate the difference in the methanol extractable OC fractions among these methods. On this basis, a new method is developed to provide more reliable $MAC_{MeS\text{-}BrC}$ values for aerosol samples.

2. Methodology

2.1. Field sites

$PM_{2.5}$ filter samples were collected at four sites in China, namely, Nam Co, Lhasa, Zhangbo and Yangdian (Table S1). Nam Co is a typical remote area on the Tibetan Plateau where local residents burn yak dung for heating and cooking. The aerosol particles emitted from these combustion activities have an important contribution to glacier retreat on the Tibetan Plateau (Li et al., 2016a). Several studies have been conducted on the OC and element carbon (EC) ratios and $MAC_{WS\text{-}BrC}$ values at this site (Chen et al., 2015; Hu et al., 2017). Lhasa is the largest city on the south-central Tibetan Plateau; the aerosols in this city are greatly influenced by fossil combustion (Li et al., 2016a). Zhangbo and Yangdian are two typical rural areas in Guanzhong and Huabei Plain, respectively, with serious air pollution in East China.

The $PM_{2.5}$ samples collected at Nam Co were directly emitted from the yak dung combustion plumes (Chen et al., 2015), which were classified as biomass aerosols. The $PM_{2.5}$ samples collected in the ambient environment at other three sampling sites were classified as ambient aerosols. Due to different sources, the light absorption characteristics of aerosol in two categories are different.

2.2. Extract assembly

A total of 33 aerosol samples were collected for the experiments (Table S1). The filter samples from the urban and rural sites were acidified by fumigation with 37% HCl for 24 h to remove carbonate carbon which interferes the measurement of EC and OC by the carbon analyzer before the experiments followed the practical protocols provided in previous studies (Bosch et al., 2014; Chen et al., 2013; Li et al., 2016a; Pio et al., 2007). The carbonate carbon removed by HCl fumigation accounted for approximately 5.5 ± 2.6% of the total OC of the study aerosols. The analytical procedure in this study is presented in Fig. S1. First, a subsample (punch #1) of the original filter was cut out for the measurement of initial OC mass. Second, a 3.8 cm^2 subsample (punch #2) was cut out and treated with 38 mL methanol using a sandwich filter assembly to prevent the loss of particles from the filter (Fig. 1). In summary, the subsample was punched and placed in a pre-

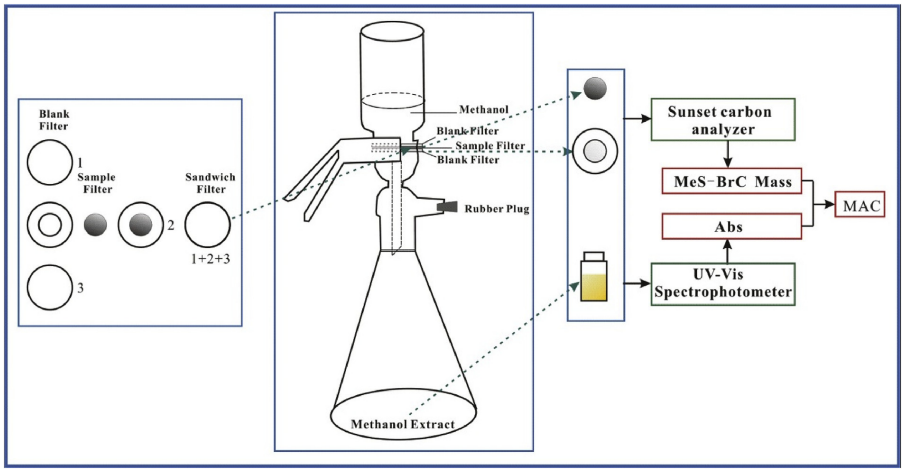

Fig. 1. Filtration unit developed in this study to extract MeS-BrC.

combusted quartz filter (pore size: 0.45 μm, Pall TissuquartzTM) with an opening of the same area. The reassembled filter samples were then placed between two pre-combusted quartz filters with the bottom of the subsample facing upward. The thusly formed three-filter sandwich was placed on the glass sand core funnel of a vacuum filtration assembly as presented in Fig. 1. After blocking the funnel, 38 mL methanol was added to the filter in three times to keep the long residence time, and the total residence time of the methanol lasted for approximately 1 h to ensure a high OC fraction extracted by methanol. The remaining methanol was then pumped through the filter. Thereafter, the filters were dried in glass petri dishes at 60 °C for 2 h. Punches of 0.526 cm^2 were obtained from the center of the original filter samples, the methanol-treated filter subsamples and the bottom filters of the sandwich filtration assembly. OC and EC of the punched samples were measured using a thermal-optical transmittance (TOT) carbon analyzer (Sunset Laboratory, Tigard, OR, USA) following the IMPROVE-A protocol. The sum of the OC masses of the two punches from the sandwich filtration assembly was regarded as the methanol-insoluble OC fraction. The difference between the OC mass of the original sample and the methanol-insoluble OC is the mass of the OC dissolved in methanol, which was used in the calculation of $MAC_{MeS\text{-}BrC}$. Third, a subsample (punch #3) was sonicated in ultrapure water to obtain the $MAC_{WS\text{-}BrC}$ value. The detailed method has been described in our previous article (Li et al., 2016c).

2.3. Light absorption measurement and calculation

The light absorption spectra of WS-BrC and MeS-BrC were measured using an ultraviolet−visible (UV−Vis) absorption spectrophotometer (SpectraMax M5, USA), by scanning from 200 to 700 nm with a step size of 5 nm. The MAC value was calculated based on the Beer-Lambert law (Bosch et al., 2014; Kirillova et al., 2014):

$$MAC = \frac{Abs}{C.L} \times \ln(10) \quad (1)$$

where Abs is the light absorbance measured directly by the spectrophotometer, L is the absorbing path length (1 cm); C is the mass of OC dissolved in methanol (MeS-BrC) or ultrapure water (WS-BrC).

The mass of WS-BrC was directly measured by the TOC analyzer, while the mass of MeS-BrC was obtained by indirect calculation due to the interference of methanol as follow:

$$MeS-BrC = OC_{original} - OC_{2,sandwich} - OC_{3,sandwich} \quad (2)$$

where $OC_{original}$ is the total OC mass of original filter; $OC_{2,sandwich}$ and $OC_{3,sandwich}$ are the OC mass of middle and bottom filters extracted by methanol in the sandwich filtration assembly present in Fig. 1.

Under the assumption that the OC soluble in water can also be dissolved in methanol, MAC of the water-insoluble OC (MAC_{WIOC}) can be calculated as the following ratio:

$$MAC_{WIOC} = \frac{[Abs_{365,\ methanol} - Abs_{365,\ water}]}{([MeS-BrC]-[WS-BrC]).L} \times \ln 10 \quad (3)$$

where $Abs_{365,\ methanol}$ and $Abs_{365,\ water}$ are the light absorbance measured at 365 nm of filtered methanol and water extracts; [MeS-BrC] and [WS-BrC] are the mass of MeS-BrC and WS-BrC.

3. Results and discussion

3.1. The loss of methanol insoluble particulate carbon in three previous methods

The loss of methanol insoluble particulate carbon from the filter during the methanol extraction was considered insignificant and negligible in a previous study (Cheng et al., 2017), although it has been reported that this phenomenon will cause $MAC_{MeS\text{-}BrC}$ underestimation (Chen and Bond, 2010; Kirillova et al., 2016). Herein, to evaluate the loss of methanol insoluble particulate carbon into methanol from the filter, light absorption of the methanol extracts using the third method in Table 1 was measured before and after filtration. If the light absorbance at wavelength of 365 nm (Abs_{365}) of the methanol extract after filtration was lower than that before

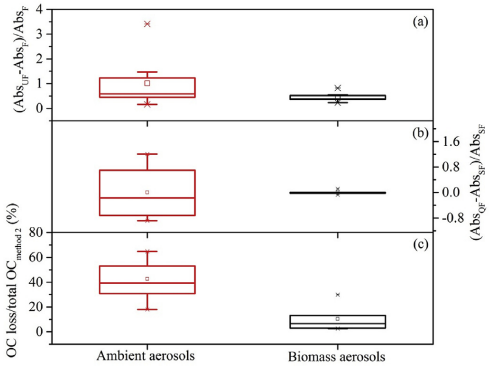

Fig. 2. The increase ratios of Abs_{365} of the unfiltered methanol extracts (Abs_{UF}) compared to those of Abs_{365} of the filtered extracts (Abs_F) (a), the increase ratios of Abs_{365} of the extracts filtered by a quartz filter (Abs_{QF}) compared to those of Abs_{365} of the extracts filtered a by syringe filter (Abs_{SF}) (b), and the ratio of OC loss to total OC of original filter samples using method 2 in Table 1.

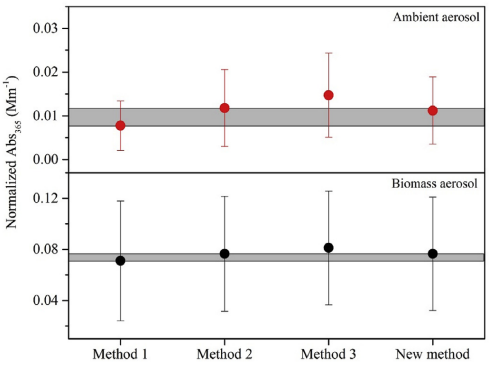

Fig. 3. Normalized light absorbance of MeS-BrC at 365 nm by four different extraction methods. Note: the large standard deviation (SD) for mean values was attributed to the large variation in the particulate carbon mass in each collected sample.

filtration, the loss of methanol insoluble particulate carbon from the filter must occur. Although this approach provides an indirect estimate, the particle loss can thus be evaluated effectively. For instance, due to the detachment of methanol insoluble particulate carbon, Abs_{365} for the unfiltered extracts of ambient and biomass aerosols increases approximately 101% and 45%, respectively compared to those of filtered extracts (Fig. 2a), suggesting that the loss of the methanol insoluble particulate carbon does exit in previous methods. Moreover, by collecting these detached OC and those remaining OC on methanol-extracted filters together and measuring by TOT carbon analyzer, the mass of MeS-BrC could be overestimated by 10% and 43% for the biomass and ambient extracts, respectively (Fig. 2c) if we assume methanol completely extracts OC of the filter samples (as presented by Huang et al., 2018, i.e., method 2 in Table 1). In contrast, the new extraction method developed in this study is reliable for obtaining accurate MeS-BrC mass and thus reliable $MAC_{MeS\text{-}BrC}$ values by preventing the detachment of the methanol insoluble particulate carbon, which is also verified by the similar average Abs_{365} values compared with the previous filtration methods (Fig. 2b). Additionally, the larger Abs increase of the ambient aerosol extracts due to the detachment of methanol insoluble particulate carbon might be explained by the lower fraction of MeS-BrC (i.e., a low ratio of methanol-soluble OC to total OC of the original filter sample) and the existence of large mineral particles with an easy detachment inclination which can be the coating of carbonaceous matter in ambient aerosols (Fig. S2); meanwhile, the finer biomass combustion carbon particles adhere to the filter paper more easily compared to the ambient particles. Thus, failing to consider the particle loss would cause large uncertainties in MAC estimation, especially for the ambient aerosols.

3.2. Abs values of MeS-BrC by four different methods

The MeS-BrC in the ambient and biomass aerosols was extracted using the existing three methods (Table 1 and Text S1) and the method we developed in this study. The Abs_{365} values were measured and compared. The results indicated that the Abs_{365} values of MeS-BrC using the new method were between those obtained using the first two methods but slightly lower than those obtained using the third method (Fig. 3). Moreover, the differences in Abs_{365} among the methanol extracts from these four methods were statistically insignificant for both ambient and biomass aerosols ($p > 0.05$, $N = 33$) (Table S2). Therefore, we propose that the complex treatments of sonication and a longer residence time do not significantly contribute to a larger amount of carbon extracted. Additionally, it is demonstrated that the syringe filter in the previous three methods and the quartz filter paper in this new method do not cause significant differences in the Abs_{365} values (Fig. S3). Consequently, it is reasonable to adopt the new method developed in this study to investigate the light absorption of MeS-BrC quantitatively and accurately. However, it should also be pointed out that the theoretical mass absorption cross-section at 365 nm (MAC_{365}) of the methanol extracts based on the Abs_{365} values obtained using the third method should be the highest among these four methods due to the elevated Abs_{365} values as a result of the sonication treatment, although the increase is statistically insignificant ($p > 0.05$, $N = 33$). In addition, the theoretical MAC_{365} divergence of the ambient aerosols between the third method and the new method would be larger than that of the biomass aerosols, which may also indicate that the OC in biomass aerosols is more easily extracted by methanol even without sonication treatment, but sonication treatment has a relatively large effect on OC faction extracted by methanol in ambient aerosols.

3.3. WS-BrC versus MeS-BrC and the light absorption properties

Approximately 93.0 ± 3.8% (87–96%) of the biomass combustion sourced OC could be extracted within 1 h by methanol in this study, which is likely the lower bound of the previously reported values of 92%–98% for wood burning aerosols (Chen and Bond, 2010). Meanwhile, the average methanol extractable OC fraction of the ambient aerosols was approximately 79.3 ± 10.0% (55%–93%) (Fig. S2), which was lower than the average value of 89% for the ambient aerosols in Beijing (Cheng et al., 2017). This phenomenon was possibly because, on the one hand, the aerosol sources were different between this study and the previous ones, and on the other hand, the previous two studies failed to consider the methanol insoluble particulate carbon detachment from the filter during analysis. Correspondingly, the extractable OC fractions by ultrapure water were small (63.3 ± 13.3% and 55.2 ± 29.1% for the biomass and ambient aerosols, respectively), close to the previously reported values (Cong et al., 2015; Graham et al., 2002; Srinivas;

Sarin, 2013). All these results disprove the assumption in several previous studies that methanol extracts almost all the OC from filters (Huang et al., 2018; Kirillova et al., 2016; Zhu et al., 2018), thus causing $MAC_{MeS\text{-}BrC}$ underestimation, especially for the ambient aerosols.

By using the new method, the MAC_{365} values of the methanol-extracted biomass OC and ambient OC were 1.55 ± 0.43 $m^2\ g^{-1}$ (1.07–2.44 $m^2\ g^{-1}$) and 1.14 ± 0.50 $m^2\ g^{-1}$ (0.55–1.51 $m^2\ g^{-1}$), respectively, in this study. The MeS-BrC fraction has higher MAC values than the WS-BrC fraction across the near-UV wavelength range (Fig. 4), consistent with previous results (Chen and Bond, 2010; Kirchstetter et al., 2004; Sun et al., 2007; Zhang et al., 2013). It is clear that the MAC_{365} value of OC from biomass combustion sourced aerosols were higher than that of OC from ambient aerosols; moreover, the MAC_{365} values in Lhasa were lower than those at the other two sites (Table S3) because the fossil fuel contribution to the aerosols in Lhasa was larger than those of the other two sites (Li et al., 2016b). Furthermore, the OC/EC ratios in Lhasa, Zhangbo and Yangdian were 3.4, 7.1 and 7.3, respectively, reflecting the larger fossil fuel contribution of the Lhasa aerosol as reported in previous studies (Hu et al., 2017; Li et al., 2016b). Therefore, it is crucial to obtain the reliable light absorption of OC in the atmosphere not only in the heavily polluted regions but also in the background remote regions of the Tibetan Plateau because there contains the largest number of glaciers outside the polar regions which has been experiencing dramatic retreat due to the climate change and the deposition of light-absorbing impurities (Kang et al., 2019). Thus, quantitative investigation of the light-absorbing OC and its effect on glaciers should be taken seriously.

The OC compounds that were only extractable by methanol (i.e., WIOC) were more light-absorbing than the WS-BrC compounds (Fig. 5 and Table S3). The estimated average MAC_{WIOC} values at 365 nm for the biomass and ambient aerosols were 2.34 ± 0.78 $m^2\ g^{-1}$ and 1.59 ± 0.76 $m^2\ g^{-1}$, approximately 2.3 and 1.6 times of the estimated $MAC_{WS\text{-}BrC}$ values, respectively. Previous studies have suggested that this strong light-absorbing WIOC are likely polycyclic aromatic hydrocarbons with a large molecule weight or certain large molecules containing conjugated aromatic rings (Apicella et al., 2004; Chen and Bond, 2010; Zhang et al., 2013), which could be produced during fossil fuel and biomass combustion in both flaming and smoldering combustion states (Evans and Milne, 1987; Schauer et al., 2001). Correspondingly, the less light-absorbing WS-BrC compounds were identified as humic-like substance and protein-like substances (Sun et al., 2007; Wu et al., 2019).

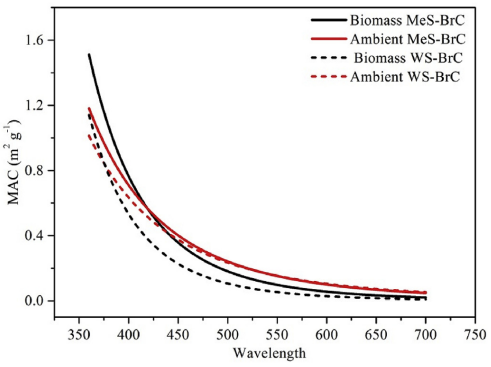

Fig. 4. Average MAC spectra of WS-BrC and MeS-BrC in the ambient and biomass aerosols.

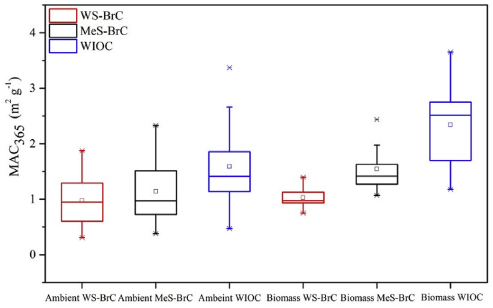

Fig. 5. Average MAC_{365} of the water and methanol extracts of ambient and biomass aerosols.

As a BrC proxy, Abs_{365} of WIOC also exhibited a strong correlation with WIOC mass in both the ambient and biomass aerosols besides the significant correlation between WS-BrC and its Abs value (Fig. S4), which suggested that a significant fraction of WIOC is consisted of BrC chromophores. Therefore, the study of MeS-BrC in aerosols can facilitate a better understanding of its role in climate forcing. In addition, the new method in this study provides a reliable and quantitative measurement for this kind of MeS-BrC.

4. Conclusion

By comparing the sandwich filtration assembly developed in this study with the three previous methods, we proved that the three existing methods do experience the detachment of methanol insoluble particulate carbon from the filter during extraction, which causes large overestimation in the calculation of the MeS-BrC mass and eventually leads to the underestimation of $MAC_{MeS\text{-}BrC}$. Correspondingly, the sandwich filtration method provides not only comparable light absorption data of the methanol extracts with the existing methods using traditional sonication process but also the reliable amount of the methanol-extractable OC. Thus, the sandwich filtration method can be utilized to measure the light absorption ability of the methanol-soluble BrC in atmospheric aerosols more accurately by overcoming the particulate carbon loss problem.

Declaration of competing interest

The authors declare no competing financial interest.

CRediT authorship contribution statement

Fangping Yan: Methodology, Investigation, Resources, Writing - original draft, Writing - review & editing. **Shichang Kang:** Validation, Writing - review & editing, Supervision, Project administration, Funding acquisition. **Mika Sillanpää:** Writing - review & editing. **Zhaofu Hu:** Investigation, Writing - review & editing. **Shaopeng Gao:** Resources, Writing - review & editing. **Pengfei Chen:** Resources, Writing - review & editing. **Sangita Gautam:** Investigation. **Satu-Pia Reinikainen:** Writing - review & editing. **Chaoliu Li:** Conceptualization, Validation, Writing - review & editing, Supervision, Funding acquisition.

Acknowledgements

This study was supported by the second Tibetan Plateau Scientific Expedition and Research Program (STEP) (2019QZKK0605), the NSFC (41971096, 41675130 and 41630754), the Strategic Priority Research Programme of the Chinese Academy of Sciences, Pan-Third Pole Environment Study for a Green Silk Road (Pan-TPE) (XDA20040501), and the State Key Laboratory of Cryospheric Science (SKLCS-ZZ-2017). This study is part of a framework across the HTP: Atmospheric Pollution and Cryospheric Change (APCC).

Appendix A. Supplementary data

Supplementary data related to this article can be found at https://doi.org/10.1016/j.envpol.2020.114300.

References

Anderson, T.L., Charlson, R.J., Schwartz, S.E., Knutti, R., Boucher, O., Rodhe, H., Heintzenberg, J., 2003. Climate forcing by aerosols–a hazy picture. Science 300, 1103–1104.

Andreae, M.O., Gelencsér, A., 2006. Black carbon or brown carbon? The nature of light-absorbing carbonaceous aerosols. Atmos. Chem. Phys. 6, 3131–3148.

Apicella, B., Alfè, M., Barbella, R., Tregrossi, A., Ciajolo, A., 2004. Aromatic structures of carbonaceous materials and soot inferred by spectroscopic analysis. Carbon 42, 1583–1589.

Bosch, C., Andersson, A., Kirillova, E.N., Budhavant, K., Tiwari, S., Praveen, P., Russell, L.M., Beres, N.D., Ramanathan, V., Gustafsson, Ö., 2014. Source-diagnostic dual-isotope composition and optical properties of water-soluble organic carbon and elemental carbon in the South Asian outflow intercepted over the Indian Ocean. J. Geophys. Res.: Atmosphere 119 (11), 743-711,759.

Chen, B., Andersson, A., Lee, M., Kirillova, E.N., Xiao, Q., Krusa, M., Shi, M., Hu, K., Lu, Z., Streets, D.G., 2013. Source forensics of black carbon aerosols from China. Environ. Sci. Technol. 47, 9102–9108.

Chen, P., Kang, S., Bai, J., Sillanpää, M., Li, C., 2015. Yak dung combustion aerosols in the Tibetan Plateau: chemical characteristics and influence on the local atmospheric environment. Atmos. Res. 156, 58–66.

Chen, Y., Bond, T.C., 2010. Light absorption by organic carbon from wood combustion. Atmos. Chem. Phys. 10, 1773–1787.

Cheng, Y., He, K., Du, Z., Engling, G., Liu, J., Ma, Y., Zheng, M., Weber, R., 2016. The characteristics of brown carbon aerosol during winter in Beijing. Atmos. Environ. 127, 355–364.

Cheng, Y., He, K., Engling, G., Weber, R., Liu, J.M., Du, Z.Y., Dong, S.P., 2017. Brown and black carbon in Beijing aerosol: implications for the effects of brown coating on light absorption by black carbon. Sci. Total Environ. 599–600, 1047–1055.

Cong, Z., Kang, S., Kawamura, K., Liu, B., Wan, X., Wang, Z., Gao, S., Fu, P., 2015. Carbonaceous aerosols on the south edge of the Tibetan Plateau: concentrations, seasonality and sources. Atmos. Chem. Phys. 15, 1573–1584.

Evans, R.J., Milne, T.A., 1987. Molecular characterization of the pyrolysis of biomass. Energy Fuels 1, 123–137.

Graham, B., Mayol-Bracero, O.L., Guyon, P., Roberts, G.C., Decesari, S., Facchini, M.C., Artaxo, P., Maenhaut, W., Köll, P., Andreae, M.O., 2002. Water-soluble organic compounds in biomass burning aerosols over Amazonia 1. Characterization by NMR and GC-MS. J. Geophys. Res.: Atmosphere 107. LBA 14-11-LBA 14-16.

Hu, Z., Kang, S., Li, C., Yan, F., Chen, P., Gao, S., Wang, Z., Zhang, Y., Sillanpää, M., 2017. Light absorption of biomass burning and vehicle emission-sourced carbonaceous aerosols of the Tibetan Plateau. Environ. Sci. Pollut. Res. Int. 24, 15369–15378.

Huang, R.J., Yang, L., Cao, J., Chen, Y., Chen, Q., Li, Y., Duan, J., Zhu, C., Dai, W., Wang, K., Lin, C., Ni, H., Corbin, J.C., Wu, Y., Zhang, R., Tie, X., Hoffmann, T., O'Dowd, C., Dusek, U., 2018. Brown carbon aerosol in urban Xi'an, Northwest China: the composition and light absorption properties. Environ. Sci. Technol. 52, 6825–6833.

Kang, S., Zhang, Q., Qian, Y., Ji, Z., Li, C., Cong, Z., Zhang, Y., Guo, J., Du, W., Huang, J., You, Q., Panday, A.K., Rupakheti, M., Chen, D., Gustafsson, Ö., Thiemens, M.H., Qin, D., 2019. Linking atmospheric pollution to cryospheric change in the Third Pole region: current progress and future prospects. Nat. Sci. Rev. 6, 796–809.

Kirchstetter, T.W., Novakov, T., Hobbs, P.V., 2004. Evidence that the spectral dependence of light absorption by aerosols is affected by organic carbon. J. Geophys. Res.: Atmosphere 109, D21208. https://doi.org/10.1029/2004JD004999.

Kirillova, E.N., Andersson, A., Han, J., Lee, M., Gustafsson, Ö., 2014. Sources and light absorption of water-soluble organic carbon aerosols in the outflow from northern China. Atmos. Chem. Phys. 14, 1413–1422.

Kirillova, E.N., Marinoni, A., Bonasoni, P., Vuillermoz, E., Facchini, M.C., Fuzzi, S., Decesari, S., 2016. Light absorption properties of brown carbon in the high Himalayas. J. Geophys. Res.: Atmosphere 121, 9621–9639.

Laskin, A., Laskin, J., Nizkorodov, S.A., 2015. Chemistry of atmospheric brown carbon. Chem. Rev. 115, 4335–4382.

Li, C., Bosch, C., Kang, S., Andersson, A., Chen, P., Zhang, Q., Cong, Z., Chen, B., Qin, D., Gustafsson, O., 2016a. Sources of black carbon to the Himalayan-Tibetan Plateau glaciers. Nat. Commun. 7, 12574.

Li, C., Chen, P., Kang, S., Yan, F., Hu, Z., Qu, B., Sillanpää, M., 2016b. Concentrations and light absorption characteristics of carbonaceous aerosol in $PM_{2.5}$ and PM_{10} of Lhasa city, the Tibetan Plateau. Atmos. Environ. 127, 340–346.

Li, C., Yan, F., Kang, S., Chen, P., Hu, Z., Gao, S., Qu, B., Sillanpää, M., 2016c. Light absorption characteristics of carbonaceous aerosols in two remote stations of the southern fringe of the Tibetan Plateau, China. Atmos. Environ. 143, 79–85.

Lin, G., Penner, J.E., Flanner, M.G., Sillman, S., Xu, L., Zhou, C., 2014. Radiative forcing of organic aerosol in the atmosphere and on snow: effects of SOA and brown carbon. J. Geophys. Res.: Atmosphere 119, 7453–7476.

Pio, C.A., Legrand, M., Oliveira, T., Afonso, J., Santos, C., Caseiro, A., Fialho, P., Barata, F., Puxbaum, H., Sanchez-Ochoa, A., 2007. Climatology of aerosol composition (organic versus inorganic) at nonurban sites on a west-east transect across Europe. J. Geophys. Res.: Atmosphere 112, D23S02. https://doi.org/10.1029/2006JD008038.

Polidori, A., Turpin, B.J., Davidson, C.I., Rodenburg, L.A., Maimone, F., 2008. Organic $PM_{2.5}$: fractionation by polarity, FTIR spectroscopy, and OM/OC ratio for the Pittsburgh aerosol. Aerosol. Sci. Technol. 42, 233–246.

Saleh, R., Hennigan, C., McMeeking, G., Chuang, W., Robinson, E., Coe, H., Donahue, N., Robinson, A., 2013. Absorptivity of brown carbon in fresh and photo-chemically aged biomass-burning emissions. Atmos. Chem. Phys. 13, 7683–7693.

Schauer, J.J., Kleeman, M.J., Cass, G.R., Simoneit, B.R., 2001. Measurement of emissions from air pollution sources. 3. C1–C29 organic compounds from fireplace combustion of wood. Environ. Sci. Technol. 35, 1716–1728.

Shamjad, P., Tripathi, S., Pathak, R., Hallquist, M., Arola, A., Bergin, M., 2015. Contribution of brown carbon to direct radiative forcing over the Indo-Gangetic Plain. Environ. Sci. Technol. 49, 10474–10481.

Srinivas, B., Sarin, M., 2013. Light absorbing organic aerosols (brown carbon) over the tropical Indian Ocean: impact of biomass burning emissions. Environ. Res. Lett. 8, 044042.

Sun, H., Biedermann, L., Bond, T.C., 2007. Color of brown carbon: a model for ultraviolet and visible light absorption by organic carbon aerosol. Geophys. Res. Lett. 34, L17813. https://doi.org/10.1029/2007GL029797.

Wu, G., Ram, K., Fu, P., Wang, W., Zhang, Y., Liu, X., Stone, E.A., Pradhan, B.B., Dangol, P.M., Panday, A.K., Wan, X., Bai, Z., Kang, S., Zhang, Q., Cong, Z., 2019. Water-soluble Brown carbon in atmospheric aerosols from Godavari (Nepal), a regional representative of south Asia. Environ. Sci. Technol. 53, 3471–3479.

Xie, M., Chen, X., Holder, A.L., Hays, M.D., Lewandowski, M., Offenberg, J.H., Kleindienst, T.E., Jaoui, M., Hannigan, M.P., 2019. Light absorption of organic carbon and its sources at a southeastern US location in summer. Environ. Pollut. 244, 38–46.

Yan, J., Wang, X., Gong, P., Wang, C., Cong, Z., 2018. Review of brown carbon aerosols: recent progress and perspectives. Sci. Total Environ. 634, 1475–1485.

Zhang, X., Lin, Y.H., Surratt, J.D., Weber, R.J., 2013. Sources, composition and absorption Angstrom exponent of light-absorbing organic components in aerosol extracts from the Los Angeles Basin. Environ. Sci. Technol. 47, 3685–3693.

Zhang, Y., Forrister, H., Liu, J., Dibb, J., Anderson, B., Schwarz, J.P., Perring, A.E., Jimenez, J.L., Campuzano-Jost, P., Wang, Y., 2017. Top-of-atmosphere radiative forcing affected by brown carbon in the upper troposphere. Nat. Geosci. 10, 486.

Zhu, C.S., Cao, J.J., Huang, R.J., Shen, Z.X., Wang, Q.Y., Zhang, N.N., 2018. Light absorption properties of brown carbon over the southeastern Tibetan Plateau. Sci. Total Environ. 625, 246–251.

Supporting Information for

Environmental Pollution

A new method for extraction of methanol-soluble brown carbon: Implications for investigation of its light absorption ability

Fangping Yan[a,b,c], Shichang Kang[c,d,e], Mika Sillanpää[f], Zhaofu Hu[c,e], Shaopeng Gao[a], Pengfei Chen[c], Sangita Gautam[a,e], Satu-Pia Reinikainen[b], Chaoliu Li[a,d*]

[a]Key Laboratory of Tibetan Environment Changes and Land Surface Processes, Institute of Tibetan Plateau Research, Chinese Academy of Sciences, Beijing 100101, China

[b] LUT School of Engineering Science, Lappeenranta University of Technology, P.O. Box 20, 53851, Lappeenranta, Finland

[c]State Key Laboratory of Cryospheric Sciences, Northwest Institute of Eco-Environment and Resources, Chinese Academy of Sciences, Lanzhou, 730000, China

[d]CAS Center for Excellence in Tibetan Plateau Earth Sciences, Chinese Academy of Sciences, Beijing 100085, P.R. China

[e]University of Chinese Academy of Sciences, Beijing 100049, China

[f]Department of Civil and Environmental Engneering, Floride International University, Miami, FI, USA.

Corresponding author:

*E-mail: lichaoliu@itpcas.ac.cn;

Address: Building 3, Yard 16, Lincui road, Chaoyang district, Beijing, China, 100101

List of Supplemental Figures

Figure S1. Flowchart of the measurement of the light absorption ability of the carbonaceous matter.

Figure S2. The ratios of WS-BrC and MeS-BrC masses to the OC mass in the original ambient and biomass aerosols.

Figure S3. Significant relationship between Abs_{365} of the methanol extract filtered by quartz filter paper (new method) and the syringe filter (previous methods).

Figure S4. Significant correlations between light absorption of WIOC (WSOC) at a wavelength of 365 nm ($Abs_{365, WIOC}$; $Abs_{365, WSOC}$) and the WIOC (WSOC) mass in the ambient aerosols (a) and (c) and biomass aerosols (b) and (d); $Abs_{365, WIOC}=Abs_{365, methanol}-Abs_{365, water}$.

List of Supplemental Tables

Table S1. Information of the sampling sites and collected samples.

Table S2. The average Abs_{365} values of the ambient and biomass aerosols extracted with methanol using the three previous methods and the one in this study.

Table S3. Comparison of MAC_{WS-BrC}, $MAC_{MeS-BrC}$ and MAC_{WIOC} values between this study and other previous studies.

Text S1. Method comparison

To compare the results of the new method with those of the three previous methods, another subsample (punch #4) was treated using the following method. First, a 3.8 cm^2 sample was soaked in 38 mL methanol for 1 h; then, the solution was sonicated for 1 h; after keeping the solution at room temperature for 20 h, it was sonicated for another 1 h. Light absorbance of the extract was measured after each step. The analyzed extracts in the cuvettes during each step were returned to the bottles to maintain the same volume during the experiment. The weights of the extracts were measured before and after each measurement, and the extract loss was 0.68%±0.08% on average during the whole measurement process. Although it is difficult to obtain the exact amount of carbon dissolved in methanol by these three methods, the light attenuation value of each step can be compared with the value of our new filtration process. This comparison is valid under the hypothesis that the more carbon is dissolved in methanol, the more notable the light attenuation will be observed.

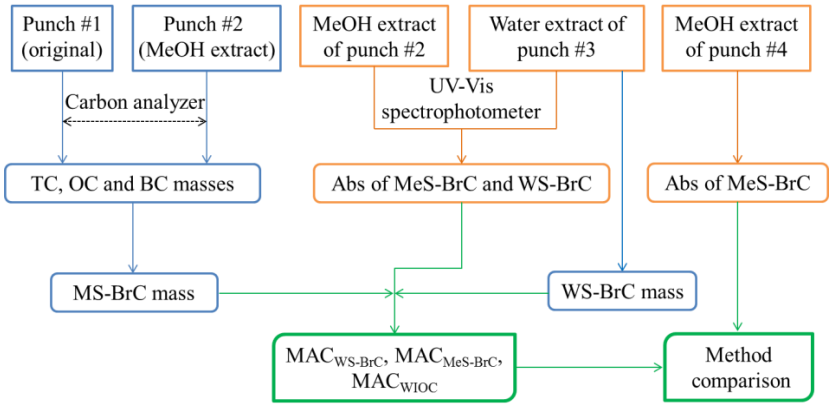

Figure S1. Flowchart of the measurement of the light absorption ability of the carbonaceous matter.

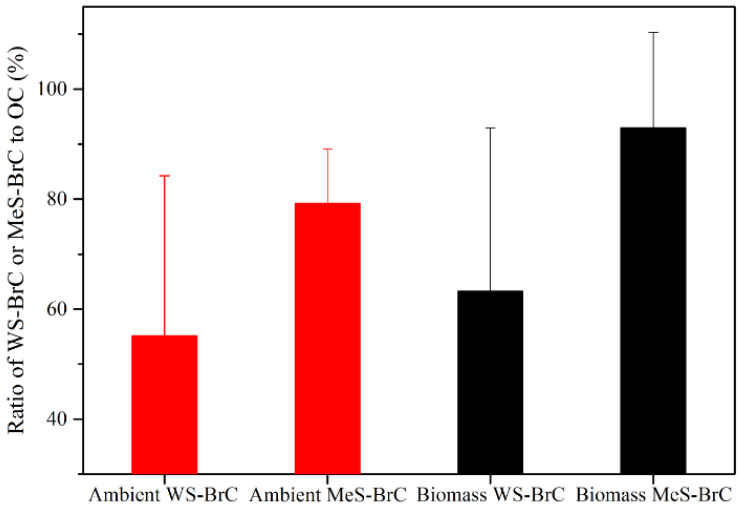

Figure S2. The ratios of the WS-BrC and MeS-BrC mass to OC mass in the original ambient and biomass aerosols.

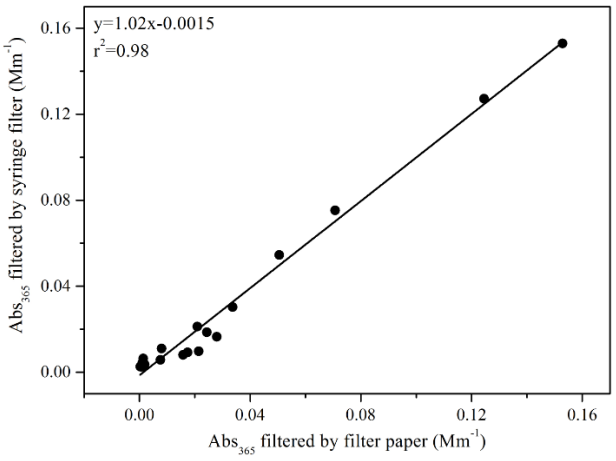

Figure S3. Significant relationship between Abs_{365} of the methanol extract filtered by the quartz filter paper (new method) and the syringe filter (previous methods).

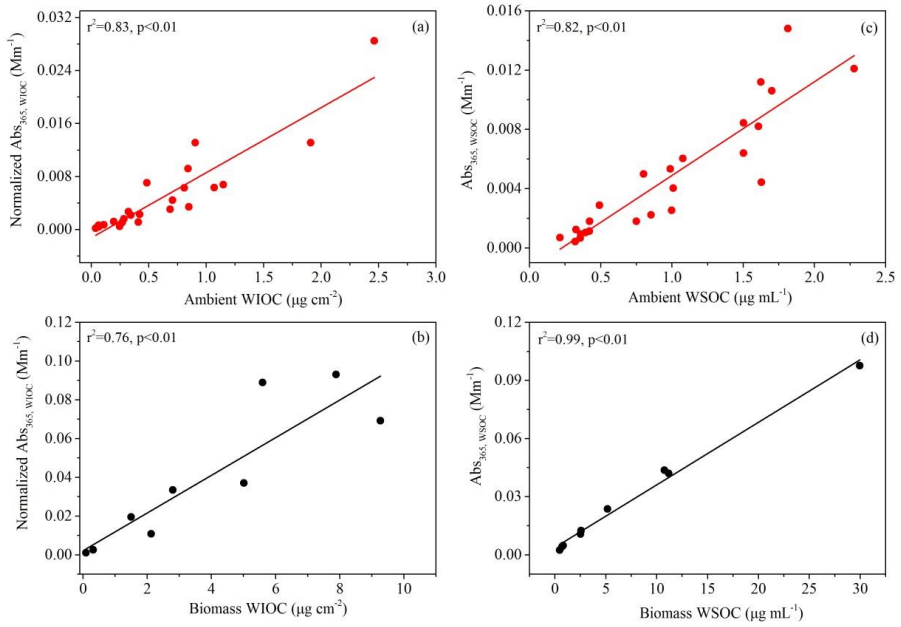

Figure S4. Significant correlations between light absorption of WIOC (WSOC) at a wavelength of 365 nm ($Abs_{365, WIOC}$; $Abs_{365, WSOC}$) and the WIOC (WSOC) mass in the ambient aerosols (a) (c) and biomass aerosols (b) (d); $Abs_{365, WIOC}=Abs_{365, methanol}-Abs_{365, water}$.

Table S1. Information of the sampling sites and collected samples.

Sampling site	Regions	Latitude (N) /longitude (E)	Collecting period (YY.MM)	No.
Nam Co	Tibetan Plateau, remote site	30°46′23″/90°57′48″	2018.08	9
Lhasa	Tibetan Plateau, urban site	29 °38′32″/91 °02′14″	2018.05-07	7
Zhangbo	Guanzhong Plain, rural site	34 °26′44″/109 °10′04″	2018.05- 2019.01	8
Yangdian	Huabei Plain, rural site	35 °53′32″/116 °35′40″	2019.05-10	9

Table S2. The average Abs_{365} values (mean±SD) of the ambient and biomass aerosols extracted with methanol using the three existing methods and the newly developed method.

Method	$Abs_{365,\ methanol}$ (Mm^{-1}) ($*10^{-2}$)	
	Ambient aerosols	Biomass aerosols
Method 1	0.78±0.56a	7.11±4.68b
Method 2	1.18±0.88a	7.66±4.50b
Method 3	1.47±0.96a	8.12±4.45b
New method	1.12±0.79a	7.65±4.44b

Note: 'a' indicates the statistically insignificance of the $Abs_{365,\ methanol}$ of ambient aerosols among the four methods; 'b' indicates the statistically insignificance of $Abs_{365,\ methanol}$ of the biomass aerosols among the four methods.

Table. S3. Comparison of $MAC_{WS\text{-}BrC}$, $MAC_{MeS\text{-}BrC}$ and MAC_{WIOC} values of the aerosols between this study and other previous studies.

Site	Collected period （YY.MM）	Size	$MAC_{WS\text{-}BrC}$ ($m^2\ g^{-1}$)	$MAC_{MeS\text{-}BrC}$ ($m^2\ g^{-1}$)	MAC_{WIOC} ($m^2\ g^{-1}$)	Reference
Nam Co	2018.08	$PM_{2.5}$	1.08±0.23	1.64±0.59	2.61±1.06	This study
Lhasa	2018. 05-08	$PM_{2.5}$	0.64±0.22	0.86±0.24	1.22±0.54	This study
Zhangbo	2018. 05-12	$PM_{2.5}$	0.96±0.35	1.10±0.35	1.63±0.70	This study
Yangdian	2018.05-2019.01	$PM_{2.5}$	1.25±0.39	1.54±0.54	2.03±0.92	This study
Bejing, China	2011. 08	$PM_{2.5}$	0.44±0.06	0.58±0.07	0.98±0.34	(Cheng et al., 2017)
Beijing, China	2011.12	$PM_{2.5}$	1.22±0.11	1.45±0.26	1.66±0.48	(Cheng et al., 2016)
NCO-P, Nepal	2013.06-2014.11	PM_{10}	0.57±0.18	0.69±0.17		(Kirillova et al., 2016)
Los Angeles Basin	2010.05-06	$PM_{2.5}$	0.71	1.58		(Zhang et al., 2013)

References

Cheng, Y., He, K.-b., Du, Z.-y., Engling, G., Liu, J.-m., Ma, Y.-l., Zheng, M., Weber, R.J., 2016. The characteristics of brown carbon aerosol during winter in Beijing. Atmospheric Environment 127, 355-364.

Cheng, Y., He, K.B., Engling, G., Weber, R., Liu, J.M., Du, Z.Y., Dong, S.P., 2017. Brown and black carbon in Beijing aerosol: Implications for the effects of brown coating on light absorption by black carbon. Sci Total Environ 599-600, 1047-1055.

Kirillova, E.N., Marinoni, A., Bonasoni, P., Vuillermoz, E., Facchini, M.C., Fuzzi, S., Decesari, S., 2016. Light absorption properties of brown carbon in the high Himalayas. Journal of Geophysical Research: Atmospheres 121, 9621-9639.

Zhang, X., Lin, Y.H., Surratt, J.D., Weber, R.J., 2013. Sources, composition and absorption Angstrom exponent of light-absorbing organic components in aerosol extracts from the Los Angeles Basin. Environ Sci Technol 47, 3685-3693.

ACTA UNIVERSITATIS LAPPEENRANTAENSIS

872. ZHIDCHENKO, VICTOR. Methods for lifecycle support of hydraulically actuated mobile working machines using IoT and digital twin concepts. 2019. Diss.

873. EGOROV, DMITRY. Ferrite permanent magnet hysteresis loss in rotating electrical machinery. 2019. Diss.

874. PALMER, CAROLIN. Psychological aspects of entrepreneurship – How personality and cognitive abilities influence leadership. 2019. Diss.

875. TALÁSEK, TOMÁS. The linguistic approximation of fuzzy models outputs. 2019. Diss.

876. LAHDENPERÄ, ESKO. Mass transfer modeling in slow-release dissolution and in reactive extraction using experimental verification. 2019. Diss.

877. GRÜNENWALD, STEFAN. High power fiber laser welding of thick section materials - Process performance and weld properties. 2019. Diss.

878. NARAYANAN, ARUN. Renewable-energy-based single and community microgrids integrated with electricity markets. 2019. Diss.

879. JAATINEN, PEKKO. Design and control of a permanent magnet bearingless machine. 2019. Diss.

880. HILTUNEN, JANI. Improving the DC-DC power conversion efficiency in a solid oxide fuel cell system. 2019. Diss.

881. RAHIKAINEN, JARKKO. On the dynamic simulation of coupled multibody and hydraulic systems for real-time applications. 2019. Diss.

882. ALAPERÄ, ILARI. Grid support by battery energy storage system secondary applications. 2019. Diss.

883. TYKKYLÄINEN, SAILA. Growth for the common good? Social enterprises' growth process. 2019. Diss.

884. TUOMISALO, TEEMU. Learning and entrepreneurial opportunity development within a Finnish telecommunication International Venture. 2019. Diss.

885. OYEDEJI, SHOLA. Software sustainability by design. 2019. Diss.

886. HUTTUNEN, MANU. Optimizing the specific energy consumption of vacuum filtration. 2019. Diss.

887. LIIKANEN, MIIA. Identifying the influence of an operational environment on environmental impacts of waste management. 2019. Diss.

888. RANTALA, TERO. Operational level performance measurement in university-industry collaboration. 2019. Diss.

889. LAUKKANEN, MINTTU. Sustainable business models for advancing system-level sustainability. 2019. Diss.

890. LOHRMANN, CHRISTOPH. Heuristic similarity- and distance-based supervised feature selection methods. 2019. Diss.

891. ABDULLAH, UMMI. Novel methods for assessing and improving usability of a remote-operated off-road vehicle interface. 2019. Diss.

892. PÖLLÄNEN, ILKKA. The efficiency and damage control of a recovery boiler. 2019. Diss.

893. HEKMATMANESH, AMIN. Investigation of EEG signal processing for rehabilitation robot control. 2019. Diss.

894. HARMOKIVI-SALORANTA, PAULA. Käyttäjät liikuntapalvelujen kehittäjinä - Käyttäjälähtöisessä palveluinnovaatioprosessissa käyttäjien tuottama tieto tutkimuksen kohteena. 2020. Diss.

895. BERGMAN, JUKKA-PEKKA. Managerial cognitive structures, strategy frames, collective strategy frame and their implications for the firms. 2020. Diss.

896. POLUEKTOV, ANTON. Application of software-defined radio for power-line-communication-based monitoring. 2020. Diss.

897. JÄRVISALO, HEIKKI. Applicability of GaN high electron mobility transistors in a high-speed drive system. 2020. Diss.

898. KOPONEN, JOONAS. Energy efficient hydrogen production by water electrolysis. 2020. Diss.

899. MAMELKINA, MARIA. Treatment of mining waters by electrocoagulation. 2020. Diss.

900. AMBAT, INDU. Application of diverse feedstocks for biodiesel production using catalytic technology. 2020. Diss.

901. LAAPIO-RAPI, EMILIA. Sairaanhoitajien rajatun lääkkeenmääräämistoiminnan tuottavuuden, tehokkuuden ja kustannusvaikuttavuuden arviointi perusterveydenhuollon avohoidon palveluprosessissa. 2020. Diss.

902. DI, CHONG. Modeling and analysis of a high-speed solid-rotor induction machine. 2020. Diss.

903. AROLA, KIMMO. Enhanced micropollutant removal and nutrient recovery in municipal wastewater treatment. 2020. Diss.

904. RAHIMPOUR GOLROUDBARY, SAEED. Sustainable recycling of critical materials. 2020. Diss.

905. BURGOS CASTILLO, RUTELY CONCEPCION. Fenton chemistry beyond remediating wastewater and producing cleaner water. 2020. Diss.

906. JOHN, MIIA. Separation efficiencies of freeze crystallization in wastewater purification. 2020. Diss.

907. VUOJOLAINEN, JOUNI. Identification of magnetically levitated machines. 2020. Diss.

908. KC, RAGHU. The role of efficient forest biomass logistics on optimisation of environmental sustainability of bioenergy. 2020. Diss.

909. NEISI, NEDA. Dynamic and thermal modeling of touch-down bearings considering bearing non-idealities. 2020. Diss.

LUT University

ISBN 978-952-335-525-5
ISBN 978-952-335-526-2 (PDF)
ISSN-L 1456-4491
ISSN 1456-4491
Lappeenranta 2020